Pharmacological modulation of Excitation - Inhibition balance in Autism Spectrum Disorders
a translational approach

Ajram, Laura Ann

Awarding institution:
King's College London

Pharmacological modulation of Excitation – Inhibition balance in Autism Spectrum Disorders: A translational approach

Laura Ann Ajram

A thesis submitted for the degree of

Doctor of Philosophy

Institute of Psychiatry, Psychology and Neuroscience

King's College London

2018

Acknowledgements

I would first like to thank my supervisors, Dr. Grainne McAlonan, Dr. Stephen Mitchell and Prof. Declan Murphy for their constant support and guidance throughout this journey. I am indebted to them for their input, feedback, encouragement and overwhelming patience. I would like to thank Dr Grainne McAlonan in particular, for providing support above and beyond the call of duty throughout the ups and downs of the past four years.

Thank you to Dr Mark Tricklebank and Dr Po Wah-So for helpful conversations and feedback along the way. Thank you also to Dr Jamie Horder for sharing his expertise in magnetic resonance imaging techniques and his patience whilst teaching me and assisting with data analysis throughout the thesis.

Thank you to all members of the MAGA team, both current and past (Dr Grainne McAlonan, Dr Jamie Horder, Dr Andreina Mendez, Dr Louise Brennan, Dr Janneke Zinkstock, Dr Tasos Galanopoulos, Dr Rob Wichers, Dr Ben Lloynes, Dr Iulia Dudd and Dr Valeria Parlatini) for assisting with recruitment, scanning and ensuring the smooth running of the MAGA protocol. Thank you to all staff at the Centre for Neuroimaging Sciences, particularly Prof. Steve Williams, Prof. David Lythgoe and the team of radiographers who performed the MAGA scans, and to Charlotte Pretzsch and Dr Hester Velthuis for continuing MAGA in my absence. A huge thank you to all participants who took part in the study.

I would like to thank the neurochemistry group at Eli Lilly and Co. for welcoming me into their team during my placement. I am particularly grateful to Dr Stephen Mitchell for his supervision and assistance with planning and carrying out pre-clinical experiments, and to Dr Nadia Malik and Dr Marcin Ligocki for teaching me essential surgical and microdialysis techniques, and for keeping me sane during the long days of microdialysis studies. I would also like to offer my sincere gratitude to Guy Carter and Sandra Sossick for undertaking huge amounts of sample analyses for this thesis, despite their own busy schedules.

I am especially grateful to other members of the Forensic and Neurodevelopmental Sciences department, who have provided support and friendship over the course of this PhD, including the LEAP girls; Daisy Crawley, Hannah Hayward and Dr. Antonia San Jose Caceres. In particular I would like to thank Dr. Alice Durieux and Dr. Ines Pote- it has been a privilege to share this experience with you. Thank you for your constant support and advice, often accompanied by sushi, gin and cake.

Thank you to my friends for keeping me relatively sane throughout this process- especially Katherine, Florence, Maria, Stephanie, Susie, Anna, Maanti, Aidan, Beatrice and Malcolm- your messages, visits and reminders that I made the right decision have been invaluable. A special shout out to the 'man high' girls – our group chats have kept me laughing and your love and support has been ever-present. I would also like to give an extra special thank you to Hannah- I really couldn't have done this without your encouragement, parcels of brownies and gin in the post and the well-timed messages and calls telling me to keep going. Thank you for everything you do- I couldn't ask for a better best friend.

Ru – thank you for being the perfect antidote to my 'science brain', my anchor in the storm that was writing this thesis and my rock ever since. Thank you for being you- you're the best, and I'm the luckiest.

Most importantly- to my family (Mum, Dad, Grandma, Zak and Alfie), thank you for always believing in me and for your endless encouragement, patience, faith and love. Thank you for teaching me to believe in myself. I wish I could have completed this in Grandma's lifetime, but I know she has been with me every step of the way. Last of all, to Zak- you are an amazing inspiration and a shining example of how amazing people with ASD are- don't ever change. Thank you for reminding me every day to work hard, I hope this makes you proud.

Acknowledgement of funding bodies

Laura Ajram (LA) is a recipient of an Industrial Cooperative Awards in Science & Technology (CASE) studentship (MR/K01725X/1), jointly funded by the Medicines Research Council (MRC) and Eli Lilly and Co. Funding for this PhD was provided in part by Autism Speaks Grant Number 8132 and support was provided by The Sackler Centre for Translational Neurodevelopment at King's College London; and EU-AIMS (European Autism Interventions), which receives support from the Innovative Medicines Initiative Joint Undertaking under Grant Agreement No. 115300, the resources of which are composed of financial contributions from the European Union's Seventh Framework Programme (Grant FP7/2007–2013). Additional support was provided by the National Institute for Health Research (NIHR) Biomedical Research Centre for Mental Health at South London and Maudsley NHS Foundation Trust and Institute of Psychiatry, Psychology and Neuroscience at King's College London.

The views expressed in this thesis are those of LA and not necessarily those of the NHS, the NIHR, the Department of Health or Eli Lilly and Co. This thesis was written by LA and critically evaluated by Dr Grainne McAlonan (GMA), Dr Stephen Mitchell (SM) and Prof. Declan Murphy (DGM), with additional support from Dr Mark Tricklebank (MT) and Dr Po Wah-So (PWS).

Statement of contribution

The work presented in this thesis would not have been possible without the help and contribution of several people:

AG: Anastasios Galanopoulos
MAM: Maria (Andreina) Mendez
BL: Ben Lloynes
CM: Clodagh Murphy
DL: David Lythgoe
DM: Daniel Meek
DGM: Declan Murphy
DR: Dene Robertson
GB: Gareth Barker
GC: Guy Carter
GI: Glynis Ivin
GMA: Grainne McAlonan
ID: Iulia Dudd
JZ: Janneke Zinkstock
LA: Laura Ajram
LB: Louise Brennan
MH: Martin Heasman
ML: Marcin Ligocki
MT: Mark Tricklebank
MW: Mark Ward
NM: Nadia Malik
PWS: Po Wah-So
RE: Richard Edden
RM: Roger Moore
RW: Robert Wichers
SM: Stephen Mitchell
SS: Sandra Sossick
SW: Steve Williams
VP: Valeria Parlatini

Clinical research

LA, GMA and JH conceived and designed the study. AM, JH and LA recruited participants. The daily running of the clinical study would not have been possible without the help of clinicians and researchers (AG, AM, BL, DM, GMA, JH, JZ, LB, RW, VP) and staff at the Behavioural Genetics Clinic at the Maudsley Hospital (DM, CM) and the Maudsley Hospital Pharmacy (GI, MH). Imaging data was acquired with the help of researchers (JH, AM) and radiographers at the Institute of Psychiatry, Psychology and Neuroscience. Assistance with scanning protocols and data acquisition was provided by SW, DL, RE and GB. LA collected the data. LA and JH analysed MRS data, and JH performed all fMRI analyses.

Pre-clinical research

LA, SM and GMA conceived and designed the studies. Microdialysis probe implantation surgeries were performed by LA, NM, ML and SM. Probe placement experiments were performed by LA and MW, and probe recovery experiments were performed by SM. All sample analyses were performed by GC, SM and SS. Statistical analyses for microdialysis experiments were performed using in-house software by RM.

List of related publications and presentations

Publications

LA Ajram, A Carvalho Pereira, A Durieux, H Velthuis, M Petrinovic, and GM McAlonan. (2018) The contribution of [1H] Magnetic Resonance Spectroscopy to the study of excitation-inhibition in autism. *Progress in Neuro-Psychopharmacology and Biological Psychiatry*. **89** p 236-244.

LA Ajram, J Horder, MA Mendez, A Galanopoulos, L Brennan, R Wichers, D Robertson, C Murphy, J Zinkstok, G Ivin, M Heasman, D Meek, M Tricklebank, G Barker, D Lythgoe, R Edden, S Williams, DG Murphy and GM McAlonan. (2017) Shifting brain inhibitory balance and connectivity of the prefrontal cortex of adults with autism spectrum disorder. *Transl Psychiatry*. **7** (5) e1137.

LA Ajram and M Tricklebank. (2017) Why is pharma so scared of psychiatric drug discovery? *Integrative Neuroscience Research.* **1** (1)

Published abstracts

LA Ajram, J Horder, MA Mendez, I Dudd, A Galanopoulos, R Wichers, D Meek, G Barker, D Lythgoe, S Williams, R Edden, DG Murphy and GM McAlonan. (2016) PT698. Shifting Excitation/Inhibition balance in Autism Spectrum Disorder. *International Journal of Neuropsychopharmacology.* **19** (1) p 54

LA Ajram, J Horder, A Galanopoulos, I Dudd, R Wichers, S Williams, DG Murphy and GM McAlonan. (2015) P001. Pharmacological modulation of brain excitatory/inhibitory balance

in autism spectrum disorder. *Proceedings of the British Pharmacological Society; PA2 online.* **13** (3)

LA Ajram, J Horder, A Galanopoulos, A Durieux, D Meek, R Wichers, S Williams, DG Murphy and GM McAlonan. (2015) Pharmacological modulation of brain excitatory/inhibitory balance in autism spectrum disorder. *Journal of Intellectual Disability Research.* **59** (9) p 794

LA Ajram. (2015) S.12.01 Pharmacological modulation of excitatory/inhibitory balance in autism spectrum disorder. *European Neuropsychopharmacology.* 25 (Supplement 2) p S127

LA Ajram, J Horder, A Galanopoulos, I Dudd, R Wichers, S Williams, DG Murphy and GM McAlonan. (2014) 008P. Glutamate and GABA in autism spectrum; a clinical in-vivo magnetic resonance spectroscopy assay. *Proceedings of the British Pharmacological Society; PA2 online.* **12** (3)

Oral presentations

LA Ajram et al. Pharmacological modulation of excitatory/inhibitory balance in autism spectrum disorder

Presented at 28th ECNP Congress, 29 Aug- 1 Sept 2015, Amsterdam, The Netherlands

LA Ajram et al. Glutamate and GABA in Autism Spectrum: A clinical in-vivo Magnetic Resonance Spectroscopy assay

Presented at the International Meeting for Autism Research (IMFAR), 14-16 May 2015, Salt Lake City, USA

LA Ajram et al. Pharmacological modulation of Excitation/Inhibition imbalance in Autism Spectrum Disorder; a clinical in vivo MRS study

Presented at the EU-AIMS Annual General Meeting, 13-14 April 2015, Paris, France

LA Ajram et al. Pharmacological modulation of inhibitory/excitatory imbalance in Autism Spectrum Disorder

Presented at SFARI's Autism Research Social at the Society for Neuroscience (SfN) Annual Meeting, 17 Nov 2014, Washington DC, USA

Poster Presentations

LA Ajram et al. Shifting brain inhibitory balance and connectivity of the prefrontal cortex of adults with autism spectrum disorder

Presented at the International Meeting for Autism Research (IMFAR), 10-13 May 2017, San Francisco, USA

LA Ajram et al. Shifting excitation/inhibition balance in autism spectrum disorder

Presented at 30th CINP World Congress, 3-5 July 2016, Seoul, South Korea

*Winner of 'Student Encouragement' Award for poster presentation *

LA Ajram et al. Modulating excitation: inhibition imbalance in ASD as a means of 'fractionating the spectrum'; an in vivo, clinical [1H]-MRS assay

Presented at the International Meeting for Autism Research (IMFAR), 11-14 May 2016, Baltimore, USA

LA Ajram et al. Pharmacological modulation of brain excitatory/inhibitory balance in autism spectrum disorder

Presented at Pharmacology 2015, 15-17 December 2015, London, UK

LA Ajram et al. Pharmacological modulation of excitatory/inhibitory balance in autism spectrum disorder

Presented at the International Meeting for Autism Research (IMFAR), 14-16 May 2015, Salt Lake City, USA

LA Ajram et al. Pharmacological modulation of excitatory/inhibitory balance in autism spectrum disorder

Presented at ECNP Workshop on Neuropsychopharmacology for Junior Scientists in Europe, 12-15 March 2015, Nice, France * Winner of Poster Prize *

LA Ajram et al. Glutamate and GABA in autism spectrum; a clinical in-vivo magnetic resonance spectroscopy assay.

Presented at Pharmacology 2014, 16-18 December 2014, London, UK

LA Ajram et al. Glutamate and GABA in autism spectrum: a clinical in-vivo magnetic resonance spectroscopy assay

Presented at GABA in Health and Disease, 13-14 Nov 2014, Washington DC, USA

LA Ajram et al. Glutamate and GABA in autism spectrum: a clinical in-vivo magnetic resonance spectroscopy assay

Presented at Translational Neuroscience, 13-14 Nov 2014, Washington DC, USA

Abstract

There are currently no effective pharmacologic treatments for the core symptoms of Autism Spectrum Disorder (ASD); and candidate treatments are often assumed to act in a similar way in people with and without ASD. This may not be the case, as there is recent evidence that the excitatory (E) glutamate and inhibitory (I) GABA systems, which are crucial to brain development and function, are altered in ASD. Abnormalities of E-I balance at rest in ASD are described in the literature, however findings often contradict and mostly stem from cross-sectional studies. To date, no prior studies of ASD have examined the 'responsivity' of the E-I system to pharmacologic challenge.

No single technique can fully capture E-I dynamics in the living brain, however E-I balance can be measured at a number of 'levels', using different species-specific modalities. Hence, in the present thesis, I aimed to explore the effect of pharmacologically modulating E-I balance at the i) intracellular, ii) functional, and iii) extracellular level, in both humans, and an animal model of ASD (the *Neurexin1α* knock out rat), after a pharmacological challenge with the E-I acting drug, riluzole.

To first capture E-I dynamics at the intracellular level, I investigated riluzole-evoked changes in bulk tissue levels of E-I neurotransmitters in the medial prefrontal cortex (mPFC) and basal ganglia (BG)- regions known to be important in ASD- using Magnetic Resonance Spectroscopy and *ex vivo* tissue analyses in humans and rats, respectively. In humans, I compared the change in 'Inhibitory Index' - the GABA fraction within the pool of glutamate plus GABA metabolites - post riluzole challenge in adult men with (n = 17) and without (n = 20) ASD. Despite comparable baseline measures of GABA and Glx (glutamate + glutamine) in the mPFC, I found the response of the Inhibitory Index to riluzole to be diametrically

opposite in men with and without ASD. In contrast, in the BG, I reported a significant group difference in baseline Glx, in which the ASD cohort had lower Glx levels compared to controls, yet both groups responded in the same direction to riluzole challenge, with an increase in the Inhibitory Index. These findings were partially replicated in the *Neurexin1α* knock out rat- with lower subcortical glutamate also reported in an equivalent basal ganglia region (the caudate putamen), compared to wild type controls. However, no differences in E-I responsivity were observed in the rodent in either strain or brain region.

Given the reported group differences in E-I responsivity profile of the human mPFC, and that E-I imbalances are likely to affect the whole brain, I next explored the responsivity of functional connectivity of the mPFC with the rest of the brain, using resting-state functional Magnetic Resonance Imaging (rs-fMRI). In the ASD group, functional connectivity was abnormal at baseline, but restored to control levels after riluzole administration. Conversely, riluzole had no effect on the functional connectivity in the control group, thus highlighting again a group difference in responsivity.

Finally, to examine whether extracellular changes in E-I dynamics were driving differences in functional connectivity, I explored neurotransmitter efflux into the extracellular space in the living rat brain, using *in vivo* microdialysis. However, riluzole had no measurable effect on glutamate nor GABA efflux in either wild type, or *Neurexin1α* knock out rats.

Overall, I have, for the first time, identified that E-I balance at both the intracellular and functional level may be shifted in adult men with ASD, and that the brain in ASD is pharmacologically different to that of controls. This has implications for future drug discovery in ASD and the results of this thesis could be translated forwards to enhance future

clinical trial design. Further to this, I found the *Neurexin1α* knock out rat to have a comparable baseline biology to the human condition, which may support its use in future studies of back-translate these findings. Such work will be necessary to further understand E-I pharmacology in ASD, and further validate E-I balance as a tractable therapeutic treatment target for this increasingly prevalent condition.

Table of Contents

List of Figures

Chapter 5

Chapter 6

Chapter 7

List of Tables

List of Abbreviations

[1H]MRS	Proton Magnetic Resonance Spectroscopy
2-OG	2-Oxoglutarate
3Rs	Replacement, Refinement and Reduction
3T	3 Tesla
AAT	Aspartate Aminotransferase
Ac	Anterior Commisure,
Acbc	Nucleus Accumbens Core,
Acbsh	Nucleus Accumbens Shell,
ACN	Acetonitrile
aCSF	Artificial Cerebrospinal Fluid
ADHD	Attention Deficit Hyperactivity Disorder
ADI	Autism Diagnostic Interview
ADOS	Autism Diagnostic Observation Schedule
AHRQ	Agency for Health Care Reserach and Quality
ALS	Amyotrophic Lateral Sclerosis
AMARES	Advanced Method for Accurate, Robust and Efficient Spectral Fitting
AMPA	A-Amino-3-Hydroxy-5-Methyl-4-Isoxazole Propionic Acid
AQ	Autism Quotient
Aralar	Aspartate-Glutamate Carrier;
ASD	Autism Spectrum Disorder
ASL	Arterial Spin Labelling
Asp	Aspartate
BBB	Blood Brain Barrier
BET	Brain Extraction Tool
Bis-Tris (buffer)	2-[bis(2-hydroxyethyl)amino]-2-(hydroxymethyl)propane-1,3-diol
BOLD	Blood Oxygenation Level Dependent
Ca^{2+}	Calcium ion
CAMHS	Child and Adolescent Mental Health Services
cAMP	Cyclic AMP
CBT	Cognitive Behavioural Therapy
Cc	Corpus Callosum
CE	Collision Energy

Cg	Cingulum
Cg1	Cingulate Cortex Area 1,
Cg2	Cingulate Cortex Area 2
CGI	Clinical Global Impression
Cho	Choline
CID	Collision Induced Dissociation
Cl^-	Chloride ion
C_{max}	Maximum concentration
CNS	Central Nervous System
CNV	Copy Number Variation
CpG	C (Cytosine) base followed by G (Guanine) base
CPu	Caudate Putamen,
Cr	Creatine
CSF	Cerebrospinal Fluid
CXP	Collision Cell Exit Potential
D	Deuterium
DP	Declustering Potential
DP	Dorsal Peduncular Cortex,
DSM	Diagnostic and Statistical Manual of Mental Disorders
E-I	Excitation-Inhibition
EAAT	Excitatory Amino Acid Transporter
E_{cl}^-	Equilibrium potential for Chloride
EPI	Echo Planar Imaging
EPSC	Excitatory Post Synaptic Current
EPSP	Excitatory Post Synaptic Potential
ESI	Electrospray Ionisation
FDA	US Food and Drug Administration
Fmi	Forceps Minor Corpus Callosum,
fMRI	Functional Magnetic Resonance Imaging
FSL	FMRIB Software Library
FSPGR	Fast SPoiled Gradient Echo
FWHM	Full Width at Half Maximum
FXMRp	Fragile X Mental Retardation Protein
GABA	γ-aminobutyric acid

GABA-T	GABA Transaminase
$GABA_A$	GABA A Receptor
$GABA_B$	GABA B Receptor
GAD	Glutamic Acid Decarboxylase
GAT	GABA Transporter
GDH	Glutamate Dehydrogenase;
GKAP	Guanylate Kinase-Associated Protein.
GLT-1	Glutamate Transporter 1
Glx	Glutamate and glutamine combined
GM	Grey Matter
HEC	Hydroxyethyl Cellulose
HPLC	High Performance Liquid Chromatography
IL	Infralimbic Cortex
IPAC	Interstitial nucleus of the Posterior limb of the Anterior Commissure
IPSP	Inhibitory Post Synaptic Potential
IQ	Intelligence Quotient
JMRUI	Java Based Magnetic Resonance User Interface
K^+	Potassium ion
KCC2	Potassium-Chloride Co-Transporter
KO	Transgenic knock-out
LC/MS	Liquid Chromatography/Mass Spectroscopy
LC-MS/MS	Liquid Chromatography/Dual Mass Spectroscopy
LD_{50}	Lethal Dose in 50% of animals
Lo	Lateral Olfactory Tract,
LV	Lateral Ventricle
M1	Primary Motor Cortex
M2	Secondary Motor Cortex,
MCFLIRT	Motion Correction FMRIB Linear Image Registration Tool
MECP2	Methyl CpG binding protein 2
MEGAPRESS	Meshcher-Garwood Point Resolved Spectroscopy
MELODIC	Multivariate Exploratory Linear Optimized Decomposition into Independent Components
mGluR	Metabotropic Glutamate Receptor
MI	Myoinositol

MM	Macromolecule
MPEP	2-methyl-6-phenylethyl-pyrididine
mPFC	medial Prefrontal Cortex
MRS	Magnetic Resonance Spectroscopy
MS	Mass Spectroscopy
Ms	Medial Septal Nucleus
Na^+	Sodium ion
NAA	N-Acetyl-Aspartate
NHS	National Health Service
NKCC1	Sodium-Potassium-Chloride Co-Transporter
NL3	Neuroligin 3
NMDA	*N*-Methyl-D-Aspartate
NMDAR	*N*-Methyl-D-Aspartate Receptor
NRXN1α	Neurexin 1 α
$NRXN1\alpha^{-/-}$	Neurexin 1 α Knock Out (homozygous)
OCD	Obsessive Compulsive Disorder
P-Gp	P-Glycoprotein
p.o.	Per Os (Oral Dosing)
PDD-NOS	Pervasive Developmental Disorder, Not Otherwise Specified
PET	Proton Emission Tomography
PFC	Prefrontal Cortex
Pir	Piriform Cortex,
PK	Pharmacokinetics
PLD	Post-Labelling Delay
Ppm	Parts per million
PRESS	Point Resolved Spectroscopy
PRL	Prelimbic Cortex,
PSD-95	Post Synaptic Density Protein - 95
Rf	Rhinal Fissure
RF	Radiofrequency
rs-fMRI	Resting State fMRI
RSN	Resting State Network
S1	Primary Somatosensory Cortex,

S2	Secondary Somatosensory Cortex
s.c	Sub Cutaneous
SSA	Succinic Semi Aldehyde;
STAI	State Trait Anxiety Inventory
T2	T2 Relaxation Time
TCA	Tricarboxylic Acid Cycle
TE	Echo Time
TI	Inversion Time
TMS	Tetramethylsilane
TR	Repetition Time
UBE3A	Ubiquitin protein ligase E3A
VGAT	Vesicular GABA Transporter
VGluT	Vesicular Glutamate Transporter
V_m	Membrane potential
WM	White Matter
WSC	Water Scaling Constant

Chapter 1

General Introduction

Some of the information presented in Chapter 1 has been published in *Progress in Neuro-Psychopharmacology and Biological Psychiatry* (See Appendix 1):
Ajram et al. (2018) The contribution of [1H] Magnetic Resonance Spectroscopy to the study of excitation-inhibition in autism. *Prog Neuro-Psychopharm & Biol Psych*. 89, 236-244.

1.1 Introduction to Autism Spectrum Disorder

Autism Spectrum Disorder (ASD) is an increasingly common neurodevelopmental condition. The frequency of ASD diagnoses in both adults (Brugha et al., 2011) and children (Russell et al., 2014) has increased globally over the last 50 years and is currently reported at around 1% in the UK, with an estimated 4 times more males affected than females (Ehlers & Gillberg, 1993). Previously split into the subcategories of Autism, Asperger's, Childhood Disintegrative Disorder and Pervasive Developmental Disorder Not Otherwise Specified (PDD-NOS) in the Diagnostic and Statistical Manual of Mental Disorders (DSM) version 4 (American Psychiatric Association, 2000), ASD is now treated as one umbrella term by the DSM-5 (American Psychiatric Association, 2013). For a diagnosis of ASD under the new DSM-5 criteria, the following four benchmarks must be met; 1) persistent difficulties with social interaction and communication, 2) restricted, repetitive behaviour patterns, 3) symptoms must be present from early childhood, and 4) symptoms must limit everyday functioning (Table 1.1). Core symptoms can range from mildly to severely debilitating and are often complicated by secondary features such as hyperactivity, inattention and intellectual impairment (O'Brien & Pearson, 2004; Reiersen & Todd, 2008).

Detail	Example
A. Persistent deficits in social communication and social interaction across contexts (not accounted for by general development delays)	
A1. Deficit in socio-emotional reciprocity	Abnormal social approach Lack of normal back and forth conversation Lack of initiation of social interaction
A2. Deficit in nonverbal communicative behaviours	Abnormal eye contact and body language Lack of facial expression and gestures
A.3 Deficits in developing and maintaining relationships appropriate to developmental level	Difficulty playing with and making friends Difficulty adjusting behavior to suit social context Absence of interest in others
B. Restricted, repetitive patterns of behavior, interests or activities	
B.1 Stereotyped or repetitive speech, movement or interest in objects	Unusual language Unusual hand and body movements Nonfunctional play with objects
B.2 Excessive adherence to routines, ritualized patterns of verbal or nonverbal behavior	Insistence on rigidity Rituals Excessive resistance to change
B.3 Highly fixated interests that have abnormal intensity or focus	Preoccupations Unusual interests or fears
B.4 Abnormal reactivity to sensory aspects of the environment	Adverse response to specific sounds or textures
C. Symptoms must present in early childhood (but may not fully manifest until social demands exceed ability)	
D. Symptoms together limit and impair everyday functioning	

Table 1.1: DSM-5 criteria for ASD diagnosis

All conditions of A, C and D must be met, with an additional 2 of 4 from B. *Adapted from DSM-5* (American Psychiatric Association, 2013)

There is increasing evidence that clinicians are able to reliably identify children with ASD as young as 2 years of age (Charman & Baird, 2002), and traits of ASD and related disorders may be recognised even earlier (Charman et al., 2000). However, despite better general awareness of ASD and improved early diagnostic tools (Luyster et al., 2009), most individuals do not receive a diagnosis until they reach school age (Yeargin-Allsopp et al., 2003); and a considerable number are not diagnosed until adulthood (Aggarwal & Angus, 2015; Geurts & Jansen, 2011). Early indicators include; lack of joint attention or shared enjoyment, limited social play, delayed onset of language and unusual 'insistence on sameness'. An ASD diagnosis is based upon behavioural observations combined with evidence from a detailed developmental history. The diagnosis can be confirmed using the gold standard diagnostic tools; the Autism Diagnostic Observation Schedule (ADOS) (Lord et al., 2000), that a trained individual conducts with the patient; and the Autism Diagnostic Interview-Revised (ADI-R) (Lord, Rutter, & Couteur, 1994), which is an interview conducted with the parent/carer; alongside a comprehensive multidisciplinary review.

If a diagnosis is not given in childhood, identifying ASD later in life becomes increasingly difficult. Though the ADOS has a specific module designed for use in verbal adults (module 4), the materials and activities are designed for children, i.e. 'Telling a story from a book' or 'Imaginative play', which may not be age-appropriate. Additionally, the ADOS module is selected on the basis of verbal ability, which may not always parallel cognitive ability (Gotham et al., 2007). Furthermore, as symptoms must be present from an early age to support an ASD diagnosis, in older individuals a detailed developmental history may not be available from a parent, or may be flawed due to incorrect recall and recall-bias (Schutte et al., 2015). Self- report can be used in lieu of parental interview; the Autism-Spectrum Quotient (AQ) is a self-reported questionnaire which can be useful in adults to assess the

degree of autistic traits, but as patients often lack insight into their own condition, it cannot be used as a stand-alone diagnostic tool (Baron-Cohen et al., 2001; Sizoo et al., 2015). Furthermore, the AQ has recently been shown to have poor predictive validity in 'real world' clinical settings. In development, the AQ was found to be highly effective at identifying ASD traits in those with a clinical diagnosis of ASD, compared to healthy controls, however in a clinical setting the AQ's predictive power is poor, and may therefore lead to 'false negative' results (Ashwood et al., 2016).

Recognition of autistic symptoms in general is clearer in children, with defined developmental markers in childhood against which progress can be compared. In contrast, such references do not exist in adulthood and can be confused by cultural differences. In addition, under long term social pressure to 'fit in', adults may have developed coping or masking techniques, either consciously or unintentionally. For example, training oneself to make eye contact during conversation, using learned jokes, or making contextually appropriate gestures or remarks (imitating facial expressions, or making sympathetic sounds in response to bad news). This 'masking' of symptoms is especially common in women with ASD (Lai et al., 2011).

Considering the difficulties of diagnosing ASD in adulthood, it is conceivable that the prevalence of ASD in this age group is higher than is currently estimated, with many adults remaining undiagnosed and untreated, or misdiagnosed with other psychiatric disorders. This may also link to the scarcity of autism research in adults, as shown by a recent assessment which found only 15% of ASD research in the UK exclusively focused on adults with the condition, with the majority of studies focusing on children, or adolescents (Pellicano et al., 2014). Hence, though it is prudent and necessary to initiate studies of neurodevelopmental

disorders as early in development as possible, this may have come at the expense of research into those already living with the condition as an adult.

The pervasive idea that ASD is a neurodevelopmental, and therefore primarily a childhood, disorder may also contribute to the limited research in this age group. In reality, ASD is a lifelong condition, which persists as the brain matures and changes through life. It is important to note that findings from research in children cannot necessarily be extrapolated to adults- because the adult brain may respond differently. For example, differences in responsivity to drugs across ASD age groups have been reported by Hollander et al (2012), who observed significant decreases in repetitive behaviours in adults with ASD taking fluoxetine, yet only a modest effect in children with the disorder (Hollander, Phillips, et al., 2005). A similar pattern of efficacy differences has been observed using fluvoxamine (McDougle et al., 1996, 2000). Thus, it should not be assumed that the adult brain is just a larger child's brain- and this must be taken into consideration when attempting to identify treatments to alleviate the difficulties of living with ASD as an adult.

1.1.1 Living with ASD as an adult

The importance of providing mental health support for adults with autism is becoming increasingly recognised, for example by the UK government's 2009 Autism Act and subsequent extension, 'Think Autism' in 2014. However, in reality, clinical services for adults remain markedly limited (UK Government, 2009, 2014). In particular, the transition from childhood to adulthood is a difficult time, involving the loss of school structure and support, and (in the UK) the transition from Child and Adolescent Mental Health Services (CAMHS) to Adult Services. For those adults with ASD, but an IQ>70 and no co-morbid psychiatric conditions, gaining support from adult services is near impossible, as they do not

fit into either learning disability or mental health streams (Pilling et al., 2012).

The core symptoms of autism; difficulties in social interaction, communication and restricted interests, do not typically lend themselves to successful adult relationships in the workplace and in social settings. Only 15% of people with an ASD in the UK are in employment (NAS, 2016), many of whom experience difficulty maintaining employment, not due to performance, but due to the requirement to interact and engage with colleagues (Vogeley et al., 2013). For high functioning individuals able to work, employment not only offers a financial income, but a chance to contribute and be valued in the community (Capo, 2001; Scott et al., 2015). In addition to poor employment opportunities, studies (admittedly conducted prior to the availability of early intervention strategies) predict that over half of patients have poor outcomes in terms of independent living, and forming peer relationships (Billstedt et al., 2005; Howlin et al., 2004, 2013).

Though many people with ASD are able to live fully functional lives, a large proportion are severely debilitated and require full time care. Compounding the difficulties autistic patients face are co-occurring health, psychiatric and developmental disorders thought to affect up to 70% of individuals (Lugnegård et al., 2011). The presence of these additional challenges are strongly associated with reduced quality of life, increased need for professional help and poorer prognosis (Carlsson et al., 2013; Levy et al., 2010; Mattila et al., 2010). Subsequently, the emotional, social and financial cost to these individuals and their families can be huge, particularly in areas where access to services and support is inadequate. It is estimated that autism costs the UK £32 billion per year; more than cancer (£12bn), heart disease (£8bn) and stroke (£4bn) combined (Buescher et al., 2014). The absence of pharmacological treatment options for the core symptoms of ASD and sometimes sub-optimal response of comorbidities

to conventional medications (Reiersen & Todd, 2008) contributes to the cost of ASD; yet the increased rate of diagnosis has not led to a proportional increase in available treatments.

1.1.2 Current treatment options

There are currently no pharmacological treatments for the core symptoms of restricted, repetitive behaviours, and social and communication difficulties in ASD. Repurposed medications have proven useful in managing associated behaviours; for example; the antipsychotics risperidone and aripiprazole are FDA-approved for the treatment of irritable behaviour in ASD (Dinnissen et al., 2014; Ghanizadeh et al., 2015; Sharma & Shaw, 2012), though they also have many detrimental side effects. Despite their efficacy in reducing challenging and repetitive behaviours, they also induce weight gain, sedation and extrapyramidal symptoms (Jannsen Pharmaceuticals Ltd, 2009; Otsuka America Pharmaceutical, Inc, 2002). Additionally, methylphenidate is often prescribed for ADHD (though this also comes with potential side effects) and people with ASD may be especially sensitive to these (Reiersen & Todd, 2008; Research Units on Pediatric Psychopharmacology Autism Network, 2005). Buspirone may also be prescribed with some efficacy, to reduce anxiety (Hsia et al., 2014). However, no pharmaceutical intervention has yielded results in terms of improving social communication as a primary outcome.

Due to the current lack of pharmacological treatments, non-pharmacological treatment strategies have become the cornerstone of ASD management. Educational intervention (communication skills, play, addressing behavioural problems), psychotherapy (applied behaviour analysis) and cognitive behavioural therapy (CBT- restructuring maladaptive thoughts and behaviours) have all been successful in improving patient quality of life (Myers & Johnson, 2007), though more evidence is needed to fully assess their effectiveness (AHRQ, 2011).

Despite the relative success of these measures, there is a pressing need for effective pharmacological treatments for core deficits. The high level of phenotypic variability in ASD, by which one patient may present as high functioning yet another with the same disorder may be non-verbal, likely reflects the marked aetiological heterogeneity of the disorder, and has made the identification of a common underlying pathology challenging. If the biology was better understood this could point drug development in the direction of viable pathways to target. To advance drug discovery in this field, it is therefore of the utmost importance that we continue attempts to expose the underlying patho-aetiology of the disorder.

1.1.3 Aetiology

Autism was originally viewed as a result of inadequate mother-child bonding, specifically a cold attitude on the mother's part, in what became known as the 'refrigerator mother theory' (Bettelheim, 1967). Today, the notion of parental fault is generally disregarded, and it is widely accepted that there is a neurobiological underpinning to ASD.

It is well established that genetics play an important role in the development of ASD. Early twins studies suggested familial hereditability estimates of 56-95% (Colvert et al., 2015), but the role of genes in ASD is best demonstrated by the presence of syndromic forms, such as Fragile X syndrome and Retts syndrome, which have a clear genetic cause (a single gene mutation of the Fragile X Mental Retardation protein (FXMRp) or methyl CpG binding protein 2 (MECP2) genes, respectively (Amir et al., 1999; Verkerk et al., 1991). In addition, up to 1000 susceptibility genes have been identified, each accounting for a very small fraction of ASD cases (Berg & Geschwind, 2012). It has been suggested that the genes contributing to ASD fall within 3 main groups: those affecting the glutamate/GABA synapse; those involved in chromatin remodelling; and those causing alterations to gene transcription

and splicing (De Rubeis et al., 2014).

Genetics are not solely responsible however; multiple environmental risk factors have also been identified, such as advanced parental age (Lampi et al., 2013), early prenatal maternal viral infection (Atladóttir et al., 2010) and environmental chemical exposure (Al-Hamdan et al., 2018; Kalkbrenner et al., 2014). However, aside from syndromic forms of ASD, no single genetic alteration or environmental factor has been identified as sufficient or necessary to develop an ASD. Instead, it is likely that most cases originate from an interplay of genetic predisposition and environmental exposures, which converge onto common molecular pathways involved in key neurodevelopmental processes (Baudouin, 2014; Persico & Bourgeron, 2006). For example, based on evidence that exposure to toxins such as valproic acid and maternal immune activation in prenatal life directly alters glutamate metabolism (Wei et al., 2016) and the GABA transcriptome (Dickerson et al., 2014; Richetto et al., 2014) respectively in the foetal brain; a candidate pathway susceptible to both genetic (above) and environmental risk factors for ASD is the glutamate-GABA system.

Although a range of both genetic and environmental risk factors for ASD are now appreciated to act on glutamate-GABA pathways (Banerjee et al., 2013; Baudouin, 2014; The Autism Genome Project Consortium, 2007), the first forays implicating this molecular pathway in ASD pathology stemmed from the association of ASD with increased rates of epilepsy- a condition known to arise from altered excitatory (E) and inhibitory (I) signalling in the brain (Tuchman & Cuccaro, 2011; Tuchman & Rapin, 2002). Whilst the high frequency of comorbidity of epilepsy with ASD could indicate shared symptomatology or even simply similar diagnostic criteria, it is thought likely to be due to a common underlying pathology; a disruption of the E-I system (Lai et al., 2014). Furthermore, other conditions which are well accepted to be at least partly due to disruption of E-I balance are also often

linked to ASD; for example Obsessive Compulsive Disorder (OCD), Attention Deficit Hyperactivity Disorder (ADHD), anxiety and depression (Avoli & de Curtis, 2011; Kariuki-Nyuthe et al., 2014; Lydiard, 2003; Mann et al., 2014; Purkayastha et al., 2015). Early developmental problems, such as intellectual disability and ADHD are most commonly observed to accompany ASD in childhood (Leyfer et al., 2006; Matson & Shoemaker, 2009; Simonoff et al., 2008), whilst in ASD in adulthood, in addition to ADHD and anxiety disorders, mood disorders are common (Croen et al., 2015; Ghaziuddin et al., 2002; Hofvander et al., 2009; Sterling et al., 2008). A comprehensive list of the conditions highly associated with ASD and their proposed pathophysiology are found in Table 1.2.

Though for brevity the present thesis focuses on GABA and glutamate pathways as the principle controllers of E-I balance, they should not be viewed in isolation as they interact with, and can be modulated by, a number of other neurochemical pathways. Serotonin in particular is a particularly influential modulator of E-I balance. For example, in the frontal cortex, hippocampus and cerebellum, serotonin induces a decrease of glutamate transmission and a parallel increase in GABA (Ciranna, 2006). Likewise, dopamine affects glutamate function with different effects depending on the receptor, cell type and brain region, involved. In the striatum for instance, D1 receptors potentiate responses mediated by NMDA receptors, whereas D2 receptors depress AMPA responses (Tseng & O'Donnell, 2004). Given the importance of serotonin and dopamine in modulating E-I balance, it is unsurprising that disruptions to these systems have also been implicated in the pathology of ASD (Muller et al., 2016; Pavăl, 2017). The importance of these neurotransmitters is highlighted in Table 1.2, where disruptions of serotonin and dopamine, amongst others, have been linked to disorders often co-morbid with ASD (Clarke et al., 2014; Gleason et al., 2010; Helton & Lohoff, 2015; Spencer et al., 2005; Vaswani et al., 2003). Hence, although I focus on GABA

and glutamate in the present thesis, it is important to highlight that these are two of many neurochemicals altered in the pathogenesis of ASD.

Taken together, these associations strongly implicate differences in the E –I system as a potential underlying cause of ASD, and hence a potential therapeutic target. Maintaining a balance of excitatory to inhibitory neural control is essential from conception throughout the entire lifespan. Any alteration to this system could therefore have profound and far reaching effects on both neurodevelopmental processes and the subsequent formation of coherent networks.

Condition	Co-morbidity risk	Further information	Proposed Disease Mechanism
General Medical			
Epilepsy	5-30% (Besag, 2017; Tuchman et al., 2013; Viscidi et al., 2013)	Onset in childhood or adolescence (Tuchman & Rapin, 2002)	E-I Imbalance & cortical interneuron dysfunction (Avoli & de Curtis, 2011)
Gastrointestinal problems	17-70% (Adams et al., 2011)	Common symptoms include chronic constipation, diarrhoea and abdominal pain	Altered gut microbiota (de Theije et al., 2014) may affect GABA (Kang et al., 2018; Lin, 2013) and other neurotransmitters (Clarke et al., 2014)
Genetic syndromes	<5%	Fragile X (Verkerk et al., 1991) Rett Syndrome (Castro et al., 2013) Tuberous Sclerosis (Gipson et al., 2015)	Single genetic mutation
Psychiatric			

Anxiety	42-56% (Hofvander et al., 2009; Mattila et al., 2010; Simonoff et al., 2008)	Common across all age groups	GABA dysfunction (Lydiard, 2003) and Serotonergic dysfunction (Gleason et al., 2010; Vaswani et al., 2003)
Depression	12-70% (Hofvander et al., 2009; Mattila et al., 2010; Simonoff et al., 2008)	Common in adults, less so in children (Ghaziuddin et al., 2002; Hofvander et al., 2009)	E-I imbalance (Mann et al., 2014; Pehrson & Sanchez, 2015; Veeraiah et al., 2014) Serotonergic dysfunction (Helton & Lohoff, 2015)
Obsessive Compulsive Disorder	7-24% (Hofvander et al., 2009; Lugnegård et al., 2011; Simonoff et al., 2008)	May fit the 'repetitive behaviors domain' of ASD	E-I imbalance (Kariuki-Nyuthe et al., 2014; Naaijen et al., 2015) Serotonergic dysfunction (Soomro, 2012)
Developmental			
Intellectual disability	~30% (Centers for Disease Control and Prevention, 2014)	IQ<70	Genetic (Moeschler & Shevell, 2006) or unexplained

Attention Deficit Hyperactivity Disorder (ADHD)	28-44% (Leyfer et al., 2006; Simonoff et al., 2008)	May now be diagnosed in addition to ASD under DSM-V, where DSM-IV did not allow co-morbid diagnosis. The current prevalence of co-morbid diagnosis is therefore likely higher than reported.	Dopamine dysregulation (Spencer et al., 2005, 2007) E-I imbalance (Purkayastha et al., 2015)

Table 1.2: Comorbid conditions common to Autism Spectrum Disorders

Adapted from Lai et al. 2014.

1.2 The Excitation - Inhibition System

Glutamate and γ-aminobutyric acid (GABA) are respectively the major excitatory and inhibitory neurotransmitters in the brain. The processes by which each of these neurotransmitters is synthesized, released, removed from the synaptic and extra-synaptic cleft and metabolized are all tightly regulated and have, for many years, been targets for drug discovery. They are found in all brain regions and have multiple neurobiological functions, mediated by different types of receptors. A balanced interaction between glutamate and GABA is essential for effective neurotransmission from conception and throughout the whole lifespan. The regulation of E-I balance is particularly important during neurodevelopment, where GABA and glutamate act in synchrony to regulate the proliferation, migration and differentiation of neuronal cells. Balanced neurotransmission is also essential for synaptic maturation, refinement of neuronal circuitry and eventually the regulation of cognition, emotion and behaviour (Luján et al., 2005).

1.2.1 Pharmacology

1.2.1.1 Synthesis

The amino acid glutamine is synthesised by astrocytes and converted to glutamate via the enzyme glutaminase in both glutamatergic and GABAergic neurons. In excitatory neurons, glutamate is transported into vesicles via vesicular glutamate transporters (vGluT) and released into the synaptic cleft upon depolarisation of the neuron. In inhibitory neurons, glutamate is converted to GABA, by the glutamic acid decarboxylase (GAD) enzyme. GAD exists in two isoforms, GAD_{65} and GAD_{67}, which have different molecular weights (65 and 67 kDa respectively), properties, and subcellular localization (Erlander et al., 1991). GABA is then transported to vesicles for release via vesicular GABA transporters (vGAT). Upon

release, neurotransmitters are taken up by high affinity membrane transporters back into neurons and surrounding glia, where they are recycled for continued use. Glutamate may be converted to glutamine for storage in astrocytes via glutamine synthase, or converted to GABA via GAD in GABA-synthesising inter-neurons (Rowley et al., 2012). In this way, GABA and glutamate are in constant flux, each continuously contributing to the synthesis of the other (Figure 1.1).

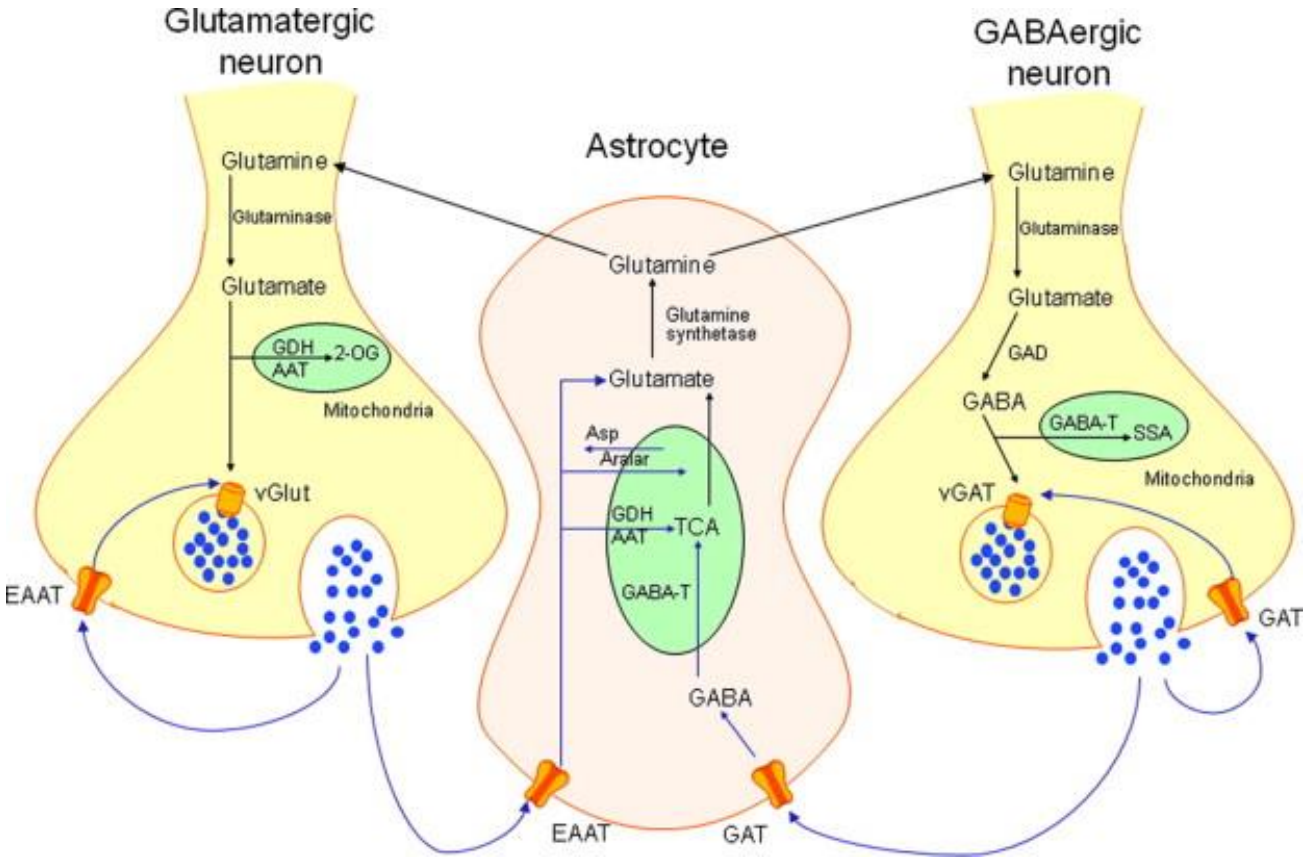

Figure 2.1: Synthesis, release and metabolism of glutamate and GABA

Glutamine is converted to glutamate via the enzyme glutaminase, which then goes on to either be released by excitatory neurons, or converted to GABA via the enzyme glutamic acid decarboxylase in inhibitory neurons. Neurotransmitters are taken up into astrocytes and neurons to be recycled to glutamate and glutamine, thus the cycle re-starts. Adapted from Rowley et al., 2012.

Abbreviations: 2-OG, 2-oxoglutarate; AAT, aspartate aminotransferase; Aralar, aspartate-glutamate carrier; Asp, aspartate; EAAT, excitatory amino acid transporter; GABA-T, GABA transaminase; GAD, glutamic acid decarboxylase; GAT, GABA transporter; GDH, glutamate dehydrogenase; SSA, succinic semi aldehyde; TCA, tricarboxylic acid cycle; vGAT, vesicular GABA transporter; vGlut, vesicular glutamate transporter.

1.2.1.2 Receptors and signalling pathways

Neuronal action potentials initiate neurotransmitter release into the synaptic cleft, where they act on multiple pre- and postsynaptic receptors (Figure 1.2), triggering a signalling cascade within the cell that modulates neuronal activity. Excitatory synaptic transmission is initiated by glutamate binding to either ionotropic (AMPA, NMDA or Kainate) ion channel receptors, or metabotropic G protein-coupled receptors ($mGluR_{1\text{-}5}$). Activation of ionotropic receptors opens the ion channel and allows influx and efflux of sodium (Na^+), potassium (K^+) and calcium (Ca^{2+}) ions, to produce an Excitatory Post Synaptic Potential (EPSP) and fast neuronal activity. In comparison, metabotropic receptors are G protein-coupled, and therefore have a relatively slower action, as ligand activation first evokes secondary messenger signalling cascades prior to ion channel modulation.

GABA receptors are also grouped according to their activation mechanism; $GABA_B$ receptors are G protein coupled, and are found pre- and postsynaptically, whereas $GABA_A$ receptors are ionotropic, postsynaptic chloride (Cl^-) ion channels. Upon binding to the $GABA_A$ receptor, GABA evokes a conformational change, which allows the receptor to facilitate the passive influx or efflux of Cl^- ions, dependent upon the neuronal equilibrium potential for chloride (E_{Cl^-}). During postnatal life, this presents as an influx, which results in inhibitory synaptic transmission.

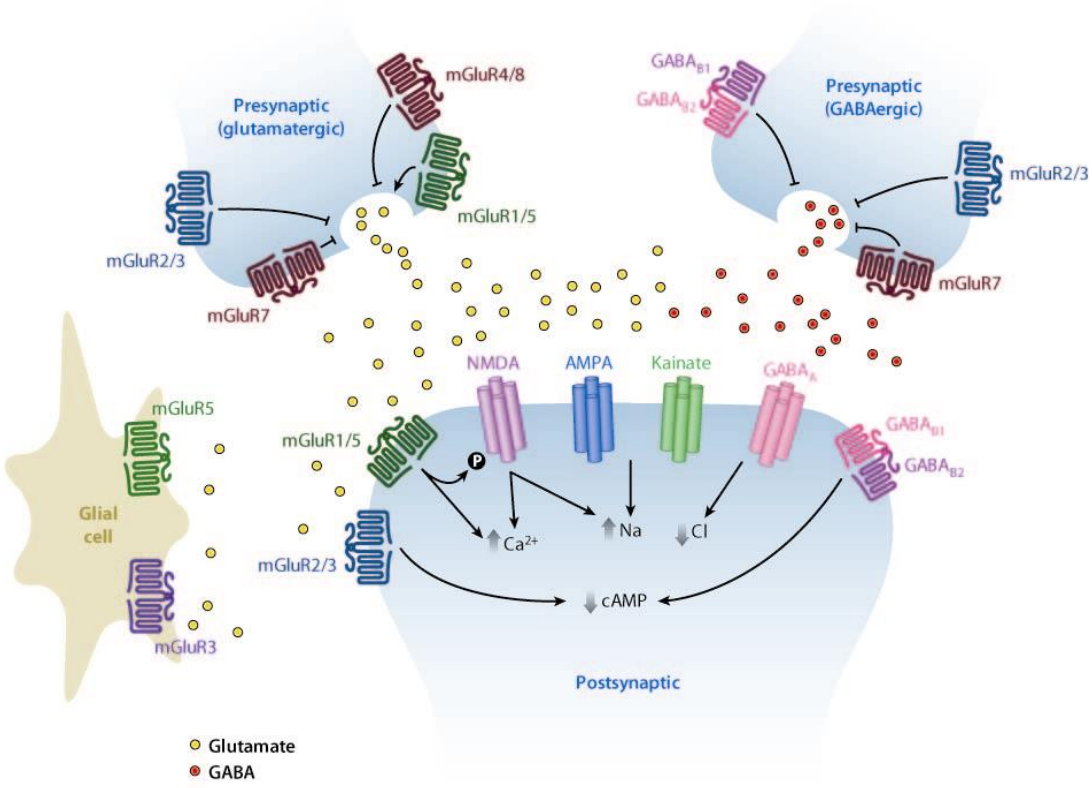

Figure 1.3: Schematic representation of glutamate and GABA receptors at the synapse

Glutamate (yellow circles) and GABA (red circles) are released from presynaptic terminals, diffuse across the synaptic cleft, and activate receptors located on postsynaptic neurons. Additionally, glutamate and GABA can act at receptors on nearby astrocytes and as retrograde transmitters on presynaptic nerve terminals. Figure taken from Niswender & Conn, 2010.

Abbreviations: mGluR, metabotropic glutamate receptor; GABA$_{A/B}$, GABA $_A$ and $_B$ receptors; NMDA, N-Methyl-D-aspartic acid receptor; AMPA, α-amino-3-hydroxy-5-methyl-4-isoxazolepropionic acid receptor; Ca^{2+}, calcium; Na, sodium; Cl, chloride; cAMP, cyclic adenosine monophosphate

Prenatally however, GABA acts very differently. Over the time course of synaptic development in utero, GABA synapses develop first, prior to their glutamatergic counterparts. Hence GABA initially plays an excitatory role, before 'switching' to its eventual inhibitory purpose after birth.

Initially, immature neurons have a high level of intracellular Cl^- ions compared to the extracellular space; therefore when activated by GABA, the relative difference of E_{Cl^-} (positive) to the resting membrane potential (V_m), causes a net Cl^- efflux via a sodium-potassium-chloride co-transporter (NKCC1) and membrane depolarisation (Ben-Ari et al., 2012). The 'switch' to inhibition is thought to occur at birth, as preclinical studies indicate a dramatic reduction of intracellular Cl^- immediately prior to, and post-delivery, in response to maternal oxytocin released during labour (Tyzio et al., 2006). Additionally, around the same time, there is a distinct change in neuronal chloride co-transporter expression; NKCC1 expression decreases, and is superseded by expression of potassium-chloride co-transporter, KCC2 (Clayton et al., 1998). The decrease in intracellular Cl^- means that the relative difference between E_{Cl^-} and V_m is now negative, therefore, in mature postnatal neurons, lower intracellular Cl^- results in a net Cl^- influx via KCC2 and membrane hyperpolarisation (see Figure 1.3).

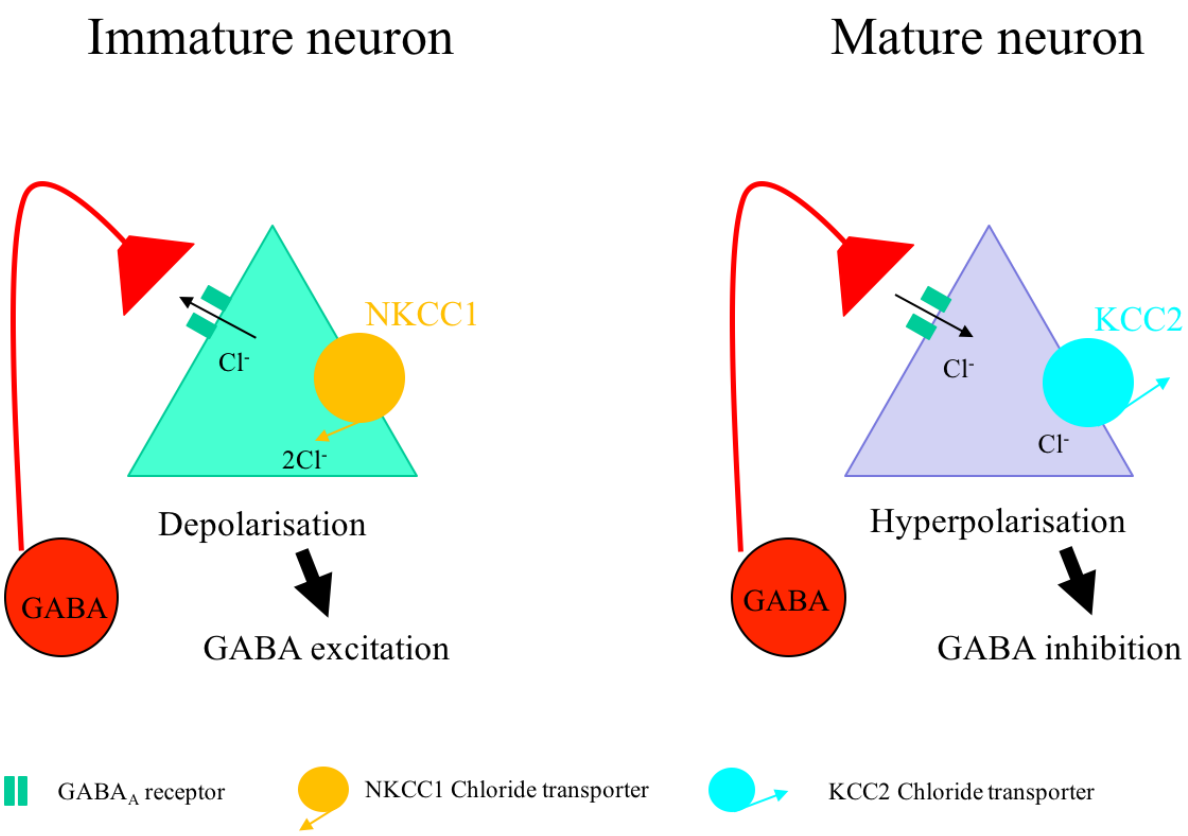

Figure 1.3: The developmental GABA switch from excitation to inhibition

The shift in GABA function is partly determined by the sequential development of two chloride transporters; NKCC1 develops first and imports Cl^- upon $GABA_A$ receptor activation, and KCC2 develops later, and exports Cl^- upon receptor activation. This causes depolarization and hyperpolarization of the neuron respectively.

Abbreviations: NKCC1, sodium-potassium-chloride co-transporter; Cl-, chloride ion; KCC2, potassium-chloride co-transporter

1.2.2 Glutamate and GABA in neurodevelopment

Glutamate and GABA act together to initiate and control events such as neural proliferation, migration, differentiation and synaptogenesis during prenatal brain development and throughout postnatal life (Luján et al., 2005).

Prenatally, the proliferation of neuronal progenitor cells is fundamental for generating neurons in the correct sequence and location in the brain. Glutamate and GABA receptor emergence and activation are believed to regulate this system, and have been identified as instrumental in controlling DNA synthesis in dividing neurons (Ben-Yaakov & Golan, 2003; Haydar et al., 2000; LoTurco et al., 1995). Post creation, most neurons migrate from their site of origin to their intended destination in the cortex, thus creating the complex patterning and organization of the brain regions. This too is dependent upon the emergence of GABA and glutamate control at the correct time. For example, in the prefrontal cortex, glutamate acts as a chemoattractant signal to guide incoming neurons (Behar et al., 1999). For these neurons to effectively signal, they need to be positioned and anchored together. This is achieved by a complex structure of cell adhesion proteins, most notably neurexins and neuroligins, which work together to maintain synaptic stability. These structures are essential for effective glutamatergic and GABAergic transmission, and any abnormalities can cause profound implications for E-I signalling. Their role in ASD is discussed in further detail in section 1.3.

In addition to correctly positioning cortical neurons, glutamate also alters cortical neuron cytoarchitecture prenatally, and during the first postnatal days. Pyramidal neurons are the primary excitation unit in the prefrontal cortex, but are also found in abundance throughout the cerebral cortex, and in the hippocampus and amygdala; areas known to be associated with advanced cognitive function (Spruston, 2008). During pyramidal neuron development,

glutamate regulates selective inhibition of dendritic growth and dendritic pruning (at non-toxic levels). Some studies also show a role for glutamate in encouraging dendritic growth and branching of cerebellar granule cells (Pearce et al., 1987) and hippocampal cells (Mattson et al., 1988). This complex guidance system, mediated by progressive GABA and glutamate activity, allows neurons to grow towards their postsynaptic targets, ready to form synapses, which enable neurons to fire and wire together. Hence, what begins as a diffuse and overlapping networks of neuronal contacts, is in time refined (through repeated E-I activity) into better defined local circuits, which may interact to form extensive neural networks.

With such complex shifts in excitatory - inhibitory function in the perinatal period, it is easy to imagine that slight alterations in E –I balance could significantly alter the effectiveness of neural signalling and could potentially give rise to subtle, but wide-ranging differences in the neural networks which coordinate complex behaviours in ASD.

1.3 Excitation – Inhibition Imbalance in ASD

The development and firing of neural networks are co-ordinated by excitatory glutamate, and inhibitory GABA transmission, hence alterations to this system have been proposed to be key to the pathology of ASD (Coghlan et al., 2012; Gao & Penzes, 2015; Uzunova et al., 2016). Indeed, many known aetiological and genetic risk factors for ASD appear to affect the balance of this system (for more details please see below).

Initially, this may lead to disruption of neurogenesis, neuronal proliferation and migration and synaptogenesis (Packer, 2016). However on a grander scale, such disruptions to brain cytoarchitecture would inevitably result in affected brain regions being unable to generate connections that give rise to fully effective functional networks (Courchesne et al., 2007;

Ecker & Murphy, 2014; Stanfield et al., 2008) and thus behaviour would be affected.

1.3.1 Genetic and preclinical evidence

There is an accumulation of evidence from genetic and preclinical studies to support a role for differences in E-I in ASD.

Genetically determined abnormalities in GABA and glutamate signalling pathways have consistently been associated with ASD. The $GABA_A$ receptor may be of particular significance, as studies of ASD susceptibility genes have identified chromosome 15q11-q13 as a region of interest, and this contains three $GABA_A$ receptor subtype genes (β3, γ3 and α5) (Pizzarelli & Cherubini, 2011). Mutations in this region, and in particular those in the β3 subunit (Chaste et al., 2014; Isles et al., 2016; Shao et al., 2003), convey a high risk for ASD. Additionally, evidence for the link between $GABA_A$-β3 and autism has been shown in a mouse knock-out model, in which an absence of the β3 subunit caused behavioural difficulties relevant to autism; such as repetitive and stereotyped behaviours (stereotypical cage circumnavigation and 'tail chasing') in addition to poor motor co-ordination and learning deficits (DeLorey et al., 1998). Likewise, $GABA_A$-α5 alterations have been reported in adults with ASD, namely in a preliminary PET study reporting significantly reduced binding to the α5 subunit across multiple brain regions (Mendez et al., 2013), although this finding was not replicated in a larger cohort (Andersson et al., 2017). Post-mortem studies in ASD have also pointed to GABA abnormalities including reduced mRNA levels for multiple $GABA_A$ and $GABA_B$ receptor subtypes (Fatemi et al., 2014; Fatemi & Folsom, 2015; Oblak et al., 2009, 2010) and $GABA_A$ and $GABA_B$ receptor protein levels have been are reported to be lower the cingulate cortex of adults (Fatemi et al., 2010; Oblak et al., 2010) and prefrontal

cortex of children with ASD (Mori et al., 2012). Furthermore, single cell transcriptomic data suggest that inhibitory neurons may be a major neuron subtype affected by the disruption of ASD gene networks (Wang, Zhao, Lachman, & Zheng, 2018).

Studies have also uncovered associations between ASD and polymorphisms in genes involved in glutamatergic signalling pathways. Fragile X Syndrome, the most common genetic form of ASD-like behaviours, is caused by a single gene mutation affecting fragile X mental retardation protein (FXMRp) (Verkerk et al., 1991). In healthy individuals, FXMRp acts to negatively regulate postsynaptic glutamate receptor ($mGluR_5$) activity, and its absence leads to excessive excitatory activity, which presents as an autism-like phenotype (Lozano et al., 2014; Yu & Berry-Kravis, 2014). Furthermore, genetic (Dölen et al., 2007) and pharmacological (Mehta et al., 2011) reduction of mGluR activity in rodent models, have been shown to significantly improve ASD-like behaviours. However, pharmacological attempts to reduce mGluR activity in humans with ASD have since failed in clinical trials (Berry-Kravis et al., 2016; Scharf et al., 2015), suggesting the E-I imbalance in ASD is not straightforward. For example, the numbers of glutamate receptors have also been reported to be altered in ASD; $mGluR_5$ has been shown to be significantly higher in ASD (Fatemi et al., 2011), whereas reduced NMDA receptor expression gives rise to ASD-like behaviours in mice (Gandal et al., 2012). Such alterations in receptor density and activity will no doubt affect synaptic efficacy, but coupled with this, there is emerging evidence that the structural integrity of the synapse itself is also affected in ASD.

Cell adhesion molecules neurexin and neuroligin, and scaffolding proteins Post Synaptic Density – 95 (PSD-95) and SHANK act together to establish the structural architecture of E-I synapses (see Figure 1.4). Anchoring of the pre- and post-synaptic neuron terminals via this matrix is essential to synapse formation, alignment and stability (Lee & Sheng, 2000).

Impairment of any one component therefore, could result in irregular molecular assembly of the synapse, and hence faulty E-I neurotransmission (Futai et al., 2007; Südhof, 2008; Zhao et al., 2017).

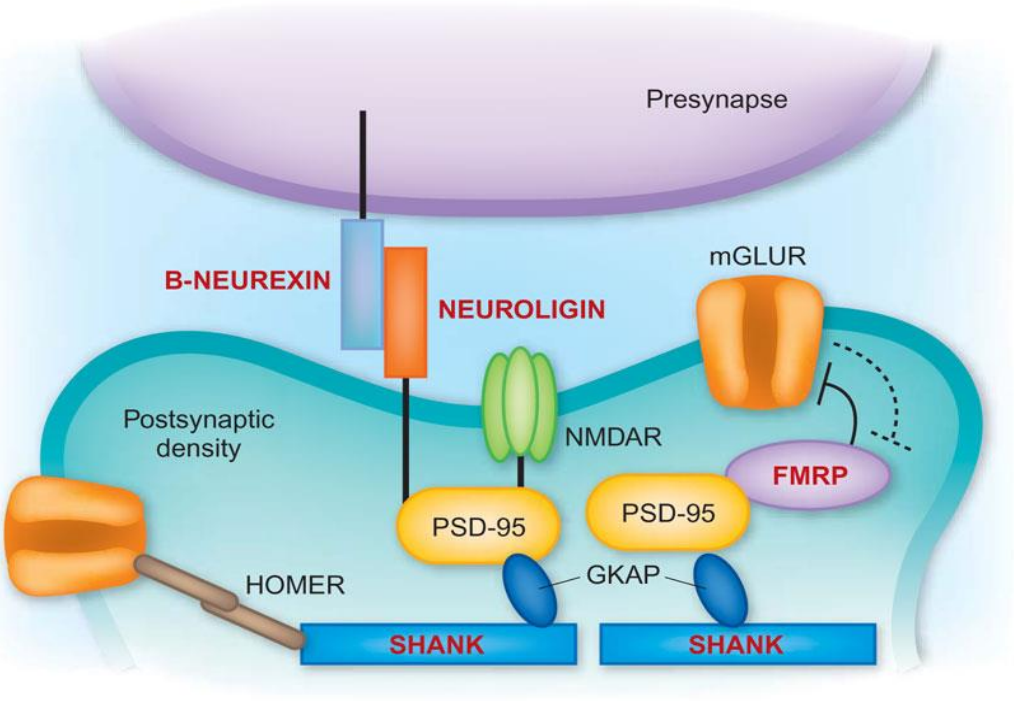

Figure 1.4: Neuroligin-Neurexin complexes stabilize the synapse

Neurexin, a presynaptic neuronal adhesion molecule, interacts with neuroligins (its post-synaptic equivalent), which in turn bind intracellularly to Post Synaptic Density protein 95 (PSD-95). SHANK proteins form a matrix to anchor this complex. Figure taken from State, 2010**.**

Abbreviations: mGluR, metabotropic glutamate receptor; NMDAR, N-methyl-D-aspartate receptor; FMRP, Fragile X Mental Retardation Protein; PSD-95, Post Synaptic Density protein 95; GKAP, guanylate kinase-associated protein.

Of this group of synaptic proteins, the neurexin-neuroligin complex is one of the most studied trans-synaptic pairs in ASD. Distinct pairings of these families play discrete roles during synaptogenesis; for example, neuroligin-1 regulates excitatory synapse formation (Song et al., 1999), whereas neuroligins -2 and -3 regulate inhibitory synapse formation and maturation (Levinson et al., 2005; Varoqueaux et al., 2004). In connecting the pre- and post-synaptic neurons, neurexin-neuroligin interactions mediate signalling across the synapse, which in turn modulates synaptic activity and determines the properties of neuronal networks. It is therefore unsurprising that genetic alterations to this process have been linked to cognitive deficits, such as those seen in autism. Several copy number variants (CNVs) across the two families have been associated with ASD, with the highest prevalence for mutations in *Neurexin-1* (Ching et al., 2010; Feng et al., 2006; Kim et al., 2008; Yan et al., 2008) and *Neuroligin-3* (Jamain et al., 2003; Yanagi et al., 2012; Yu et al., 2011). Considering the essential role of neurexins and neuroligins in structuring the synapse, and the clear link to ASD in humans, genetically modified animal models have been created to explore the disrupted synaptic mechanisms in ASD.

Neurexin1α homozygous knock out (*Nrxn1α*$^{-/-}$) mice have been reported to have weak excitatory synaptic strength and reduced excitatory post synaptic current (EPSC) frequency compared to wild type controls (Etherton, Blaiss, Powell, & Südhof, 2009). Additionally, knock out mice have fewer spontaneous and evoked excitatory and inhibitory neurotransmitter release events (Kattenstroth et al., 2004; Missler et al., 2003; Zhang et al., 2005). Behavioural abnormalities have also been observed in the knock-outs; including increased grooming behaviours, decreased startle response and impaired nest building and social investigation (Dachtler et al., 2015; Etherton, 2009; Grayton et al., 2013; Laarakker et al., 2012). More recently, a rat model of *Neurexin1α* deletion became available. This animal

has persistent non-social cognitive deficits, such as hyperactivity, reduced learning ability and inattention (Esclassan et al., 2015). Though the human condition can never be fully replicated in an animal model, the features observed in *Neurexin1α* rodents may proxy the repetitive behaviours, cognitive deficits and inflexibility/stereotypy which are core to the human condition and therefore provide a useful model to study mechanisms underpinning ASD in the laboratory (Etherton et al., 2009; Grayton et al., 2013).

Thus, the combined evidence from the aforementioned genetic and pre-clinical studies strongly suggest that E-I imbalance is relevant to the pathophysiology of ASD. However, directly measuring this imbalance *in vivo* in the living human brain has proved to be challenging. There is hope however, as recent advances in magnetic resonance imaging has enabled safe, *in vivo* quantification of brain metabolites in both healthy individuals, and those with ASD.

1.3.2 E-I in the living human brain – metabolite levels

The first approach to assessing levels of both glutamate and GABA in autistic patients was to study plasma metabolite concentrations, which were taken as an indication of what may be happening in the brain. Findings were inconsistent using this method, for example, glutamate serum levels were found to be significantly higher in children (Hassan et al., 2013) and adults (Shinohe et al., 2006) with ASD, yet high serum levels of GABA have also been reported in ASD populations (Dhossche et al. 2002). Such inconsistencies may have arisen because the blood-brain barrier does not permit free movement of metabolites between intracranial and plasma compartments. This is especially true for GABA, which is known to be unable to cross this barrier (Van Gelder & Elliott, 1958). Measuring E-I by proxy may therefore not be the best approach. Rather, direct measures of neurotransmitters in the living brain are needed

to understand E-I balance *in situ*. Direct measures of glutamate, and more recently, GABA, using Magnetic Resonance Spectroscopy (MRS) are now possible. Using this technique, E-I levels can be quantified in a predefined brain region of interest, in an awake, living human brain.

MRS studies in ASD have largely focused on the basal ganglia and prefrontal cortex. ASD is believed to be a disorder of network connectivity (Mohammad-Rezazadeh et al., 2016; Nomi & Uddin, 2015), and considering the extent of executive function, socio-emotional and repetitive behaviours observed in this condition, the subcortical and prefrontal networks sub serving these activities have been linked to both socio-communication deficits and repetitive behaviours in ASD (Calderoni et al., 2014; Estes et al., 2011; Holmboe et al., 2010; Horder et al., 2013; Kalbe et al., 2010; Kratsman et al., 2016; Martínez-Sanchis, 2015; Prat et al., 2016; Qiu et al., 2010). Consistent with this, both structural and signalling abnormalities of these regions have been associated with the core symptoms of ASD (Haznedar et al., 2006; Hollander et al., 2005; Prat, 2016; Schmitz et al., 2007, 2008). However, the results from studies comparing baseline metabolite levels in these regions (and other brain areas) between groups are still at variance (see Table 1.3; and for a complete review see Ajram et al., 2018, Appendix 1).

Multiple MRS studies have reported an excess of glutamate across the brain in ASD, for example in the frontal cortex (Hassan et al., 2013; Joshi et al., 2013), amygdala and hippocampal regions (Page et al., 2006) and auditory cortex (Brown et al., 2013). Yet others, including research from my own department, have found that there is lower resting glutamate levels in ASD participants in the subcortex (Horder et al., 2013), cingulate (Tebartz van Elst et al., 2014) and anterior cingulate cortex (Bernardi et al., 2011). Still others have found no

differences in glutamate levels across the brain (Ajram et al., 2017; Carvalho Pereira et al., 2017; Cochran et al., 2015; DeVito et al., 2007; Hardan et al., 2008; Libero et al., 2015; Tebartz van Elst et al., 2014).

Though fewer in number, MRS studies of GABA are more consistent and generally find lower GABA in the ASD brain; for example GABA has been shown to be lower in the frontal cortex (Harada et al., 2011; Kubas et al., 2012), motor and auditory regions (Gaetz et al., 2014) of children with the disorder. Again, others have also observed no differences in brain GABA in ASD (Ajram et al., 2017; Brix et al., 2015; Carvalho Pereira et al., 2017; Gaetz et al., 2014; Harada et al., 2011).

Brain Region	Metabolite measured	
	Glx or Glutamate	**GABA**
Anterior cingulate cortex	↑ Hassan et al. 2013 * ↑ Joshi et al. 2013 • ↑ Bejjani et al. 2012 * ↓ Tebartz van Elst et al. 2014 ∇ ↓ Bernardi et al. 2011 ∇ ≡ Libero et al. 2015 ∇ ≡ Cochran et al. 2015 •	↓ Cochran et al. 2015 • = Brix et al. 2015 *
Medial prefrontal cortex	= Carvalho Pereira et al. 2017 •* = Ajram et al. 2017 ∇	= Carvalho Pereira et al. 2017 •* = Ajram et al. 2017 ∇
Amygdala	↑ Page et al. 2006 ∇	
Hippocampus	↑ Page et al. 2006 ∇	
Basal Ganglia **Striatum**	↓ Horder et al. 2013 ∇ ↑ Hassan et al. 2013 *	≡ Harada et al. 2011*
Thalamus	≡ Hardan et al. 2008 *	
Frontal lobe	↑ Hassan et al. 2013 *	↓ Harada et al. 2011* ↓ Kubas et al. 2012 *
Lenticular nuclei		≡ Harada et al. 2011*
Motor cortex		↓ Gaetz et al. 2014 *
Visual cortex		≡ Gaetz et al. 2014 *
Auditory cortex	↑ Brown et al. 2013b ∇	↓ Gaetz et al. 2014 *
Cerebellum	≡ Tebartz van Elst et al. 2014 ∇ ≡ DeVito et al. 2007 * ↑ Hassan et al. 2013 *	

Table 1.3: [1H]MRS quantified glutamate and GABA differences for patients with ASD

1.5 Tesla; 3 Tesla; 4 Tesla; * Children; • Adolescent; ∇ Adult. A comprehensive review of MRS studies in ASD can be found in Ajram et al., 2018 (Appendix 1).

Discrepancies between studies may be due to a number of factors, most notably the inevitable differences in patient demographics that arise when investigating such a heterogeneous population. In particular, variations in current medication and the presence of comorbid mental or physical health symptoms, such as anxiety or epilepsy, may alter results, as some patients may consequently have pharmacologically altered E-I balance or alterations attributable to a co-occurring condition (Pizzarelli & Cherubini, 2011). Likewise, inconsistencies between studies of different ages are not surprising given reports that glutamate also varies across age groups and brain regions in typically developed participants (Kaiser et al., 2005; Sailasuta et al., 2008) and metabolite levels may 'normalise' with age in people with ASD (Aoki et al., 2012; Ipser et al., 2012). Ultimately however, participant variability may stem from the fact that even 'pure' ASD is a highly heterogeneous disorder (Ecker et al., 2013), and not all individuals necessarily share the same E-I profile.

Practically, between-study differences in experimental protocol may also contribute to divergent MRS findings. Different scanner field strengths and protocols will provide different measures of metabolites, as (due to their structural similarity) glutamate, glutamine and GABA are difficult to isolate and quantify at lower field strengths such as 1.5T (Puts & Edden, 2012) and are often combined into one measure of 'Glx' in these studies (e.g. Bernardi et al. 2011; DeVito et al. 2007 and Horder et al. 2013). At field strengths of 3T or above, with specific scanner parameters, such as J-edited MEGAPRESS (MEshcher-GArwood Point RESolved Spectroscopy) (Edden & Barker, 2007; Mescher et al., 1998) and specialised software tools (Edden et al., 2014; Naressi et al., 2001), GABA and glutamate/glutamine can be isolated and separately quantified, allowing us to observe them as independent components of the E-I system (although in the majority of studies the GABA measure is a combined signal with lipid macromolecules). Considering the difference in

metabolite composition, it may therefore not be appropriate to compare results at different field strengths.

1.3.3 Measuring E-I responsivity in the human brain

The fact that E-I balance is not static (and so may contribute to this failure to replicate study results) has been largely overlooked in the literature. As is evident from Table 1.3, the majority of research concerning E-I metabolite levels in ASD has focused on either glutamate alone, or only GABA levels. However, glutamate and GABA do not exist in isolation *in vivo* - the system is in constant flux (Hyder et al., 2013; Rothman et al., 2011, 2012; Sibson et al., 1998). Control of this flux may well be abnormal in ASD, as glutamic acid decarboxylase (GAD) levels, which converts glutamate to GABA, have been found to be lower in ASD (Fatemi et al., 2002; Yip et al., 2007, 2009), and altered in ASD animal models (Wei et al., 2016; Zhang et al., 2014). Differences in E-I flux, and subsequent responsivity of the E-I system, may therefore need to be taken into consideration in studies of E-I in ASD, yet this has not been directly examined *in vivo.*

1.3.3.1 Choice of drug

To examine system dynamics, one approach is to provide a challenge to the system and capture its response. This may be achieved pharmacologically, and in the experiments reported in this thesis I elected to use the drug riluzole, because it has broad actions on E-I and should therefore modulate E-I transmission in a range of participants.

Riluzole is an FDA-approved medication for the treatment of amyotrophic lateral sclerosis (ALS) and has actions at both GABA and glutamate targets. For example, in both *in vitro* and

in vivo studies, riluzole has been shown to inhibit pre-synaptic release of glutamate (Cheramy et al., 1992; Doble, 1996; Jehle et al., 2000), potentiate postsynaptic $GABA_A$ receptor function (He et al., 2002) and block GABA reuptake into the striatum (Mantz et al., 1994). In addition to its direct actions on glutamate and GABA pathways, riluzole may also modulate E-I via its additional effects on ion channel activity. For example, *in vitro* studies have shown riluzole to decrease sodium (Wang et al., 2008) and potassium (Zona et al., 1998) channel activity, as well as inhibiting ionotropic glutamate receptor currents (namely NMDA and Kainate; Debono et al. 1993).

In this instance, the polypharmacology of riluzole may be advantageous; as a modulator of the E-I system through both glutamatergic and GABAergic mechanisms, riluzole should have the potential to modulate E-I flux in the majority of individuals. Importantly, riluzole has a well-established pharmacokinetic and safety profile; and a single dose can reach peak plasma concentration within a relatively short time frame (1 hour) with relatively low risk of adverse effects (Le Liboux et al., 1997).

1.3.3.2 Choice of brain region

It is clear from Table 1.3 that E-I imbalances are found in a variety of brain regions in ASD. For the present study, the dorsomedial prefrontal cortex (containing the anterior cingulate cortex) and a sub-cortical region targeting the left basal ganglia were selected as targets as both are associated with the social, communication, affective and cognitive functions which are disrupted in autism (see page 60 for further detail). The larger area of the dorsomedial prefrontal cortex was selected as the region of interest, rather than the anterior cingulate alone, in order to compare results with other ongoing studies in the department which used

the same methodology. This was also a technical decision, as a large region is needed to capture a good signal, thus the voxel extends beyond the size of the ACC.

1.3.3.3 Choice of modality

Responsivity of the E-I system can be investigated at multiple levels in the human brain, each of which tell us something different. As explored in section 1.3.2, MRS enables sampling of bulk intracellular measures of metabolites and will allow for comparisons of E-I responsivity at a tissue level. In the present thesis, I therefore opted to utilise this technique to investigate whether the intracellular dynamics of the E-I system differs in ASD. However, MRS is not sensitive to differences in synaptic events, therefore it is not possible to know what proportion of the metabolites measured are a result of active neurotransmission. An additional approach may therefore help to assess E-I responsivity in terms of its influence on brain function.

1.3.4 E-I in the living human brain – functional impact

Functional connectivity as measured using fMRI refers to the extent that activity across interconnected brain regions is synchronized (Friston, Worsley, Frackowiak, Mazziotta, & Evans, 1994); i.e. what fires together wires together (Hebbian theory -Hebb 1949). As 'firing' is primarily determined by the balance between glutamate-driven excitation, and inhibitory GABA feedback signalling within local microcircuits (Buzsáki et al., 2007; Kapogiannis et al., 2013; Magistretti & Pellerin, 1999), functional connectivity measures can be used to as a proxy measure of inter-regional glutamatergic and GABAergic drive. For example, in typical individuals, prefrontal glutamate concentration correlates with the strength of prefrontal functional connectivity (Duncan et al., 2013); and posteromedial cortex glutamate and GABA

predict intrinsic functional connectivity of the default mode network (Kapogiannis et al., 2013). Likewise, local GABA concentration predicts the extent of inhibition within the motor network (Stagg et al., 2014) and striatal GABA levels relate to functional connectivity of the basal ganglia (Haag et al., 2015). Any changes to E-I balance may therefore have widespread influence on the regulation of the functional connectivity of resting state networks. However, functional connectivity can also be modulated through multiple neurotransmitter systems, and this should be remembered when interpreting the results from fMRI studies.

It is well established in the literature that functional connectivity, potentially stemming from E-I differences, is altered in ASD (Hahamy, Behrmann, & Malach, 2015; Jann et al., 2015; Just, Keller, Malave, Kana, & Varma, 2012; Schipul, Keller, & Just, 2011). Under-connectivity across long-distance networks in ASD has been fairly consistently reported in ASD (Cherkassky, Kana, Keller, & Just, 2006; Just, Cherkassky, Keller, & Minshew, 2004; Just et al., 2012; Washington et al., 2014), particularly in networks incorporating the prefrontal cortex, for example the default mode network (DMN) where reduced connectivity in ASD has been linked to severity of social symptoms (Assaf et al., 2010; Weng et al., 2010). By contrast, others have found over-connectivity in shorter distance networks in ASD (Uddin et al., 2013). For example, social impairments and repetitive behaviours have been linked to *increased* connectivity within cortico-striatal circuitry (Delmonte et al., 2013). Taken together, there appears to be a loss of long range neural coherence, coupled with, perhaps compensatory, increases in short-range cortico-subcortical connectivity in ASD at rest (reviewed by Rane et al. 2015). However, to date, no one has examined the dynamics of this system and whether functional connectivity in ASD is 'fixed', or if it can be shifted by E-I modulation.

Hence, the present thesis also incorporated a resting state fMRI study to examine whether there are group differences in the response of functional connectivity of networks associated with ASD after E-I challenge with riluzole.

As noted above, the MRS and functional connectivity measures used in the human studies in this thesis have limitations. For instance, MRS is a direct measure of glutamate and GABA but only at a 'bulk' tissue (and mainly intracellular) level; and fMRI is an indirect measure of network activity that does not directly measure extracellular levels of neurotransmitters in the living brain. Examination of neurotransmitter efflux into the extracellular space is however possible in animal models using *in vivo* microdialysis.

1.3.5 E-I in the rodent brain – sampling the extracellular space

Microdialysis is an established sampling technique for the *in vivo* measurement of neurotransmitter efflux into the extracellular space of discrete brain regions (see methods section 2.2.4.2 for further detail). For example, microdialysis has proven effective at capturing increases in prefrontal and caudate efflux of glutamate following amphetamine (Del Arco, Martínez, & Mora, 1998) and haloperidol treatment respectively (Yamamoto & Cooperman, 1994). Pertinently, this technique has also captured decreases in glutamate efflux from the ventral posterolateral nucleus of the thalamus following riluzole administration in prior rodent studies (Abarca et al., 2000). GABA can also be reliably captured using this method (Wydra et al., 2013), and most importantly both glutamate and GABA may be sampled from the same brain region at the same time; and measures can be taken at multiple time points over a few hours, in freely moving, live rodents (Zapata et al., 2009).

To investigate extracellular E-I responsivity using this technique, it was first necessary to select an appropriate animal model of ASD. It is essentially impossible to capture the complex and heterogeneous phenotype of the human condition with one genetic or environmental alteration, and consequently a broad array of animals modelling different aspects of ASD have been generated (Burrows et al., 2015; Esclassan et al., 2015; Liu et al., 2016; Mabunga et al., 2015; Shinoda et al., 2013; Stewart et al., 2014). For my study, I selected the *Neurexin1α* homozygous knock out rat (*Nrxn1α*$^{-/-}$), as previously described in section 1.3.1, because it models disruption at glutamate and GABA synapses, and hence potentially the E-I imbalance, which is associated with ASD. To mirror the human arm of the experiment, *Nrxn1α*$^{-/-}$ rats or wild type controls were given either a single oral dose of riluzole, or equivalent vehicle (placebo), and GABA and glutamate efflux were measured. To my knowledge, this is the first time that E-I response to pharmacological challenge has been investigated in *Nrxn1α*$^{-/-}$ rats.

1.4 The present thesis: aims and hypotheses

The evidence presented thus far suggests that E-I imbalances contribute to the pathology of ASD, yet to date, nobody has ever investigated what is likely to be a crucial element - E-I *responsivity*. This is important as differences in E-I pathways in ASD may not necessarily be best understood by capturing data in the 'resting state' or at a single time point. Instead, what is important in ASD may be the responsivity, or flux, of the E-I system.

To assess E-I responsivity, we can examine how the system is – or is not – shifted by a challenge. To this end, riluzole was selected as a pharmacological probe to activate both glutamate and GABA pathways.

There is no single modality which can fully assess whether there are E-I responsivity differences in the living brain, therefore I employed a range of modalities to probe E-I at different resolutions – i) bulk tissue, ii) functional network and iii) extracellular levels. I could address i) and ii) in humans but needed to address iii) in an animal model; the *Nrxn1α*$^{-/-}$ knock-out rat (see Figure 1.5).

1.4.1 Clinical Studies

1.4.1.1 E-I responsivity of adult men with ASD: 1[H]MRS

1[H]MRS was used to investigate whether the responsivity of bulk E-I metabolites differed between adult men with and without ASD at the intracellular level, when challenged with the pharmacological probe, riluzole. The targets selected for MRS study were the dorsomedial prefrontal cortex (Chapter 3) and the basal ganglia (Chapter 4).

1.4.1.2 E-I responsivity of adult men with ASD: Resting state fMRI

The selected brain regions do not act in isolation, rather they function as part of wider brain networks. Therefore, where a group difference in MRS measured E-I responsivity was found (in the dorsomedial prefrontal cortex, see Chapter 3), resting state fMRI was used to investigate the functional connectivity of that brain region with the rest of the brain. I hypothesized that there would be an ASD-control difference in resting state functional connectivity response to riluzole challenge. Specifically, I anticipated the ASD group would demonstrate reduced functional connectivity of the prefrontal cortex at baseline, compared to controls, and that functional connectivity of this region would increase upon administration of riluzole. Comparatively, I hypothesised that riluzole would not affect the functional connectivity of the control group, as they would re-balance E-I after a rilzuole challenge. This study is reported in Chapter 3.

1.4.2 Pre-clinical studies

1.4.2.1 Validating the *Neurexin1α*$^{-/-}$ rat as a model of E-I imbalance observed in the human studies: *Ex vivo*

Prior to investigating responsivity differences in the *Nrxn1α*$^{-/-}$ rat, I first investigated whether baseline E-I differences between the knock out rat and wild type controls were comparable to the clinical cohort in terms of their baseline neurochemistry. Equivalent brain regions to the human study were dissected (prefrontal cortex and caudate putamen) and the bulk intracellular level of metabolites in the tissue were assessed. This study is reported in Chapter 5.

1.4.2.2 E-I responsivity of *Neurexin1α*$^{-/-}$ rats: *Ex vivo*

I next examined bulk intracellular differences in E-I metabolites *ex vivo* in the prefrontal cortex and caudate putamen of *Nrxn1α*$^{-/-}$ and wild type rats after riluzole administration. Specifically, I tested the hypothesis that there would be group differences in E-I responsivity, in terms of bulk measures of E-I metabolites, which would match the results of the human MRS study. This approach is reported in Chapter 5.

1.4.2.3 E-I responsivity of *Neurexin1α*$^{-/-}$ rats: *In vivo* microdialysis

Finally, I used *in vivo* microdialysis to investigate changes in extracellular flux of E-I metabolites, after riluzole administration. Specifically, glutamate and GABA efflux in the medial prefrontal cortex and caudate putamen were compared following administration of riluzole or 1% HEC (vehicle) in wild type and *Nrxn1α*$^{-/-}$ rats. I hypothesised that there would be group differences in responsivity to riluzole in terms of local extracellular neurotransmitter efflux. This study is reported in Chapter 6.

1.4.3 Summary of thesis plan

To summarise, the following thesis will examine E-I responsivity at the intracellular, functional and extracellular levels:

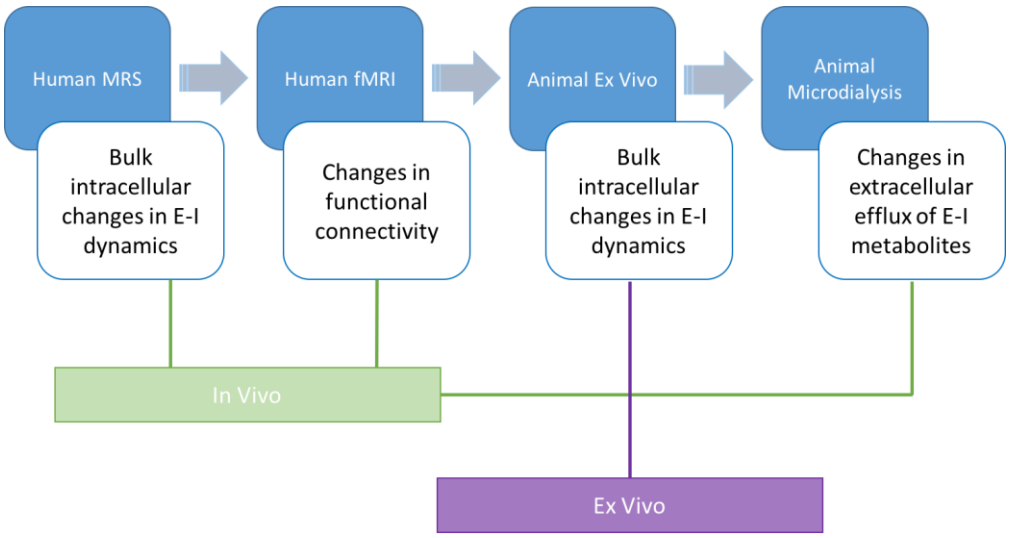

Figure 1.5: Schematic representation of study design and the level at which E-I responsivity will be examined

Chapter 2

General Methods

2.1 Measuring E-I in humans

2.1.1 Study design

A case-control, crossover repeated measures study was designed to compare *in vivo* metabolite levels 'at rest' (placebo) and when 'activated', by a standard 50 mg oral dose of riluzole. A placebo condition was deemed essential to control for non-specific effects such as anxiety which may independently alter E-I dynamics in both the patient and control population (Lydiard, 2003).

Participants were scanned on two occasions, one week apart to ensure full drug 'wash-out' between scans (riluzole half-life is estimated at 12 hours (Le Liboux et al., 1997)). The order of drug administration was pseudo-randomised (crossover) to ensure half of participants received placebo on their first visit, and half received riluzole. The participant, clinicians and study lead were blind to this randomisation to exclude bias.

At the start of each session, a brief medical assessment was performed by a study clinician to check normal heart rate, blood pressure and respiratory function before participants were given either a capsule of riluzole or matched placebo to swallow with water. The tablet was administered 45 minutes prior to the participant entering the scanner, to ensure data collection began at the time of estimated peak drug effect (1-hour post dose). During the wait period, participants completed study questionnaires. After the scan, participants were re-

assessed by a clinician and completed an adverse-effect form before leaving the facilities. See Table 2.1 for an overview of the study design:

	Prior to Scan	First Scan	Second Scan
Recruitment	X		
Patient Information and Informed Consent	X		
Medical Assessment (via questionnaire and physical examination)	X	X	X
Questionnaires	X	X	X
Oral administration of placebo/riluzole		X	X
MRI Scan		X	X
Adverse Effects Interview		X	X

Table 2.1: Study overview

An example time course of events throughout the duration of the study.

On both visits, the total scan duration was approximately 60 minutes. During this time, a structural MRI image was obtained, followed by two MRS acquisitions, then resting state fMRI. If there was time remaining, Arterial Spin Labelling (ASL) data were also acquired but were not used in this thesis. See Figure 2.1 for an overview of the scan timeline:

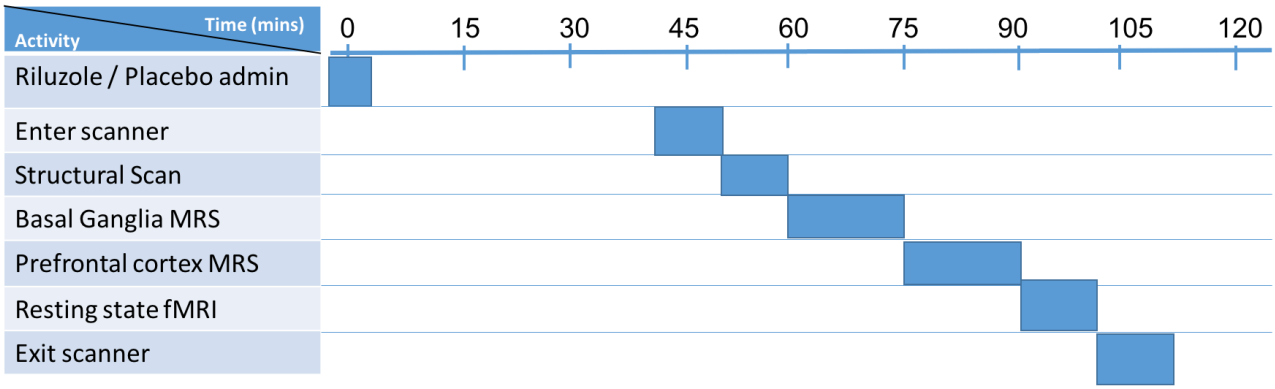

Figure 2.1: Timetable of in-scanner events

An example time course of events from the time of drug administration. Riluzole or placebo was administered at time zero, followed by a 45-minute wait, during which time study questionnaires were completed. The participant entered the scanner 45 minutes post-dose and the structural scan was performed. MRS data acquisition began 60 minutes after drug administration, followed by fMRI. Total scan duration was 60 minutes. Timeline is not to scale.

2.1.2 Study materials and compounds

The study was performed on a 3 Tesla (3T) GE Excite II Magnetic Resonance Imaging scanner (GE Medical Systems, WI, USA) at the Centre for Neuroimaging Sciences, Kings College London, UK.

2.1.2.1 Drug and placebo

Riluzole was obtained from the manufacturer, Sanofi, UK, and dispensed by the Maudsley Hospital Pharmacy (South London and the Maudsley NHS Foundation Trust, UK).

Placebo, ascorbic acid (vitamin C), was obtained from the manufacturer, Dalkeith Laboratories Ltd, UK, and dispensed by the Maudsley Hospital Pharmacy. Both riluzole and placebo were encapsulated by a pharmacist such that both tablets appeared identical, and drug administration was double-blind. The drug or placebo assignment information was held by the Maudsley Hospital Pharmacy and the Chief Investigator, who performed the randomization using a computer algorithm (Haahr, 1998).

2.1.2.2 Study Questionnaires

In the wait time between drug administration and the scanning protocol, participants were invited to complete a series of questionnaires:

Autism Spectrum Quotient (AQ): A screening instrument of 50 statements which measures autistic traits in adults. The subject was asked to indicate to what extent they agree with the statements, for example: 'I find social situations easy'. Scores range from 0-50, with the diagnostic cut off being >32 (Baron-Cohen et al., 2001).

State-Trait Anxiety Inventory (STAI): We asked participants to complete the 'State' part of the STAI as a measure of current anxiety levels before both scans. Scores range between 20-80, with a higher score indicating higher anxiety (Spielberger et al., 1970).

Obsessive Compulsive Inventory- Revised (OCI-R): This questionnaire comprises of 18 questions which measure to what extent obsessive and compulsive traits interfere with the subject's life (Abramowitz & Deacon, 2006). A score of >21 indicates obsessive compulsive disorder, with the mean score of an OCD patient being 28 (Foa et al., 2002). This was used in this study as an additional measure of mental state, and as a proxy measure of current traits of rituals and compulsions, which are found in ASD but are not always well documented by the ADOS.

Barkley's Current Scale: The participant was asked to complete the Barkley's self-assessment, which measures inattention and hyperactivity (Barkley & Russell, 2011). The same questionnaire was then given to the participant to take home for an informant (family member/friend) to complete to assess the participant's insight to their symptom presentation.

2.1.3 Participants

2.1.3.1 Recruitment

We recruited a total of 37 adult men aged 18-60, 17 of which had a confirmed ASD diagnosis, and 20 age- and IQ-matched controls. Adults with ASD were recruited from a database of patients at the Maudsley Behavioural Genetics Clinic who had consented to be contacted for research. Control participants were recruited from the local community. All potential participants were provided with information sheets (see Appendix 2) and had the

study rationale and protocol explained verbally. Written, informed consent was obtained prior to study commencement, by a trained member of the research team (see Appendix 3).

2.1.3.2 Inclusion and Exclusion criteria

Men with ASD had their clinical diagnosis of autism spectrum disorder confirmed using the Autism Diagnostic Observation Schedule and where an informant was available, Autism Diagnostic Interview – Revised. This was usually carried out in the clinic at the time of their initial diagnosis; if this was the case, it was not repeated for the study.
Participant suitability was assessed using a thorough pre-recruitment screening questionnaire, completed over the phone with a researcher.

Inclusion criteria for all participants were; IQ above 70; absence of current psychoactive medication, and being medication free for a minimum of 6 weeks to avoid potential confounds from drug interactions. For the same reason, only participants who consumed less than 28 units of alcohol per week, and smoked less than 4 cigarettes per day were deemed eligible for inclusion. Exclusion criteria for all participants were; comorbid psychiatric or medical condition which may affect brain development (e.g. epilepsy or psychosis), head injury, or genetic or chromosomal disorder associated with ASD (e.g. Fragile X or tuberous sclerosis). In the ASD group, known genetic disorders were screened by checking patient records for any outstanding diagnoses. Additionally, both groups were asked if they had any knowledge of chromosomal or genetic disorders within their family, or if they had ever had tests for, or been told they had a chromosomal or genetic disorder themselves. Participants were also excluded if they had a recent history of psychoactive substance abuse, drug allergy (particularly to E-I acting drugs) or any contraindication to MRI scanning, for example metal in the body. Full exclusion criteria and rationale are provided in Appendix 4.

2.1.4 Magnetic Resonance Spectroscopy

Proton Magnetic Resonance Spectroscopy ([1H]MRS) is a rapidly developing neuroimaging technique that allows non-invasive *in vivo* analysis and quantification of neurochemicals and their metabolites. Using this methodology, it is possible to quantify excitatory and inhibitory neurotransmitters (glutamate and GABA) within specific, pre-defined regions of brain tissue; and thus, to examine the potential biochemical underpinnings of neurological and psychiatric disorders. MRS has the advantage of being non-invasive, without the need for injections, or radioactive materials. As such, patients tend to be more comfortable and the level of study compliance for repeat visits is high.

2.1.4.1 The Physics of 1[H]MRS

2.1.4.1.1 Nuclear magnetic resonance

[1H]MRS works on the principle that hydrogen (^{1}H) nuclei, otherwise known as protons, are in constant precession (spinning around their own axes); which contributes to the induction of a magnetic moment. As shown in Figure 2.2 A, in the absence of a magnetic field, protons 'at rest' (without artificial stimulation) are in random alignment. The application of an external magnetic field (B_o) generated by an MRI scanner magnetizes a proportion of protons and causes them to align themselves along the magnetic field lines (Figure 2.2 B). This produces a net magnetisation effect, longitudinal to the applied magnetic field. Under normal circumstances, the aligned hydrogen nuclei continue to precess around their axes with the frequency of their precession being proportional to the applied magnetic field strength according to the Lamor equation:

$$\omega_0 = \gamma \beta_0$$

Where ω_0 represents precessional (Lamor) frequency (MHz), γ is the gyromagnetic ratio (MHz/T) and β_0 is magnetic field strength (T).

2.1.4.1.2 Excitation, relaxation and MR signal acquisition

The application of a radiofrequency (RF) pulse, B_{rf}, (an additional time-dependent magnetic field, equal to the Lamor frequency) causes the nuclei to absorb energy, and transition to a higher energy state, thus creating an overall excitation effect. The RF is usually applied perpendicular to B_o (Figure 2.2 C), which alters the original direction of proton alignment, and causes the protons to spin at a new angle, away from B_o. This new angle of proton orientation is termed the *flip angle* and is directly proportional to the direction and amplitude of the applied RF pulse (usually 90 degrees). This changing of the direction of proton alignment causes an induced current in the coil of the scanner- this current can be measured and is commonly referred to as the MR signal.

When the RF pulse stops, the protons return to their original lower energy state, and line up with the direction of the scanner's magnetic field once more (Figure 2.2 D). This return to equilibrium is termed *relaxation,* specifically 'T1 longitudinal relaxation' and is defined as the time taken for the protons to realign with B_o after a radiofrequency pulse application. During relaxation, protons 'decay' and release their absorbed energy. As the protons return to their original alignment, the magnetic fields of the individual protons interact with each other and exchange energy. This results in an overall loss of signal, and is termed 'T2 transverse relaxation'. Both T1 and T2 times vary, depending on the intrinsic properties of the tissue

that is being imaged. We can therefore use this information to distinguish between different tissue types in the brain, i.e. structural MRI.

Multiple RF pulses are applied during a single scan, at a predetermined rate, termed repetition time (TR). Together with the inversion time (TI- time between different pulse sequences) and echo delay time (TE- time between the application of the RF pulse and the detection of the response signal) they affect the appearance of the signal readout; variations in these parameters can affect both the image contrast and the overall duration of the scan.

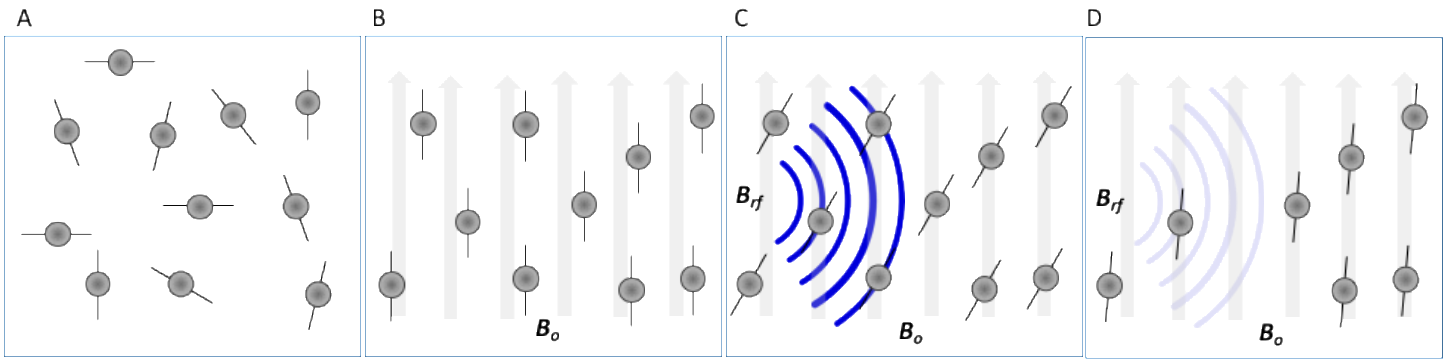

Figure 2.2: Schematic representation of proton behaviour in an MRI scanner

A) Hydrogen atoms, or protons, outside a scanner orientate in random directions;

B) once under the influence of the strong magnetic field (B_o) created by the scanner, the protons align with the direction of the magnetic field;

C) a radiofrequency pulse (B_{rf}) is applied perpendicular to B_o and the protons tilt and change their direction of alignment;

D) once the applied radiofrequency pulse fades, protons return to their equilibrium position, as in (B) and release energy in the form of their own radiofrequency signal- this is termed 'decay' and can be measured and quantified.

2.1.4.2 Generating a structural MR image

The MR signal obtained from an MRI scan does not immediately translate to a structural image. First, the signal must be expressed in an intermediate form, in k-space, before being reconstructed into an image via a Fourier Transform. The final image is given as a map of pixels in grey scale- each one representing a spatial location, and coloured to indicate the level of tissue contrast.

Tissues with high proton density will release a larger signal (brighter) than those with lower proton density (darker). Additionally, the longer a signal takes to decay, the lower the signal intensity will be and the darker the pixel will appear. We can externally manipulate tissue contrast by varying parameters such as the TE, TR and flip angle; to achieve a T1-weighted image, the TR must be short, in order to reduce the recovery time before the application of the next RF pulse, whereas T2-weighted images are dependent upon long TE times, given that TE controls the amount of T2 decay that can occur. MR sequences can be designed to give different weightings to either T1 or T2, depending on the needs of the researcher. T1-weighted imaging shows tissues with high fat content (e.g. white matter) as bright and compartments filled with water (e.g. CSF and ventricles) as dark, and is therefore used to demonstrate anatomical structures. In comparison, T2-weighted images show the opposite- water filled regions are bright and tissues with high fat are dark. This is especially useful for demonstrating pathology since most lesions are associated with an increase in water content, and are easily identifiable as bright spots.

The present study included an initial structural MRI scan, namely a 3D fast spoiled gradient-recalled echo (FSPGR) acquisition (number of slices = 124, slice thickness= 1.1mm, inversion time (TI) = 450 ms, repetition time (TR) = 7.084 ms, echo time (TE) = 2.84 ms,

field of view= 280 mm, flip angle= 20^{o}). This was then used to set the voxel locations for the spectroscopy scans.

2.1.4.3 Defining a region of interest

[1H]MRS data acquisition was performed in two regions of interest; a medial prefrontal cortical region, comprising the anterior cingulate cortex (primarily grey matter), and a subcortical region; in the left basal ganglia, comprising of the head of the caudate, the anterior putamen and the global pallidus internal capsule, plus white matter tracts (see Figure 2.3) using the following parameters:

Bilateral dorsomedial prefrontal cortex; 25 (left-right) x 30 (superior-inferior) x 40 (anterior-posterior) mm^3; TR = 2000 ms, TE = 68 ms.

Left basal ganglia; 35 x 25 x 30 mm^3; TR = 1800 ms, TE = 68 ms.

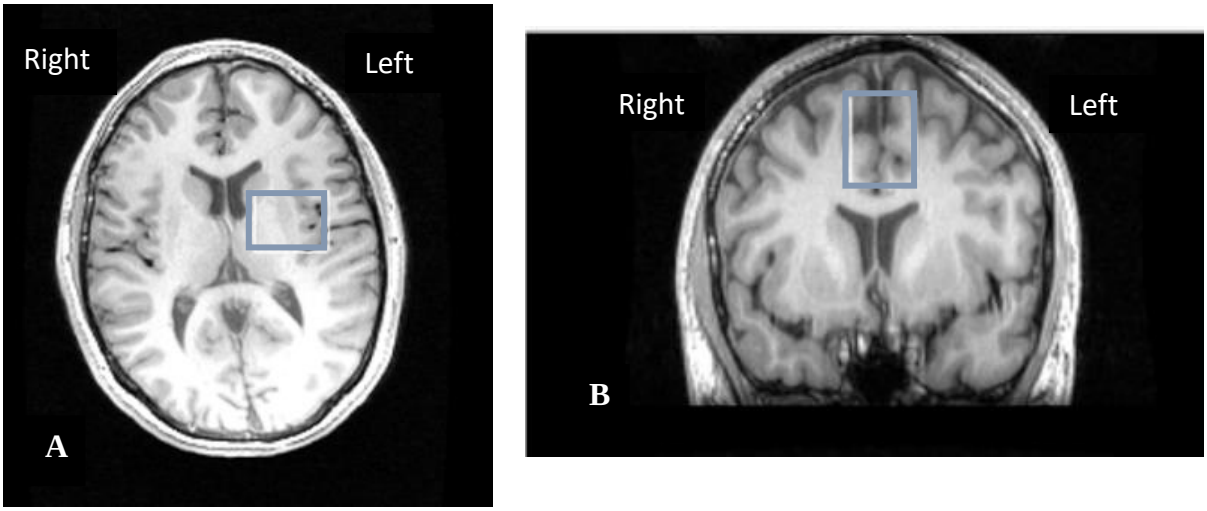

Figure 2.3: Examples of placement of [1H]MRS voxels

A. Example of subcortical voxel placement, including the head of the caudate, putamen and internal globus pallidus.
B. Example of anterior cingulate cortex voxel placement

2.1.4.4 Generating a metabolite spectrum

In MRS, instead of using the MR signal to construct images, the frequency information is used to identify chemical compounds. Specific molecules within a scanning region of interest can be identified by the way in which their protons behave in the applied magnetic field sequences of the scanner. Within a given field strength, protons in different molecules experience different levels of 'chemical shielding', whereby surrounding electron clouds affect the magnetic field experienced by the proton; i.e. if the electrons are close to the proton, there is a shielding effect and the proton 'experiences' a minimally smaller magnetic field. The extent to which the shift caused by shielding occurs, depends on the structure of the molecule and the position of the proton within the molecule- for this reason, it is known as **'chemical shift'**. As such, each molecule has a specific chemical shift, which can be used

to identify it. Much like with MRI structural data, a Fourier Transform is applied to the MRS data output to separate the signal into individual frequencies, which are expressed in the form of a magnetic resonance spectrum. The spectrum is a plot of signal intensity on the y-axis (roughly proportional to metabolite concentration), versus chemical shift on the x-axis. Chemical shift is reported in magnetic field-independent units; parts per million (ppm) of the proton frequency, so the output is the same regardless of the magnetic strength of the scanner. The position of a peak on the x-axis measures the chemical shift relative to a reference (by convention, the chemical shift of tetramethylsilane (TMS) protons is defined as 0 ppm) and can be used to identify chemicals (see Figure 2.4 and Table 2.2).

In principle, the area under each peak is proportional to the number of protons contributing to the metabolite of interest, however this is not an absolute concentration, but rather an indication of the level of metabolite, which can be compared between time points or between groups (but not interpreted in terms of physical concentration directly).

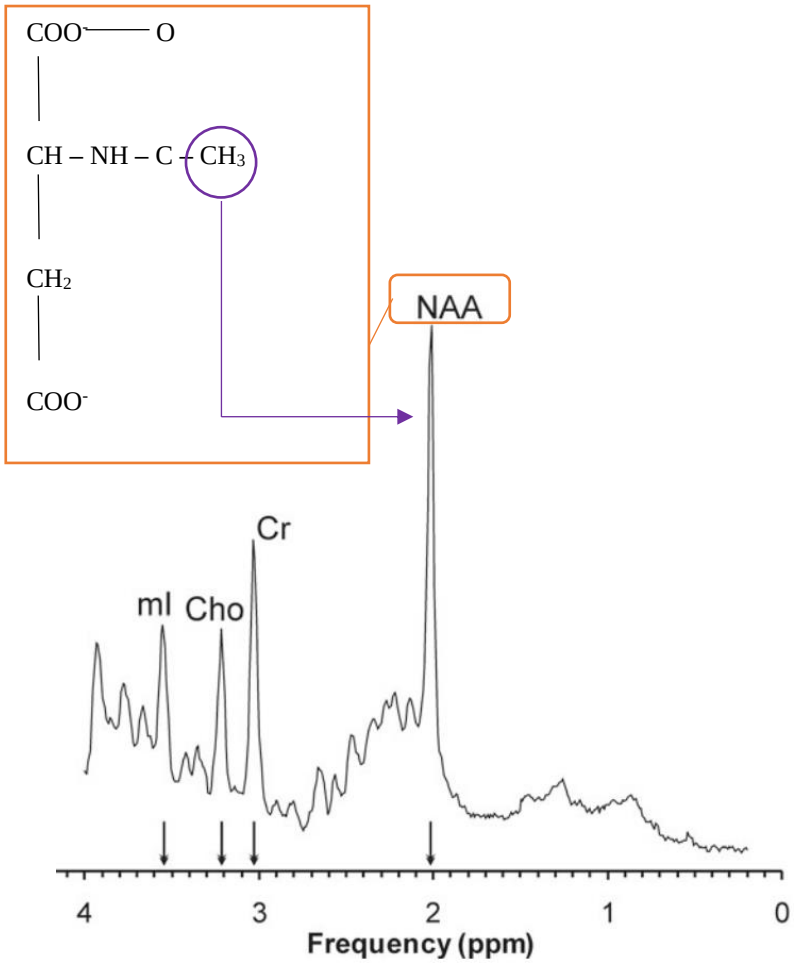

Figure 2.4: An example [1H]MRS spectrum

A spectrum is a frequency analysis (Fourier Transform) of the signal that is detected during an MRS study. The height of the peak is equivalent to the strength of the signal and the position on the x-axis is determined by the degree of chemical shift, which is specific to each chemical and can be used to identify it. N-acetly-aspartate (NAA) can be identified by the large peak at 2 ppm, which is due to the combined J-coupling effect of the three protons in its CH_3 group. If shown, the water peak would be at 4.7 ppm. The water peak is suppressed in most MRS spectra as it would be dramatically larger than the metabolic peaks. *Figure adapted from Blüml and Panigrahy, 2013.*

Chemical shift (ppm)	Metabolite	Properties
0	Tetramethylsilane (TMS)	Reference
2.0	N-Acetyl-Aspartate (NAA)	Neuronal marker
2.2 - 2.4	Glutamine/GABA	Neurotransmitters
3.0	Creatine (Cr)	Energy metabolism
3.2	Choline (Cho)	Cell membrane marker
3.5	Myoinositol (mI)	Glial cell marker
4.7	Water	-

Table 2.2: Observable metabolites using [1H]MRS

Various metabolites and neuronal markers can be identified by their degree of chemical shift, measured in parts per million (ppm). Note that some metabolites have multiple peaks, but the ones most useful for quantification are listed above.

In addition to chemical shift, the spectrum is also modulated by **J-coupling**. J-coupling is the result of the interaction between neighbouring protons; uncoupled protons yield single peaks, whereas coupled protons give peaks split into two or three. The resulting distinct peak pattern and size tells us about bond distance and bond angles and helps to identify molecules. For example, the three protons of the -CH_3 group of NAA combine to create one large peak at 2 ppm, which is characteristic of NAA (Figure 2.4). J-coupling modulates signal intensity depending on the sequence type and acquisition parameters of the scan. The most important parameter is the **Echo delay Time** (TE) (time between the applied RF pulse and signal readout). During this time, the signal from each metabolite peak relaxes with its own characteristic **T2-relaxation time** (a measure of signal decay) and the signal amplitude of J-coupled proton is modulated. Long echo times (TE ≈ 135 ms) simplify spectra by reducing

the number of detectable peaks, and are therefore mostly used in clinical practise where clear peak identification is needed. By contrast, short echo times (TE< 35 ms) allows the detection of an increased number of metabolites and give a better signal to noise ratio than long TE. One common pulse sequence is Point RESolved Spectroscopy (PRESS), a 90^{o} - 180^{o} - 180^{o} sequence of RF pulses, which gives better visualisation of metabolites with longer relaxation times. Whilst this sequence captures glutamate clearly, GABA has proven difficult to reliably measure, mainly due to the large overlap between GABA peaks (at 3.0 ppm, 2.3 ppm and 1.9 ppm) and those of other metabolites which are present in much higher concentrations. GABA is found in the human brain at around 1mM, significantly lower than most other metabolites, and 40,000 times lower than water (Puts & Edden, 2012).

MEshcher-GArwood Point RESolved Spectroscopy (MEGAPRESS) is, at this stage, the standard technique for obtaining GABA measurements in MRS, and can be incorporated into the basic PRESS sequence. Unlike conventional PRESS, MEGA-PRESS can separate the GABA signal from that of other metabolites, by taking advantage of known J-couplings within the GABA molecule. Using a 'difference-edited technique', MEGA-PRESS collects two datasets which differ in the way they affect GABA spin. In one set, an editing pulse is applied at 1.9 ppm which selectively refocuses the GABA signal at 3.0 ppm- this is referred to as 'ON'. In the second, control dataset, the editing pulse is either not applied, or applied at a different frequency that does not affect GABA signals or any other metabolite of interest- this is referred to as 'OFF'. During processing of the data, the ON signal is subtracted from the general OFF signal, to leave only the data affected by the GABA-specific editing pulse, i.e. GABA (Edden & Barker, 2007; Mescher et al., 1998). This process is referred to as J-difference editing.

2.1.4.5 Spectral data processing

In this study, MRS spectra were pre-processed using SAGE (Spectroscopy Analysis, GE Healthcare Technologies, WI, USA) spectral analysis software (SAGE 2007, GE Healthcare Technologies, WI, USA) to perform the edit ON – edit OFF subtraction, to extract the subtraction (difference) spectrum, the unedited spectrum (equivalent to a conventional PRESS spectrum) and the unsuppressed water spectrum. These spectra were further processed and quantified using JMRUI (Java based Magnetic Resonance User Interface) version 4 software (Naressi et al., 2001) and each participant's raw data was checked for quality to ensure adequate signal to noise ratio and absence of artefacts. If required and appropriate, artefacts were removed using JMRUI peak fitting and removal algorithm to restore data integrity. Metabolite concentrations were estimated using the AMARES algorithm (Advanced Method for Accurate, Robust and Efficient Spectral fitting of noisy MRI data). In the subtraction spectrum; GABA (+ macromolecule) at 3.0 ppm, Glx (Glutamate + Glutamine; as the measure of glutamate) as two peaks at 3.8 and 3.75 ppm and N-acetylaspartate (NAA) at 2.01 ppm were estimated. In the unedited spectrum; Choline at 3.19 ppm, Creatine at 2.99 ppm and, NAA at 2.01 ppm were estimated. To correct for inter-subject variations in water levels, each metabolite was multiplied by an individual Water Scaling Constant (WSC);

$$Water\ Scaling\ Constant\ (WSC) = \frac{1}{Water\ Amplitude}$$

$$Metabolite_{Water\ corrected} = Metabolite_{Raw\ value} \times WSC$$

Additionally, partial volume effects (group variation in proportions of grey matter (GM), white matter (WM) and cerebrospinal fluid (CSF) in the [1H]MRS voxels) are a potential confound in spectroscopy. This is of particular relevance to the present study, as previous literature has indicated volumetric differences between ASD and control participants (Haznedar et al., 2006). To assess voxel composition, the initial structural MRI scan was segmented into GM, WM and CSF using SPM2 (UCL). The position of the voxel was then registered to the corresponding segmented structural scan and the GM, WM and CSF content of this region was calculated using in-house software. Assuming CSF contains negligible amounts of the metabolites of interest, all data was corrected for varying levels of CSF in the voxel as follows:

$$CSF\ Correction\ Factor\ = \frac{1}{(1 - CSF)}$$

$$Metabolite_{\ CSF\ corrected}\ =\ Metabolite_{\ Water\ corrected}\ \times\ CSF\ correction\ Factor$$

2.1.4.6 Limitations of [1H]MRS

Though sequences such as MEGAPRESS have greatly advanced our ability to measure the GABA signal, there remain some problems in the reliability of its detection. When MEGAPRESS is implemented at 3T using the standard acquisition parameters of a 68 ms echo time (TE), as in the present study, there is potential for contamination of the GABA peak with co-edited macromolecular (MM) signals (Edden et al., 2012; Henry et al., 2001; Rothman et al., 1993). This is because the ON pulse applied at 1.9 ppm, also affects the MM signal at 3.0 ppm, the same frequency as the GABA signal. As a result, the final edited GABA measure is contaminated with MM and potentially as much as 45% of the total GABA signal output is known to be due to MM, rather than GABA alone (Mullins et al.,

2014). Modifications to the MEGAPRESS sequence have been devised that reduce the MM signal (Harris et al., 2015; Henry et al., 2001), though this often results in also diminishing the GABA signal, which is small to begin with. The most common approach therefore, is to acknowledge the presence of MM within the GABA signal and report it as such - it is often referred to as GABA+MM or GABA+. Whilst this allows for comparison across studies, there is always the query over whether results are driven by GABA or MM.

Likewise, depending upon the magnetic field strength of the scanner used, it is not always possible to differentiate between glutamate and its metabolite glutamine, due to the overlap of their resonant peaks. As a result, the combined signal is commonly reported as Glx (Ramadan et al., 2013).

The need to supress the large water signal in order to detect metabolites also poses a problem, as insufficient and variable methods of suppression may result in variation of metabolite levels across subjects and studies.

Another cause for inter-study variation is the way in which we choose to express metabolite levels. It is common in MRS literature for metabolite concentrations to be expressed as a ratio, relative to a metabolite which is deemed to be more stable- most often this is creatine. This is problematic in atypical brains however; creatine levels have been shown to be disrupted in ASD, with reductions in the thalamus, insula, corpus callosum (Friedman et al., 2003) and head of the caudate (Levitt et al., 2003); and increased levels in amygdala-hippocampal regions (Page et al., 2006) and the medial prefrontal lobe (Murphy et al., 2002). This widespread variability in creatine findings has reduced its use as an internal reference

point (Rackayova et al., 2017), and therefore the present study used absolute measures of metabolites only to avoid such confounds.

Finally, and perhaps most importantly, [1H]MRS, specifically when applying MEGAPRESS techniques, is inherently limited by the size of the voxel and the lack of specificity and spatial resolution within the voxel. [1H]MRS is essentially a crude tool which restricts us to bulk measurements of metabolites- i.e. a specific region of interest's capacity to *hold* metabolites- we cannot say whether these metabolites are active or metabolic, or specify whether they originate in neurons or in extracellular space. This macroscopic approach may provide insight into gross regional metabolite changes, but does not allow for circuit level analysis.

2.1.5 Resting State Functional Magnetic Resonance Imaging

Unlike Magnetic Resonance Imaging, which maps brain structure, or Magnetic Resonance Spectroscopy, which measures metabolite concentration, Functional Magnetic Resonance Imaging (fMRI) measures and maps brain activity.

2.1.5.1 Concept

fMRI was initially based on the premise that whilst performing a task, or action, specific areas of the brain are engaged; for example, the motor cortex is active during movement. It is now known that certain brain networks are also active 'at rest', i.e. even when the brain is not engaged in a specific task, certain regions which are known to function together are active in synchrony (Biswal et al., 1995). These so-called resting state networks can be examined to investigate the brain's functional organisation and to examine whether it is altered in psychiatric disorders.

As in the construction of MR images (described in detail in the previous section), acquisition of fMRI data relies on the magnetisation of hydrogen atoms, which are manipulated with various applied radiofrequency pulses, and emit a signal which is measured. When neural activity in any particular area of the brain increases, this is matched by a slight increase of around 1% in the detected MR signal. Rather than a direct correlation between neural activity and MR signal output, the change in signal is an indirect effect caused by the change in regional blood flow which follows neural activity.

This is dependent on two factors; firstly, oxygenated and oxygen-depleted blood have slightly different magnetic properties due to the bonding of haemoglobin. When oxygenated, haemoglobin is diamagnetic (repelled by a magnetic field), but paramagnetic (attracted to a magnetic field) when deoxygenated. Deoxygenated blood therefore slightly distorts the magnetic field in its immediate vicinity, creating microscopic field inconsistencies, which lead to the shortening of the T2 relaxation time within the tissue voxel- this is termed *static dephasing*. Therefore, variations in tissue oxygenation as a result of altered blood supply caused by regional changes in brain activity can be mapped by T2*-weighted MRI (Holdsworth & Bammer, 2008).

The second effect is the somewhat paradoxical fact that neural activity prompts an increase in blood flow in surplus of that needed to satisfy the increase in oxygen metabolism, and thus blood actually becomes more oxygenated shortly after neural activity increases. This *blood oxygenation level dependent* (BOLD) effect is the basis for fMRI (Ogawa et al., 1990). At rest, the brain remains highly active, and these patterns of activity can reveal particular networks of areas which work together, so called *resting state networks* (RSNs) (Biswal et al., 1995). Resting state networks reflect the functional connectivity between different brain

regions, irrespective of their anatomical or structural connectivity. The strength of these RSNs can be affected by disease and can therefore be used to understand network activity in psychiatric disorders (Garrity et al., 2007; Greicius, 2008; van de Ven et al., 2004).

2.1.5.2 Resting state fMRI BOLD data acquisition

The most common image sequence for fMRI acquisition is *echo planar* imaging (EPI), in which data is captured during a succession of rapid field gradient reversals following RF excitation of protons. As in MR imaging, the contrast that is achieved is determined by several acquisition parameters, such as the TE, TR and flip angle. The speed at which images are acquired means that a whole brain may be imaged in as little as a few seconds, and the imaging is less sensitive to motion (i.e. head movement) than conventional MR. Furthermore, this speed also allows for the capturing of rapidly changing physiological processes such as blood flow and kinetic energy (DeLaPaz, 1994).

In the present study (Chapter 3), resting state fMRI acquisition parameters were as follows: an EPI sequence, TR = 2 seconds, TE = 30 ms, 256 volumes. Slice thickness = 3 mm, number of slices = 38, slice spacing = 0.3 mm. Each slice comprised of 64 x 64 voxels with a field of view of 240 mm, for a final voxel size of 3.75 mm x 3.75 mm x 3.3 mm. Pulse and respiration parameters were also acquired during the fMRI scan, for the purposes of correcting for physiological artefacts (or *noise*) in the fMRI dataset, using a photoplethysmogram pulse oximeter and a chest band, respectively.

2.1.5.3 Resting state fMRI BOLD data processing

Once data is acquired, the observed changes in the BOLD signal are reconstructed into a 4-dimensional time series which reflects the changes in neuronal activity. The data undergo multiple pre-processing steps, including;

Slice-time correction- as multiple 'slices' of the brain are being scanned in quick succession, the BOLD signal is sampled at different time points through different layers in the brain. Ideally, we want data from the whole brain at the same time point- correcting for slice timing allows us to see whole sections as if they were sampled at the same time, to prevent errors arising from a region spanning multiple slices. For each voxel, slice timing correction examines the time course, and shifts it by a small amount to interpolate between the points sampled to provide the time course that would have been observed had every slice within a volume been sampled at the same time.

Motion correction- due to the rapid sampling of multiple slices in a short space of time, errors can arise from movement, however small, which may cause the brain to be in the wrong location for some images, or cause loss of data entirely if the movement is so gross the head moves out of the selected scanning volume. Motion correction is particularly important in resting state fMRI, when global brain activity is taken into account, and especially when comparing control and patient groups, who may significantly differ in their ability to remain still whilst in the scanner for extended periods of time. Effects of motion can be removed by correcting for motion-related components (as regressors) within the general linear model analysis, and further corrected when comparing across subjects by also normalising to a standard brain space, or co-registration. Brain normalisation is initiated by segmenting the brain into its component GM, WM and CSF tissue types and overlaying the structural and

functional images, thereby linking the functional data to the anatomical. Scans are then spatially normalised, establishing a one-to-one correspondence between the brains of different participants with a common template brain. This allows us to both determine what happens generally across individuals, and also identify any differences between groups, within a particular study and across other studies. Linear registration using a program such as SPM (UCL) accounts for major differences in head shape and positioning (though positioning should be somewhat accounted for by initial head placement in the scanner by radiographers), before nonlinear registration *warps* the brain images and accounts for smaller differences in anatomy (Friston, Ashburner, & Wellcome, 1997).

Spatial smoothing is performed to average individual data points with their neighbours and thus lower the signal to noise ratio, increase sensitivity and increase the validity of statistical tests by normalising the error distribution of each point. However, this technique does reduce spatial accuracy of the data and may result in misrepresentation of where specifically activation is taking place (Mikl et al., 2008).

Lastly, **high-pass filtering** is performed to 'clean' the final data signal and separate out any remaining noise. If you know the signal frequency you should be obtaining, you can remove any frequencies too low to be relevant, i.e. remove low frequencies and *pass through high frequencies.*

The main approach to resting state fMRI data, and the one used in the present study, concerns connections between regions (functional connectivity). A commonly used method for analysing this is a hypothesis-driven seed-based analysis. This approach uses an extracted BOLD time course from an *a priori* region of interest and examines the temporal correlation

between this signal and the time course from all other brain regions. In this way, a functional connectivity map of correlation between a chosen region and the rest of the brain can be created. This map allocates Z scores for each voxel, showing how well its time series correlates with the time series of the seed region. Two regions are said to be functionally connected if the time series of their activation are correlated (Biswal et al., 1995; Fox et al., 2005).

In the present study, fMRI data were processed using FSL 5.0.0. The following pre-processing steps were applied: motion correction using MCFLIRT; slice-timing correction using Fourier-space time-series phase-shifting; non-brain removal using BET; spatial smoothing using a Gaussian kernel of FWHM 5 mm; grand-mean intensity normalisation of the entire 4D dataset by a single multiplicative factor; and highpass temporal filtering (Gaussian-weighted least-squares straight line fitting, with sigma = 50.0 s).

Manual inspection and removal of artefactual connectivity components was then carried out using hypothesis-free Probabilistic Independent Component Analysis as implemented in MELODIC (Multivariate Exploratory Linear Decomposition into Independent Components) Version 3.10, part of FSL (Analysis group, FMRIB, Oxford; Jenkinson, Beckmann, Behrens, Woolrich, & Smith, 2012). The decisions as to whether to exclude each component from a given fMRI scan were made by a researcher blind to group and to drug status.

2.1.5.4 Limitations of resting state fMRI

A much-criticised limitation of fMRI is that it does not measure neuronal function directly, rather it is a measure of secondary physiological correlates of neural activity- it is therefore not truly quantitative and there is always a risk that group or individual differences are

physiological rather than neurological. Additionally, caution must be exercised in processing fMRI data, hence the need for the extended measures described above. Further care must be taken when interpreting the data; in many pathologic conditions, cerebral blood volume and cerebral blood flow may be perturbed, and so the BOLD effect in these regions might present differently than in healthy regions despite otherwise normal underlying neuronal activity.

Additionally, whilst spatial resolution is highly accurate, temporal resolution of fMRI is inherently limited by the slow speed of the BOLD response, and therefore sub-millisecond neural activity is not fully captured (Glover, 2011).

2.2 Measuring E-I in rodents

The following pre-clinical protocols (Figure 2.5) were designed to complement the human study described above (section 2.1.1). Two separate studies were undertaken; firstly, an initial investigation into the pharmacokinetic profile of riluzole at the selected experimental dose was performed in wild type rats only (detailed in Chapter 5). Next, an *in vivo* microdialysis study determined the effect of riluzole on E-I efflux of extracellular neurotransmitters and metabolites in wild type and *Neurexin 1 alpha* (α) knock out (*Nrxn1α*$^{-/-}$) rats (detailed in Chapter 6). Brain tissue collected from this study was also analysed to evaluate the effect of riluzole on bulk tissue levels of E-I neurotransmitters (Chapter 5).

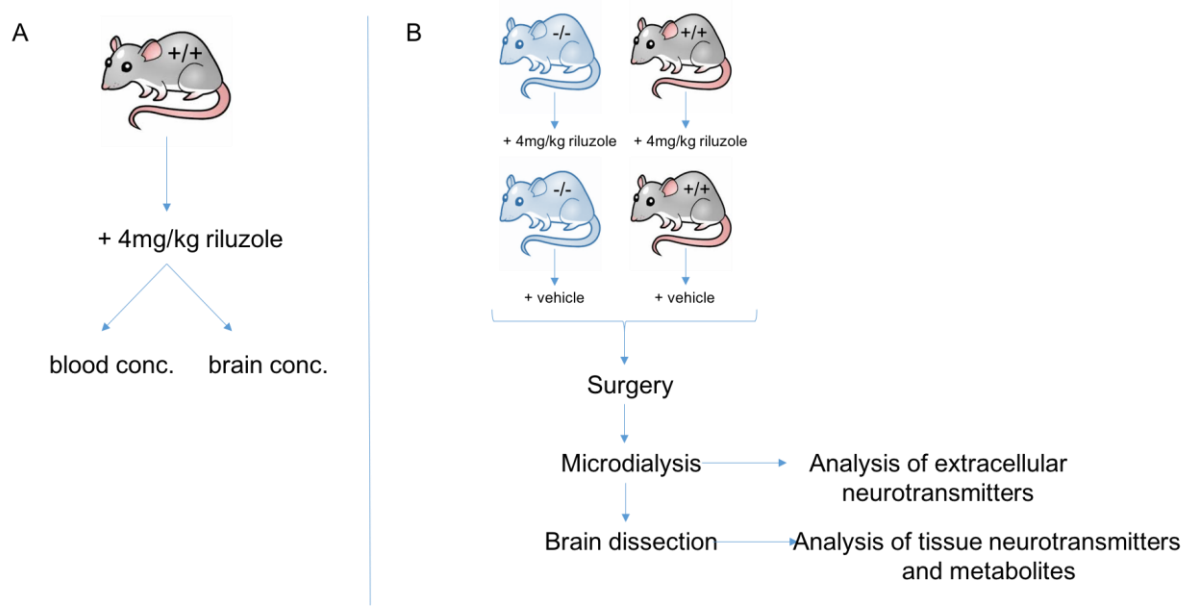

Figure 2.5: Representation of pre-clinical study designs

A. Pharmacokinetic study of blood and brain tissue concentrations of riluzole after a single, oral 4 mg/kg dose of riluzole in wild type (+/+) adult Wistar rats.

B. *In vivo* microdialysis and *ex vivo* tissue analysis of wild type (+/+) and *Nrxn1α*$^{-/-}$ (-/-) rats after either 4 mg/kg oral dose of riluzole or equivalent vehicle.

2.2.1 Animals

Adult male *Nrxn1α* $^{-/-}$ rats and littermate controls were sourced from SAGE labs (now Horizon Discovery, USA) and housed at Eli Lilly in standard conditions; 07:00 to 19:00 light phase, constant temperature (21°C) and humidity, *ad libitum* food and water, and environmental enrichment.

Nrxn1α $^{-/-}$ rats contain a biallelic deletion, specifically, a 16 base pair (ACCACTCTCTACATCG) frameshift deletion in exon 1 of the Nrxn1 gene (see Figure 2.6), which was confirmed using sequencing techniques by the manufacturer.

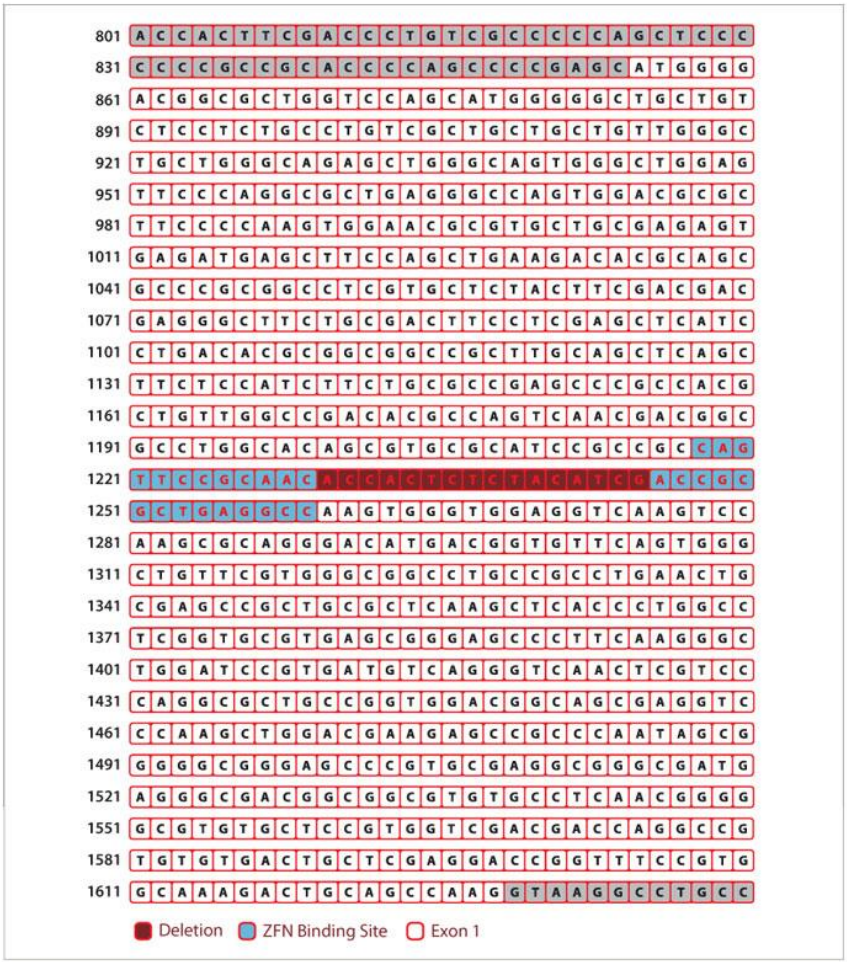

Figure 2.6: Location of the 16 base pair deletion in the Nrxn1 gene

Nrxn1α $^{-/-}$ rats contain a deletion (red) in the Nrxn1 gene in exon 1 (white)

2.2.2 Drug and vehicle

Riluzole was obtained from SIGMA (Sigma, UK) and formulated in 1% HEC (hydroxyethyl cellulose; containing 0.25% Tween 80 and 0.05% antifoam) at 4 mg/kg (2 ml/kg).
Vehicle was 1% HEC.

2.2.2.1 Dose calculation

50 mg oral dose of riluzole was administered in the human imaging study. To achieve an equivalent dose in the pre-clinical studies, a dose translation from human to rodent was calculated using body surface area as a guide (Reagan-Shaw et al., 2008):

$$\textbf{Human equivalent dose (mg/kg)} = \textbf{Animal dose (mg/kg)} \times \frac{\textbf{Animal Km}}{\textbf{Human Km}}$$

where *Km* is the body weight to surface area ratio (human *Km* = 37; rat *Km* = 6) as defined by FDA guidelines (USA Food and Drug Administration, 2002).

50 mg human dose is equivalent to 0.625 mg/kg for a standard 80 kg male or female, therefore using the above formula, where the human *Km* = 37 and rat *Km* = 6, the equivalent rat dose is 3.85 mg/kg.

A 4 mg/kg dose in adult rats is consistent with previous dosing regimens in neuropathic pain experiments (Chew et al., 2014) and experiments investigating glutamate transporter activity (Sung et al., 2003).

2.2.3 Pharmacokinetics of riluzole

The following study aimed to determine riluzole brain and plasma concentration over a time course of 4 hours in adult male Wistar rats.

12 male Wistar rats were dosed orally (p.o.) with 4 mg/kg riluzole. Animals were culled 0.5, 1, 2 or 4 hours after drug administration by a non-Schedule 1 procedure by exposure to a rising concentration of CO_2 delivered at 10 L/min for 2.5 min, n=3/group. Blood was collected by cardiac puncture into Li-heparin tubes and placed on a rotating table. Following removal of blood, the brains were removed and the forebrain cut at the level of the optic chiasm (using a 2 mm brain dissection block), weighed and then frozen on dry ice. Plasma was separated by centrifugation at 3,000 rpm for 7 min (Centaur 2; MSE) and frozen on dry ice. Brain and plasma samples were stored at -80°C pending analysis by Liquid Chromatography and Mass Spectroscopy (LC-MS/MS; see section 2.2.6 for further details).

2.2.4 Effect of riluzole on E-I responsivity; *in vivo* microdialysis

The following study aimed to determine the effect of riluzole on GABA and glutamate efflux in the medial prefrontal cortex (mPFC) and caudate putamen (CPu) of 16 wild type rats and 15 *Nrxn1*$\alpha^{-/-}$ rats.

2.2.4.1 Surgical implantation of microdialysis probes

Rats were anaesthetised with Isoflurane® (2.5% in O_2 at 1 L/min) and administered the analgesic Buprenorphine® (0.075 ml subcutaneously (s.c.)), before being positioned on the

stereotaxic frame. Surgical anaesthesia was then maintained at 2-2.5% Isoflurane® in O_2 at 0.5 L/min, and body temperature was maintained at 36-37˚C using a heated pad.

MAB 4.7.4 and MAB 4.7.3 microdialysis probes (cuprophan membrane; 6 kDa cut-off; MicroBiotech AG, Sweden) were implanted stereotaxically into the medial prefrontal cortex and caudate putamen, respectively, of each rat whilst being perfused with artificial cerebrospinal fluid at a flow rate of 1.5 µl/min (aCSF; containing NaCl 141 mM, KCl 5 mM, $MgCl_2$ 0.8 mM and $CaCl_2$ 1.5 mM) using the following coordinates:

From bregma and dura surface, with nose bar set to -3.3 mm:

Medial prefrontal cortex, 4 mm probe (MAB 4.7.4);

Anterior +3.0 mm

Lateral ±1.5 mm

Vertical (from dura) -5.0 mm

Angle = 12 degrees

Caudate putamen, 3 mm probe (MAB 4.7.3);

Anterior +0.3 mm

Lateral -3.0 mm

Vertical (from dura) -6.0 mm

Probes were fixed in place with two scull screws and dental cement. Animals were allowed to recover in a thermacage (28-30˚C) before being returned to their individual home cage.

2.2.4.2 *In vivo* microdialysis

2.2.4.2.1 Concept

Microdialysis allows for the sampling, and subsequent quantification, of neurotransmitters from the interstitial space in discrete brain regions. The principle element which enables this sampling is the microdialysis probe, which is used to capture molecules from the extracellular space. Once the probe is inserted into the brain tissue, constant perfusion of a solution (in this case, aCSF) begins, and substances on the outside surface of the dialysis membrane diffuse through the membrane into the probe along their concentration gradient (see Figure 2.7). The perfusate is infused slowly and continuously through the length of the dialysis probe into the outflow tubing where it can be collected for quantification. It is presumed that the amount of neurotransmitter measured in the resulting sample, or dialysate, will depend upon the level of synaptic activity and therefore neurotransmitter efflux in that brain region (see Chefer et al. 2009 for a full review). Importantly for the present study, both GABA and glutamate efflux can be reliably captured using this methodology (Bourdelais & Kalivas, 1992; Dietze & Kuschinsky, 1992).

2.2.4.2.2 Protocol

The day after probe implantation, 4 animals per experimental day were connected to the microdialysis rig. This consisted of a liquid swivel suspended on a counterbalanced arm, connected to an infusion pump filled with aCSF. Prior to attaching the animals to the rig, a single sample was collected over 6 minutes at a flow rate of 5 µl/min to measure aCSF alone and ensure the rig was functional. The sample was also analysed along with all other samples in order to identify potential contaminants.

The rats were then attached and flow rate reduced to 1.5 µl/min for a 90 minute pre-sample settling period. Dialysate samples were collected at 20 minute intervals thereafter for a total

of 15 samples. After six ‘baseline’ samples (120 min) were collected, animals were administered with either 4 mg/kg riluzole or vehicle (1% HEC) p.o. All samples were immediately frozen on dry-ice and stored at -80°C pending analysis by LC-MS/MS.

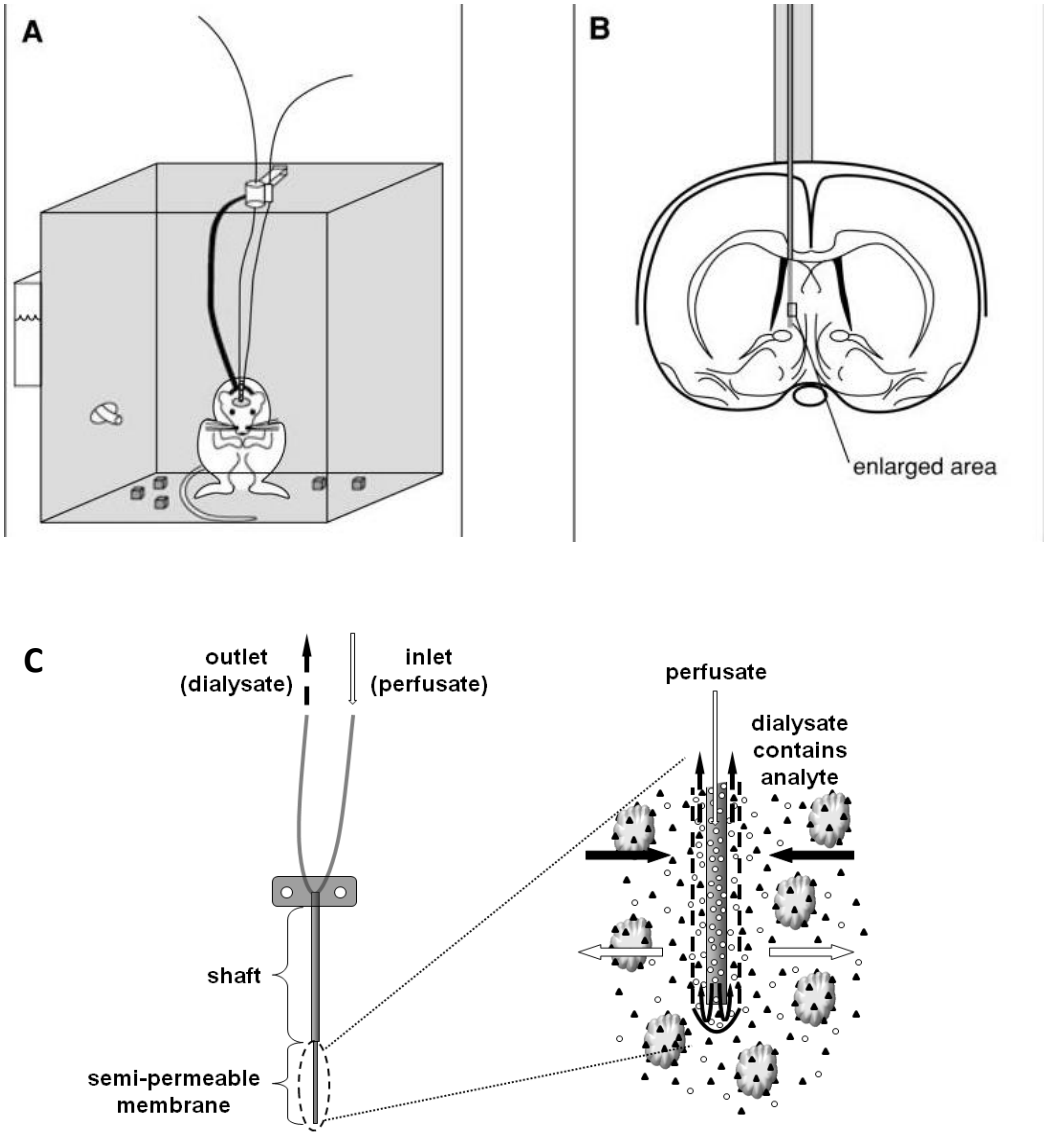

Figure 2.7: Schematic illustration of a microdialysis rig (A, B) and probe (C)

A. The microdialysis probe is surgically implanted into the rodent brain; the inlet is connected to an infusion pump, and the outlet attached to a sample tube to collect the dialysate
B. The probe is implanted into a specific brain region
C. Artificial CSF (perfusate) is perfused into the microdialysis probe via the inlet, and dialysate containing neurotransmitters of interest is collected via the outlet

Images adapted from Chefer et al. 2009.

2.2.4.3 Limitations of *in vivo* microdialysis

Microdialysis has a few key disadvantages which must be considered. Firstly, it has limited time resolution, particularly in this study, as samples are collected over a period of 20 minutes- therefore samples do not provide real time information regarding changes in the extracellular environment.

Secondly, microdialysis is an invasive technique and some tissue damage is likely to occur during probe implantation- at least 220 μm, and potentially as much as 1 mm, surrounding the probe has shown signs of trauma which affect neurotransmitter release in some studies (Borland et al., 2005). However, as all animals will undergo the same surgery, it is expected that this particular limitation will not preclude comparisons across groups.

Additionally, the efficiency or 'recovery' of the probe itself may be questioned. The recovery is defined as the percentage of metabolites measured (recovered) in the immediate vicinity of the probe, relative to the (estimated) amount of metabolite present in the wider space in which the probe sits. Several factors can affect recovery, including but not limited to; flow rate, length of the probe membrane (longer = more recovery), temperature and molecular weight/shape of the substance being recovered. An *in vitro* assay was therefore performed to estimate the recovery of the microdialysis probes used in the present study, in order to better estimate the local extracellular concentration of riluzole in each region (see Appendix 5).

Finally, the dimensions of the microdialysis probes indicate that samples cannot be taken directly from the synaptic cleft, rather they may detect compounds further from the site of release. A critical question therefore, is whether dialysate measures are reflective of true

synaptic release and/or uptake of the measured analyte, or whether they represent 'overflow' of neurotransmitters from non-synaptic sources, e.g. astrocytes and glia.

Action potential-controlled release of neurotransmitters requires the opening of Na^+ and Ca^{2+} channels, which may be experimentally blocked by tetrodotoxin (TTX) or excluding calcium from the perfusate, respectively. This approach has conclusively shown that dopamine, norepinephrine, serotonin, and acetylcholine present in brain dialysates is derived from action-potential controlled release (reviewed by Westerink 2000 and Westerink et al. 1988). However, basal dialysate levels of GABA and glutamate have shown no dependence on Na^+ and Ca^{2+} channels using this method and growing evidence suggests that synaptic GABA and glutamate are only involved in short distance signalling which may not reach the microdialysis probe (Del Arco, Segovia, Fuxe, & Mora, 2003). Hence, the extracellular concentrations of glutamate and GABA may therefore not provide a reliable indication of their synaptic exocytotic release. Many microdialysis studies show changes in extracellular GABA and glutamate following pharmacological modulation, yet the origin of these changes is unknown. One proposal is that changes to Glu-GABA levels could reflect changes in the activation of neuron-astrocyte networks, rather than absolute levels of neurotransmitters released from synaptic terminals (for review- see Del Arco et al. 2003).

2.2.5 Effect of riluzole on E-I responsivity; *ex vivo*

Following microdialysis, brain tissue was dissected and analysed to investigate bulk intracellular tissue measures of GABA and glutamate in the prefrontal cortex (PFC), caudate putamen (CPu) and thalamus (Th) of 16 wild type rats and 15 *Nrxn1α* $^{-/-}$ rats.

2.2.5.1 Protocol

Animals were culled by a non-Schedule 1 procedure by exposure to a rising concentration of CO_2 delivered at 10L/min for 2.5 min, prior to decapitation by guillotine. Brains were removed and the following regions dissected; PFC, CPu, Th and bilateral cerebellum (Cb). For consistency, dissections were performed using a brain dissection block according to the method outlined in section 2.2.5.2. Time from dose to dissection was recorded. Samples were weighed and then frozen on dry ice prior to storing at -80^{o}C pending analysis. Samples were dansylated and derivatized (section 2.2.6.1) before analysis by LC-MS/MS (section 2.2.6.2).

2.2.5.2 Brain dissection

Brains regions were dissected using a cutting block based on Heffner et al's method for rapid dissection of the rat brain (Heffner et al., 1980). Both the cutting block and single edged razor blades were kept on ice during dissection. The rat brain was rapidly removed and placed on its dorsal surface in the block (Figure 2.8).

Blade 1 (red line in Figure 2.8) was inserted tangential to the most posterior aspect of the olfactory tubercles. Two blades (orange line, Figure 2.8) were then inserted anterior to the first at intervals of 2 mm. Two further blades (green line, Figure 2.8) were inserted posterior to the first at intervals of 2 mm. All blades were removed from the block with the coronal brain slice attached and placed on a glass plate over crushed ice, and brain regions were then dissected bilaterally as shown in Figure 2.9.

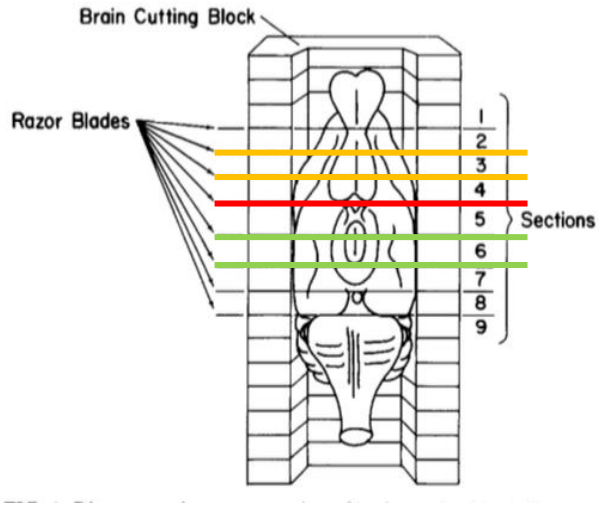

Figure 2.8: Diagrammatic representation of brain cutting block

Representation of brain orientation and razor placement (coloured lines) to obtain coronal sections. Figure adapted from Heffner, Hartman, and Seiden 1980.

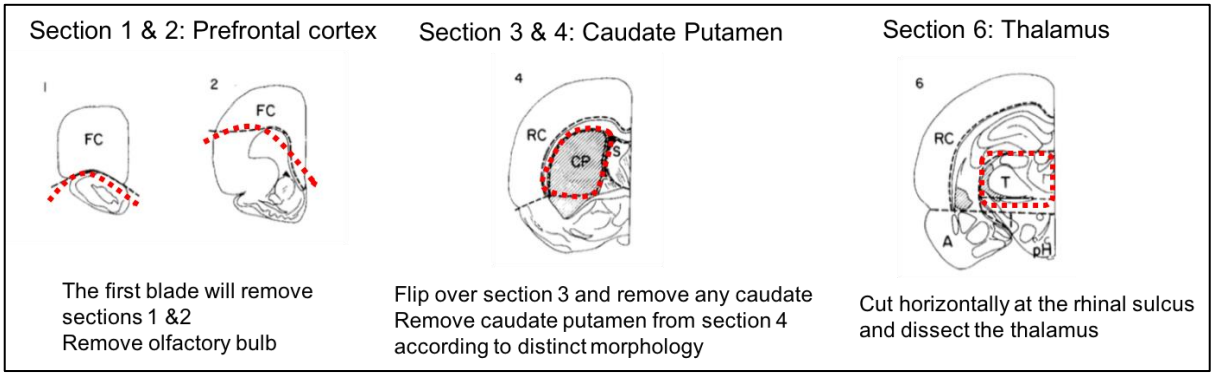

Figure 2.9: Dissection guide for coronal brain slices

Dissections were performed along the red dashed line to dissect individual brain regions. Section numbers refer to those in Figure 2.8.

2.2.6 Sample analysis

Brain tissue, plasma and microdialysis dialysate sample analysis was performed at Eli Lilly using in house protocols. Analyses were performed by SS and GC; a brief description of their methodology is outlined below.

2.2.6.1 Dansylation and derivatization

2.2.6.1.1 Brain tissue preparation

Brain tissue samples were homogenised prior to analysis. Briefly, samples were defrosted on ice and ice-cold acetonitrile (ACN) was added at a 90:10 ratio with H_2O. The tissue was then sonicated for 30 seconds using a Vibro sonic probe set at 50% amplitude. The resultant homogenous suspension was then allowed to stand in the fridge at 4^{o}C for 30 minutes to aid protein precipitation. The samples were then briefly vortexed before being spun at 20,000 x g for 15 minutes at 8^{o}C. 80 µl of supernatant was then carefully decanted off into a clean 2 ml screw top vial tube. Samples were then derivatized using a dansylation method.

2.2.6.1.2 Sample dansylation

High performance liquid chromatography (HPLC) is the method of choice for separation, identification and quantitative determination of different metabolites in a solution (see section 2.2.6.2). However, many metabolites of interest cannot be detected by HPLC as they do not possess the necessary properties. Dansylation is a chemical derivatization method which introduces these properties (e.g. increased molecular weight or hydrophobicity) into the sample to increase their sensitivity for detection (Tapuhi et al., 1981; Walker, 1994). Dansylation was performed in accordance with standard methods, which were adapted for the purposes of this experiment (Cai, Zhu, & Li, 2010). Briefly; to each brain, plasma and

dialysis sample, buffer (1M Bis-Tris, pH10), deuterated internal standards and dansyl chloride (0.1% w/v in acetone) were added and mixed.

Internal standards are necessary for controlling for differences in extraction, chromatography and detection between samples and are often an isotopically labelled version of the molecule to be quantified. In the present study, stable deuterium (D) labelled isotopes of GABA (D6-GABA) and glutamic acid (D5-Glutamic acid) were used.

Samples were vortexed and heated at 65^{o}C for 30 min, then evaporated to dryness under a stream of purified N_2 at 65^{o}C for 90 min. Samples were re-suspended in 50:50 (v/v) ACN:H_2O containing 10 mM ammonium formate and 0.06% formic acid. Samples were then centrifuged at 13,000 rpm for 10 min at ambient temperature and samples loaded into vials for chromatography. A portion of sample (10 µl) was also directly loaded onto the liquid chromatography – mass spectrometer (LC-MS/MS) (API 4000, Sciex, Canada) using a chilled auto-sampler (PAL HTC-xt, CTC Analytics, Switzerland).

2.2.6.2 Liquid Chromatography – Mass Spectroscopy (LC-MS/MS)

High Performance Liquid Chromatography (HPLC) is a form of column chromatography, in which a sample in liquid form is injected into the LC and the different chemical components are separated as they travel at different speeds through the column. The output of the LC column is then directed into a mass spectrometer (MS) where it is ionized (using electrospray ionization- ESI) and a mass spectrum is generated. Different metabolites can then be identified according to their position on the resultant mass spectrum. MS/MS refers to the combination of two mass analysers in one mass spectrometer. Hence using LC-MS/MS

allows for further increased sensitivity and therefore specificity. This is of particular importance for detecting metabolites with similar molecular weights.

In the present study, chromatographic separation of dansylated samples (including drug standards) was performed under a 13 min gradient (including washout and a re-equilibration step) using Shimadzu LC-20AD XR binary pumps (plus a CBM-20 controller) and a 2.6 μm Phenomenex Kinetex, XB-C18 HPLC column. Samples were prepared by 1:10 dilution in internal standard and calibration curves for each metabolite and for riluzole were run at the end of each batch of samples for quantification. Mobile phase A consisted of ACN:H_2O 5:95 (v/v), 2 mM ammonium formate and 0.06% formic acid, and mobile phase B; ACN:H_2O 95:5 (v/v), 2 mM ammonium formate and 0.06% formic acid.

LC-MS/MS was operated with both negative and positive ESI transition ion detection modes (negative for glutamate and glutamine; positive for GABA). A 120 ms dwell time was used on the majority of analytes (except for GABA at 25 ms) with MS conditions optimized individually by infusion of the dansylated derivative (see Table 2.3):

Transition ions measured (ESI negative ionization mode):

Glutamic acid was detected by monitoring the m/z 378.1 → 143.9 transition and its D5 analog internal standard at 384.2 → 234.0 (collision energy; -22 V, collision cell exit potential; -9 V).

Glutamine was detected by monitoring the m/z 378.1 → 234.0 transition (collision energy; -33 V, collision cell exit potential; -7 V).

Transition ions measured (ESI positive ionization mode):

GABA was detected by monitoring the m/z 343.0 → 170.2 transition and its D6 analog internal standard at 343.0 → 170.2 (collision energy; 25 V, collision cell exit potential; 12V).

Negative transition ion mode		
Glutamic acid Dwell 120 ms; DP -85; CE -22; CXP -9	m/z 379.1 → 143.9	Rt2.75 min
D5-Glutamic acid Dwell 120 ms; DP -90; CE -29; CXP -6	m/z 384.2 → 234.0	Rt2.75 min
Glutamine Dwell 120 ms; DP -95; CE -33; CXP -7	m/z 378.1 → 234.0	
Positive transition ion mode		
GABA Dwell 25 ms; DP 66; CE 25; CXP 12	m/z 337.0 → 170.2	Rt3.25 min
GABA –D6 Dwell 25 ms; DP 66; CE 26; CXP 14	m/z 343.0 → 170.2	Rt3.25 min

Table 2.3: LC-MS/MS detection conditions

Conditions for the detection of glutamate, glutamine and GABA using LC-MS/MS

Mass/charge number of ions (m/z): *The units of the horizontal axis of a mass spectrum. In mass analysis, electrons are taken from molecules to create charged ions. The number of electrons removed is the charge number.*

Dwell time: *The time in which the m/z ion signal is collected.*

Collision energy (CE): *To obtain structural information, analyte ions are fragmented by colliding them with neutral molecules in a process known as Collision Induced Dissociation (CID). Voltages are applied to the analyte ions to add energy to the collisions and create more fragmentation; the higher the CE, the more fragmentation.*

De-clustering potential (DP): *An applied voltage which helps prevent ions from clustering together*

Collision cell exit potential (CXP): *The CXP focuses and accelerates the ions towards the detector.*

2.2.7 Data analysis

2.2.7.1 Pharmacokinetics of riluzole

Riluzole in the brain and plasma were expressed as mean (± SEM) ng/g and ng/ml respectively. A brain:plasma ratio was calculated as brain concentration of riluzole/plasma concentration. Graphs were produced using GraphPad Prism Version 7 (GraphPad Software, USA).

2.2.7.2 Microdialysis and *ex vivo* samples

Microdialysis data were expressed as a percentage change from a pre-dosing control period. This was obtained by averaging the three samples collected prior to drug delivery (=100%) and expressing values as a percentage change from this value. The amount of analyte and drug in each microdialysate sample was recorded in ng/mL using their respective calibration curves. Statistical analyses were undertaken using 2-way ANOVA with Repeated Measures (SAS) using log transformed percentage data and comparing the response profiles post drug or vehicle administration. Riluzole levels were expressed as a molar concentration and compared using linear regression in GraphPad Prism.

Levels of neurotransmitter in *ex vivo* brain tissue were recorded in ng/g tissue wet weight. Statistical analyses were undertaken using 2 way- ANOVA (SAS) to test for main effect of drug, main effect of group and drug by group interactions. The SAS package allowed for missing values that were an occasional issue with collection of microdialysis samples. This was achieved through 'multiple imputation', whereby each missing value was replaced with a set of plausible values that represent the uncertainty about the right value to impute. The multiply imputed datasets are then analysed using standard methods, as would be used for complete datasets (SAS Institute, 2018). A probability value of $p<0.05$ was considered to be statistically significant for all analyses.

2.2.8 Tissue histology for verification of probe placement

In order to verify the placement of the microdialysis probes, a supplementary experiment was conducted to visually check the approximate probe location. Two adult male Wistar rats (Charles River, UK), of a similar age and kept in the same conditions as the experimental cohort, were used as subjects. Rats were anaesthetized with Isoflurane® (2.5% in O_2 at 1 L/minute) and administered the analgesic Buprenorphine® (0.075 ml subcutaneously) before being positioned on the stereotaxic frame. Surgical anaesthesia was then maintained at 2-2.5% Isoflurane® in O_2 at 0.5 L/min, and body temperature was maintained at 36-37◦C using a heated pad. In place of a microdialysis probe, a needle of similar proportions was implanted stereotaxically into the medial prefrontal cortex and caudate putamen, at co-ordinates outlined in section 2.2.4.1. A small amount of Toluidine Blue dye (1 µl) was injected into the tract using a Hamilton microsyringe.

Animals were culled immediately by a non-Schedule 1 procedure of decapitation by guillotine, whilst under anaesthetic sedation. Brains were removed and stored in 4% Formalin at room temperature. Formalin-fixed brains were 'snap' frozen in a beaker of isopentane cooled in a cardice (CO_2) bath prior to cryo-sectionning. The cerebellum was cut with a razor to give a flat surface, and the brain was mounted onto the (pre-cooled) specimen disc with an OCT mounting medium, Shandon™ Cryochrome embedding resin (Thermo Scientific™, UK).

Sections were performed, anterior to posterior, on a Leica CM1900 Cryostat (Leica Microsystems, GmbH), with the tissue temperature maintained at -18^{o}C. 30 µm thick sections were cut and 'lifted' onto room temperature ColorFrost Plus™ microscope slides (Thermo Scientific, UK). They were air-dried and scanned unstained on a Aperio AT Scanscope (Leica Biosystems).

Images were acquired using the Aperio ScanScope AT slide scanner which digitizes whole/part sections from 3x1" glass files (proprietory .tif style) and stores files to the Lilly supported server; YE02aperioprd01. This is maintained and interfaced through Aperio Spectrum Digital Image Library (eSlide Manager Version 12.2.1.5006). The images were viewed using the Aperio Software application, ImageScope.

Probe placement:

The following mPFC co-ordinates were chosen for the microdialysis study to best replicate and map to the region of interest selected in the human MRS study: bregma +3.0 mm, lateral ±1.5 mm, vertical (from dura) -5.0 mm, angle: 12 degrees in bregma plane. Though experimental co-ordinates were +3.0 mm from bregma, Figure 12 in Paxinos and Watson's stereotaxic rat brain atlas was used for comparison (+2.76 mm from bregma) to best match the anatomy depicted in the atlas (Paxinos & Watson, 2009).

The following CPu co-ordinates were chosen to best replicate and map to the region of interest in the human MRS study, the basal ganglia: bregma +0.3 mm, lateral ±3.0 mm, vertical (from dura) -6.0 mm. Though experimental co-ordinates are + 0.3 mm from bregma, Figure 31 in Paxinos and Watson's stereotaxic rat brain atlas was used for comparison (+ 0.24 mm from bregma) to best match the anatomy depicted in the atlas. Using these co-ordinates, I visualized the ideal probe placement using the Paxinos and Watson brain atlas (Paxinos & Watson, 2009), and compared this image with the actual placement observed. See Figure 2.10 and 2.11 for prefrontal cortex and caudate putamen placements, respectively.

The staining and visible probe tract in both brain regions confirmed the microdialysis probes had most likely collected samples from the regions of interest.

A

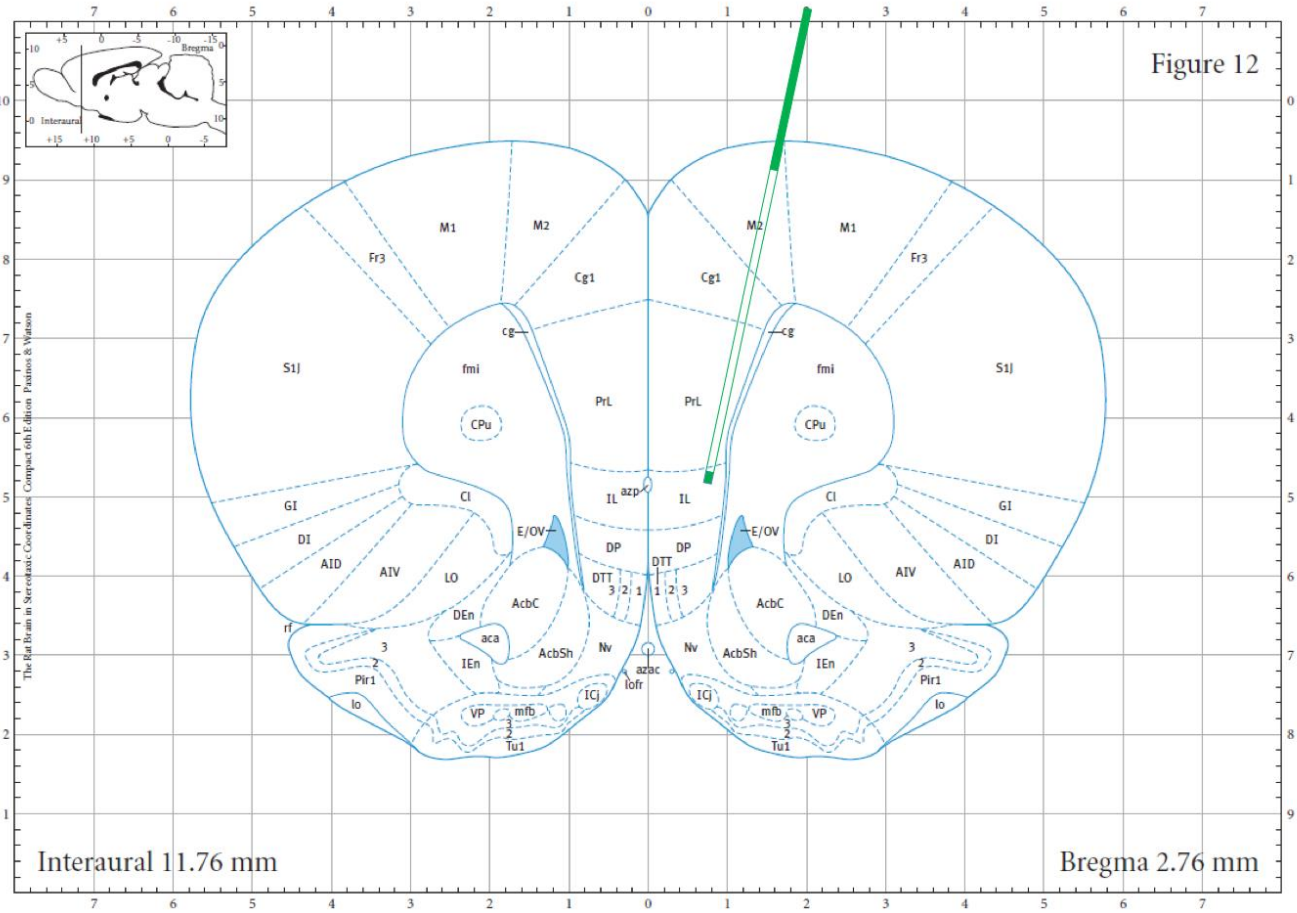
Figure 12
Interaural 11.76 mm
Bregma 2.76 mm
M1
M2
Fr3
Cg1
cg
S1J
fmi
PrL
CPu
GI
DI
AID
AIV
LO
Cl
E/OV
IL
azp
DP
DTT
AcbC
DEn
aca
AcbSh
Nv
IEn
Pir1
lo
VP
mfb
Tu1
ICj
rf
azac
lofr

B

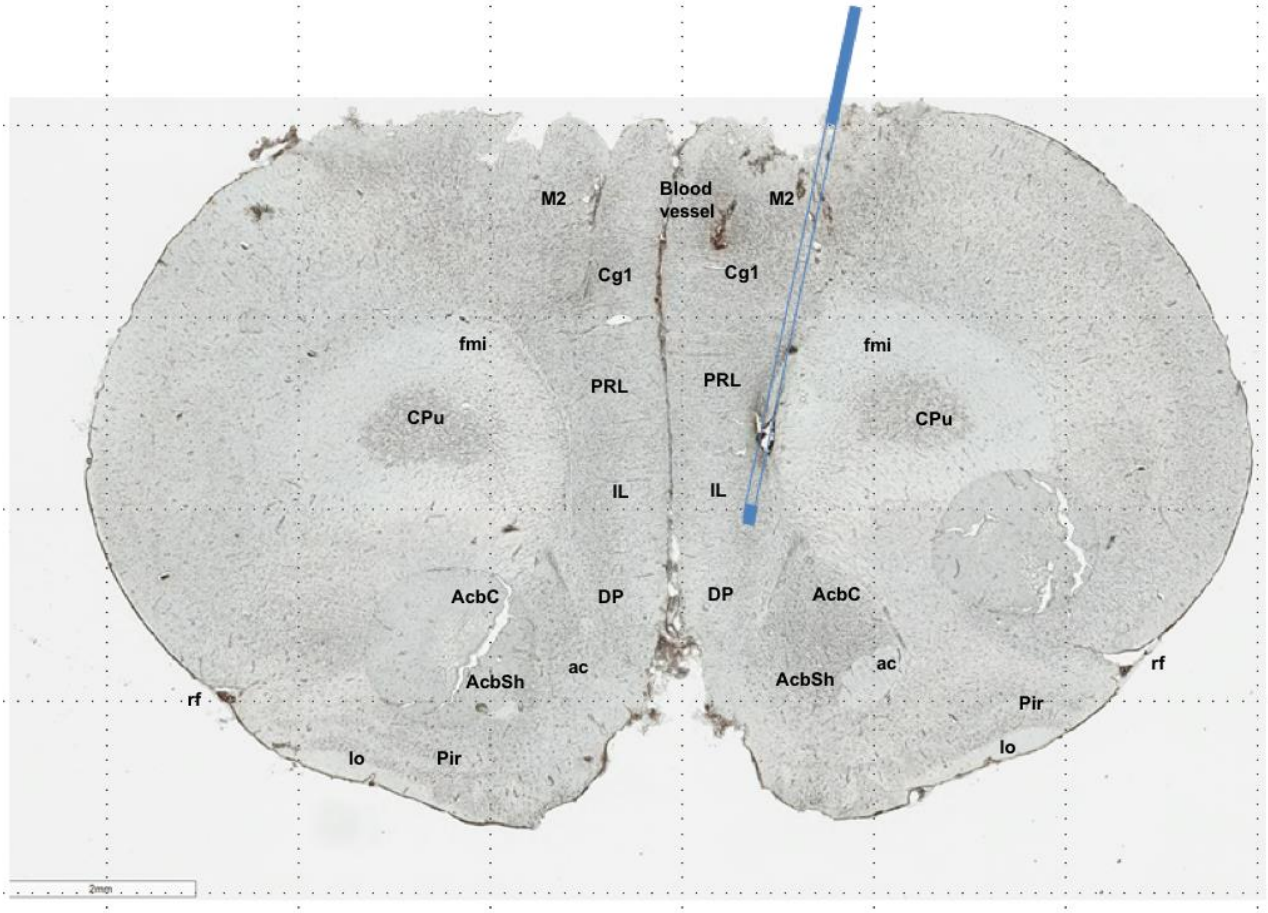
M2
Blood vessel
Cg1
fmi
PRL
CPu
IL
AcbC
DP
ac
AcbSh
rf
lo
Pir

C

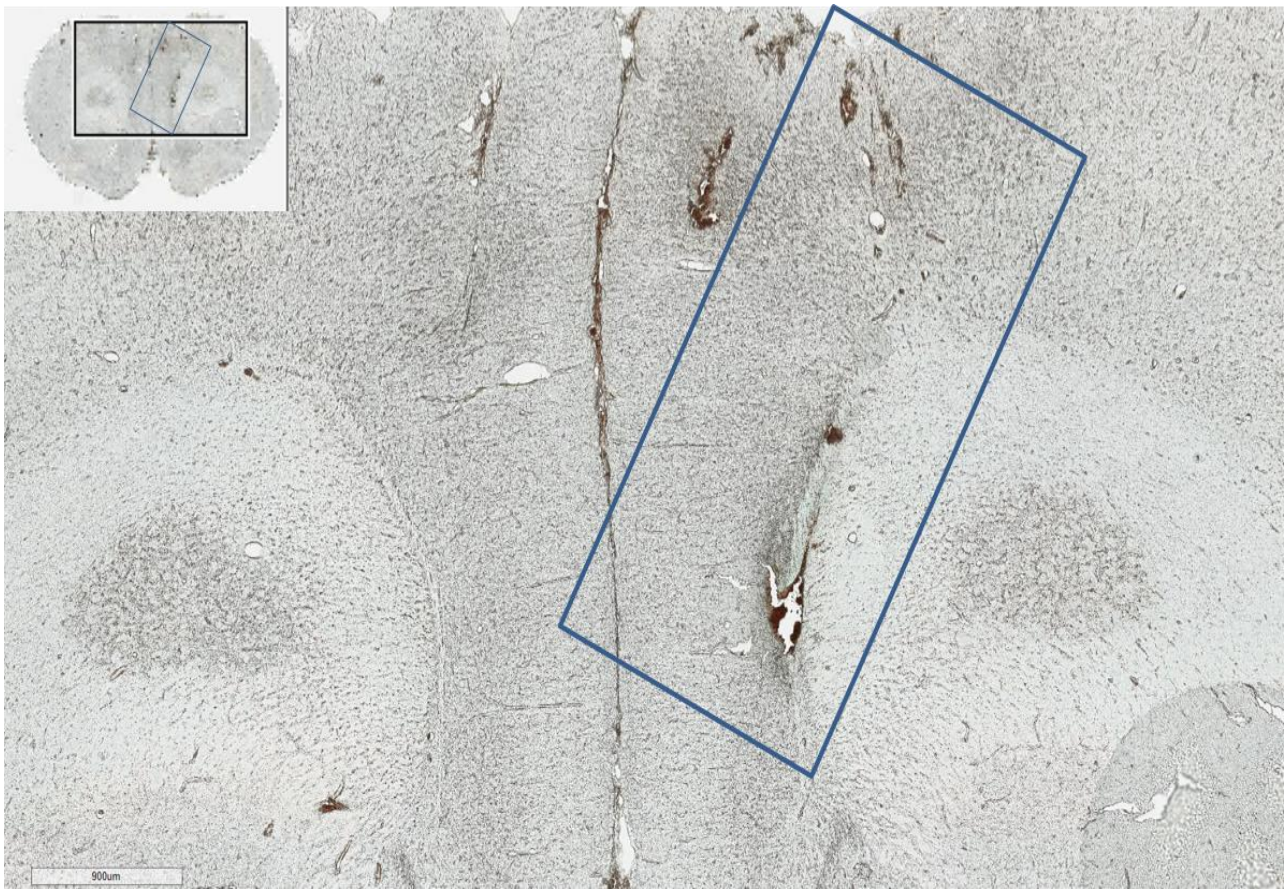

Figure 2.10: Microdialysis probe placement- medial prefrontal cortex

A) Imagined probe placement using atlas stereotaxic co-ordinates, 4 mm microdialysis probe depicted in green

B) Representative example of actual probe placement, 4 mm microdialysis probe depicted in blue

C) Close up view of probe tract terminating in the infralimbic layer 2 region. Toluene blue stains the area where the microdialysis probe would lie.

Abbreviations: ac; anterior commisure, AcbC; nucleus accumbens core, AcbSh; nucleus accumbens shell, Cg1; cingulate cortex area 1, Cpu; caudate putamen, DP; dorsal peduncular cortex, fmi; forceps minor corpus callosum, IL; infralimbic cortex, lo; lateral olfactory tract, M2; secondary motor cortex, Pir; piriform cortex, PRL; prelimbic cortex, rf; rhinal fissure

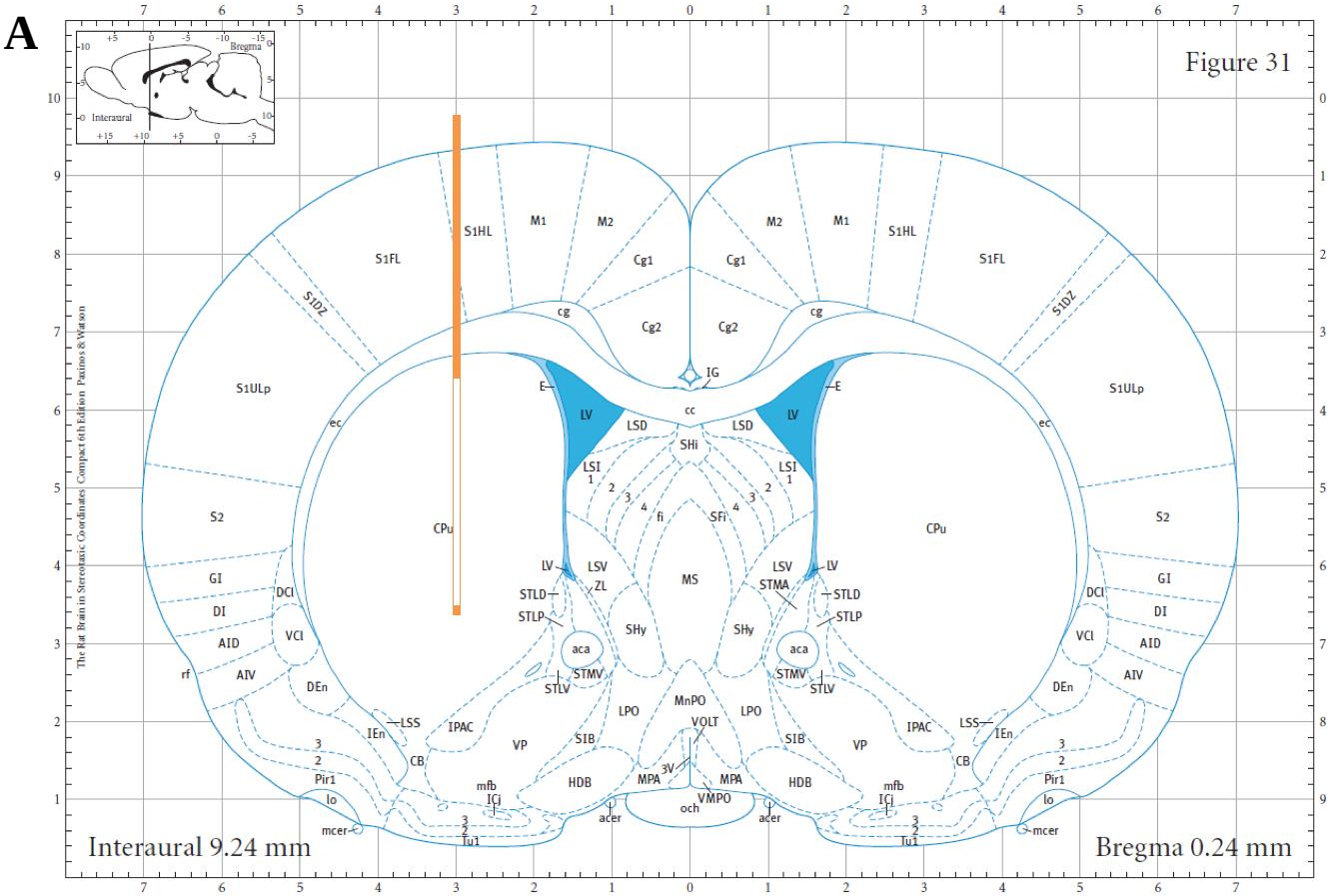
A
Figure 31
Bregma
Interaural
The Rat Brain in Stereotaxic Coordinates Compact 6th Edition Paxinos & Watson
S1HL
M1
M2
Cg1
Cg2
cg
S1FL
S1DZ
S1ULp
ec
E
IG
cc
LV
LSD
SHi
LSI
fi
SFi
CPu
S2
GI
DCl
DI
AID
VCl
AIV
rf
DEn
LSS
IEn
IPAC
CB
VP
SIB
Pir1
lo
mcer
mfb
ICj
HDB
LPO
MnPO
VOLT
3V
MPA
VMPO
och
acer
Tu1
MS
SHy
aca
STMV
STLV
STLD
STLP
ZL
STMA
Interaural 9.24 mm
Bregma 0.24 mm


B
M1
M2
S1
cg
cg2
LV
cc
CPu
MS
S2
ac
rf
IPAC
Pir
lo
2mm

C

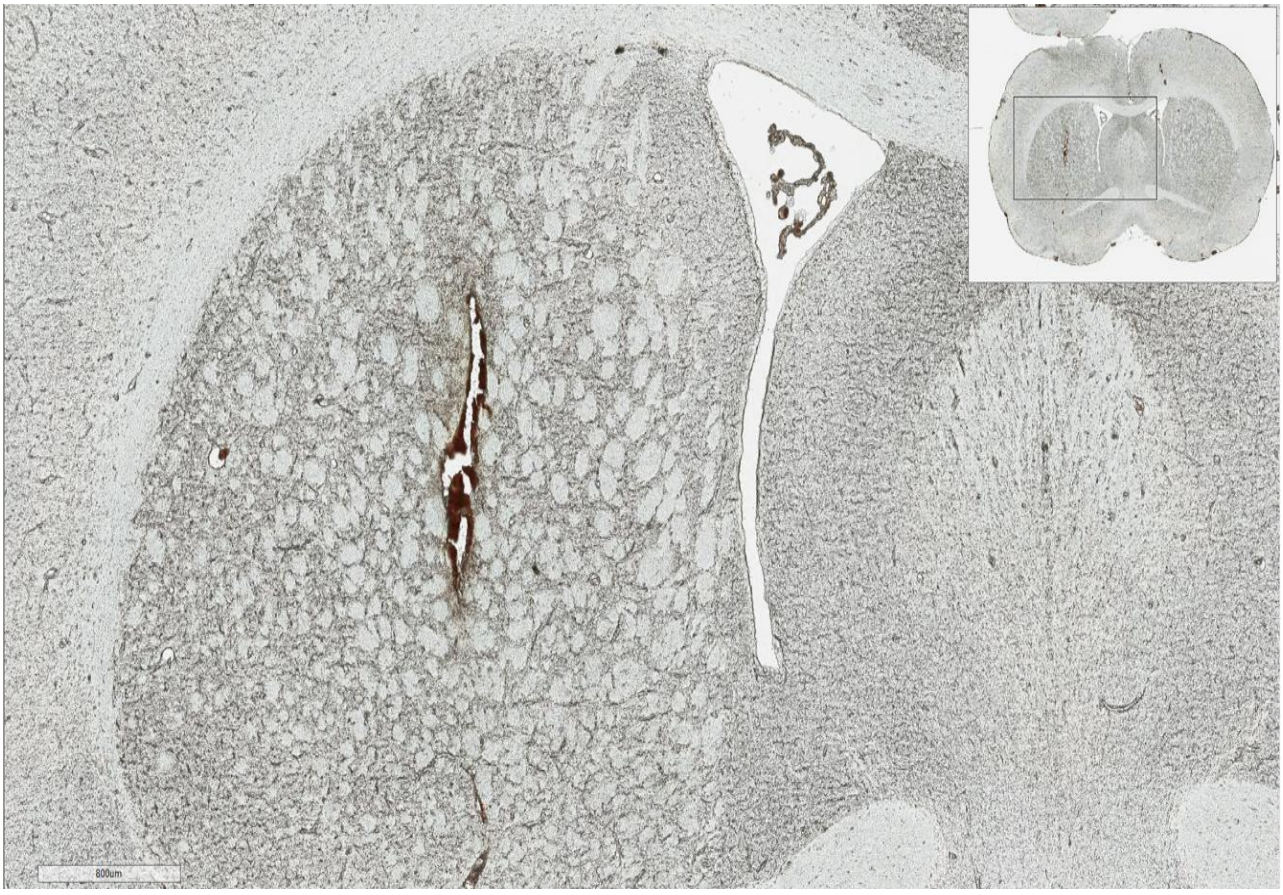

Figure 2.11: Microdialysis probe placement- caudate putamen

A) Imagined probe placement using atlas stereotaxic co-ordinates, 3 mm microdialysis probe depicted in orange

B) Representative example of actual probe placement, 3 mm microdialysis probe depicted in orange

C) Close up view of probe tract terminating in the centre of the caudate putamen. Toluene blue stains the area where the microdialysis probe would lie.

Abbreviations: ac; anterior commissure, cc; corpus callosum, cg; cingulum, cg2; cingulate cortex area 2, CPu; caudate putamen, IPAC; interstitial nucleus of the posterior limb of the anterior commissure, lo; lateral olfactory tract, LV; lateral ventricle, M1; primary motor cortex, M2; secondary motor cortex, MS; medial septal nucleus, Pir; piriform cortex, rf; rhinal fissure, S1; primary somatosensory cortex, S2; secondary somatosensory cortex

2.3 Ethical considerations

2.3.1 Clinical research

Ethical approval for all aspects of the clinical research outlined in the present thesis was provided by Camden and Islington London NHS Research Ethics Committee; study reference 13/LO/0091. Written, informed consent was obtained by all participants prior to study commencement, by a trained member of the research team (see Appendix 3).

2.3.2 Pre-clinical research

All housing and experimental procedures were performed in compliance with guidelines set by the Animal Care and Use Committee of Eli Lilly and Company and the U.K Home Office Animals Scientific Procedures Act 1986. Research was carried out under Project Licence; PPL30/3226. All efforts were made to minimize animal suffering and to reduce the number of animals used in accordance with the 3Rs (Replacement, Refinement and Reduction).

2.4 Concluding remarks

Conducting clinical and pre-clinical research in both an academic group, and in an industry research setting allowed me to have access to different expertise and equipment, whilst gaining a wide variety of research skills. The array of different techniques available enabled me to investigate E-I pharmacology at multiple different levels; namely the E-I dynamics of intracellular human (Chapters 3 and 4) and rodent (Chapter 5) brain regions, the functional connectivity of those brain networks (Chapter 3), and finally E-I dynamics in the extracellular synaptic space in an animal model of ASD (Chapter 6).

However, back and forward translating the findings of these different approaches between animal and human studies proved challenging- the implications of which are discussed further in Chapter 7.

Chapter 3

Shifting brain inhibitory balance and connectivity of the prefrontal cortex of adults with autism spectrum disorder

Previous investigations into Excitation (E) – Inhibition (I) balance in the living ASD brain have returned inconsistent findings using both MRS and fMRI techniques. One explanation for this may be that differences in E-I pathways in ASD are not static - they are in constant flux- and therefore are not best captured at a single time-point (i.e. 'at rest'). However, no-one has examined E-I flux or 'responsivity' to challenge in ASD. The following paper published in Translational Psychiatry (2017) aimed to test the hypothesis that there are group differences in the *dynamics* of E-I balance in the living ASD brain. I investigated this on two different levels; intracellular changes in E-I flux, using MRS; and network level changes in connectivity using fMRI.

OPEN

Citation: Transl Psychiatry (2017) 7, e1137; doi:10.1038/tp.2017.104

www.nature.com/tp

ORIGINAL ARTICLE

Shifting brain inhibitory balance and connectivity of the prefrontal cortex of adults with autism spectrum disorder

LA Ajram[1,6], J Horder[1,6], MA Mendez[1,2], A Galanopoulos[1,2], LP Brennan[1,2], RH Wichers[1,2], DM Robertson[2], CM Murphy[1,2], J Zinkstok[2], G Ivin[3], M Heasman[3], D Meek[2], MD Tricklebank[4], GJ Barker[4], DJ Lythgoe[4], RAE Edden[5], SC Williams[4,7], DGM Murphy[1,2,7] and GM McAlonan[1,2,7]

Currently, there are no effective pharmacologic treatments for the core symptoms of autism spectrum disorder (ASD). There is, nevertheless, potential for progress. For example, recent evidence suggests that the excitatory (E) glutamate and inhibitory (I) GABA systems may be altered in ASD. However, no prior studies of ASD have examined the 'responsivity' of the E–I system to pharmacologic challenge; or whether E–I modulation alters abnormalities in functional connectivity of brain regions implicated in the disorder. Therefore, we used magnetic resonance spectroscopy ([1H]MRS) to measure prefrontal E–I flux in response to the glutamate and GABA acting drug riluzole in adult men with and without ASD. We compared the change in prefrontal 'Inhibitory Index'—the GABA fraction within the pool of glutamate plus GABA metabolites—post riluzole challenge; and the impact of riluzole on differences in resting-state functional connectivity. Despite no baseline differences in E–I balance, there was a significant group difference in response to pharmacologic challenge. Riluzole increased the prefrontal cortex inhibitory index in ASD but decreased it in controls. There was also a significant group difference in prefrontal functional connectivity at baseline, which was abolished by riluzole within the ASD group. Our results also show, for we believe the first time in ASD, that E–I flux can be 'shifted' with a pharmacologic challenge, but that responsivity is significantly different from controls. Further, our initial evidence suggests that abnormalities in functional connectivity can be 'normalised' by targeting E–I, even in adults.

Translational Psychiatry (2017) **7,** e1137; doi:10.1038/tp.2017.104; published online 23 May 2017

INTRODUCTION

Autism spectrum disorder (ASD) is a neurodevelopmental condition, which impacts on three 'core' domains of function–social interaction, social communication and repetitive behaviours or interests. ASD has its origins in very early (prenatal) development, and persists through to adulthood.[1] It is clinically diverse; the core difficulties can range in severity from mild to severe, and they are often accompanied by secondary conditions, such as anxiety and depression, especially in adulthood.[2] This phenotypic variability likely reflects the marked aetiological heterogeneity of the disorder, and has made the identification of a common underlying pathology challenging. As a result, there are currently no effective pharmacological treatments for the core symptoms.

There is hope however, as genetic, post-mortem and preclinical laboratory studies indicate that the differences in the balance between the brain's excitatory (E) glutamate and inhibitory (I) GABA systems may be one of the final 'common pathways' in ASD.[3] This is perhaps especially true for GABA. For example, genetic studies have consistently implicated genes regulating $GABA_A$ receptor expression with ASD,[4,5] whereas environmental risk factors for ASD, such as exposure to maternal inflammation in prenatal life, have been shown to disrupt gene expression across GABA pathways.[6–8]

Direct *in vivo* measurement of glutamate and, more recently, GABA, is now possible in humans using proton magnetic resonance spectroscopy ([1H]MRS). However, studies of glutamate and GABA at baseline in ASD are at variance.[9–14] For example, some have reported an excess of glutamate in the cortex[9] and plasma,[15] and in the amygdala and hippocampal regions.[10] Conversely, we have reported lower levels of glutamate in the subcortex.[12] GABA has been reported to be lower in the frontal cortex of children with ASD,[11] yet higher in plasma.[16] Still others have observed no differences in brain glutamate and GABA in ASD.[13,17]

This divergence of findings may at least partly reflect between-study differences in (for example) the brain regions examined, age of participants, medication history and the presence of common comorbid mental health symptoms such as anxiety (mediated by GABA[18]). However, all prior studies examined E–I without challenging the system, and it is also possible that differences in glutamate and GABA 'flux' contribute to the variety of findings reported. This is because glutamate is a precursor of GABA, and

[1]Department of Forensic and Neurodevelopmental Sciences, The Sackler Centre for Translational Neurodevelopment, Institute of Psychiatry, Psychology and Neuroscience, King's College London, London, UK; [2]Behavioural and Developmental Psychiatry Clinical Academic Group, South London and Maudsley NHS Trust, London, UK; [3]Pharmacy Department, South London and Maudsley NHS Foundation Trust, London, UK; [4]Department of Neuroimaging, Institute of Psychiatry, Psychology and Neuroscience, King's College London, London, UK and [5]Department of Radiology and Radiological Science, Johns Hopkins University School of Medicine, Baltimore, MD, USA. Correspondence: Dr GM McAlonan, Department of Forensic and Neurodevelopmental Sciences, The Sackler Centre for Translational Neurodevelopment, Institute of Psychiatry, Psychology and Neuroscience, King's College London, 16 De Crespigny Park, London SE5 8AF, UK.
E-mail: grainne.mcalonan@kcl.ac.uk
[6]These authors contributed equally to this work.
[7]These authors contributed equally to this work.
Received 5 April 2017; accepted 10 April 2017

there is continuous 'flux' between glutamate and glutamine, and glutamate and GABA in the brain.[19–23] Glutamic acid decarboxylase (GAD) is a rate limiting enzyme in the glutamate/GABA-glutamate cycle, and has been reported to be abnormal in ASD.[24,25] Thus, E–I 'dynamics' (as opposed to the static state) may be critical in ASD—but this has never been directly studied *in vivo*.

Regional E–I dynamics may have widespread influence by regulating the functional connectivity of resting-state brain networks. For example, in typical individuals, prefrontal glutamate concentration has been shown to correlate with the strength of prefrontal functional connectivity;[26] whereas local GABA concentration predicts the extent of inhibition within the motor network.[27] However, although altered functional connectivity measures are commonly reported in ASD (for example, see refs 28–30), no-one has examined if these can be modulated through E–I.

Therefore, we conducted the present study to compare E–I and functional connectivity responsivity of the prefrontal cortex in adult men with and without ASD. We selected the prefrontal cortex as a region of interest (ROI), because this region is reliably implicated in the core symptoms in ASD, including deficits in theory of mind[31,32] and the regulation of socio-emotional responses.[33] We used [1H]MRS and resting-state functional magnetic resonance imaging (fMRI) to measure (respectively) change in the E–I flux and functional connectivity of the prefrontal lobe following a pharmacological challenge with the drug riluzole. Our MRS measure of E–I flux was the fraction of GABA within the total measured pool of GABA plus glutamate and glutamine (Glx), which we defined as the 'Inhibitory Index'. Our measure of functional connectivity was the strength of correlation (parameter estimate; PE) between activity in the prefrontal cortex and the rest of the brain.

We selected the drug riluzole because it has a broad range of actions at both GABA and glutamate targets,[34,35] and it should therefore modulate glutamate–GABA flux in a majority of individuals. For example, riluzole blocks the pre-synaptic release of glutamate, facilitates $GABA_A$ receptor activity[36,37] and has been reported to shift glutamate–glutamine flux in bipolar disorder.[38] Importantly, however, the pharmacokinetic and safety profile of riluzole is well-established; and a single oral dose of 50 mg riluzole, as used here, reaches a peak plasma concentration 1 h after oral administration[39] and has a very low risk of adverse effects.

MATERIALS AND METHODS

Participants

A priori calculations indicated that a sample size of $n = 12$ is sufficient to capture a 10% change in MRS measured metabolite concentration at 80% power, $\alpha = 0.05$;[40] and this is in line with the minimum number needed for typical fMRI activations.[41] However, to increase confidence in our results, a total of 37 adult males participated in the study; 17 individuals with ASD and 20 unaffected controls (Table 1). Each individual had two scans and so each acted as their own 'control'; this reduced the inter-subject variability to improve power.

Individuals with ASD were recruited through the National Autism and ADHD Service for Adults at the Maudsley Hospital, London; a specialist diagnostic service for adults. All ASD individuals had a consensus clinical diagnosis of ASD led by a consultant psychiatrist using ICD10 research criteria;[42] and reached Autism Diagnostic Observation Schedule (ADOS)[43] algorithm cut-offs in both communication and social domains.

Inclusion criteria were: IQ score above 70; absence of current psychoactive medication; and being medication free for a minimum of 6 weeks, to avoid possible confounds from drug interactions. Exclusion criteria were: a comorbid psychiatric or medical disorder that might affect brain development, for example, epilepsy or psychosis, head injury, or any genetic or chromosomal disorder associated with ASD, for example, tuberous sclerosis or fragile X syndrome. The ASD group scored significantly higher (as expected) in their self-rated autism symptom scores (autism quotient; $P < 0.001$), and anxiety (STAI; $P < 0.005$), but the groups did not differ in age or IQ ($P = 0.44$ and 0.15, respectively), see Table 1.

Table 1. Participant demographic and clinical symptoms

	ASD	*Control*	T *(df)*	P-*value*
Number	17	20	N/A	
Age (years)	33 (2.5)	30 (1.9)	−0.79 (35)	0.44
FSIQ	114 (3.0)	120 (3.5)	1.48 (31)	0.15
AQ	32 (2.2)	13 (1.1)	−0.76 (24)	0
STAI, State	35 (3.3)	24 (0.8)	−3.3 (18)	0.004
OCI	25 (3.9)	7 (1.1)	−4.5 (19)	0
ADI-R ($n = 8$) A domain	14 (3.4)			
ADI-R B domain	13 (2.2)	N/A		
ADI-R C domain	5 (0.8)			
ADOS ($n = 16$) A domain	7 (0.7)	N/A		
ADOS B domain	4 (0.5)			

Abbreviations: ADI-R, Autism Diagnostic Interview—revised (Domain A, social interaction; Domain B, communication; Domain C, restrictive and repetitive patterns of behaviour); ADOS, Autism Diagnostic Observation Schedule; AQ, autism quotient; ASD, autism spectrum disorder; FSIQ, Full Scale Intelligence Quotient; N/A, not applicable; OCI, Obsessive Compulsive Inventory; STAI State, State/Trait Anxiety Inventory. Groups differed in their neuropsychological tests of symptoms linked to ASD, but not in age or IQ score (Students *t*-test).

All participants provided written informed consent. Ethical approval for this study was provided by Camden and Islington London NHS Research Ethics Committee, study reference: 13/LO/0091.

Procedure

Each participant was scanned on two occasions, one week apart. MRI scanning began 1 h after oral administration of a capsule containing either 50 mg riluzole, or an equivalent placebo. The order of administration was randomised and double-blind, so that neither the researcher nor participant knew which capsule was given. We further controlled for order effects by ensuring that approximately half the individuals in each group had placebo first and the other half had riluzole first.

[1H]MRS data acquisition

[1H]MRS data were acquired on a 3 Tesla (3T) GE Excite II Magnetic Resonance Imaging scanner (GE Medical Systems, Milwaukee, WI, USA). The scanning protocol included an initial structural MRI scan, namely a 3D inversion recovery prepared fast spoiled gradient-recalled echo (IR-FSPGR) acquisition (number of slices = 124, slice thickness = 1.1 mm, inversion time (TI) = 450 ms, repetition time (TR) = 7.084 ms, echo time (TE) = 2.84 ms, field of view = 280 mm, flip angle = 20°). This was then used to set the voxel location for the spectroscopy scans.

Single voxel J-edited MEGAPRESS [1H]MRS spectra were then acquired in a prefrontal cortex region of interest using previously described methods.[12] More specifically, we obtained spectra from the bilateral dorsomedial prefrontal cortex ($25 \times 30 \times 40$ mm^3; TR = 2000 ms, TE = 68 ms), which included the anterior cingulate cortex. See Figure 1a for an illustration of the voxel placement.

[1H]MRS data analysis

[1H]MRS spectra were pre-processed using GE SAGE software (SAGE 2007, General Electric Healthcare Technologies, Milwaukee, WI, USA) to perform an edit ON–edit OFF subtraction, to extract the unedited spectrum (equivalent to conventional PRESS spectrum) and also to extract the unsuppressed water spectrum. These spectra were then quantified using jMRUI version 4 software.[44] Each [1H]MRS spectrum was manually checked for quality to ensure adequate signal-to-noise ratio and absence of artefacts (Figure 1b). If required, artefacts were removed using jMRUI peak fitting and removal algorithm, if this was sufficient to restore data integrity.

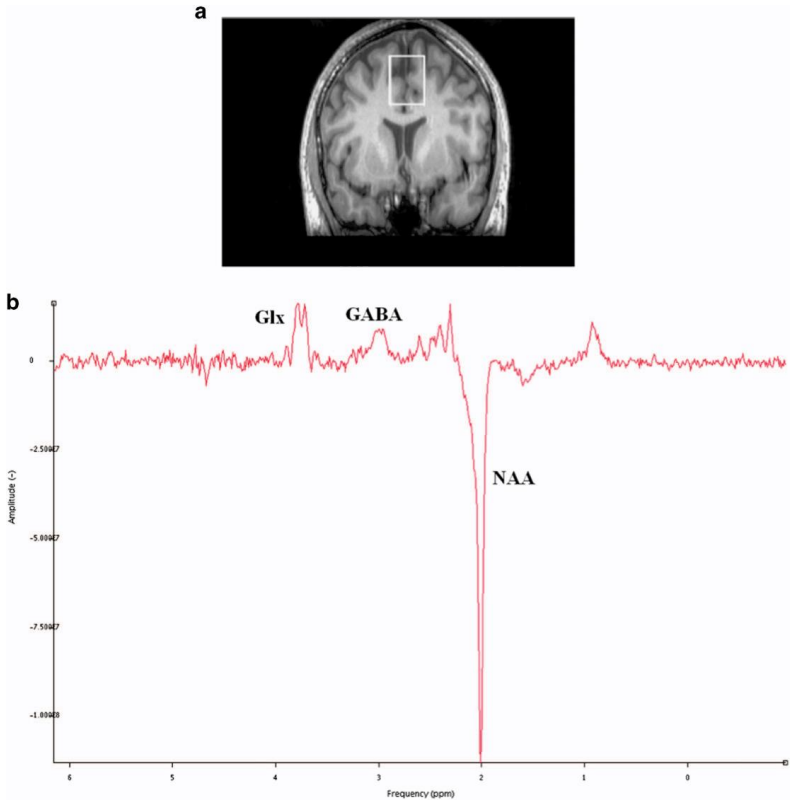

Figure 1. [1H]MRS voxel positions and example spectra. (**a**) Cortical region of interest; medial prefrontal cortex (mPFC) ($25 \times 30 \times 40$ mm^3) outlined in white, comprising primarily of anterior cingulate cortex. (**b**) Example spectroscopy output from the prefrontal voxel (Glx (glutamate+glutamine); GABA; *N*-acetylaspartate (NAA) identified using jMRUI spectroscopy software.

Metabolite concentrations were estimated using the AMARES algorithm. In the subtraction spectrum; GABA (including macromolecule[45]) at 3 p.p.m., Glx (Glutamate+Glutamine; as the measure of glutamate) as two peaks at 3.8 and 3.75 p.p.m. and *N*-acetylaspartate (NAA) at 2.01 p.p.m. were estimated. In the unedited spectrum; choline at 3.19 p.p.m., creatine at 2.99 p.p.m. and NAA at 2.01 p.p.m. were estimated. Absolute metabolite concentrations (in institutional units) were then calculated by dividing the amplitude of each peak by the amplitude of the unsuppressed water peak from the water spectrum at 0.00 p.p.m.

To quantify E–I flux, an 'Inhibitory Index' was defined as the fraction of GABA relative to total GABA plus Glx, within each voxel, for each subject: that is, Inhibitory Index = GABA/(GABA+Glx). This inhibitory index does not represent an absolute ratio of GABA to glutamate molecules in the brain tissue, as [1H]MRS has different sensitivities for these two molecules. Rather, the inhibitory index is a relative measurement that theoretically ranges from 0 to 1. Therefore, a value approaching zero would indicate relatively more Glx (excitation); values close to 1 would indicate more GABA (inhibition).

[1H]MRS voxel composition calculation

Group differences in proportion of white matter, grey matter and cerebrospinal fluid contained in the voxel (partial volume effects) are a potential confound for spectroscopy, and a particular consideration for the present study, as previous literature has found volumetric group differences between control and ASD subjects.[46] The structural MRI was first segmented into grey matter, white matter and cerebrospinal fluid (CSF) using SPM2.[47] The position of the [1H]MRS voxel was then registered to the corresponding segmented structural scan and the grey matter, white matter and CSF content of this region was calculated using in-house software. We found no group differences in the percentage composition of grey or white matter in the ROI, nor did this change in the presence of riluzole (Supplementary Table 1). There was however, a significant difference in the percentage CSF composition in ASD. In light of this, we corrected each metabolite for individual CSF levels prior to analysis and controlled for both water and CSF levels, as previously described.[12]

Resting state fMRI BOLD data acquisition

Immediately after [1H]MRS acquisition, in the same scanning session, resting state functional MRI data were acquired. Resting state fMRI acquisition parameters were as follows: an echo-planar imaging (EPI) sequence, TR = 2 s, TE = 30 ms, 256 volumes. Slice thickness = 3 mm, number of slices = 38, slice spacing = 0.3 mm. Each slice comprised of 64×64 voxels with a field of view of 240 mm, for a final voxel size of 3.75 mm × 3.75 mm × 3.3 mm. Pulse and respiration parameters were also acquired during the fMRI scan, for the purposes of correcting for physiological artefacts in the fMRI dataset, using a photoplethysmogram pulse oximeter and a chest band, respectively.

Resting state fMRI BOLD data analysis

fMRI data were processed using FSL 5.0.0. The following pre-processing steps were applied: motion correction using MCFLIRT; slice-timing correction using Fourier-space time-series phase-shifting; non-brain removal using Brain Extraction Tool (BET); spatial smoothing using a Gaussian kernel of full width at half maximum (FWHM) 5 mm; grand-mean intensity normalisation of the entire 4D dataset by a single multiplicative factor; and highpass temporal filtering (Gaussian-weighted least-squares straight line fitting, with sigma = 50.0 s).

Manual inspection and removal of artefactual components was then carried out using hypothesis-free probabilistic independent component

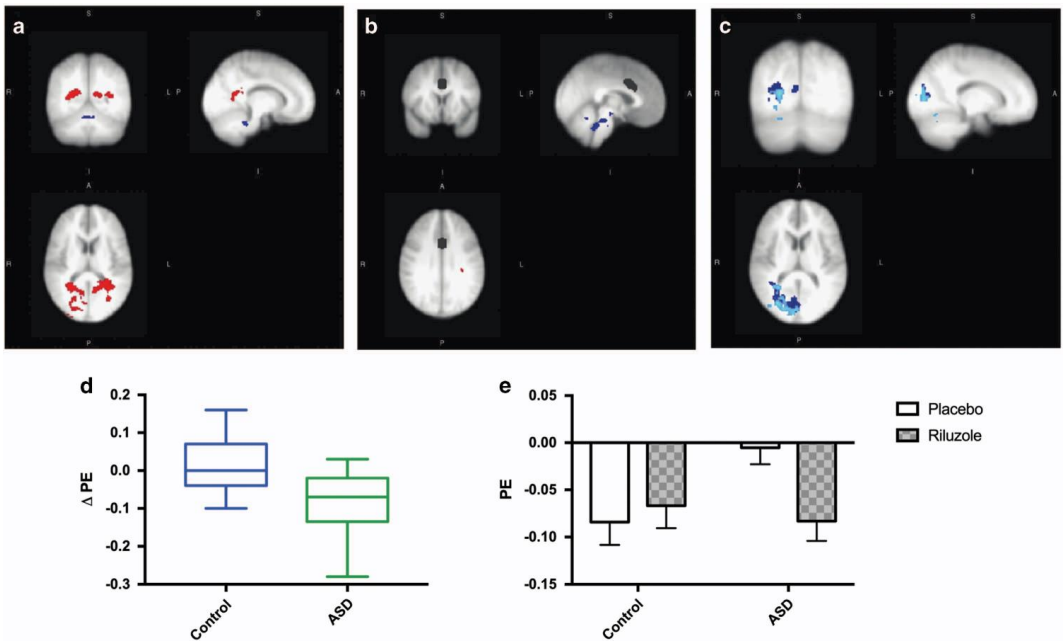

Figure 2. Functional connectivity differences between controls and ASD. (**a**) BASELINE: In the control group there was greater connectivity (an inverse correlation) between a prefrontal seed region and posterior regions compared to ASD (red). (**b**) The seed region (mPFC) is shown in black. (Also indicated is a restricted region of connectivity between mPFC and the brain stem/cerebellum (blue) in ASD at baseline). (**c**) RILUZOLE: Riluzole increased connectivity (an inverse correlation) between the prefrontal seed and posterior cortices in ASD only. Blue: riluzole < placebo ($P < 0.05$, cluster-corrected). Light blue: voxels in which the within-subjects effect of riluzole vs. placebo is negative in ASD ($P < 0.05$, cluster-corrected). (**d**) Change in functional connectivity elicited by Riluzole is significantly different between groups ($t_{(26)} = 0.394$, $P < 0.005$). (**e**) Riluzole did not alter the functional connectivity of the prefrontal lobe in controls but 'restored' functional connectivity in the ASD group to control levels post riluzole (connectivity × group Interaction, two-way repeated measures ANOVA; $F_{(1,\ 26)} = 9.696$, $P < 0.005$).

analysis as implemented in MELODIC (multivariate exploratory linear decomposition into independent components) Version 3.10, part of FSL.[48] The decisions as to whether to exclude each component from a given fMRI scan were made by a researcher blind to group and to drug status.

Statistical analysis

Statistical analysis of demographic, questionnaire, and [1H]MRS data were performed using IBM SPSS v.22 software (IBM SPSS Statistics for Macintosh, Version 22.0. Armonk, NY, USA). Figures were generated using GraphPad Prism version 7 for Windows (GraphPad Software, La Jolla, CA, USA). Age, IQ and self-reported questionnaire group comparisons were performed using independent samples *t*-tests. The numbers included in each MR analysis depended upon a stringent quality check of data available for each participant per analyses at each time point.

[1H]MRS. The [1H]MRS voxel composition in each group was compared using repeated measures two-way ANOVAs with 'group' as between-subjects factor and 'drug' as within-subjects factor (control $n = 20$, ASD $n = 17$). The inhibitory index could be calculated at two time points from 27 participants (that is, 54 data-points) and was therefore compared using repeated measures two-way analysis of variance with 'group' as between-subjects factor and 'drug' as within-subjects factor. Where there was a significant group × drug interaction, we also tested for a group difference in the change in inhibitory index elicited by drug. The State score measure of anxiety was included as a covariate in these analyses, as anxiety is closely linked to GABA,[49] and participants with ASD scored significantly higher than controls on measures of anxiety (Table 1).

Post-hoc the change in inhibitory index was converted to a *z*-score contribution so that the contribution of a change in glutamate to any change in the inhibitory index following riluzole could be explored using Pearson's correlation analyses; and a Fisher '*r* to *z*' transformation was used to compare correlation co-efficients between groups. For consistency across analyses, the State score measure of anxiety was included as a covariate. Finally, we screened for any unpredicted effects of group or drug on other metabolites measured (choline, creatine or *N*-acetylaspartate); any difference identified would have been subject to a threshold of $P < 0.01$ to accommodate multiple comparisons.

Resting state fMRI connectivity. The anterior cingulate region contained within the dorsomedial prefrontal cortex voxel was used as the seed in a whole brain seed-voxel resting state fMRI connectivity analysis of $n = 18$ controls and $n = 17$ ASD subjects. The seed-voxel analysis was performed using a general linear model implemented in FEAT (FMRI expert analysis tool) version 5.98 (ref. 48) as follows: for each participant, the mean signal time course from an anterior cingulate seed region (contained within the prefrontal cortex MRS voxel; see Figure 2b was first extracted using the fslmeants tool. This time course was entered as an explanatory variable (EV) in FEAT, and the participant's pulse, respiration, and the mean signal from grey, white, and CSF masks were entered as the five additional EVs of no interest. We then carried out higher-level fMRI analysis using FLAME (FMRIB's local analysis of mixed effects) stage 1. Higher-level EVs included drug (riluzole or placebo) and group (ASD or control). The *Z* (Gaussianised T/F) statistic images were thresholded using clusters determined by $Z > 2.3$ and a cluster-corrected significance threshold of $P = 0.05$.[50]

PE values from the first level fMRI data, for each participant, were our measure of the mean connectivity between the seed and the network of voxels found at the group level (Figure 2a). High absolute PE values indicate high connectivity. Full details of the fMRI result can be found in Supplementary Table 2.

Potentially confounding differences in head movement were examined by estimating mean absolute displacement and mean relative volume-to-volume motion using FSL MCFLIRT. There were no group or drug effects on either parameter (all $P > 0.8$).

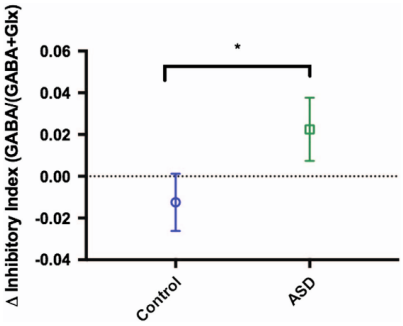

Figure 3. Riluzole increases inhibition in the prefrontal cortex of the autism spectrum disorder (ASD) group only. Riluzole increased the inhibitory index in the ASD group, not controls: *Drug × group interaction; $F_{(1, 24)} = 4.288$, $P < 0.05$. *Post-hoc* analyses demonstrate a significant difference between groups in the change in inhibitory index after riluzole administration: ANCOVA; $F_{(1, 27)} = 4.290$, $P < 0.05$. Results are expressed as mean (± s.e.m.) and are corrected for State anxiety score.

All data are expressed as mean ± s.e.m. unless otherwise specified. A significance threshold of $P < 0.05$ was adopted for all pre-planned analyses.

RESULTS

Men with ASD have significant differences in E–I responsivity

At baseline (that is, placebo), there were no group differences in the inhibitory index, or absolute levels of GABA or glutamate in the medial prefrontal cortex region. However, riluzole administration shifted the inhibitory index in opposite directions in the ASD and control groups. Specifically, riluzole increased the proportion of GABA in the prefrontal cortex of the ASD group but decreased the proportion of GABA in controls (group × drug interaction; $F_{(1, 24)} = 4.288$, $P < 0.05$). This was confirmed by a significant group difference in the change in inhibitory index elicited by riluzole ($F_{(1, 27)} = 4.29$, $P < 0.05$). There were no significant effects of group or drug on other metabolites measured (choline, creatine or *N*-acetylaspartate). Please see Figure 3.

E–I balance is regulated differently in men with and without ASD

In controls a decrease in inhibitory index (or GABA fraction) elicited by riluzole was accompanied by an increase in Glx ($r = -0.705$, $P < 0.01$), see Figure 4. In ASD, the increase in the inhibitory index (or GABA fraction) was not linked to Glx. This relationship between the change in inhibitory index and change in glutamate measure in each group was significantly different (Fisher *r* to *z* transformation, $z = 2.23$, $P < 0.01$).

Baseline functional connectivity differences in ASD are 'normalised' post riluzole

There was a significant group difference in the change in functional connectivity elicited by riluzole ($t_{(26)} = 0.394$, $P < 0.005$). Specifically, riluzole increased the minimal/absent baseline prefrontal functional connectivity in the ASD group towards the control levels; and there was no longer a group difference in functional connectivity post riluzole (Figure 2).

DISCUSSION

To the best of our knowledge, this study provides the first direct evidence that responsivity of the E–I system and functional networks in ASD is regulated differently from controls. Specifically,

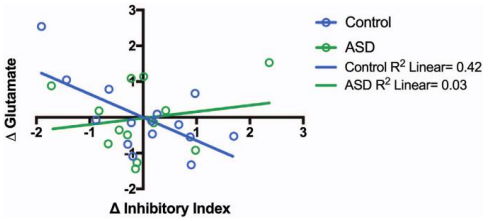

Figure 4. Inhibitory tone is regulated differently in men with and without autism spectrum disorder (ASD). The change in inhibitory index was negatively correlated with changes in Glx in controls (Pearson correlation; $r = -0.705$, $P < 0.01$), but not men with ASD ($r = 0.357$, $P = 0.28$). Furthermore, there was a significant group difference in correlation coefficient (Fisher *r* to *z* transform, $z = 2.23$, $P < 0.01$). Results are expressed as *z*-scores ((value – mean)/standard deviation) and are corrected for State anxiety score.

in men with ASD the E–I acting drug riluzole increased a prefrontal cortex inhibitory index but decreased it in controls. Riluzole also increased prefrontal functional connectivity from 'absent' at baseline in ASD, to control levels.

We found no baseline differences in the level of cortical glutamate or GABA in men with ASD relative to controls. This is consistent with some (unpublished data and refs. 17, 51), but not all,[9] previous studies. However, our results indicate that despite a comparable baseline, the E–I response to a riluzole challenge was diametrically opposite in men with ASD and controls. In controls, the decrease in the inhibitory index (or GABA fraction) was correlated with an increase in Glx. In ASD, riluzole increased the inhibitory index (or GABA fraction) without changing Glx. Overall, this pattern of results indicates that riluzole shifts flux towards GABA in ASD and towards glutamate–glutamine (Glx) in controls.

This unusual E–I responsivity in ASD may help explain other paradoxical findings from studies of the way people with ASD respond to E–I acting medications. For example, $GABA_A$/benzodiazepine receptor agonists typically have an inhibitory effect in non-ASD populations, but can sometimes cause excitation in individuals with ASD.[52,53] This opposite direction of response in ASD is important because the initial selection of drug candidates for clinical trials in ASD is often based on their action in unaffected individuals. If, however, the nature of the brain response in ASD fundamentally differs from other populations then similar outcomes cannot be anticipated, and trials are likely to be unsuccessful. This exacerbates the challenges of identifying effective pharmacological treatments for ASD. For example, a number of clinical trials have been based on the presumption that drugs which increase inhibition in other populations should also be effective in ASD. These have included the anti-epileptic medication lamotrigine, which reduces glutamate release in the cortex, and D-cycloserine, a partial agonist at the NMDA glutamate receptor. However, neither approach has been successful in ASD.[54–56]

The cause of such E–I responsivity differences in ASD is unknown. However, they may have their origins in early developmental abnormalities, and perhaps especially in the GABA inhibitory system. For example, in ASD, it has been proposed that there is a delay or alteration in the typical 'switch' from an excitatory action of GABA in prenatal life, to its inhibitory action in the postnatal period.[57–60] There is also evidence from a genetic model of ASD, the neuroligin knock-in mouse, indicating that GABAergic, but not glutamatergic, signalling is enhanced in early postnatal development.[18] Abnormalities in GABA pathways in ASD are also evident in later life, and these include a reduction in the levels of GAD type 65 and 67 in a number of brain regions,[24,25] and GABA receptor abnormalities in ASD, including in the anterior

cingulate component of the prefrontal cortex voxel sampled here.[61,62] Thus, in ASD, early aberrations in E–I pathways may lead to persistent alterations, not necessarily in the absolute amount of GABA or glutamate but in their flux, receptor availability and action, and hence on their subsequent influence on brain network activity.

Consistent with this, our work suggests that the typical functional connectivity of a prefrontal-posterior brain network is absent in ASD. Similar baseline differences in resting state networks in ASD have been observed before, and our findings are consistent with the 'long range underconnectivity' reported in ASD (reviewed in Geschwind and Levitt[63]). Moreover, the dorsomedial prefrontal cortex/anterior cingulate region of interest examined in our study has been specifically identified as the critical node within a disconnected system which contributes to the social difficulties found in ASD.[63,64] This accumulation of observations of long-range underconnectivity in ASD has lead to the conceptualization of the condition as a 'Developmental Disconnection Syndrome'.[63]

Developmental disconnection in ASD has been suggested to arise in two ways: (i) 'a weakening of already formed connections'; or (ii) 'a failure of certain connections to establish correct organisation *de novo*'.[63] This then has implications for the severity of the ASD phenotype, with a failure to establish correct connections theroetically leading to more severe features. Here, riluzole (re-)established a functional relationship between the prefrontal and posterior cortices in high functioning adults with ASD which was similar to controls. This implies that any developmental disconnection in our cohort of autistic men is more likely to be 'a weakening' rather than an irreversible 'failure' of connectivity *per se*. In other words, the functional architecture of brain in ASD, though not measureable at baseline, was still in place and revealed by riluzole.

Clinically, riluzole has shown promise in reducing symptoms in some[65,66] but not all individuals with ASD.[67] Thus, as expected in a spectrum condition like ASD, not everyone responds to the same extent to a drug challenge. In future studies, a neuroimaging approach such as the one used here could begin to help personalise medicine for ASD. For instance, future studies investigating clinical treatment with riluzole may be of interest in cohorts enriched with individuals who can be shown to mount a brain response to a single test dose.

The limitations of our study include the inherently limited spatial resolution of [1H]MRS, which restricts measurements to 'bulk' levels of metabolites. This macroscopic approach provides insight to the gross regional changes in E–I flux after challenge (see for example, Brennan *et al.*[38]), but does not allow for circuit level analysis. Future work is warranted to dissect the circuitry of the prefrontal cortex in more detail. One way of doing this may be to use more directed pharmacological probes, for example, specific to different GABA receptor sub-types.

We also acknowledge that, although based upon prior power calculations, the sample size for this study was still modest. This precluded further exploration of the relationship between symptom profile and E–I responsivity in ASD. Future work will be required to confirm the findings from this 'Proof of Concept' work, and determine if these are generalisable, for example, to females with ASD, to other age groups and/or to individuals with intellectual difficulties.

In conclusion, using [1H]MRS and fMRI, we found that E–I flux and functional connectivity of the prefrontal cortex are differentially regulated in adults with ASD compared with the controls. Importantly, inhibitory tone and functional connectivity can be shifted pharmacologically—and even in adults with ASD.

CONFLICT OF INTEREST

The authors declare no conflict of interest.

ACKNOWLEDGMENTS

This study was funded by Autism Speaks Grant Number 8132 and by an MRC CASE Postgraduate Studentship Award, MR/K01725X/1 (LAA). Support was also provided by The Sackler Centre for Translational Neurodevelopment at King's College London; and EU-AIMS (European Autism Interventions), which receives support from the Innovative Medicines Initiative Joint Undertaking under Grant Agreement No. 115300, the resources of which are composed of financial contributions from the European Union's Seventh Framework Programme (Grant FP7/2007–2013). Additional support was provided by the National Institute for Health Research (NIHR) Biomedical Research Centre for Mental Health at South London and Maudsley NHS Foundation Trust and Institute of Psychiatry, Psychology and Neuroscience at King's College London.

DISCLAIMER

The views expressed are those of the authors and not necessarily those of the NHS, the NIHR or the Department of Health, U.K.

REFERENCES

1 American Psychiatric Association. *Diagnostic and Statistical Manual Of Mental Disorders*, 5th edn. American Psychiatric Publishing: Arlington, VA, 2013.
2 Gillberg C, Billstedt E. Autism and Asperger syndrome: coexistence with other clinical disorders. *Acta Psychiatr Scand* 2000; **102**: 321–330.
3 Ecker C, Spooren W, Murphy DGM. Translational approaches to the biology of Autism: false dawn or a new era? *Mol Psychiatry* 2012; **18**: 435–442.
4 Ching MSL, Shen Y, Tan W-H, Jeste SS, Morrow EM, Chen X *et al.* Deletions of NRXN1 (neurexin-1) predispose to a wide spectrum of developmental disorders. *Am J Med Genet B Neuropsychiatr Genet* 2010; **153B**: 937–947.
5 Jamain S, Quach H, Betancur C, Råstam M, Colineaux C, Gillberg IC *et al.* Mutations of the X-linked genes encoding neuroligins NLGN3 and NLGN4 are associated with autism. *Nat Genet.* 2003; **34**: 27–29.
6 Fatemi SH, Reutiman TJ, Folsom TD, Huang H, Oishi K, Mori S *et al.* Maternal infection leads to abnormal gene regulation and brain atrophy in mouse offspring: Implications for genesis of neurodevelopmental disorders. *Schizophr Res* 2008; **99**: 56–70.
7 Meyer U, Feldon J, Dammann O. Schizophrenia and autism: Both shared and disorder-specific pathogenesis via perinatal inflammation? *Pediatr Res* 2011; **69**: 26R–33R.
8 Giovanoli S, Weber L, Meyer U. Single and combined effects of prenatal immune activation and peripubertal stress on parvalbumin and reelin expression in the hippocampal formation. *Brain Behav Immun* 2014; **40**: 48–54.
9 Joshi G, Biederman J, Wozniak J, Goldin RL, Crowley D, Furtak S *et al.* Magnetic resonance spectroscopy study of the glutamatergic system in adolescent males with high-functioning autistic disorder: a pilot study at 4T. *Eur Arch Psychiatry Clin Neurosci* 2013; **263**: 379–384.
10 Page LA, Daly E, Schmitz N, Simmons A, Toal F, Deeley Q *et al. In vivo* 1H-magnetic resonance spectroscopy study of amygdala-hippocampal and parietal regions in autism. *Am J Psychiatry* 2006; **163**: 2189–2192.
11 Harada M, Taki MM, Nose A, Kubo H, Mori K, Nishitani H *et al.* Non-invasive evaluation of the GABAergic/glutamatergic system in autistic patients observed by MEGA-editing proton MR spectroscopy using a clinical 3 tesla instrument. *J Autism Dev Disord* 2011; **41**: 447–454.
12 Horder J, Lavender T, Mendez MA, O'Gorman R, Daly E, Craig MC *et al.* Reduced subcortical glutamate/glutamine in adults with autism spectrum disorders: a [^{1}H] MRS study. *Transl Psychiatry* 2013; **3**: e279.
13 Brix MK, Ersland L, Hugdahl K, Grüner R, Posserud M-B, Hammar Å *et al.* Brain MR spectroscopy in autism spectrum disorder—the GABA excitatory/inhibitory imbalance theory revisited. *Front Hum Neurosci* 2015; **9**: 1–12.
14 Gaetz W, Bloy L, Wang DJ, Port RG, Blaskey L, Levy SE *et al.* GABA estimation in the brains of children on the autism spectrum: measurement precision and regional cortical variation. *Neuroimage* 2014; **86**: 1–9.
15 Shinohe A, Hashimoto K, Nakamura K, Tsujii M, Iwata Y, Tsuchiya KJ *et al.* Increased serum levels of glutamate in adult patients with autism. *Prog Neuropsychopharmacology Biol Psychiatry* 2006; **30**: 1472–1477.
16 Dhossche D, Applegate H, Abraham A, Maertens P, Bland L, Bencsath A *et al.* Elevated plasma gamma-aminobutyric acid (GABA) levels in autistic youngsters: stimulus for a GABA hypothesis of autism. *Med Sci Monit* 2002; **8**: PR1–PR6.
17 Libero LE, Reid MA, White DM, Salibi N, Lahti AC, Kana RK. Biochemistry of the cingulate cortex in autism: An MR spectroscopy study. *Autism Res* 2015; **9**: 643–657.
18 Pizzarelli R, Cherubini E. Alterations of GABAergic signaling in autism spectrum disorders. *Neural Plast* 2011; **2011**: 297153.
19 Sibson NR, Dhankhar A, Mason GF, Rothman DL, Behar KL, Shulman RG. Stoichiometric coupling of brain glucose metabolism and glutamatergic neuronal activity. *Neurobiology* 1998; **95**: 316–321.

20 Rothman DL, de Feyter HM, de Graaf RA, Mason GF, Behar KL. 13C MRS studies of neuroenergetics and neurotransmitter cycling in humans. *NMR Biomed* 2011; **24**: 943–957.
21 Rothman DL, De Feyter HM, Maciejewski PK, Behar KL. Is there *in vivo* evidence for amino acid shuttles carrying ammonia from neurons to astrocytes. *Neurochem Res* 2012; **37**: 2597–2612.
22 Hyder F, Fulbright RK, Shulman RG, Rothman DL. Glutamatergic function in the resting awake human brain is supported by uniformly high oxidative energy. *J Cereb Blood Flow Metab* 2013; **33**: 339–347.
23 Bak LK, Schousboe A, Waagepetersen HS. The glutamate/GABA-glutamine cycle: aspects of transport, neurotransmitter homeostasis and ammonia transfer. *J Neurochem* 2006; **98**: 641–653.
24 Yip J, Soghomonian J-J, Blatt GJ. Decreased GAD67 mRNA levels in cerebellar Purkinje cells in autism: pathophysiological implications. *Acta Neuropathol* 2007; **113**: 559–568.
25 Yip J, Soghomonian JJ, Blatt GJ. Decreased GAD65 mRNA levels in select subpopulations of neurons in the cerebellar dentate nuclei in autism: an *in situ* hybridization study. *Autism Res* 2009; **2**: 50–59.
26 Duncan NW, Wiebking C, Tiret B, Marjańska M, Marjańska M, Hayes DJ *et al.* Glutamate concentration in the medial prefrontal cortex predicts resting-state cortical-subcortical functional connectivity in humans. *PLoS ONE* 2013; **8**: e60312.
27 Stagg CJ, Bachtiar V, Amadi U, Gudberg CA, Ilie AS, Sampaio-Baptista C *et al.* Local GABA concentration is related to network-level resting functional connectivity. *Elife* 2014; **3**: e01465.
28 Hahamy A, Behrmann M, Malach R. The idiosyncratic brain: distortion of spontaneous connectivity patterns in autism spectrum disorder. *Nat Neurosci.* 2015; **18**: 302–309.
29 Schipul SE, Keller TA, Just MA. Inter-regional brain communication and its disturbance in autism. *Front Syst Neurosci* 2011; **5**: 10.
30 Just MA, Keller TA, Malave VL, Kana RK, Varma S. Autism as a neural systems disorder: a theory of frontal-posterior underconnectivity. *Neurosci Biobehav Rev* 2012; **36**: 1292–1313.
31 Kalbe E, Schlegel M, Sack AT, Nowak Da, Dafotakis M, Bangard C *et al.* Dissociating cognitive from affective theory of mind: A TMS study. *Cortex* 2010; **46**: 769–780.
32 Murdaugh DL, Shinkareva SV, Deshpande HR, Wang J, Pennick MR, Kana RK. Differential deactivation during mentalizing and classification of autism based on default mode network connectivity. *PLoS ONE* 2012; **7**: e50064.
33 Tebartz van Elst L, Maier S, Fangmeier T, Endres D, Mueller GT, Nickel K *et al.* Disturbed cingulate glutamate metabolism in adults with high-functioning autism spectrum disorder: evidence in support of the excitatory/inhibitory imbalance hypothesis. *Mol Psychiatry* 2014; **19**: 1314–1325.
34 Mantz J, Laudenbach V, Lecharny JB, Henzel D, Desmonts JM. Riluzole, a novel antiglutamate, blocks GABA uptake by striatal synaptosomes. *Eur J Pharmacol* 1994; **257**: R7–R8.
35 Doble A. The pharmacology and mechanism of action of riluzole. *Neurology* 1996; **47**: S233–S241.
36 Cheramy A, Barbeito L, Godeheu G, Glowinski J. Riluzole inhibits the release of glutamate in the caudate nucleus of the cat *in vivo*. *Neurosci Lett* 1992; **147**: 209–212.
37 He Y, Benz A, Fu T, Wang M, Covey DF, Zorumski CF *et al.* Neuroprotective agent riluzole potentiates postsynaptic GABAA receptor function. *Neuropharmacology* 2002; **42**: 199–209.
38 Brennan BP, Hudson JI, Jensen JE, McCarthy J, Roberts JL, Prescot AP *et al.* Rapid enhancement of glutamatergic neurotransmission in bipolar depression following treatment with riluzole. *Neuropsychopharmacology* 2010; **35**: 834–846.
39 Le Liboux A, Lefebvre P, Le Roux Y, Truffinet P, Aubeneau M, Kirkesseli S *et al.* Single- and multiple-dose pharmacokinetics of riluzole in white subjects. *J Clin Pharmacol* 1997; **37**: 820–827.
40 Stone JM, Dietrich C, Edden R, Mehta Ma, De Simoni S, Reed LJ *et al.* Ketamine effects on brain GABA and glutamate levels with 1H-MRS: relationship to ketamine-induced psychopathology. *Mol Psychiatry* 2012; **17**: 664–665.
41 Desmond JE, Glover GH. Estimating sample size in functional MRI (fMRI) neuroimaging studies: statistical power analyses. *J Neurosci Methods* 2002; **118**: 115–128.
42 World Health Organisation. *International Statistical Classification of Diseases and Related Health Problems*, 5th edn, 10th revision. WHO: Geneva, Switzerland, 2016.
43 Lord C, Rutter M, Goode S, Heemsbergen J, Jordan H, Mawhood L *et al.* Austism diagnostic observation schedule: a standardized observation of communicative and social behavior. *J Autism Dev Disord* 1989; **19**: 185–212.
44 Naressi a, Couturier C, Devos JM, Janssen M, Mangeat C, De Beer R *et al.* Java-based graphical user interface for the MRUI quantitation package. *Magn Reson Mater Phys Biol Med* 2001; **12**: 141–152.
45 Edden RAE, Puts NAJ, Barker PB. Macromolecule-suppressed GABA-edited magnetic resonance spectroscopy at 3T. *Magn Reson Med* 2012; **68**: 657–661.
46 Haznedar MM, Buchsbaum MS, Hazlett EA, LiCalzi EM, Cartwright C, Hollander E. Volumetric analysis and three-dimensional glucose metabolic mapping of the striatum and thalamus in patients with autism spectrum disorders. *Am J Psychiatry* 2006; **163**: 1252–1263.
47 UCL. SPM2. Available at: http://www.fil.ion.ucl.ac.uk/spm/software/spm2.
48 Analysis Group. FMRIB, Oxford U. FMRIB Software Library. Available at: www.fmrib.ox.ac.uk/fsl.
49 Lydiard RB. The role of GABA in anxiety disorders. *J Clin Psychiatry* 2003; **64**: 21–27.
50 Worsley KJ. Statistical analysis of activation images. In: Jezzard P, Matthews P, *et al.* (eds). *Functional MRI: An Introduction to Methods*. Oxford University Press: Oxford, UK, 2001, pp 251–270.
51 Robertson CE, Ratai EM, Kanwisher N. Reduced GABAergic action in the autistic brain. *Curr Biol* 2016; **26**: 80–85.
52 Marrosu F, Marrosu G, Rachel MG, Biggio G. Paradoxical reactions elicited by diazepam in children with classic autism. *Funct Neurol* 1987; **2**: 355–361.
53 Lemonnier E, Degrez C, Phelep M, Tyzio R, Josse F, Grandgeorge M *et al.* A randomised controlled trial of bumetanide in the treatment of autism in children. *Transl Psychiatry* 2012; **2**: e202.
54 Belsito KM, Law PA, Kirk KS, Landa RJ, Zimmerman AW. Lamotrigine therapy for autistic disorder: a randomized, double-blind, placebo-controlled trial. *J Autism Dev Disord* 2001; **31**: 175–181.
55 Posey DJ, Kem DL, Swiezy NB, Sweeten TL, Wiegand RE, McDougle CJ. A pilot study of D-cycloserine in subjects with autistic disorder. *Am J Psychiatry* 2004; **161**: 2115–2117.
56 Minshawi NF, Wink LK, Shaffer R, Plawecki MH, Posey DJ, Liu H *et al.* A randomized, placebo-controlled trial of D-cycloserine for the enhancement of social skills training in autism spectrum disorders. *Mol Autism* 2016; **7**: 2.
57 Ben-Ari Y. Excitatory actions of gaba during development: the nature of the nurture. *Nat Rev Neurosci* 2002; **3**: 728–739.
58 Ben-Ari Y, Khalilov I, Kahle KT, Cherubini E. The GABA excitatory/inhibitory shift in brain maturation and neurological disorders. *Neuroscience* 2012; **18**: 467–486.
59 Tyzio R, Cossart R, Khalilov I, Minlebaev M, Hübner Ca, Represa A *et al.* Maternal oxytocin triggers a transient inhibitory switch in GABA signaling in the fetal brain during delivery. *Science* 2006; **314**: 1788–1792.
60 Khazipov R, Tyzio R, Ben-Ari Y. Effects of oxytocin on GABA signalling in the foetal brain during delivery. *Prog Brain Res* 2008; **170**: 243–257.
61 Oblak AL, Gibbs TT, Blatt GJ. Decreased GABAB receptors in the cingulate cortex and fusiform gyrus in autism. *J Neurochem* 2010; **114**: 1414–1423.
62 Blatt GJ, Fatemi SH. Alterations in GABAergic biomarkers in the autism brain: research findings and clinical implications. *Anat Rec* 2011; **294**: 1646–1652.
63 Geschwind DH, Levitt P. Autism spectrum disorders: developmental disconnection syndromes. *Curr Opin Neurobiol* 2007; **17**: 103–111.
64 Mundy P. Annotation: the neural basis of social impairments in autism: the role of the dorsal medial-frontal cortex and anterior cingulate system. *J Child Psychol Psychiatry* 2003; **44**: 793–809.
65 Wink LK, Erickson Ca, Stigler Ka, McDougle CJ. Riluzole in autistic disorder. *J Child Adolesc Psychopharmacol* 2011; **21**: 375–379.
66 Ghaleiha A, Mohammadi E, Mohammadi M-R, Farokhnia M, Modabbernia A, Yekehtaz H *et al.* Riluzole as an adjunctive therapy to risperidone for the treatment of irritability in children with autistic disorder: a double-blind, placebo-controlled, randomized trial. *Paediatr Drugs* 2013; **15**: 505–514.
67 Grant PJ, Joseph La, Farmer Ca, Luckenbaugh Da, Lougee LC, Zarate Ca *et al.* 12-Week, placebo-controlled trial of add-on riluzole in the treatment of childhood-onset obsessive-compulsive disorder. *Neuropsychopharmacology* 2013; **39**: 1–7.

Supplementary Information accompanies the paper on the *Translational Psychiatry* website (http://www.nature.com/tp)

Supplementary Data to Ajram et al., 2017

	Mean (SEM)				RM ANOVA Between groups		RM ANOVA Within groups	
	Control		ASD					
					F	*p*	*F*	*p*
Measure	n = 20		n = 17					
	Placebo	**Riluzole**	**Placebo**	**Riluzole**				
Grey	54.5 (0.7)	49.9 (3.9)	53.8 (3.4)	53.9 (3.5)	0.2	0.67	1.3	0.27
White	22.6 (1.1)	22.3 (0.9)	22.6 (0.7)	22.2 (0.8)	0.3	0.59	1.2	0.28
CSF	23.2 (4.3)	22.2 (3.6)	20.2 (2.7)	19.5 (2.1)	6.9	**0.01**	5.9	**0.02**

Supplementary Table 1: Prefrontal cortex voxel composition

There were no significant main effects of group or drug on the proportion of grey or white matter in the prefrontal cortex voxel. There was a significant effect of riluzole ($F_{(1,32)}=6.9$, $p=0.01$) and group ($F_{(1,32)}=5.9$, $p=0.02$) on the proportion of CSF in the voxel, hence metabolite levels were corrected for CSF.

Cluster Index	Voxels	P	-log10P	Z-MAX	Z-MAX X (mm)	Z-MAX Y (mm)	Z-MAX Z (mm)	COPE-MAX	COPE-MEAN	Brain Region
Comparison of connectivity of DMPFC seed, on placebo, in ASD group vs. control group (Figure 4A), between subjects										
ASD>HV 2	831	0.0034	2.46	4.19	28	-52	16	0.21	0.121	Right occipital white matter, right intracalcarine cortex
ASD>HV 1	786	0.0049	2.31	4.01	-38	-46	22	0.218	0.084	Left cerebral white matter
HV>ASD 1	894	0.0021	2.68	3.96	12	-16	-24	0.626	0.247	Brainstem
Comparison of connectivity of DMPFC seed on riluzole vs. placebo, within the ASD group, within subjects (Figure 4C)										
Placebo> riluzole 2	1242	3.64E-06	5.44	4.01	24	-70	8	0.116	0.061	Right occipital white matter, right intracalcarine cortex, right lateral occipital cortex
Placebo> riluzole 1	462	0.0139	1.86	3.57	-58	-60	-4	0.135	0.0756	Left lateral occipital cortex
Comparison of effect of placebo vs. riluzole (negative slope of riluzole) in ASD vs. negative slope in controls (Figure 4C)										
ASD>HV 3	904	9.49E-05	4.02	3.81	24	-70	8	0.157	0.094	Right occipital white matter, right intracalcarine cortex, right lateral occipital cortex
ASD>HV 2	525	0.0063	2.2	3.79	20	-64	-22	0.204	0.0937	Right Cerebellum
ASD>HV 1	439	0.0186	1.73	3.66	-36	-40	-36	0.154	0.0888	Left cerebellum

Supplementary Table 2: Detail of fMRI result

3.1 Additional findings not included in the peer-reviewed publication

Additional analyses which were not incorporated into the publication are detailed below.

3.1.1 E-I responsivity and clinical symptoms

3.1.1.1 [1H]MRS

In the ASD cohort, where MRS data was available at two time points, the relationship between riluzole-evoked change in the inhibitory index, and clinical symptom profile was investigated. The percentage increase in the inhibitory index was shown to be inversely correlated with social ability, as measured using the ADOS (Pearson correlation; n=12, r=-0.663, p=0.019). Though there was a low n for the ADI, mainly due to advanced parental age, there was also a significant association between the ADI communication score and change in the inhibitory index (Pearson correlation; n=7, r =-0.803, p=0.03). Specifically, patients with lower social and communication scores (i.e. those who were least impaired according to the assessment) responded to riluzole with a larger percentage increase in PFC GABA fraction, than those who were deemed to have more difficulties (see Figure 3.1).

The inhibitory index at baseline (placebo condition) did not correlate with any measure from the ADOS or ADI.

3.1.1.2 Functional connectivity

There were no significant associations between baseline, or change, in functional connectivity with ADOS or ADI scores in the ASD cohort.

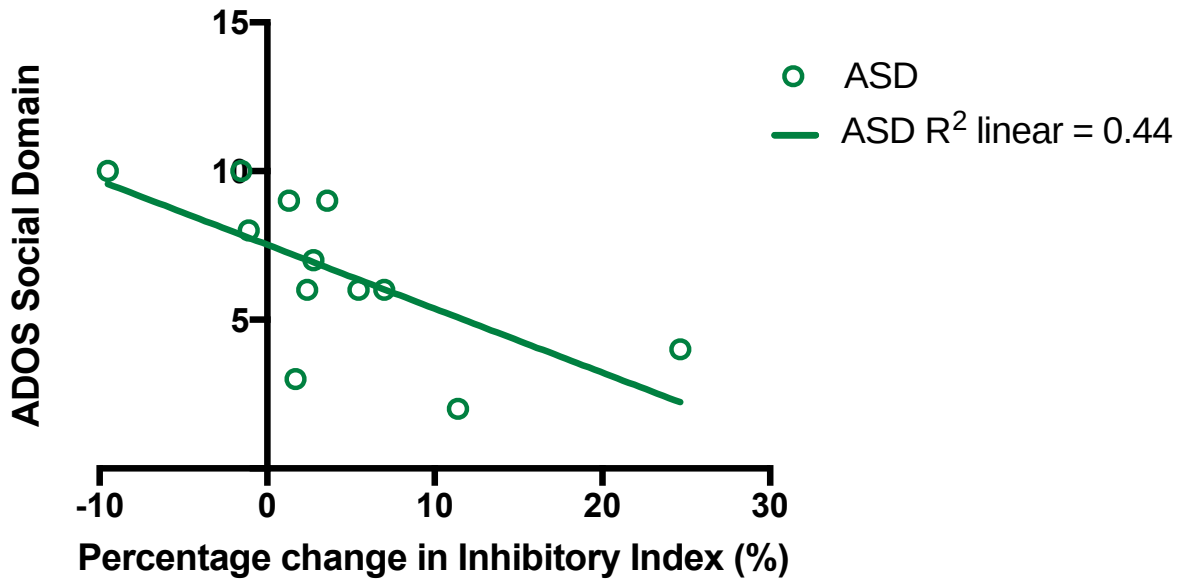

Figure 3.1: Riluzole evoked changes in PFC inhibitory index are related to core symptom domains in ASD

Riluzole-evoked percentage increase in the inhibitory index in ASD is inversely correlated with social ability, as measured by the ADOS: Pearson correlation; n=12, r=-0.663, p=0.019. Removal of the apparent outlier (x=24.7, y=4) did not affect significance (Pearson correlation with outlier removed; n=11, r=-0.71, p=0.014).

3.1.2 Metabolites levels and functional connectivity

As local changes in E-I metabolites are thought to influence wider network activity (Duncan et al., 2013; Stagg et al., 2014), the association of metabolite levels and functional connectivity were investigated.

There were no significant correlations of baseline glutamate, GABA or the inhibitory index at rest with baseline functional connectivity (data not shown). Likewise, there was no association between the riluzole-evoked change in PE and change in any MRS measure (Table 3.1). Additionally, baseline metabolite levels were not associated with the degree of change in connectivity (Table 3.1).

Group			Correlation		
			Inhibitory index	**GABA**	**Glx**
Control	*Pearson Correlation*	**Δ PE**	-0.495	-0.542	0.186
	Sig. (2-tailed)		0.213	0.166	0.66
	N		8	8	8
ASD	*Pearson Correlation*	**Δ PE**	-0.491	0.138	0.719
	Sig. (2-tailed)		0.263	0.768	0.068
	N		7	7	7
Group			**Correlation**		
			Δ Inhibitory index	**Δ GABA**	**Δ Glx**
Control	*Pearson Correlation*	**Δ PE**	0.171	0.223	0.157
	Sig. (2-tailed)		0.543	0.424	0.593
	N		15	15	14
ASD	*Pearson Correlation*	**Δ PE**	0.308	0.101	-0.17
	Sig. (2-tailed)		0.33	0.743	0.598
	N		12	13	12

Table 3.1: Correlation of MRS metabolites with functional connectivity (PE)

There were no significant associations between baseline or riluzole-evoked change in inhibitory index, glutamate or GABA with change in functional connectivity (PE) in either group.

3.2 Additional conclusions not included in the peer-reviewed publication

3.2.1 Clinical correlates- MRS

In addition to group differences in responsivity, the present study also identified a range of responses to riluzole in the ASD group; individuals with more ASD symptoms had the least shift in GABA fraction. Specifically, men with more social and communication difficulties (as measured by higher scores on the ADOS and ADI, respectively) showed the least response to riluzole (Figure 3.1). This is broadly consistent with previous findings that riluzole (Ghaleiha et al., 2013; Wink et al., 2011), and GABA acting drugs (such as arbaclofen (Frye, 2014)), have shown promise in reducing symptoms in some, but not all, ASD individuals. This may not be unexpected in a spectrum condition, but may inform the biological underpinnings of these symptoms. As there were no reported correlations between baseline GABA or glutamate measures with clinical symptoms scores, it may not be differences in baseline E-I metabolites which drives symptom severity- rather it is the lack of dynamic flux, and responsivity of the system which contributes to symptomatology.

3.2.2 Clinical correlates- fMRI

As highlighted in Ajram et al., 2017, the number of ASD participants who had both a full set of clinical assessment scores prior to scanning, and imaging data at both time points was lower than planned (ADOS n=12, ADI n=7). No clinical correlates were found with functional connectivity measures. Future investigations with a larger cohort will be necessary to increase power.

3.2.3 MRS-fMRI

It is widely established in the literature that local glutamate and GABA levels at rest determine the activity of neural networks (Duncan et al., 2013; Enzi et al., 2012; Horn et al., 2010; Kapogiannis et al., 2013; Kwon et al., 2014) . However, no one has investigated whether changes to metabolite flux correlate with changes in functional connectivity. There were no significant correlations between resting inhibitory index, GABA or glutamate levels with baseline functional connectivity of the ACC (data not shown). Likewise, there was no association between change in any MRS measure and change in ACC functional connectivity (Table 3.1). It was postulated that baseline metabolite levels may be predictive of the extent of change in functional connectivity elicited by riluzole, however no significant associations between any metabolite at rest and riluzole-evoked change in PE were found (Table 3.1).

Again, however, results are limited by the small sample size in these analyses, as not all participants obtained usable data on both scanning occasions, in both MRS and fMRI.

Finally, the present study focused on the prefrontal cortex as a region of interest, however, sub-cortical regions including the basal ganglia are also implicated in ASD. The following chapter examines the MRS findings from the subcortex.

Chapter 4

Shifting brain inhibitory balance of the basal ganglia of adults with autism spectrum disorder

4.1 Introduction

The previous chapter identified differences in the way that the adult prefrontal cortex of men with and without ASD responds to an E-I challenge with riluzole. However, subcortical pathology has also been implicated in ASD (Dawson et al., 2005; Dichter et al., 2012; Kohls et al., 2012; Langen et al., 2012; Naaijen et al., 2015). These findings are also consistent with the known role of fronto-striatal circuits in the processing of higher order cognitive and emotive information in neurotypical populations. Moreover, studies of both ASD and disorders which share traits with ASD, such as obsessive compulsive disorder (OCD), have documented a relationship between repetitive or stereotyped behaviours and abnormalities of basal ganglia structure and function (Calderoni et al., 2014; Langen et al., 2009; Rojas et al., 2006; Whiteside et al., 2004).

Therefore, in an extension to the prior chapter, (Ajram et al. 2017), I also used [1H]MRS to investigate excitatory-inhibitory flux in the basal ganglia in response to a riluzole challenge.

4.2 Methods

The research outlined in the present chapter took place as part of the study outlined in Chapter 3. The general methods are largely as described in Ajram et al., 2017 (pages 125-133). In brief, participants were scanned on two occasions, one week apart; and were given either a 50 mg oral dose of riluzole, or equivalent placebo. The order of drug administration was both randomised and double-blinded and order effects were controlled for by ensuring roughly half of participants received riluzole first, and half received placebo. MRS data acquisition began 1 hour after drug administration (see Figure 2.1 for a detailed timetable of in-scanner events).

4.2.1 [1H]MRS data acquisition

[1H]MRS data were acquired on a 3 Tesla GE Excite II Magnetic Resonance Imaging scanner (GE, USA). An initial structural scan was performed, which was then used to set the MRS voxel locations; namely a 3D inversion recovery prepared fast spoiled gradient-recalled echo (IR-FSPGR) acquisition (number of slices = 124, slice thickness = 1.1 mm, inversion time (TI) = 450 ms, repetition time (TR) = 7.084 ms, echo time (TE) = 2.84 ms, field of view=280 mm, flip angle=20°).

Single voxel J-edited MEGAPRESS spectra were then acquired in the left basal ganglia (see Figure 4.1 for example voxel placement) according to the following parameters:

Left basal ganglia, comprising of the head of the caudate, lateral thalamus and caudate putamen; 35 x 25 x 30 mm^3; TR = 1800 ms, TE = 68 ms.

The left basal ganglia was selected to correspond with previous data collection from this region in our department, and to enable future cross-study comparisons of different E-I interventions in this region (Horder et al. 2013 and unpublished data from Murphy lab, IOPPN). To avoid lateralisation effects, only right handed participants were recruited (see Appendix 4).

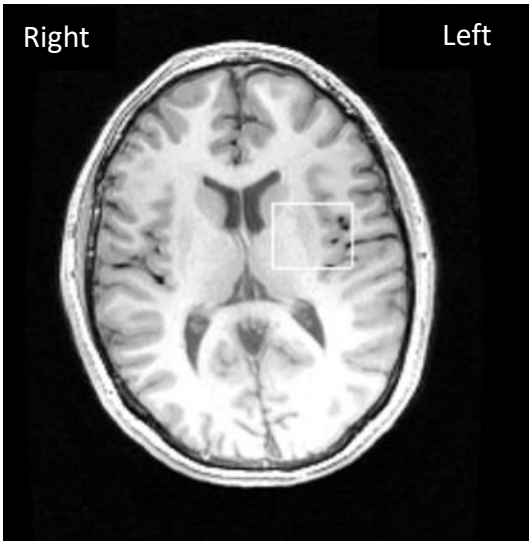

Figure 4.1: [1H]MRS basal ganglia voxel position

Basal ganglia region of interest outlined in white (35 x 25 x 30 mm^3) incorporating the head of the caudate, lateral thalamus and caudate putamen.

4.2.2 [1H]MRS data analysis

[1H]MRS data were pre-processed using previously described methods (see Chapter 2, section 2.1.4.5). Briefly, the unedited MRS spectrum and unsuppressed water spectrum were extracted using GE SAGE software (SAGE 2007, GE Healthcare, USA), prior to quantification of metabolites using jMRUI version 4 software (Naressi et al., 2001). Each spectrum was manually checked for quality (see Figure 4.2).

Metabolite concentrations were estimated at 3.0 ppm for GABA and Glx at two peaks; 3.8 ppm and 3.75 ppm. Absolute measures were calculated by dividing the peak amplitude by that of the unsuppressed water peak at 0.00 ppm.

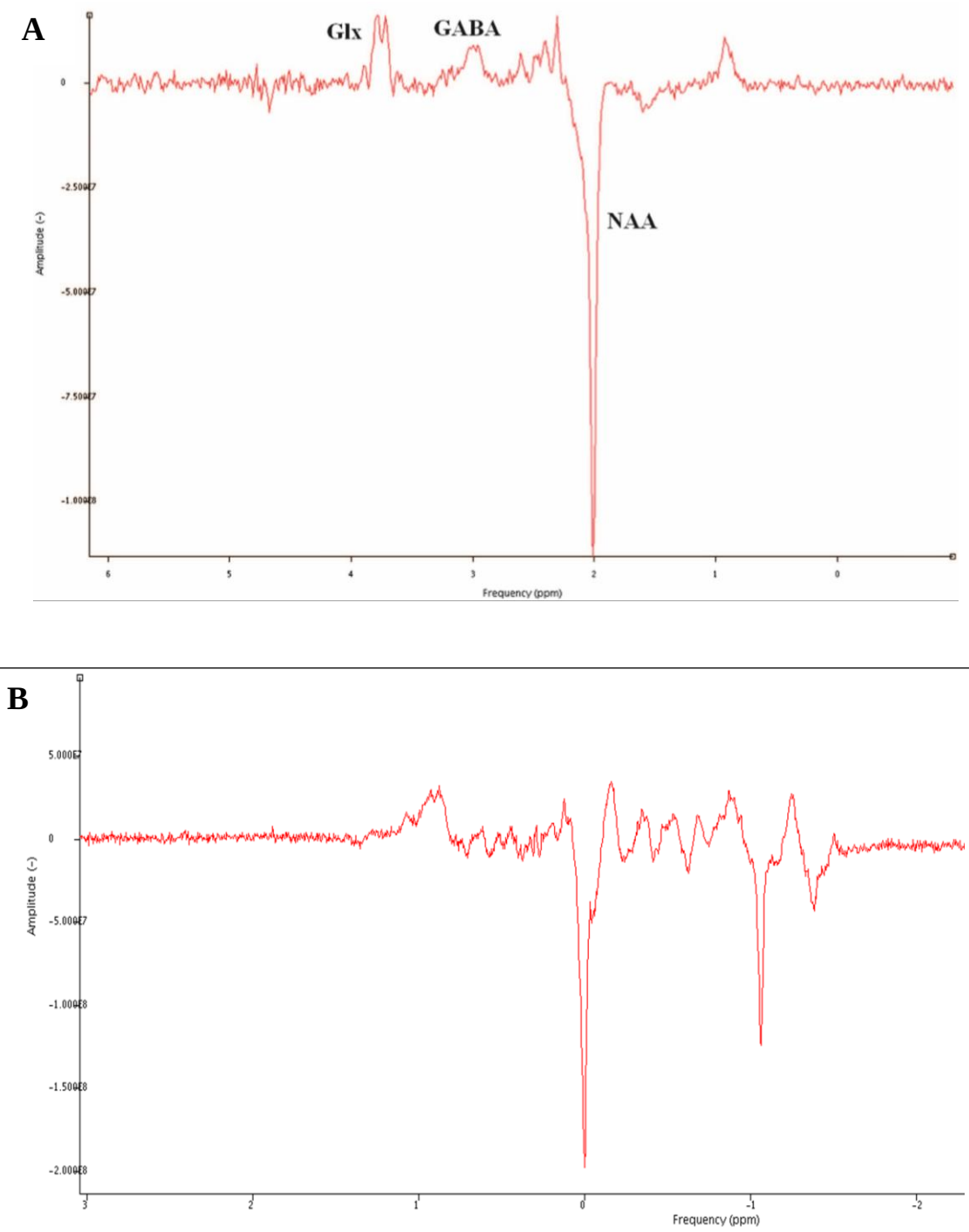

Figure 4.2: Example of good (A) and poor (B) quality [1H[MRS spectra

4.2.3 [1H]MRS voxel composition calculation

As described in further detail in Chapter 2 (section 2.1.4.5), partial volume effects are a potential confound for spectroscopy. Therefore, the relative levels of grey matter (GM), white matter (WM) and cerebrospinal fluid (CSF) were measured. No significant group differences were found in either grey or white matter (see Table 4.1). Assuming negligible levels of metabolites of interest in the CSF, all metabolite values were corrected for CSF variation.

Region	Measure	Mean (SEM)				RM ANOVA Between groups		RM ANOVA Within groups	
		Control, n=20		ASD, n= 17		*F*	*p*	*F*	*p*
		Placebo	Riluzole	Placebo	Riluzole				
Basal ganglia	**Grey**	50.1 (1.1)	44.9 (3.6)	47.1 (3.2)	50.1 (1.3)	1.3	.26	1.4	.24
	White	42.3 (1.3)	41.0 (2.5)	42.0 (1.5)	42.1 (1.5)	1.3	.26	1.1	.24
	CSF	7.6 (1.7)	6.5 (2.5)	7.9 (1.7)	7.7 (1.5)	2.0	.16	3.6	.07

Table 4.1: Percentage tissue composition in control (n=20) and ASD (n=17) basal ganglia [1H]-MRS voxels

There was no significant effect of group or drug on percentage composition of grey or white matter, nor CSF, in the basal ganglia voxel. RM ANOVA; degrees of freedom=1 for each analysis.

4.2.4 Statistical analysis

Statistical analyses were performed using IBM SPSS v.22 software (IBM SPSS Statistics for Macintosh, Version 22.0, USA). Figures were generated using GraphPad Prism version 7 for Windows (GraphPad Software, USA). Participant group comparisons were performed using independent samples t-tests. The numbers included in each MR analysis depended upon a stringent quality check of data available for each participant per analyses at each time point.

The [1H]MRS voxel composition in each group was compared using repeated measures two-way analysis of variance (RM 2-way ANOVA) with 'group' as between-subjects factor and 'drug' as within-subjects factor (control n=20, ASD n=17). A complete dataset of two time points for Glx levels was obtained for 29 participants and was compared using a RM 2-way ANOVA. Likewise, a complete dataset of two time points for the inhibitory index was obtained for 26 participants and was compared using a RM 2-way ANOVA. The State score measure of anxiety was included as a covariate in analysis of the inhibitory index, as anxiety is closely linked to GABA (Lydiard, 2003) and participants with ASD scored significantly higher than controls on measures of anxiety. Clinical scores were compared using independent samples t-tests.

Pearson correlation analyses were also used to compare the relationship of baseline, and the change in Glx and the inhibitory index with ASD symptom scores. For consistency, the State score measure of anxiety was included as a covariate in these analyses.

4.3 Results

4.3.1 Participant demographic and clinical symptoms

As reported in Chapter 3, participants did not significantly differ in age or IQ ($p=0.44$ and 0.15 respectively). As expected, the ASD group scored significantly higher in self-rated neuropsychological tests, including assessments of autism traits (AQ; $p<0.001$), anxiety (STAI; $p=0.004$) and obsessionality (OCI-R; $p<0.001$). The average scores across the gold standard diagnostic tests for ASD were above the cut off level for a diagnosis of autism.

4.3.2 Lower resting Glx levels in the ASD basal ganglia

At baseline (placebo), there were no group differences in the inhibitory index, or absolute levels of GABA in the basal ganglia region (see Table 4.2). There was however a significant group difference in baseline Glx, see Figure 4.3 and Table 4.2 (main effect of group, $F_{(1,29)} =4.926$, $p=0.034$). Riluzole did not significantly affect Glx levels in either group.

Region	Measure	Mean (SEM)						RM ANOVA Main effect of group		RM ANOVA Main effect of drug		RM ANOVA Drug*Group	
		Control			ASD			*F (df)*	*p*	*F (df)*	*p*	*F (df)*	*p*
		n	Placebo	Riluzole	n	Placebo	Riluzole						
Basal ganglia	**Index**	*13*	0.077 (0.001)	0.078 (0.001)	*13*	0.08 (0.001)	0.081 (0.001)	2.8 (1,23)	0.11	4.4 (1,23)	**0.048**	0.31 (1,23)	0.51
	GABA	*13*	0.406 (0.02)	0.44 (0.02)	*15*	0.384 (0.03)	0.416 (0.02)	1.2 (1,25)	0.29	3.6 (1,25)	0.07	0.37 (1,25)	0.55
	Glx	*16*	0.119 (0.008)	0.122 (0.002)	*15*	0.106 (0.006)	0.102 (0.006)	4.9 (1,29)	**0.034**	0.07 (1,29)	0.94	0.35 (1,29)	0.56

Table 4.2: E-I changes in the basal ganglia of men with and without ASD, after riluzole or placebo administration.

Riluzole increased the inhibitory index in both ASD and control groups in the basal ganglia. Baseline (placebo condition) Glx was significantly lower in the ASD group. Inhibitory index and GABA analyses were corrected for State anxiety measures. GABA and Glx mean and SEM are expressed as ($x10^3$). Significant p values are highlighted in bold. df = degrees of freedom. Repeated measures ANOVA displays between group (effect of diagnosis), within group (effect of drug treatment) and drug by group interactions.

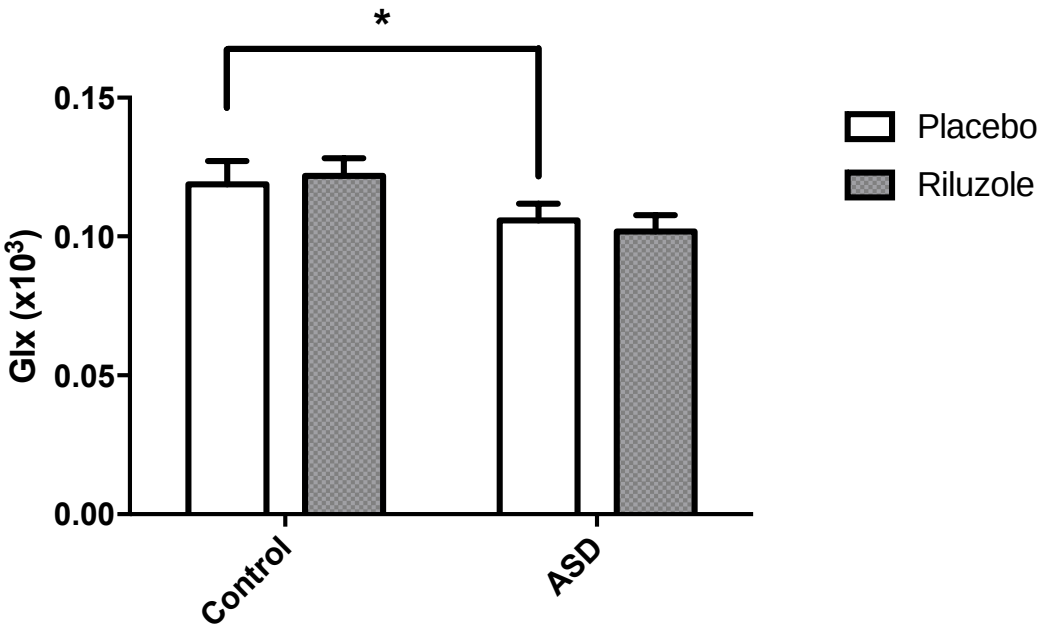

Figure 4.3: Significantly lower baseline Glx in ASD basal ganglia

Significantly lower Glx levels were observed in the ASD basal ganglia in the placebo condition, i.e. at baseline, compared to controls. ANOVA; main effect of group, $F_{(1,29)} = 4.926$, $p = 0.034$. Glx levels are presented as $x10^3$.

4.3.3 No group difference in E-I responsivity in the basal ganglia

To examine changes in E-I balance, as before, the inhibitory index was chosen as the dependent variable for further investigations.

Despite a trend towards a higher resting inhibitory index in controls, there were no statistically significant baseline group differences in inhibitory index in the basal ganglia (see Table 4.2). Riluzole increased the inhibitory index in both groups, to a similar degree, see Figure 4.4 (main effect of drug; $F_{(1,23)} = 4.382$, $p = 0.048$).

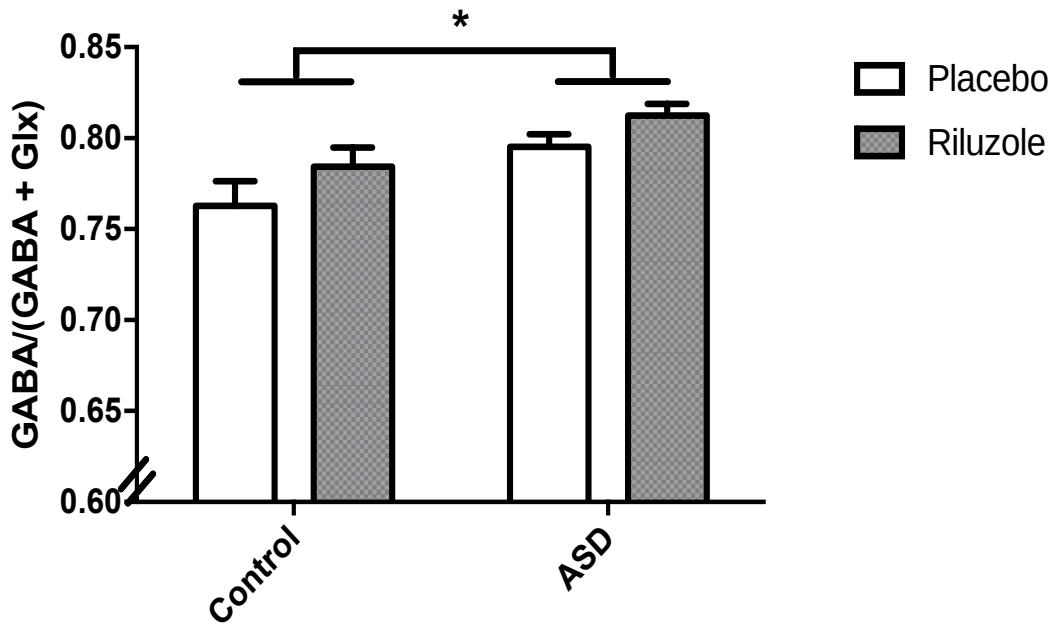

Figure 4.4: Riluzole increases the inhibitory index in the basal ganglia of both groups

Riluzole significantly increased the inhibitory index in the basal ganglia of both ASD and control participants; ANOVA; main effect of drug, $F_{(1,23)} = 4.382$, $p = 0.048$.

4.3.4 E-I responsivity and clinical symptoms

In the ASD cohort, where good quality MRS data was available at two time points, the relationship between riluzole-evoked change in the inhibitory index, and clinical symptom profile was investigated. There was no significant correlation between change in inhibitory index, or any domain of the ADOS or ADI. Likewise, there were no significant associations between baseline inhibitory index and ADOS or ADI scores. Despite the ASD cohort showing significantly lower baseline Glx compared to the control group, there were no significant correlations between Glx and ASD symptom scores (see Table 4.3). As there were no significant correlations between symptoms and responsivity, and due to the relatively low n for such correlations, it was not possible to stratify the patient population according to

degree of responsivity for the basal ganglia. This was possible to some extent in the prefrontal cortex (see previous chapter), where patients with lower social scores on the ADOS responded with the least change in the inhibitory index (Figure 3.1).

Region	Measure		Inhibitory Index	Δ Inhibitory index	Baseline Glx
Basal Ganglia	**ADOS Social**	*Pearson correlation (r)*	-0.37	0.376	-0.008
		Significance (p)	0.90	0.23	0.98
		N	14	12	15
	ADOS Communication	*Pearson correlation (r)*	0.034	0.009	-0.19
		Significance (p)	0.91	0.98	0.49
		N	14	12	15
	ADI Social	*Pearson correlation (r)*	0.614	-0.145	0.35
		Significance (p)	0.19	0.82	0.45
		N	6	5	7
	ADI Communication	*Pearson correlation (r)*	0.428	0.389	-0.89
		Significance (p)	0.40	0.52	0.85
		N	6	5	5

Table 4.3: Correlation basal ganglia E-I measures with clinical symptom scores

There were no significant correlations between the inhibitory index at baseline (placebo) or in change in the inhibitory index with any clinical measure. The ASD cohort had lower Glx level in the basal ganglia at rest, but there were no significant correlations between baseline Glx and clinical scores.

4.4 Discussion

In line with Ajram et al. (2017), this study provides direct evidence that E-I balance can be pharmacologically shifted in both the ASD and control brain. In the basal ganglia, this shift occurs to the same extent, and in the same direction in both groups, despite baseline differences in E-I balance.

4.4.1 Baseline metabolite differences

Consistent with findings from the prefrontal cortex, there were no baseline differences in the level of basal ganglia GABA in men with ASD relative to controls. However, there was a significant group difference in baseline Glx (Figure 4.3), with lower Glx in the ASD cohort. Lower subcortical glutamate in ASD is consistent with previous research from this department (Horder et al., 2013), but contradicts other findings of higher (Hassan et al., 2013) or no difference (Harada et al., 2011; Hardan et al., 2008) in glutamate indices relative to controls in the same region in ASD. This discrepancy may reflect inter-study differences, particularly in age, as both the present study and that of Horder et al., who report similar results, examined adults, whereas the others focused solely on children. Furthermore, unlike most studies, patients in the present study were psychoactive medication-free and had no co-morbid mental health conditions (particularly those with a known E-I underpinning cause, e.g. epilepsy) and therefore my findings cannot be explained by such potential confounds. Additionally, both Hassan et al. and Harada et al. recruited both male and female subjects, whereas the present study only recruited males. Brain chemistry has previously been shown to differ with age and sex in both healthy controls and ASD patients, hence differences in patient demographics may contribute to inconsistencies in the literature (Charles et al., 1994; Robinson et al., 2013; van de Lagemaat et al., 2014).

4.4.2 E-I response to challenge

In the basal ganglia, both groups responded in same way to riluzole; by increasing the inhibitory index after E-I challenge (Figure 4.4). This was in contrast to the group difference in the pattern of response to riluzole in the prefrontal cortex; whereby riluzole increased the inhibitory index in ASD, but decreased it in controls (see Appendix 6 for a table of basal ganglia and prefrontal cortex results). Collectively these findings indicate that the ASD group consistently responded with an increase in GABA tone to riluzole challenge, irrespective of the brain region tested, whereas controls had a regionally specific response profile. In the prefrontal cortex, the control group E-I balance was 'shifted' towards glutamate, whereas in the ASD group E-I balance was shifted towards GABA. In the basal ganglia, both groups shifted towards GABA (see Figure 4.5).

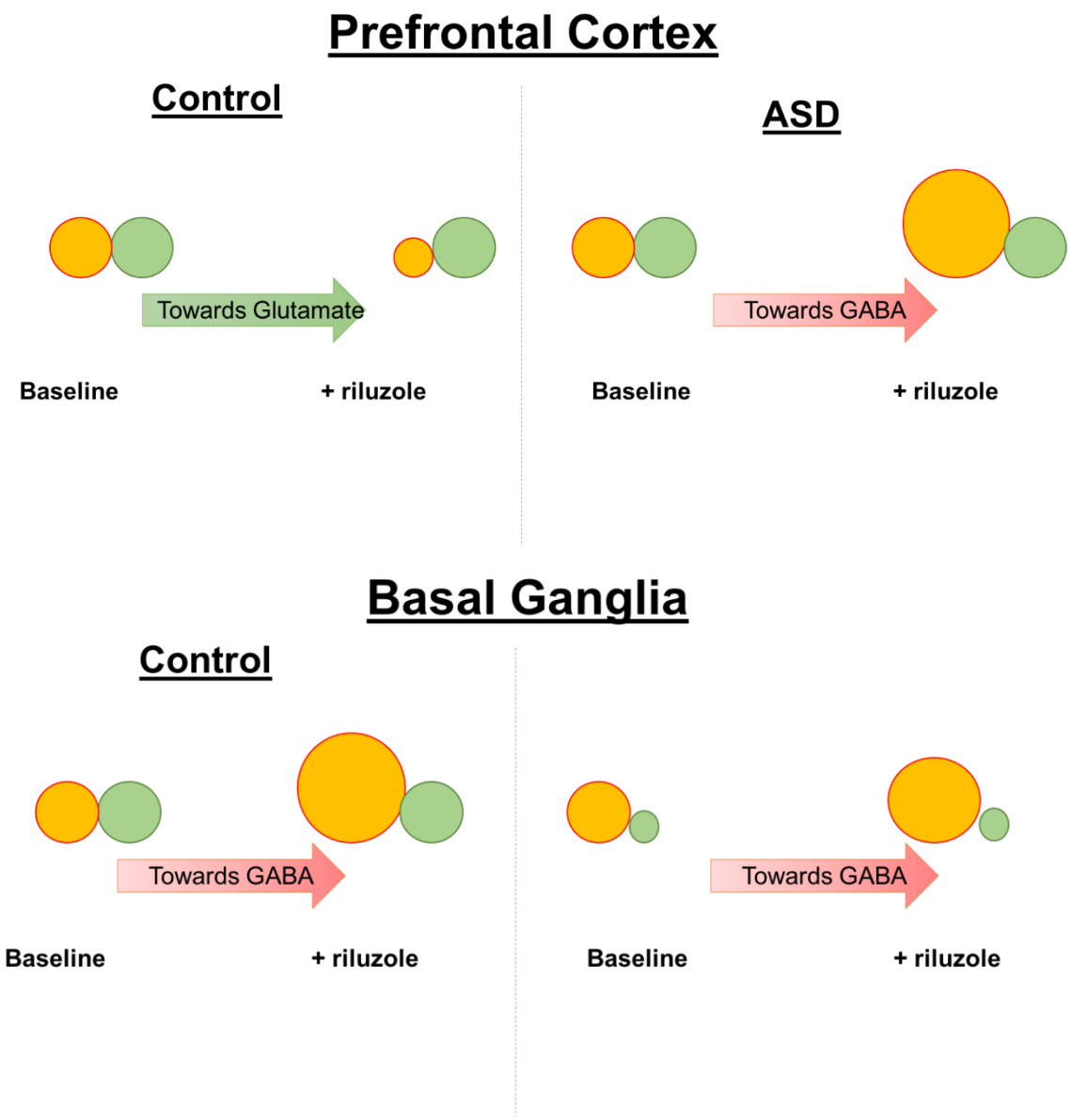

Figure 4.5: Representation of E-I shift in response to riluzole in the prefrontal cortex and basal ganglia

In the prefrontal cortex, riluzole shifted E-I balance towards glutamate in controls, but towards GABA in ASD. Conversely, in the basal ganglia; riluzole shifted E-I balance towards GABA in both groups

Key: orange circle represents GABA portion; green circle represents Glx portion; red arrow represents shift towards GABA; green arrow represents shift towards Glx. Proportions are not to scale and are intended to show direction of change, not size of change.

4.4.3 Regional cellular organisation

Though the degree of response in the two brain regions was not formally compared, it is clear that responsivity to E-I challenge is different in the prefrontal cortex and basal ganglia in controls, but not in ASD. Using MRS, it is not possible to fully understand the reason for the lack of a regionally distinct response profile in the ASD cohort, however both structural and neurochemical differences in the cortex and sub-cortex of the ASD brain compared to the typically developing brain, may play a role.

The prefrontal cortex consists primarily of excitatory pyramidal neurons, and a multitude of glial cells, which act as glutamate stores (Elston, 2003). Comparatively, the basal ganglia, in particular the striatum, is comprised primarily of GABAergic medium spiny neurons and has many inhibitory projections (Lanciego et al., 2012). Such regional differences in cellular organisation will no doubt infer differences in regional glutamate and GABA receptor distribution, which may in turn impact their availability for modulation by riluzole. For example, the degree of binding of GABA to $GABA_A$ receptors has been shown to differ throughout the control brain, depending on subunit assembly (Halonen et al., 2009) and in controls, glutamate receptors are generally more highly conserved in the PFC, compared to basal ganglia regions (Breese & Leonard, 1994). Likewise, the expression of enzymes involved in converting glutamate to GABA, which maintain E-I dynamics, such as GAD_{65} and GAD_{67} is known to differ between regions (Collins, 1972; Müller & Langemann, 1962). However, as discussed below, the composition and function of both brain regions are known to be altered in ASD (Calderoni et al., 2014; Fatemi et al., 2002; Hassan et al., 2013), which may go some way to explain why the response profile in ASD does not match that of controls.

4.4.4 Glial contribution

[1H]MRS samples the total tissue metabolite pool within both neurons and glia. The relative proportions of these two cell types differ from region to region (Pakkenberg & Gundersen, 1988; Sherwood et al., 2006), and may therefore contribute to the pattern of findings here. For example, there are a multitude of glial cells in the prefrontal cortex, which far outnumber neurons. Glial cells (astrocytes and microglia) are responsible for the uptake and storage of glutamate as glutamine, and the subsequent release of glutamine to be converted to glutamate for neurotransmission. They therefore act as a metabolic store, and are required in high quantities in the prefrontal cortex in particular due to the high metabolic demand of maintaining highly active prefrontal neurons with long dendritic projections (Sherwood et al., 2006). In addition to glutamate storage, glia help regulate E-I balance and maintain synaptic integrity (Auld & Robitaille, 2003; Domercq et al., 2013; Durieux et al., 2015; Graeber, 2010; Liang et al., 2006; Wake et al., 2009). In the prefrontal cortex (Chapter 3) the change in GABA fraction was correlated with the change in Glx in controls but not ASD. Therefore, it is possible that the typical neuronal-glia relationship is preserved in controls and maintains E-I balance.

In contrast, abnormalities in glia have been implicated in ASD (Bernstein et al., 2009; Durieux et al., 2015; Fatemi et al., 2008; Onore et al., 2012; Shigemori et al., 2015); and higher glial numbers have been shown in neurodevelopmental models and patients with ASD (Dickens et al., 2014; Suzuki et al., 2013). Moreover, differences in both glial number and activation state have been shown to be concentrated in prefrontal (e.g. ACC), and not in basal ganglia regions (Suzuki et al., 2013). Thus, I speculate that the proportions of cell populations contributing to E-I balance in the basal ganglia in ASD may be more similar to

controls and so the responsivity to E-I challenge is also similar. Unfortunately, MRS is not yet sensitive enough to tease out any differences in glial and neuronal alterations.

4.4.5 Receptor and enzyme contribution

As the cellular composition of both brain regions are known to be altered in ASD, so too are the regional distribution of receptors and enzymes which determine E-I balance. $GABA_A$ receptor expression has been shown to be abnormal across the ASD brain, with altered levels observed in the hippocampus (Blatt et al., 2001) and nucleus accumbens (Mendez et al., 2013). Pertinently- both $GABA_A$ and $GABA_B$ receptor expression is reportedly altered in the prefrontal cortex and anterior cingulate cortex of children and adults with ASD compared to controls (Fatemi et al., 2010, 2014; Mori et al., 2012; Oblak et al., 2009, 2010). This may go some way to explain why the effect of riluzole in the prefrontal cortex is different in ASD and controls, as one mechanism of action of riluzole is to potentiate GABA receptor activity.

Likewise, glutamate receptor expression is known to be altered across the brain in ASD- particularly in the cerebellum, where lower AMPA and higher NMDA and $mGluR_5$ receptors have been reported (Fatemi et al., 2011; Purcell et al., 2001). A near-significant trend towards increased $mGluR_5$ levels in the prefrontal cortex of ASD patients was reported by Lohith et al., (2013), yet lower levels in the same region and in animal models have been reported by others (Chana et al., 2015). With limited available post-mortem samples, it is difficult to fully map receptor levels across the human ASD brain, yet regional inconsistencies in receptor expression and perhaps function are apparent, which may interfere with riluzole's efficacy and could contribute to the pattern of results presented in this chapter. Similarly, the expression of enzymes which regulate glutamate-GABA flux is compromised in ASD. The majority of investigations into GAD_{65} and GAD_{67}, which convert glutamate to

GABA, focus on the cerebellum (Fatemi et al., 2002; Yip et al., 2007, 2009), where the concentration of enzymes is reportedly lower than in controls. In animal models, however, such as the valproic acid mouse model of ASD, the basal ganglia and prefrontal cortex have been examined. In these animals, GAD_{67} was found to be lower in the prefrontal cortex, but increased in the basal ganglia, whereas GAD_{65} was reduced in both regions (Wei et al., 2016). GAD_{65} is associated with synaptic terminals, and is therefore thought to impact synapatic transmission, whereas isoform 67 is associated with axonal regions and maintains metabolic stores (Esclapez, Tillakaratne, Kaufman, Tobin, & Houser, 1994; Martin & Rimvall, 1993). Both synaptic function, and metabolic stores of E-I metabolites awaiting use in transmission, may therefore be altered in ASD. Additionally, further metabolic alterations have been reported in the prefrontal cortex of patients with ASD by Shimmura et al., (2013), who highlighted decreased levels of kidney-type glutaminase in the anterior cingulate cortex, inferring altered glutamate-glutamine balance, which again, may impact the responsivity of the ASD prefrontal cortex.

Taken in combination; differences in regional cellular composition, receptor availability, and transmitter metabolic pathways may converge to create group differences in responsivity of the ASD brain, and may go some way to explain the differences observed in the prefrontal cortex in the present study.

Furthermore, the finding of altered baseline functional connectivity of the prefrontal cortex in the ASD group in Chapter 3, could also be considered as a contributing factor to regional responsivity differences. Therefore, whilst it is possible that the MRS response difference in GABA might explain the functional connectivity response, it could in fact, be the other way around. Thus, one cannot know whether by altering FC of the rest of brain with ACC in

ASD, a secondary effect is a shift in metabolite in this 'reconnected' region. Long-range connections are complex and thus the shift in connectivity may have been accompanied by metabolite shifts in multiple inter-connected subcortical and cortical components of this pathway including in posterior cortices. Unfortunately, I did not acquire MRS across whole brain, which might have helped to understand the relationship between metabolite shifts and functional connectivity changes.

The explanations suggested above may well be an over-simplification. Although both the control and ASD groups responded in the same direction to riluzole challenge in the basal ganglia, it is unclear whether this is a 'normal' response in ASD and indeed the baseline E-I was abnormal in this region in the ASD group. The MRS voxels used in these experiments incorporated, multiple anatomical structures. Both cortical and sub-cortical voxels captured a mix of CSF, grey matter and white matter; and although the voxel composition was segmented to control for variation in tissue composition, the target was sizeable. The basal ganglia voxel itself encroached upon the thalamus, insula, internal capsule and caudate putamen and it is well documented that the size, in terms of both volume and surface area, of basal ganglia structures is altered in ASD (Estes et al., 2011; Sato et al., 2014; Schuetze et al., 2016), therefore the ASD voxel in our studies and in work by other teams may capture different parts of the basal ganglia than the voxel in control group. That being said, there were no significant group differences in the percentage composition of either voxel in either grey or white matter (Supplementary Table 1 and Table 4.1), but it is impossible to tell which anatomical regions the relevant proportions of tissue belong to.

The relative proportions of white (PFC ~ 40%, basal ganglia ~ 20%), but not grey matter (~50% in both PFC and basal ganglia) differed between the two brain regions tested, though

since there were no differences in each voxel's composition between groups and variations in voxel composition were accounted for, the tissue composition at the level of grey/white matter is unlikely to account for the differences in regional responsivity in the groups.

4.5 Limitations

Thus, [1H]MRS is a valuable, yet relatively 'crude' measure of E-I balance, and can only show bulk measures of total metabolite levels within relatively large regions of brain. As a result, MRS is unlikely to be sensitive to synaptic levels of neurotransmitters and should not therefore be assumed to measure neural signalling (Dager et al., 2008). Additionally, the metabolite measures acquired do not reflect absolute concentrations of GABA and glutamate; as they are contaminated with other signals (e.g. the GABA signal also contains macromolecule and is reported as GABA+; and the Glx signal is a combination of glutamate and its metabolite glutamine). It is possible therefore that the presence of these additional molecules may confound results (see General methods, section 2.1.4.6 for further details). Steps to minimise the impact of these combined signals are now available, using suppression and editing techniques (Edden et al., 2012; Harris et al., 2015; Ramadan et al., 2013; Shungu et al., 2016). Whilst this technology was not available for the present study, future work should utilise these techniques to aim for a 'pure' sample of glutamate and GABA.

I also acknowledge that, although based upon prior power calculations, the sample size for this study was still modest. However, according to previously published data from our scanner, n=12 is sufficient to detect a 10% alteration in E-I levels at a power of 0.8 (Stone et al., 2012). I can be confident therefore that any significant findings (such as the group difference in basal Glx levels) are sufficiently powered, and similarly, findings of no difference are unlikely to be due to a lack of power. In analyses where no significant results

were found, for example where there were no group differences in response to riluzole in the basal ganglia, sample analysis calculations indicate that a total n of 262 would be necessary to find a statistically significant difference between groups (Clin Calc LLC, 2018). If putative differences were obtained with such large numbers, they may be statistically significant, but are unlikely to be clinically significant.

Finally, this study was intended as an initial 'Proof of Concept' study to test responsivity differences in ASD, but was not powered to examine symptom correlates. To accommodate correlation analyses, with an estimated moderate-large effect size (r=0.5) between acute changes in the inhibitory index and primary symptom measures, at α=0.05 and a power of 0.9, the sample size would need to be n=31. Thus, the absence of a relationship between symptoms and E-I responsivity in ASD may represent a false negative finding. Future work will be required to confirm the findings from this study (particularly with regards to clinical correlates) in a larger cohort and determine if these are generalisable, for example, to females with ASD, to other age groups and/or to individuals with intellectual difficulties.

4.6 Conclusions

For the first time, I have shown that E-I balance can be pharmacologically 'shifted' in control subjects and in patients with an established E-I imbalance. Furthermore, the nature of responsivity to E-I challenge differs between adult men with and without ASD. Specifically, the control subjects' response to riluzole in the prefrontal cortex and basal ganglia is in opposite directions, whilst participants with ASD respond in the same direction, irrespective of brain region. While this evidence that E-I balance can be modulated in ASD gives reason

for hope in the search for pharmacological treatment options, I have also shown that the response in the ASD brain is pharmacologically atypical. The latter may have important implications for drug development and suggests we cannot assume that drugs work in the same way in the neurodevelopmental spectrum as in unaffected individuals.

4.7 Next steps

It is clear from both the MRS and fMRI data presented thus far that there are alterations in E-I flux in ASD. However, with the techniques available in humans, it was not possible to tell how changes to metabolite levels at a cellular level drive changes in functional connectivity. Direct measurement of changes in extracellular E-I (efflux) following riluzole administration may help address this question and therefore, I used a rat model – the *Neurexin1α* knock-out.

Chapter 5

The *Neurexin1α* knock out rat as a model of ASD: Initial preclinical investigations

5.1 Introduction

Genetic alterations which compromise E-I synaptic stability have been consistently linked to neurodevelopmental disorders (Jamain et al., 2003; Südhof, 2008; Zhao et al., 2017). In particular, copy number variations in the *Neurexin1* gene have been repeatedly observed in patients with ASD (Bucan et al., 2009; Ching et al., 2010; Dabell et al., 2013; Feng et al., 2006; Gauthier et al., 2011; Glessner et al., 2009; Kim et al., 2008; The Autism Genome Project Consortium, 2007; Yan et al., 2008) and may contribute to 0.5% of total incidences (Etherton et al., 2009). Mostly, disruptions to the alpha (α) isoform of *Neurexin1* are implicated, and *Neurexin1α* has therefore become a target for manipulation in animal models.

Studies using *Neurexin1α* homozygous knock out (*Nrxn1α*$^{-/-}$) mice and rats have shown that removing this gene causes deficits in social behaviour which may proxy the core symptoms of the human condition (Dachtler et al., 2015; Esclassan et al., 2015; et al., 2009; Grayton et al., 2013; Laarakker et al., 2012). Additionally, *Nrxn1α*$^{-/-}$ models show abnormalities in E-I transmission, including decreased excitatory synaptic strength, reduced EPSC frequency and reduced release of both excitatory and inhibitory neurotransmitters (Etherton et al., 2009; Kattenstroth et al., 2004; Missler et al., 2003; Zhang et al., 2005). The *Nrxn1α*$^{-/-}$ rat was therefore selected as a model for continuing investigations into E-I flux in ASD. However, whilst the existing literature infers an E-I imbalance in this model, no one has directly

investigated E-I flux in a *Nrxn1-α* deficient animal. The following experiments were therefore designed to determine the face validity of the *Nrxn1α*$^{-/-}$ rat as a model of disrupted E-I and test whether the neurochemistry of the *Nrxn1α*$^{-/-}$ rat would match that of the human patient population, both at baseline, and after riluzole administration.

For consistency, the following rodent experiments aimed to mirror those undertaken in the human MRS study. First, it was necessary to establish an equivalent dose and route of administration of riluzole which would be comparable across species, and confirm the pharmacokinetics (PK) in this rat model (see Study 1, section 5.2). Next the aim was to establish whether the baseline findings of the human MRS study were comparable with the neurochemistry of the animal model at baseline. To this end, HPLC was used to capture bulk intracellular levels of metabolites in specific volumes (weights) of tissue as this method has been shown to produce equivalent results to MRS (Fatouros et al., 2000). Bulk measures of neurotransmitters were measured *ex vivo* in equivalent brain regions in rats, namely the prefrontal cortex and caudate putamen.

5.2 Study 1: Riluzole pharmacokinetics in the rodent

50 mg is the standard oral dose prescribed to adults with Amyotrophic Lateral Sclerosis (ALS) and was therefore deemed a suitable dose to use as an initial challenge for the human study (Bryson et al., 1996; Joint Formularly Committee, 2017). Using a dose translation equation, 4 mg/kg riluzole oral dose (p.o.) was calculated as the rodent equivalent to the 50 mg tablet administered to humans (see General Methods section 2.2.2.1 for full details). This dose was within the range used in previous rodent studies (Chew et al., 2014; Sung et al., 2003), with minimal side effects (which appear over 10 mg/kg), and far below the lethal dose (LD_{50}) of 85 mg/kg (Sanofi-Aventis, 2010). Riluzole at a similar dose (5 mg/kg) shows rapid brain penetration which is dependent upon plasma concentrations (Milane et al., 2009); but this data comes from intraperitoneal injections in mice. However, as the literature on riluzole PK in the rodent varies greatly in dose concentration, route of administration and animal species (Milane et al., 2009; Ravi et al., 2013; Wu et al., 2013), a PK study was conducted in wild type adult Wistar rats to establish the presence of riluzole in the rat brain and plasma after a 4 mg/kg oral dose.

5.2.1 Methods

The full protocol can be found in General Methods section 2.2.3. Briefly, 12 male Wistar rats (average weight 319.9 ± 4.1 grams) were culled by a rising concentration of CO_2 0.5, 1, 2, or 4 hours (n=3/group) after a 4 mg/kg oral dose of riluzole (in 1% HEC). Blood was collected by cardiac puncture and plasma separated by centrifugation. Following removal of blood, brains were removed and the forebrain cut at the level of the optic chiasm. Forebrains were weighed and all samples were frozen and stored at -80^{o}C pending analysis. Samples were analysed using previously described methods (General Methods section 2.2.6). Plasma and

brain concentrations of riluzole are presented as ng/ml or ng/g of sample respectively and the brain:plasma ratio was calculated as brain riluzole concentration divided by plasma riluzole concentration.

5.2.2 Results

5.2.2.1 Riluzole is present in the plasma and brain after 4 mg/kg dose

Riluzole was detected in the brain and plasma at each time point measured, with peak exposure times of 3 and 4 hours post-dose, respectively (Table 5.1 and Figure 5.1). Brain exposure was approximately 5 times that of plasma exposure, as determined by the brain/plasma ratio (see Table 5.1).

Time (hr)	Plasma Concentration (ng/ml) Mean (±SEM)	Brain Concentration (ng/g) Mean (±SEM)	Brain:Plasma Ratio Mean (±SEM)
0.5	647 (81)	3413 (507)	5.24 (0.4)
1	576 (24)	3470 (19)	6.09 (0.5)
2	1011 (72)	5683 (418)	5.67 (0.6)
4	1150 (39)	5267 (172)	4.58 (0.08)

Table 5.1: Mean riluzole brain and plasma concentrations after 4 mg/kg oral dose

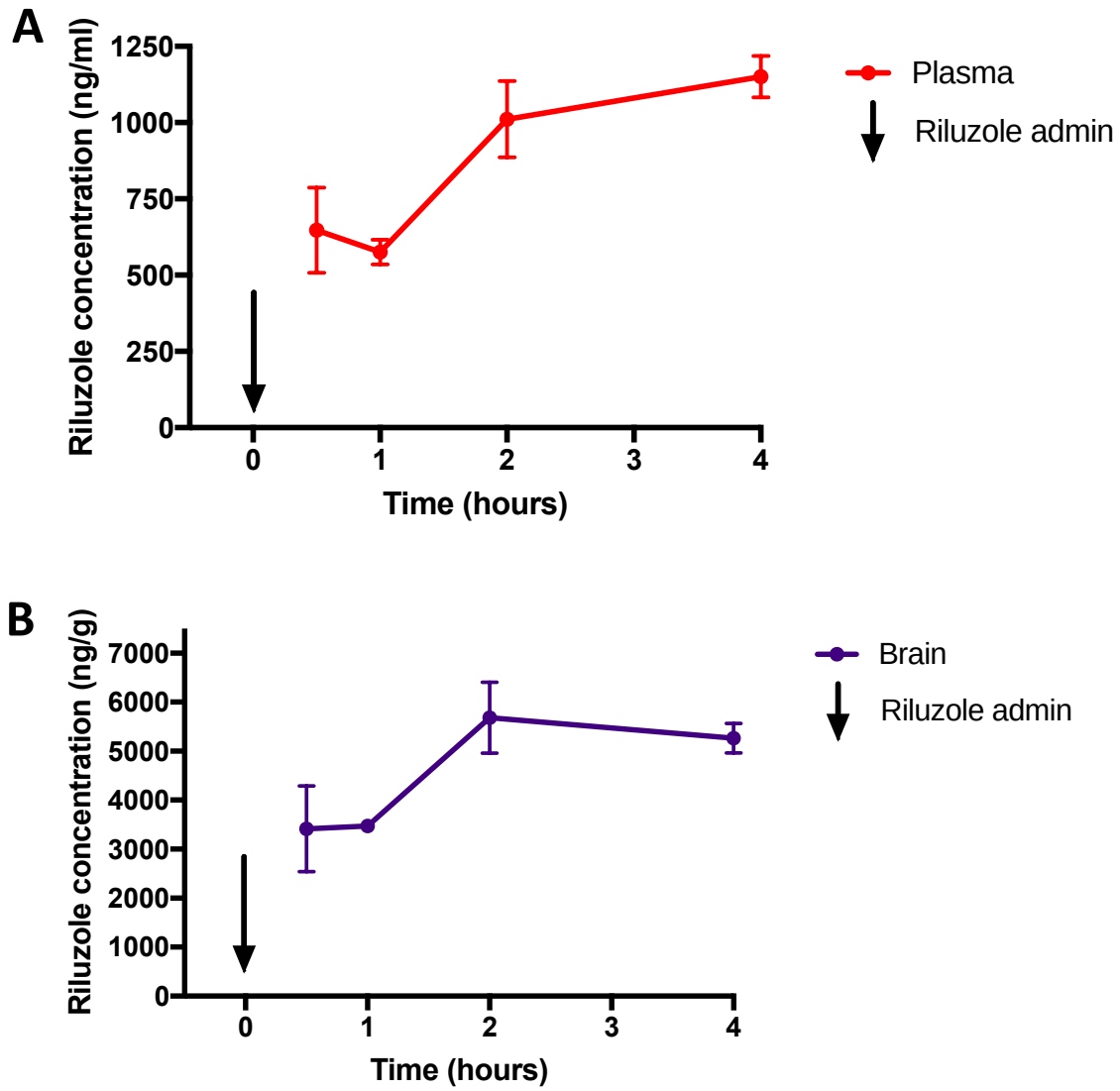

Figure 5.1: Plasma (A) and brain (B) concentration of riluzole after 4 mg/kg oral dose in wild type rats

(A) Riluzole is present in the plasma up to 4 hours post 4 mg/kg oral dose, with a peak concentration at the 4 hour time point.

(B) Riluzole is present in the brain up to 4 hours post 4 mg/kg oral dose, with a peak concentration at the 3 hour time point.

5.2.3 Conclusions

After a single oral dose of 4 mg/kg, riluzole was present in both the rat brain and plasma from the initial sampling time of 30 minutes up to 4 hours post-dose. Peak plasma concentrations were achieved at 4 hours post-dose, and peak brain concentration at 3 hours post dose. The drop in brain riluzole concentration after 3 hours, and subsequent increase in plasma levels may indicate riluzole starting to leave the brain and being effluxed through the blood-brain barrier (BBB) back to the bloodstream. Furthermore, brain exposure in the rat was found to be around five times higher than that of plasma exposure. This is consistent with previous PK studies in mice, where brain levels of riluzole were found to be four (Milane et al., 2009) or five (Colovic et al., 2004) times higher than plasma levels.

In addition to confirming the presence of riluzole in the rodent brain, this study also has implications for the previously conducted human study. Though plasma concentrations of riluzole in humans are well documented, the levels of riluzole in the human brain after dosing have not been evaluated. Whilst riluzole is able to cross the blood-brain barrier (Sanofi-Aventis, 2010), levels are impossible to directly sample in the living human brain. Assuming the brain:plasma ratio is equivalent in humans and rodents, it could be estimated that the concentration of riluzole in the human brain is likely to be around five times that of the plasma. Taken together with the known plasma levels of 50 mg oral riluzole in humans at C_{max} (1 hour post-dose) as between 52-300 ng/ml[1] or 0.2-1.2 μM (Abbara et al., 2011; Groeneveld et al., 2008; Le Liboux et al., 1997), it was anticipated that, at an estimated five

[1] This value varies greatly between and within studies, for example Le Liboux et al., record C_{max} at 1 hour post-dose as 180 ± 1220 ng/ml.

times higher concentration in the brain, riluzole would be at a concentration that should be sufficient to cause the changes in E-I dynamics observed in the human studies outlined in previous chapters.

5.3 Study 2: E-I responsivity of *Neurexin 1α* $^{-/-}$ rats (*ex vivo*)

Having established that riluzole was present in the rat brain, the next stage was to examine whether the drug had an equivalent effect on E-I responsivity of the PFC and CPu as in the human sample. Firstly, experiments investigated whether there were any initial E-I differences in *Nrxn1α* $^{-/-}$ rat at baseline, compared to wild type controls. To compare the results to the human findings, baseline GABA and glutamate levels were examined. However, as the measure of glutamate used in the human MRS studies was in fact Glx (glutamate and glutamine combined), levels of glutamine were also measured in the rodent.

5.3.1 Methods

16 adult male Wistar *Nrxn1α* $^{-/-}$ rats and 16 littermate controls were sourced from SAGE labs and housed in standard conditions (see General Methods chapter 2.2.1 for further detail). One *Nrxn1α* $^{-/-}$ rat had to be sacrificed after microdialysis surgery as the cement used to attach the probes did not bond to the skull, and was therefore excluded from all analyses to give an experimental sample of n=15 *Nrxn1α* $^{-/-}$ and n=16 wild types. Rats did not differ in weight (WT, 493.8 ± 11.6 grams; *Nrxn1α* $^{-/-}$, 495.2 ± 15.9 grams; t=0.07 (29), p=0.94) or age (WT, 23.4 ± 0.4 weeks; *Nrxn1α* $^{-/-}$, 21.7 ± 1.5 weeks; t=1.14 (29), p=0.26). See Figure 5.2.

All rats underwent microdialysis probe implantation surgery followed by *in vivo* microdialysis experiments (see General Methods section 2.2.4 for further details). Rats were dosed with either 4 mg/kg riluzole (in 1% HEC), or vehicle only (1% HEC); WT vehicle n=8, *Nrxn1α*$^{-/-}$ vehicle n=7, WT riluzole n=8, *Nrxn1α*$^{-/-}$ riluzole n=8. Following *in vivo* microdialysis, animals were culled using a non-Schedule 1 procedure by exposure to a rising concentration of CO_2 prior to decapitation by guillotine. Brains were removed and the PFC and CPu dissected and frozen pending analysis (see General Methods section 2.2.5.1 for further detail). Time from vehicle/drug administration to sample freezing (dose to dissection time, DTD) and time from euthanasia to sample freezing (post mortem interval, PMI) were recorded (Table 5.2).

Brain tissue samples were analysed using previously described methods (General Methods section 2.2.6). Independent samples t-tests were used to compare group weight, age, DTD and PMI times (within drug treatment sub-groups). One-way ANOVA was used to compare DTD and PMI times across all groups. Two-way ANOVA was used to compare regional brain weights, with region and group as the variables of interest. Baseline glutamate, glutamine and GABA levels and glutamine-glutamate ratios were compared using independent t-tests. Values were then converted to the inhibitory index. In the human MRS study, the inhibitory index was expressed as GABA/(GABA + Glx), where Glx represented the combined measure of glutamate and glutamine. For consistency across studies, the inhibitory index in the rodent was also expressed as GABA/(GABA + Glx), where Glx is the sum of glutamate and glutamine.

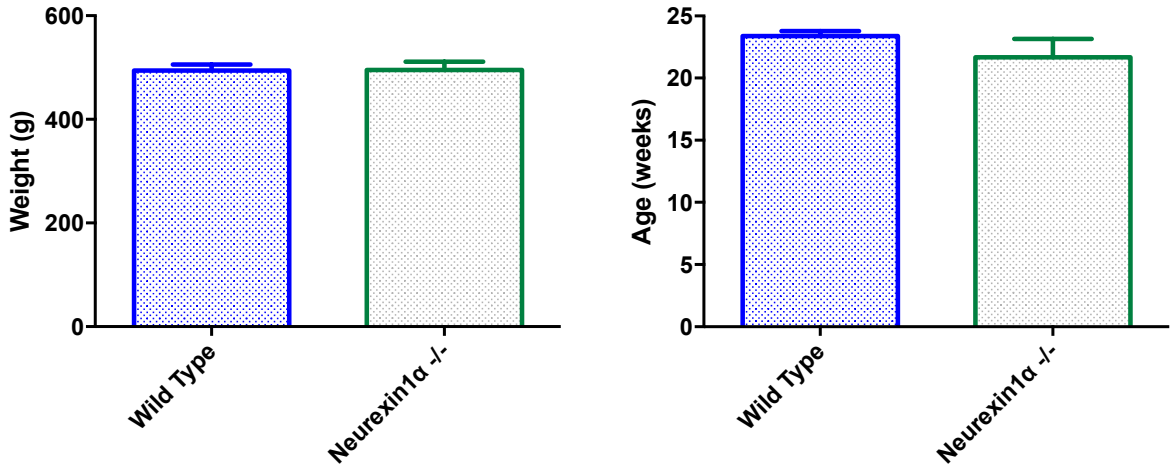

Figure 5.2: Experimental rats did not differ in weight or age

There were no significant differences between wild type and *Nrxn1α* $^{-/-}$ rats in weight (t=0.07 (df=29), p=0.94) or age (t=1.14 (df=29), p=0.26).

Time from dose to dissection (DTD), minutes (mean ± SEM)						
Wild Type vehicle (n=8)	*Neurexin1α*$^{-/-}$ vehicle (n=7)	Wild Type riluzole (n=8)	*Neurexin1α*$^{-/-}$ riluzole (n=8)	One-Way ANOVA	T-test (vehicle)	T-test (riluzole)
224.3 (3.6)	239.1 (7.6)	228.1 (4.5)	227.1 (6.5)	$F_{(3,27)}$ =1.26 p=0.31	t=1.85 (13) p=0.09	t=0.13 (14) p=0.90
Post mortem interval (PMI), minutes (mean ± SEM)						
8.4 (1.8)	7.3 (1.0)	8.9 (1.4)	9.3 (1.1)	$F_{(3,27)}$ =0.36 p=0.79	t=0.51 (13) p=0.62	t=0.21 (14) p=0.84

Table 5.2: Mean time from dose to dissection and from dissection to sample freezing

There were no significant differences between groups in time from dose to dissection, or post mortem interval (dissection to freezing time).

5.3.2 Results

5.3.2.1 Regional brain weight

There were no significant group differences when comparing the weight of each dissected brain region; main effect of group, $F_{(1,57)} = 0.08$, $p = 0.78$ (Figure 5.3).

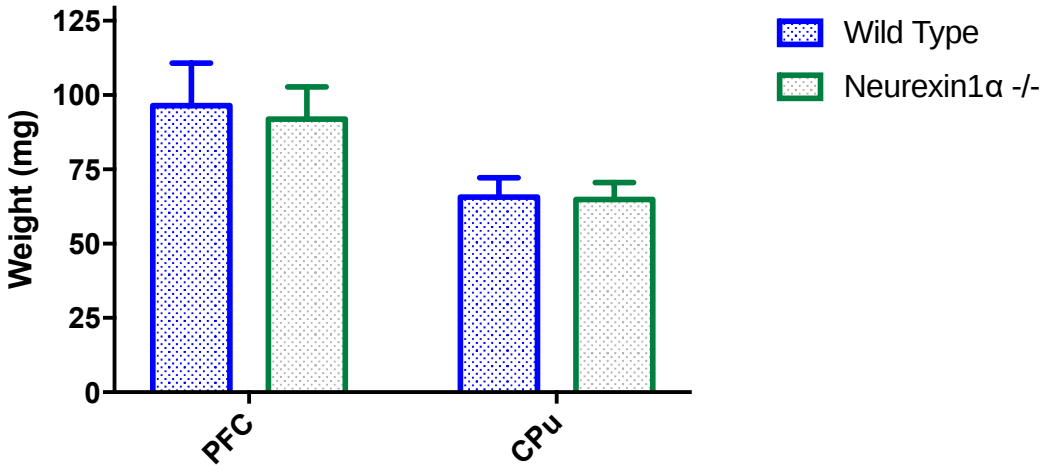

Figure 5.3: Regional brain weights

No significant group difference in regional brain weights (main effect of group; $F_{(1,57)} = 0.08$, $p = 0.78$).

5.3.2.2 Baseline metabolite levels in the rat prefrontal cortex

There were no significant group differences in baseline (vehicle) GABA or glutamate levels between wild type and *Nrxn1α*$^{-/-}$ rats in the PFC (GABA, t=0.11 (13), p=0.91; glutamate, t=0.54 (13), p=0.60, WT n=8, *Nrxn1α*$^{-/-}$ n=7), see Figure 5.4 A and B, respectively. There was however, a significant group difference in baseline glutamine in the same region (glutamine, t=3.16 (12), p=0.008, n=7/group), see Figure 5.4 C, and the ratio of glutamate to glutamine was significantly lower in *Nrxn1α*$^{-/-}$ rats compared to wild types (t=3.18 (12), p=0.008, n=7/group), Figure 5.4 D. When glutamate and glutamine levels were combined, as in the human study (Glx), there was no significant group difference between baseline levels; t=1.48 (12), p=0.16.

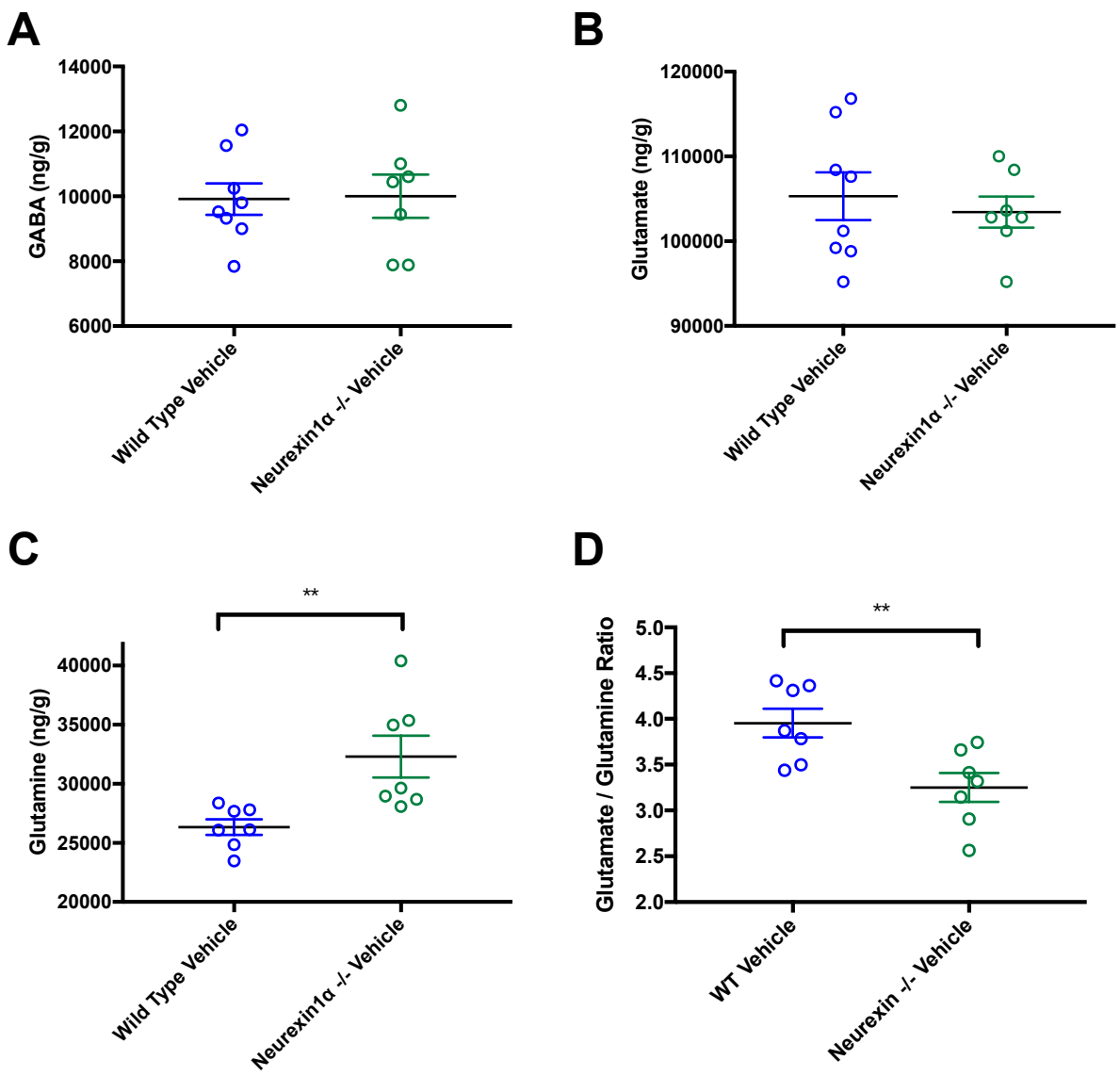

Figure 5.4: Baseline GABA (A), glutamate (B), glutamine (C) and Glu/Gln ratio (D) in the prefrontal cortex of wild type and *Nrxn1α*$^{-/-}$ rats

There were no significant group differences in baseline (vehicle) measures of GABA (A) or glutamate (B), but there was a significant group difference in baseline glutamine (C) in the PFC ($t=3.16$ (12), $p=0.008$, n=7/group). This translated to a significant group difference in the baseline glutamate-glutamine ratio ($t=3.18$ (12), $p=0.008$, n=7/group).

5.3.2.3 Baseline metabolite levels in the rat caudate putamen

There were no significant group differences in baseline (vehicle) GABA or glutamine levels between wild type and *Nrxn1α* $^{-/-}$ rats in the CPu (GABA, t=0.18 (13), p=0.86; glutamine, t=1.1 (13), p=0.31, WT n=8, *Nrxn1α* $^{-/-}$ n=7). See Figure 5.5 A and C, respectively. There was however, a significant group difference in baseline glutamate in the same region (glutamate, t=2.14 (11), p=0.05, WT n=6, *Nrxn1α* $^{-/-}$ n=7, see Figure 5.5 B), and the ratio of glutamate to glutamine was significantly lower in *Nrxn1α* $^{-/-}$ rats compared to wild types (t=2.81 (12), p=0.02, WT n=6, *Nrxn1α* $^{-/-}$ n=7, see Figure 5.5 D). When glutamate and glutamine levels were combined, as in the human study (Glx), there were no significant group differences between baseline levels; t=1.08 (11), p=0.3.

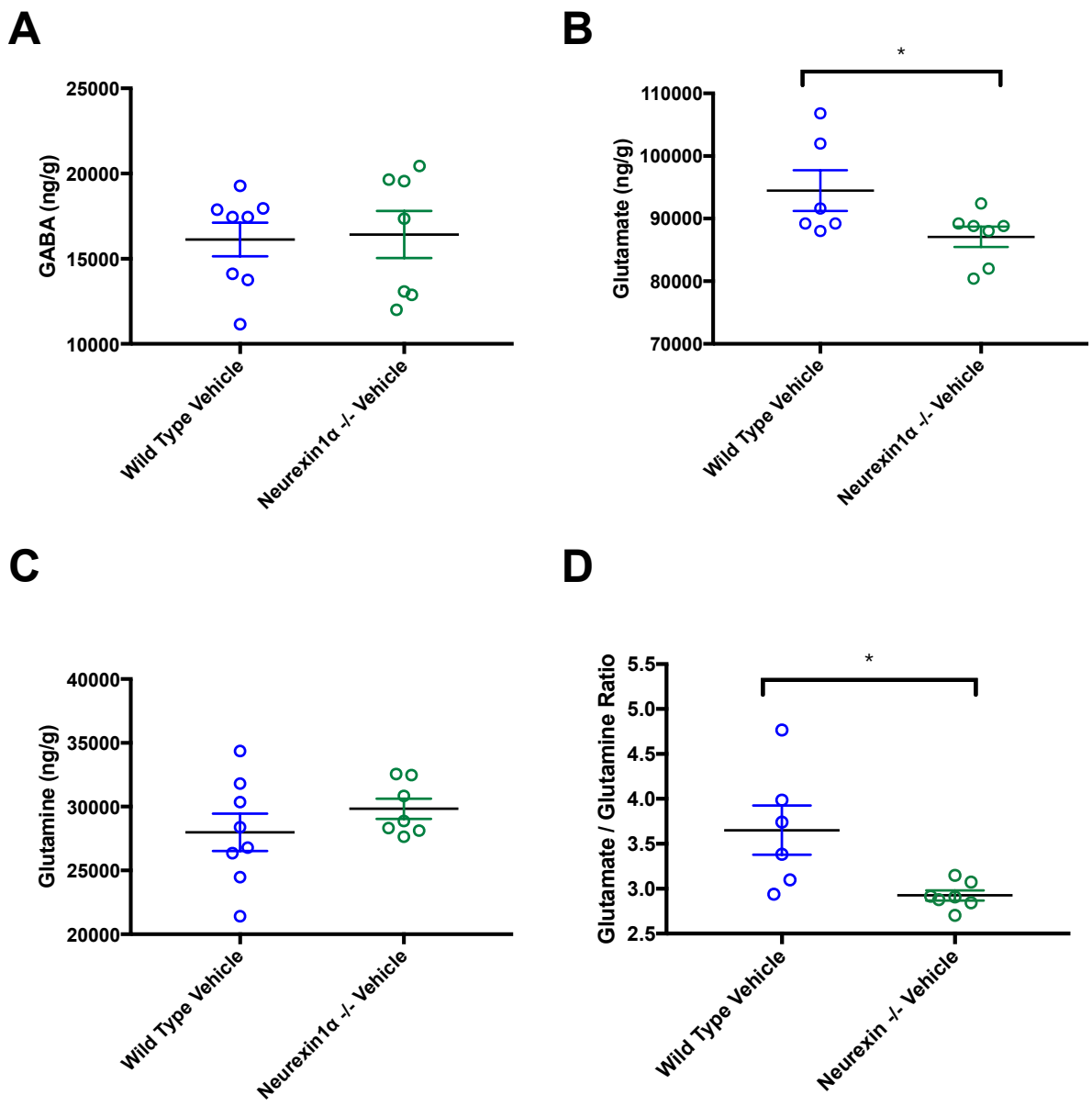

Figure 5.5: Baseline GABA (A), glutamate (B), glutamine (C) and Glu/Gln ratio (D) in the caudate putamen of wild type and *Neurexin1α*$^{-/-}$ rats

There were no significant group differences in baseline (vehicle) measures of GABA (A) or glutamine (C), but there was a significant group difference in baseline glutamate (B) in the caudate putamen (t=2.14 (11), p=0.05, WT n=6, *Nrxn1α*$^{-/-}$ n=7). This translated to a significant group difference in the baseline glutamate/glutamine ratio (t=2.81 (11), p=0.02, WT n=6, *Nrxn1α*$^{-/-}$ n=7).

5.3.2.4 No effect of riluzole on rat PFC or CPu inhibitory indices

There were no main effects of group, nor drug on the inhibitory index in the PFC (Figure 5.6 A; main effect of group; $F_{(1,25)}$ =0.06, p=0.95, and drug; $F_{(1,25)}$ =0.52, p=0.48), nor CPu (Figure 5.6 B; main effect of group; $F_{(1,27)}$ =0.93, p=0.34, and drug; $F_{(1,27)}$ =0.29, p=0.59).

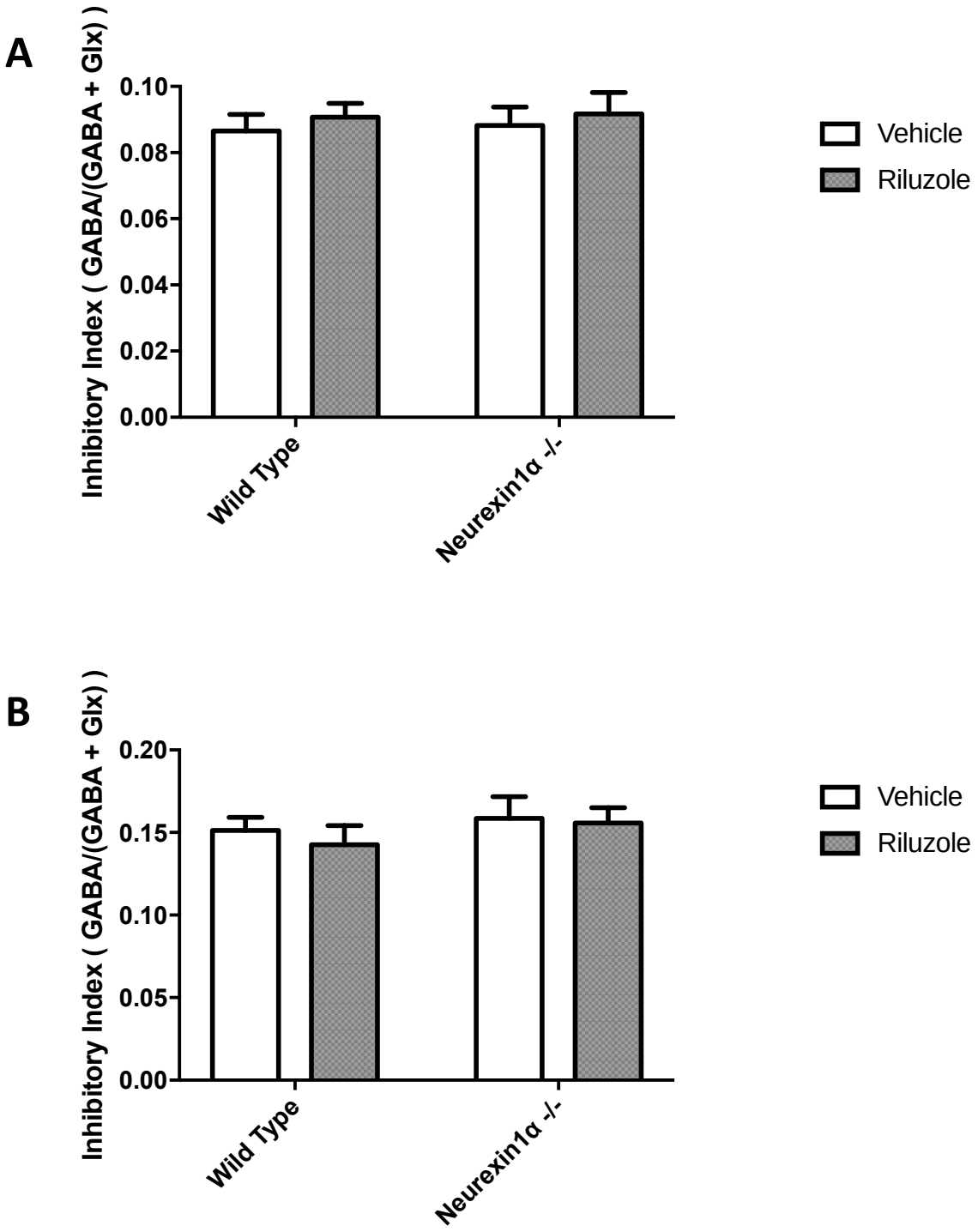

Figure 5.6: Effect of riluzole on rodent prefrontal cortex (A) and caudate putamen (B) inhibitory index

There were no significant effects of group nor drug on *Nrxn1α* $^{-/-}$ and wild type rat PFC (A), or CPu (B) inhibitory indices.

5.3.3 Discussion

In line with baseline findings from patients with ASD, *Nrxn1α*$^{-/-}$ rats had significantly lower baseline glutamate in the caudate putamen. However, despite a comparable regional E-I imbalance, unlike the human condition, no significant effects of riluzole on E-I flux were reported in either brain region. This could indicate either a lack of efficacy of riluzole in engaging the relevant targets to produce an observable response, or alternatively could be due to technical issues relating to study design and translation.

5.3.3.1 Study design

Groups did not differ in weight, or age, and dissected brain regions were equivalent weights across all groups. The time taken to perform the dissections was similar across groups, as was the time from vehicle/riluzole dose to dissection. Total time from dose to sample collection was around 4 hours for all groups (see Table 5.2).

5.3.3.2 Baseline E-I balance of the rat prefrontal cortex

There were no group differences in baseline GABA, or glutamate levels in the PFC of wild type and *Nrxn1α*$^{-/-}$ rats. However, the *Nrxn1α*$^{-/-}$ group had significantly higher levels of prefrontal glutamine (Figure 5.4 C). Additionally, glutamate-glutamine ratios were significantly lower in the *Nrxn1α*$^{-/-}$ rats compared to wild type controls (Figure 5.4 D).

The increased glutamine, and accompanying lower glutamine-glutamate ratios found in the *Nrxn1α*$^{-/-}$ PFC are consistent with reports of altered glutamine in the human condition. For example, lower glutamate-glutamine ratios have been reported in the anterior cingulate cortex

(ACC) of ASD patients compared to controls (Shimmura et al., 2013); and in the only human MRS study to measure isolated glutamine, Cochran et al. (2015) reported increased levels in the ACC of children with ASD.

The cause of the shift towards glutamine in the *Nrxn1α*$^{-/-}$ group is unknown, however disruptions to the regulation of the glutamine-glutamate cycle are a contributing factor to E-I imbalance in ASD, and may play a role here (Fatemi et al., 2002; Shimmura et al., 2013). Glutamine synthetase for example (which converts glutamate to glutamine in glial cells), is reportedly higher in the ACC of animal models of ASD (Silvestrin et al., 2013) and may represent increased astrocytic clearance of glutamate in ASD. Additionally, ACC glutaminase, which converts glutamine back to glutamate in neurons, is lower in ASD patients (Shimmura et al., 2013). Both may theoretically result in a shift towards glutamine, rather than glutamate, as observed here. Additionally, the regulation of this cycle occurs in glial cells, which themselves are known to be altered in the ASD PFC. Microglial density is reportedly increased in the PFC of $mGluR_5$ knock out autism mouse models, and both number, organisation and activation states of microglia have been reported as abnormally high in patients and animal models (Morgan et al., 2010, 2012; Suzuki et al., 2013; Vargas et al., 2005).

5.3.3.3 Baseline E-I balance of the rat caudate putamen

There were no group differences in baseline GABA, glutamine, nor combined Glx in the CPu. However, there was significantly lower glutamate in the *Nrxn1α*$^{-/-}$ group, and as a result, the glutamine-glutamate ratio was also significantly lower (Figure 5.5).

As in the PFC, it is possible that disruptions to the glutamate-glutamine system are responsible for the lower glutamate levels observed in the *Nrxn1α*$^{-/-}$ CPu. Such alterations may also be reflective of widespread glutamate dysfunction. This supports the theory of altered glutamatergic activity in ASD in both alternative animal models (Wei et al., 2015) and human studies (Horder et al., 2013).

5.3.3.4 Comparisons with human findings of the present thesis

Overall, across both brain regions tested, the baseline neurochemistry of the *Nrxn1α*$^{-/-}$ model was largely consistent with that of the human condition;

In Chapter 3, no differences in baseline GABA or Glx in the human PFC were reported, which matches the results observed in the rodent. However, when glutamate and glutamine were examined as individual metabolites in the present study, significant group differences in rodent PFC glutamine were found, which were not captured by MRS. This highlights the potential importance of separating the combined Glx measure in future MRS studies in humans, as any group differences in human glutamine levels may have been overlooked, and thus the combined Glx findings may present a false negative result.

Likewise, the baseline neurochemistry of the basal ganglia was replicated. In Chapter 4, significantly lower baseline Glx was reported in the basal ganglia of the ASD patient population. This was comparable to the lower glutamate measured in the CPu of the neurexin model of ASD.

Having established an equivalence of the model at baseline, differences in responsivity of the E-I system were next investigated.

5.3.3.5 Responsivity of the rat brain to riluzole

Unlike in the human cohort, where distinct regional differences in E-I responsivity were found, riluzole had no effect on E-I flux in either brain region tested (Figure 5.6).

At the time the brain regions were analysed (~4 hours post-dose), pharmacokinetic analyses from Study 1 indicated that riluzole was present in both the brain and plasma (Figure 5.1). Due to the time lag and difference in study protocols, the *ex vivo* animal findings at 4 hours post-dose cannot be directly compared to the findings 1 hour post-dose in the human. For both humans and rodents, the maximum effects of riluzole are thought to occur one hour post-dose (Sanofi-Aventis, 2010); therefore any changes in E-I flux at this time may have been missed in the rat. By the time data was collected at 4 hours post dose in Study 2, the system may have 'normalised', and E-I balance restored. Considering the significant delay from dose to sample measurement, it is also unknown whether riluzole was present at a sufficient concentration in the brain to produce an effect on E-I. At 4 hours post-dose in wild type rats, the average riluzole plasma level was 1150 ± 39 ng/ml. As the molar mass of riluzole is 234.2, the concentration of riluzole in the plasma at this time would therefore be around 5 μM (calculated as the weight in ng/ml divided by the molecular weight of riluzole and then multiplied by 1000 to convert from ng/ml to ng/L = (1150 / 234) x 1000 = 4.9 μM). Based upon the previously reported brain:plasma ratio in the rat, one could anticipate brain riluzole levels of approximately 5 times that of plasma, i.e. approximately 25 μM. No other studies have evaluated the effects of riluzole at this concentration *in vivo* or *ex vivo*, however

in vitro studies indicate an IC_{50} between 18 – 88 μM, which would be consistent with the estimated regional level of riluzole reported here (Debono et al., 1993; Jehle et al., 2000; Wang et al., 2008; Zona et al., 1998). The brain concentrations reached with a 4 mg/kg oral dose may therefore have been sufficient to produce a detectable shift in E-I balance, however 'total' brain region levels do not indicate the location of the drug, or whether it is bound or free in the extracellular space. They are not therefore directly comparable, and further, more localised studies of riluzole are necessary. Direct measurements of riluzole levels in the extracellular space were therefore considered in the next set of experiments.

5.3.3.6 Extra notes on the validity of the *Neurexin1α*$^{-/-}$ model

The present study focused solely on neurotransmitter levels and did not assess animal behaviour- however, some observations were made throughout the experiments which may be of relevance. Though not formally assessed, the *Nrxn1α*$^{-/-}$ rats were notably more ill-tempered than their wild type littermates, and in two instances, had to be housed individually to avoid fighting. Increased aggression is a common phenotype in animal models of ASD (Brodkin, 2007; Burrows et al., 2015; Schmeisser et al., 2012; Velez et al., 2010) including the *Nrxn1α*$^{-/-}$ (Grayton et al., 2013). Aggression was not assessed in the human arm of the study, though a considerable number of patients with ASD in the wider population report aggressive behaviour as a co-morbidity. For example in one study of 1,380 children with ASD, 68% of parents reported their child had engaged in some form of aggressive behaviour towards them (Kanne & Mazurek, 2011). Likewise in adults, 15-18% of people with ASD have been reported to engage in aggression towards others (Matson & Rivet, 2008) and 'irritability' and 'challenging behaviours' are common and disabling co-morbidities (Accordino et al., 2016).

Additionally, the *Neurexin1α* knock-outs were more prone to biting and were more difficult to handle- though not formally measured in the present study, this may be an indication of increased anxiety. Other behavioural studies of *Neurexin1α* deficient rats have previously identified heightened anxiety compared to wild type controls in the elevated plus maze (Grayton et al., 2013), and increased anxiety was also noted in the symptom profile of the patients included in the human arm of this study (see Participant Demographic Table, Chapter 3), and the general ASD population (Simonoff et al., 2008). Both of these traits add to the face validity of the model.

5.4 Limitations

Back-translating a human study into a rodent is not without limitations and despite all efforts to link the two studies, there remained discrepancies.

5.4.1 Study design

Dissected brain regions did not differ in size, though unfortunately, whole brain weights were not assessed before dissection, hence it was not possible to control for potential group differences in total brain volume. This is of particular relevance to the present thesis, as volumetric differences have been observed between ASD and control brains in humans (Haznedar et al., 2006). However, dissections were performed 'by eye', using regional landmarks, so any gross differences in brain volume would have been noticeable.

In two cases, *Nrxn1α*$^{-/-}$ rats were housed individually after displaying aggressive behaviour towards handlers. To match the groups and avoid any potential confounds, two wild type rats

could have been housed individually, as isolation may have its own effects on brain E-I balance (Lukkes et al., 2012; Sestito et al., 2011). However, in both cases, surgery was planned for the following day, hence one night of isolation was not deemed to be sufficient to cause changes in E-I balance over such a short period of time. Additionally, social isolation mostly affects juvenile rats during weaning, hence the adult rats in the present study were most likely unaffected. Finally, although the behaviour may be a characteristic phenotype, housing wild type rats singly may not have been an equivalent control, as the reaction of wild type rats to being housed singly may be different to that of a knock out animal.

Wistar rats were used as the genetic background for the *Nrxn1α*$^{-/-}$ model used in present thesis, which are an outbred stock, and are therefore genetically diverse (compared to an inbred strain, such as a Brown Norway rat). This diversity may pose disadvantages, as the sample used for the control group may have a genetically different background to those in the knock-out group, which may influence their genotype and subsequently, their phenotype (NC3Rs, 2018). To mitigate this risk, all rats were genotyped and no significant differences were noted. On the other hand, it could be argued that the human population is also heterogeneous, therefore selecting an inbred strain may not have effectively translated to the human study.

5.4.2 Study translation

Brain regions were closely matched across studies, but due to the low spatial resolution of MRS, and the potential for human error during manual brain dissection, the regions examined are not directly comparable. In the basal ganglia in particular, the rodent measures were selectively from the caudate putamen, and whilst this region was included in the basal ganglia MRS voxel, so too were others (the lateral thalamus for example). It is possible therefore that

results from the human are due to brain regions other than the caudate, which are not accounted for in the animal study.

Additionally, the analysis techniques used to capture these regions are different. Both capture bulk measures of intracellular metabolites, though MRS does so in a living, active brain, and HPLC is performed on *ex vivo* tissue post-mortem. Future work may consider using 1[H]MRS in living rodents to obtain a more direct comparison. Though GABA and glutamate measures have been successfully obtained using this method in studies of neurodevelopmental animal models (Gonçalves et al., 2017; Vernon et al., 2015), it was deemed inappropriate in the present study due to the need for E-I acting sedatives (e.g. isoflurane), which could potentially interfere with interpretation of riluzole action (Petrinovic et al., 2016).

5.5 Conclusions

The *Nrxn1α* $^{-/-}$ rat modelled the baseline regional E-I imbalance observed in the patient cohort examined in previous chapters. The *in vivo* disruptions to E-I flux seen in the patients using MRS however, were not replicated in the animal *ex vivo*. The time difference in data acquisition between studies may account for this discrepancy, hence a real-time measure of neurotransmitter flux over time *in vivo* in animals may better capture any dynamic effects of riluzole.

5.6 Next steps

In order to examine changes in E-I efflux, experiments were subsequently undertaken using *in vivo* microdialysis, which allows sampling of neurotransmitters and metabolites in the extracellular space.

Chapter 6

E-I responsivity of *Neurexin1α* knock out rats: *in vivo* microdialysis

6.1 Introduction

In the thesis thus far, E-I dynamics have been examined in both humans and animals primarily at the intracellular level, using MRS and equivalent *ex vivo* analyses, respectively. However, both of these techniques capture bulk E-I tissue measures and as a result, are not likely to be sensitive to differences in extracellular metabolite flux. In humans, fMRI was utilised as an additional approach to assess the effect of modulating E-I on brain function, which is assumed to reflect neurotransmission. However, whilst fMRI is useful, it still does not directly access extracellular levels of neurotransmitters in the living brain. Examination of neurotransmitter efflux into the extracellular space is however possible in animals using *in vivo* microdialysis.

The present study therefore aimed to use microdialysis to address extracellular E-I dynamics and test the hypothesis that there would be group differences in neurotransmitter efflux in response to riluzole. I elected to continue to use the *Neurexin1α* knock out rat (*Nrxn1α* $^{-/-}$) as it replicated at least baseline ASD E-I. Glutamate and GABA effluxes were sampled in the extra-synaptic space of the medial prefrontal cortex (mPFC) and caudate putamen (CPu) in rats, after an oral dose of 4 mg/kg riluzole, a dose which was previously demonstrated to be comparable to the human dose, and to enter the rat brain (see Chapter 5).

6.2 Methods

6.2.1 Protocol

15 adult male Wistar *Nrxn1α* $^{-/-}$ and 16 littermate control rats were sourced from SAGE labs and housed in standard conditions. Rats did not differ in weight nor age (see Figure 5.2).

The microdialysis protocol is detailed in full in General Methods section 2.2.4. Briefly, all rats underwent probe implantation surgery, followed by *in vivo* microdialysis experiments the next day. MAB 4.7.4 (4 mm) and MAB 4.7.3 (3 mm) microdialysis probes were implanted in the mPFC and CPu respectively, at the following co-ordinates (from bregma) with nose bar set to -3.3 mm:

mPFC; +3.0 mm anterior, ±1.5 mm lateral, -5.0 mm vertical (from dura); at a 12 degree angle

CPu; +0.3 mm anterior, - 3.0 mm lateral, -6.0 mm vertical (from dura)

To match the location of the human MRS voxels (bilateral medial prefrontal cortex and left basal ganglia), placement of the mPFC probe altered between left and right mPFC co-ordinates; whereas placement of the CPu probe was only in the left CPu.

From the day after probe implantation, 4 animals per experimental day were connected to the microdialysis rig. Probes were attached to the rig via an infusion pump filled with aCSF, which was continuously perfused into the rat brain at a flow rate of 1.5 µl/min. Rats were left for an initial settling period of 90 minutes, then samples were acquired at 20 minute intervals

for a total of 15 samples. After 6 'baseline' samples were collected, rats were dosed with either 4 mg/kg riluzole (in 1% HEC), or vehicle only (1% HEC) via oral gavage (p.o.); WT vehicle n=8, *Nrxn1α*$^{-/-}$ vehicle n=7, WT riluzole n=8, *Nrxn1α*$^{-/-}$ riluzole n=8.

All samples were immediately frozen on dry-ice and stored at -80°C pending analysis by LC-MS/MS (see General Methods section 2.2.6 for further details on sample analysis).

6.2.2 Data analysis

Data were represented as a 'percentage change from baseline', where the baseline was the average of the final 3 samples prior to drug/vehicle administration (i.e. the average of samples at 80-120 minutes) for each rodent. In this way, each animal was normalised to their own pre-dose control.

Repeated measures two-way ANOVA with factors of strain and treatment were used to compare any main effects of group, riluzole and time. Data from 140 to 300 minutes were included in these analyses to exclude the pre-dose settling period. In order to equalise the variance across the response range over time, it was necessary to first Log the data. To compare the difference in the effect of riluzole between groups (i.e. how responsivity to riluzole differed between the two strains), drug by strain interactions were analysed at each time point. Briefly; log estimates were calculated, and then transformed (antilogged) to 'raw values', so raw estimates = LSMean (Ril) / LSMean (Veh). This measure represents a ratio, rather than absolute difference, but may be taken as the relative effect of drug compared to vehicle. Differences in 'raw' treatment effects were again calculated as the antilog of Log

estimates, so that raw ratio estimates = LSMean (Ril_Nxn) / LSMean (Veh_Nxn) all divided by LSMean (Ril_WT) / LSMean (Veh_WT).

SAS software was used to analyse the data presented in this thesis, which was undertaken by Lilly in-house statisticians (RM). SAS was selected as it has the advantage of handling missing data without removing subjects.

Riluzole concentration in each sample was measured using LC/MS-MS, in the same manner as GABA and glutamate. Riluzole levels per dialysate sample in ng/ml were divided by the molecular weight of riluzole (234.199) and multiplied by 1000 to convert to a concentration in nM. Linear regressions were performed and then compared to determine whether the slope of riluzole in each group were equal.

6.3 Results

6.3.1 Glutamate efflux from the medial prefrontal cortex

There were no significant overall effects of rat strain or treatment type on glutamate efflux in the mPFC (strain, $F_{(1,24)}$ =0.52, p=0.47; treatment, $F_{(1,24)}$ =0.56, p=0.46, see Figure 6.1). Nor was there a main effect of time ($F_{(8,11)}$ =1.58, p=0.23). Further analyses of drug by group interactions indicated no significant effects of riluzole at any time point within strains (See Figure 6.3 B and D), and hence the response to riluzole in the wild type rats did not differ to the that of the knock outs at any time point (no significant drug by group interaction at any time).

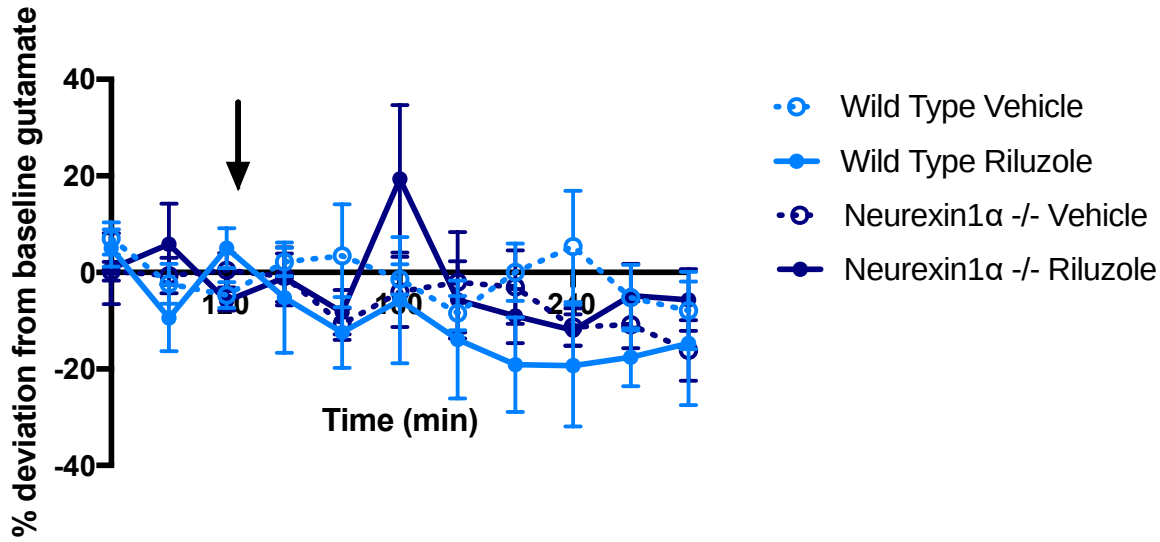

Figure 6.1: Glutamate efflux in the mPFC following riluzole administration

There were no effects of treatment, nor strain on glutamate efflux from the medial prefrontal cortex; RM Two-Way ANOVA; treatment, $F_{(1,24)} = 0.56$, $p = 0.46$; strain, $F_{(1,24)} = 0.52$, $p = 0.47$. Further analyses of drug by group interactions showed no significant differences in treatment effects between groups at any time point. Arrow indicates time of riluzole/vehicle dose (120 minutes).

6.3.2 GABA efflux from the medial prefrontal cortex

Likewise, there were no significant overall effects of drug ($F_{(1,27)} = 0.07$, $p = 0.79$) or strain ($F_{(1,27)} = 0.18$, $p = 0.67$) on GABA efflux from the mPFC (see Figure 6.2). A main effect of time almost approached significance ($F_{(8,19)} = 2.12$, $p = 0.08$), which may represent a trend towards a slight increase in GABA efflux across all groups over time. However, this may have been skewed by larger SEM values towards the end of the study timeline. There was no main effect of drug in either strain (see Figure 6.3 A and C), nor did responsivity to riluzole differ between groups at any time point (no significant drug by group interaction at any time).

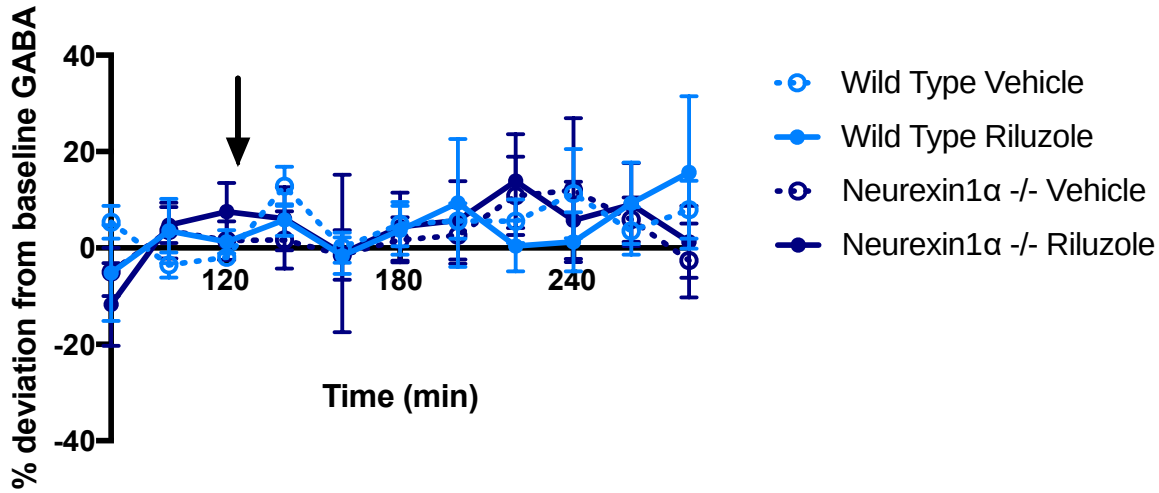

Figure 6.2: GABA efflux in the mPFC following riluzole administration

There were no effects of treatment, nor strain on GABA efflux from the medial prefrontal cortex; RM Two-Way ANOVA; treatment, $F_{(1,27)} = 0.07$, $p = 0.79$; strain, $F_{(1,27)} = 0.18$, $p = 0.67$. Further analyses of drug by group interactions showed no significant differences in treatment effects between groups at any time point. Arrow indicates time of riluzole/vehicle dose (120 minutes).

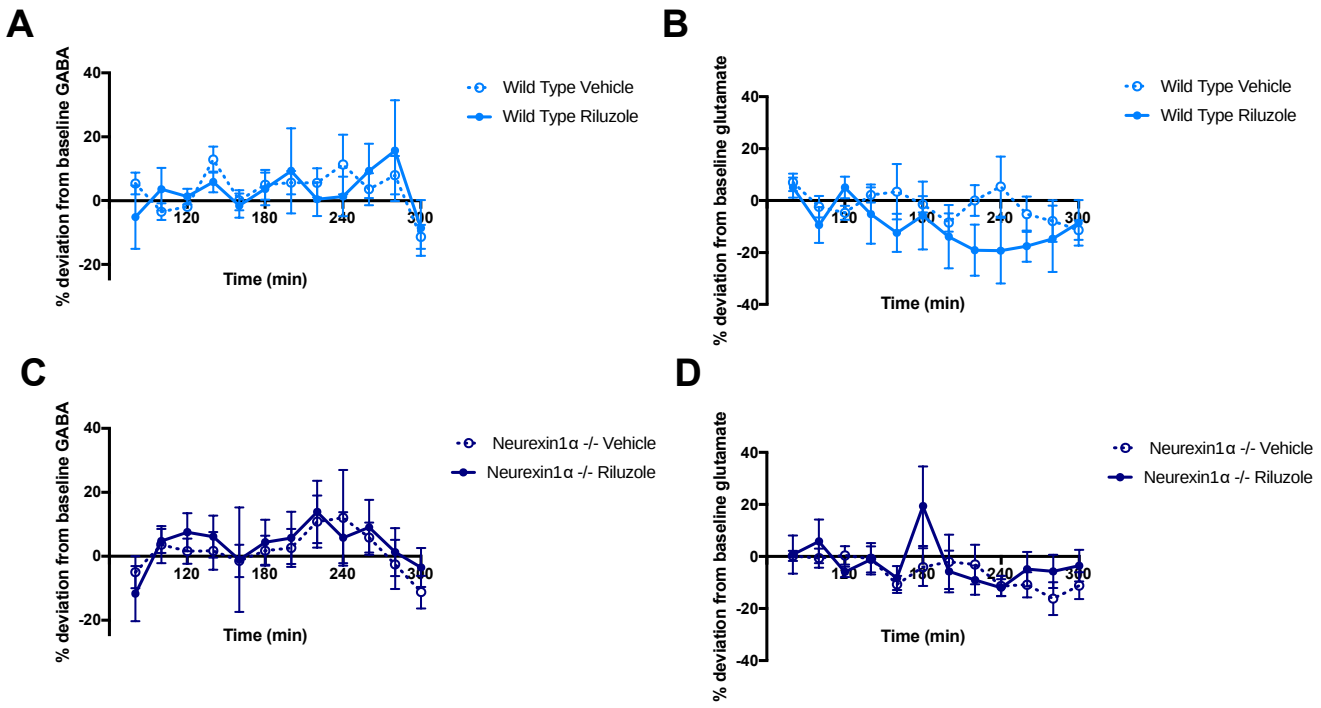

Figure 6.3: No effect of riluzole on glutamate and GABA efflux in the mPFC of wild type and *Neurexin1α* knock out rats

A) No effect of 4 mg/kg riluzole p.o. on GABA efflux in wild type rat mPFC

B) No effect of 4 mg/kg riluzole p.o. on glutamate efflux in wild type rat mPFC

C) No effect of 4 mg/kg riluzole p.o. on GABA efflux in *Nrxn1α* $^{-/-}$ rat mPFC

D) No effect of 4 mg/kg riluzole p.o. on glutamate efflux in *Nrxn1α* $^{-/-}$ rat mPFC

Riluzole/vehicle dose was administered at 120 minutes.

6.3.3 Riluzole levels in the medial prefrontal cortex

After oral dosing of riluzole at 120 minutes, riluzole rapidly entered the brain and was detected at a peak concentration of around 8 nM in the mPFC (see Figure 6.4). However, this value does not take into account that each probe samples from its immediate vicinity, and is therefore not an accurate representation of the concentration of riluzole in the wider brain region in which the probe is placed. Therefore, in a separate *in vitro* experiment (see Appendix 5), the percentage recovery of riluzole by the mPFC microdialysis probe was assessed, and found to be on average, 7.5%. The concentration observed in the present experiment was therefore extrapolated by a scale factor of 13 (100 / 7.5 = 13), and the total riluzole concentration in the wider mPFC region estimated at 100 nM (peak riluzole concentration measured multiplied by the scale factor). Riluzole concentration did not significantly differ between wild type and knock out rats (wild type slope best fit = 0.03 ± 0.003, *Nrxn1α*$^{-/-}$ slope best fit = 0.038 ± 0.004, difference in slopes; $F_{(1,26)}$ =1.98, p=0.17).

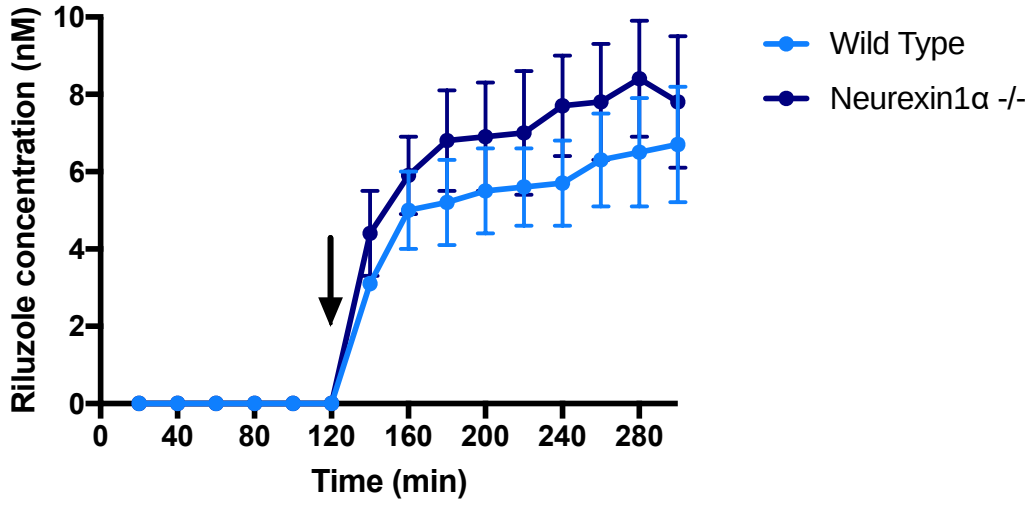

Figure 6.4: Concentration of riluzole in rat mPFC dialysate following 4 mg/kg p.o. dose

Concentration of riluzole did not significantly differ between groups; $F_{(1,26)}$ =1.98, p=0.17. Arrow indicates time of riluzole/vehicle dose (120 minutes).

6.3.4 Glutamate efflux from the caudate putamen

No main effect of treatment, group, nor time was found for glutamate efflux in the caudate putamen (see Figure 6.5; main effect of treatment; $F_{(1,22)}$ =1.7, p=0.2; strain; $F_{(1,22)}$ =2.63, p=0.12; time; $F_{(8,14)}$ =1.2, p=0.36). There was no main effect of drug in either strain (see Figure 6.7 B and D), nor did responsivity to riluzole differ between groups at any time point (no significant drug by group interaction at any time).

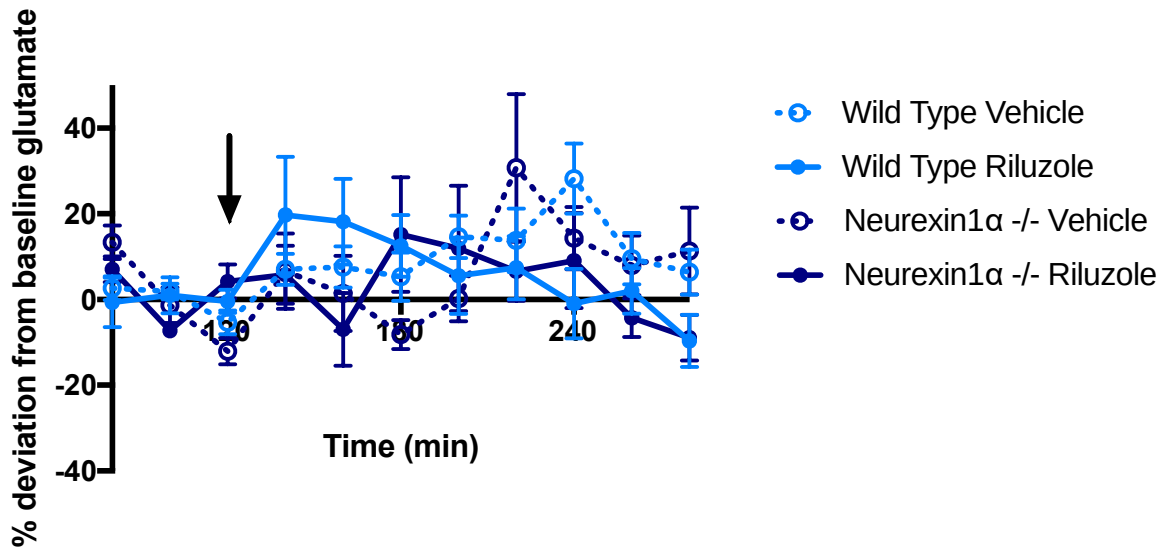

Figure 6.5: Glutamate efflux in the CPu following riluzole administration

There were no effects of treatment, nor strain on glutamate efflux from the caudate putamen; RM Two-Way ANOVA; treatment, $F_{(1,22)}$ =1.7, p=0.2; strain, $F_{(1,22)}$ =2.63, p=0.12. Further analyses of drug by group interactions showed no significant differences in treatment effects between groups at any time point. Arrow indicates time of riluzole/vehicle dose (120 minutes).

6.3.5 GABA efflux from the caudate putamen

Likewise, there were no main effects of treatment, nor time on GABA efflux of the caudate putamen; treatment, $F_{(1,27)}$ =0.99, p=0.33; time, $F_{(8,17)}$ =1.5, p=0.23. There was a trend towards a group difference; main effect of strain, $F_{(1,27)}$ =3.4, p=0.075, however this may merely represent group differences in variability, as the response profile of the *Nrxn1α* $^{-/-}$ rats was much more varied than that of the wild types (see Figures 6.6 and 6.7). There was no main effect of drug in either wild types or knock outs (see Figure 6.7 A and C, respectively), and responsivity to riluzole did not differ between groups at any time point (no significant drug by group interaction at any time).

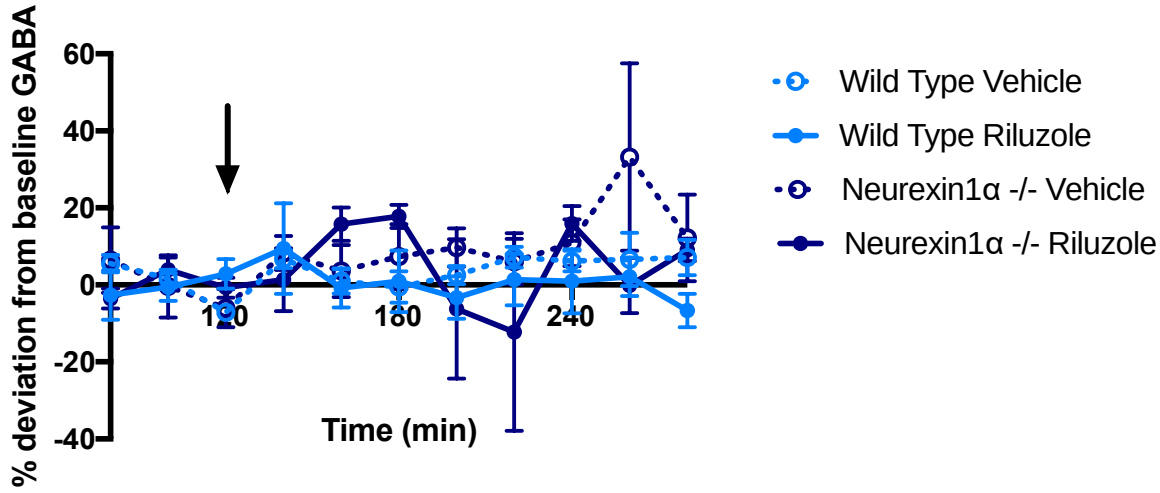

Figure 6.6: GABA efflux in the CPu following riluzole administration

There were no significant effects of treatment, nor strain on GABA efflux from the caudate putamen; RM Two-Way ANOVA; treatment, $F_{(1,27)}$ =0.99, p=0.33; strain, $F_{(1,27)}$ =3.43, p=0.075. Further analyses of drug by group interactions showed no significant differences in treatment effects between groups at any time point. Arrow indicates time of riluzole/vehicle dose (120 minutes).

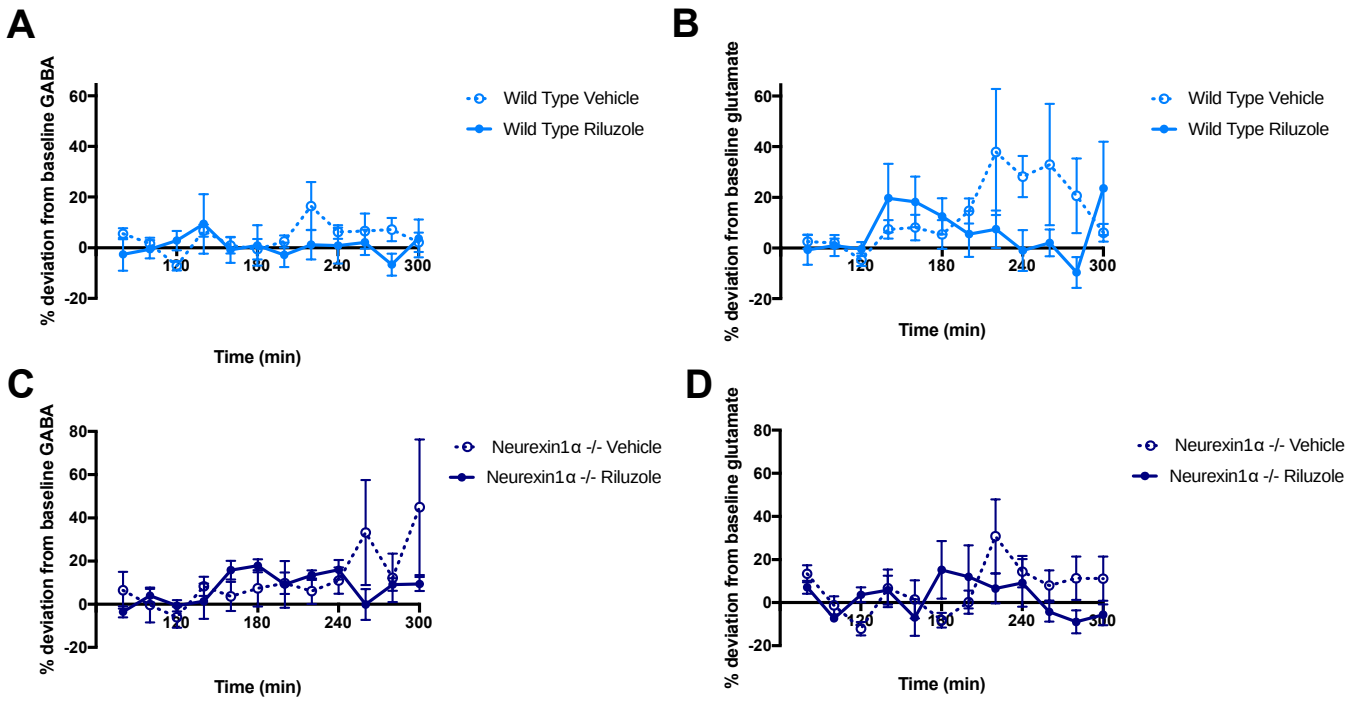

Figure 6.7: Effect of riluzole on glutamate and GABA efflux in the CPu of wild type and *Neurexin1α* knock out rats

A) No effect of 4 mg/kg riluzole p.o. on GABA efflux in wild type rat CPu

B) No effect of 4 mg/kg riluzole p.o. on glutamate efflux in wild type rat CPu

C) No effect of 4 mg/kg riluzole p.o. on GABA efflux in *Nrxn1α* $^{-/-}$ rat CPu

D) No effect of 4 mg/kg riluzole p.o. on glutamate efflux in *Nrxn1α* $^{-/-}$ rat CPu

Riluzole/vehicle dose was administered at 120 minutes.

6.3.6 Riluzole levels in the caudate putamen

After oral dosing of riluzole at 120 minutes, riluzole rapidly entered the brain and was detected at a peak concentration of around 5 nM in the caudate putamen (see Figure 6.8). As for the mPFC probe, the percentage recovery of the CPu microdialysis probe for riluzole was calculated in a separate *in vitro* experiment (see Appendix 5) and was estimated at 4.7%. By scaling up the concentration observed in the present experiment by a factor of 21 (100 / 4.7 = 21), the total riluzole concentration in the wider CPu region was estimated at around 100 nM (peak riluzole concentration measured multiplied by scale factor). Riluzole concentration did not significantly differ between wild type and knock out rats (wild type slope = 0.024 ± 0.002, *Nrxn1α*$^{-/-}$ slope = 0.027 ±0.004; difference in slopes; $F_{(1,26)}$ =0.45, p=0.51.

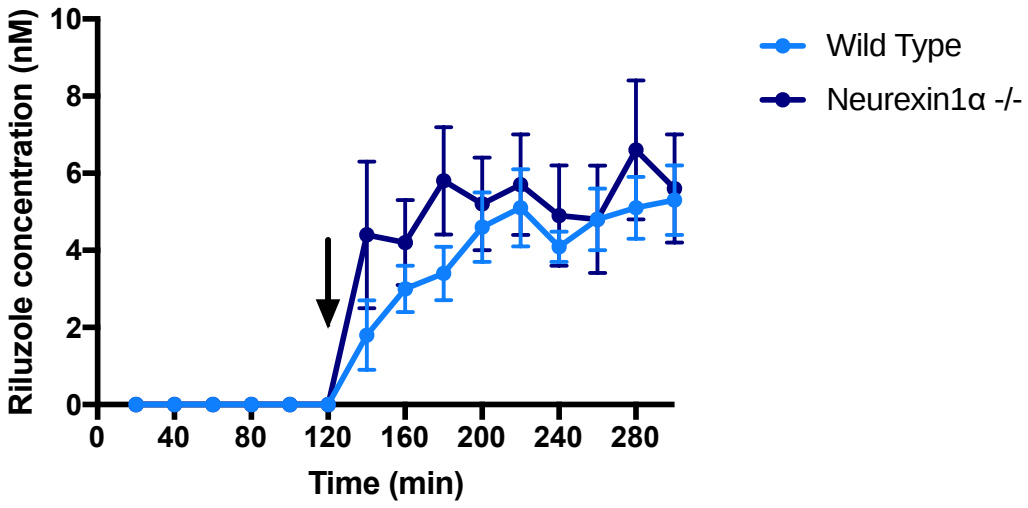

Figure 6.8: Concentration of riluzole in rat CPu dialysate following 4 mg/kg p.o. dose

Concentration of riluzole did not significantly differ between groups; $F_{(1,26)}$ =0.45, p=0.51. Arrow indicates time of riluzole/vehicle dose (120 minutes).

6.4 Discussion

The present study was conducted to investigate extracellular E-I dynamics, using microdialysis as a direct measure of neurotransmitter efflux into the extracellular space. There were no group differences in responsivity to riluzole in terms of GABA or glutamate efflux from either brain region tested, in both wild type and *Nrxn1α* $^{-/-}$ rats.

6.4.1 Neurotransmitter efflux in the medial prefrontal cortex

There were no significant effects of riluzole compared to vehicle in wild type, or *Nrxn1α* $^{-/-}$ rats on glutamate (Figures 6.1 and 6.3), or GABA (Figures 6.2 and 6.3) efflux from the medial prefrontal cortex (mPFC). Additionally, there were no overall effects of strain, treatment or time on the efflux of either metabolite when all groups were compared together.

6.4.2 Neurotransmitter efflux in the caudate putamen

Likewise, there were no significant effects of riluzole compared to vehicle in either strain on glutamate (Figure 6.5 and 6.7) or GABA (Figures 6.6 and 6.7) efflux from the caudate putamen (CPu). As in the mPFC, there were no overall effects of strain, treatment or time across all groups.

6.4.3 Riluzole levels

It is possible that these results are false negative findings because riluzole was not present in sufficient quantities to engage relevant molecular targets and evoke an E-I response. Previous *in vitro* and *in vivo* studies report the concentration of riluzole required to inhibit glutamate

release to be in the micromolar range (10 μM), whereas a 10 times higher dose (100 μM) is required for inhibition of GABA release (Cheramy et al., 1992; David Martin et al., 1993). Analyses of riluzole levels within mPFC and CPu dialysate samples in this study confirmed that riluzole was present in the brain of both strains at nano-molar concentrations, from the time of dosing (Figures 6.4 and 6.8). Specifically, riluzole presence in the brain remained continuous throughout the data collection period, with a peak concentration of extracellular (presumably free, unbound) riluzole at 8 nM and 5 nM in the PFC and Cpu, respectively. However, in order to consider the efficacy of the microdialysis probe at sampling riluzole, an estimated concentration was calculated by extrapolation (see Appendix 5), resulting in an approximate concentration of 100 nM riluzole in the extracellular space of each brain region (see section 6.3.3 and 6.3.6). Hence, whereas in Chapter 5 the 'total' *ex vivo* brain measures of riluzole suggested it was present at 25 μM, the free extracellular levels were likely to have been much lower (100 nM).

Such discrepancies between tissue and extracellular riluzole concentrations may indicate that a large proportion of riluzole is either bound in membranes, or located within compartments of the cells. It is impossible to know from the present data whether riluzole is evenly distributed across whole brain and where (intracellular or extracellular) it is acting. As riluzole acts via a multitude of mechanisms, at glutamate and GABA receptors and ion channels, it is likely that the majority of riluzole is either bound to these receptors, or partitioned in membranes.

6.4.4 Receptor availability and location

Preclinical studies suggest riluzole acts by reducing excitatory, and potentiating inhibitory neurotransmission. Amongst many actions (see Bellingham 2011 and Doble 1996 for a full review), riluzole causes inhibition of NMDA receptors (Debono et al., 1993; Prakriya & Mennerick, 2000) and sodium and potassium channels (Hebert et al., 1994; Zona et al., 1998), and potentiation of $GABA_A$ receptors (He et al., 2002; Jahn et al., 2008). However, the majority of these mechanisms were determined using *in vitro* cell cultures or brain slices, which may represent a more direct evaluation than the complex *in vivo* environment examined in the present microdialysis experiments. It is certainly possible that the abundance of other neurotransmitters in living tissue may alter, or mask riluzole's effects on E-I.

Furthermore, the majority of the literature investigating riluzole's actions on specific glutamate and GABA receptors and pathways cite the hippocampus as the primary location for these effects (He et al., 2002; Martin et al., 1993). The thalamus has also been a region of interest in previous research; a microdialysis study by Abarca et al. (2000) previously reported a significant reduction of thalamic glutamate levels after only a 2 mg/kg dose of riluzole (half that of the present study). However, this experiment was conducted in wild type rats only and riluzole administered subcutaneously, hence it cannot be directly compared with the present protocol. Nonetheless, the lack of results in the mPFC and CPu may be due to riluzole having regional efficacy, which was not captured by the present study.

The mPFC and CPu were however, specifically selected to match the human study, where effects of riluzole in both the PFC and basal ganglia were apparent (see Chapter 3 and 4). Translation between species may therefore be an issue for replication.

6.5 Limitations

A key concern when sampling neurotransmitters using microdialysis soon after probe implantation surgery is the potential tissue damage as a result of the surgery. An example of the brain tissue after probe implantation can be found in section 2.2.8 of the General Methods, where histology was performed to verify the correct placement of each probe (Figures 2.10 and 2.11). Minor damage to the surrounding tissue can be seen in both brain regions, however it must be noted that these images were captured after probes had been inserted, and removed, whereas microdialysis samples were collected only after probe insertion. Previous literature has estimated up to 1 mm of tissue damage may occur surrounding the probe (Borland et al., 2005). Tissue damage to this extent would likely invoke activation of an inflammatory response (Stenken et al., 2010), including activation of glial mechanisms, which may in turn affect E-I balance (Auld & Robitaille, 2003; Graeber, 2010). All groups underwent the same surgery; hence any effects should be consistent across all animals- however this may be a factor in why no overall group differences were found if glial mechanisms across all groups masked any effects of riluzole.

Further, it is unknown whether the way in which riluzole exerts its effects is compatible with detection by microdialysis. Previous analyses of microdialysis studies have shown that manipulations which increase neurotransmitter uptake, and simultaneously decrease neurotransmitter release, may result in no apparent change in dialysate neurotransmitter levels, even though extracellular levels may be reduced (Chefer et al., 2009). This may apply to riluzole, as it is known to both increase glutamate reuptake (Dall'Igna et al., 2013; Frizzo et al., 2004) and prevent glutamate release (Cheramy et al., 1992; David Martin et al., 1993). However other microdialysis studies have found significant effects of riluzole on glutamate efflux (Coderre et al., 2007), though admittedly using a higher dose (6 and 12 mg/kg).

Finally, whether microdialysis captures glutamate and GABA efflux in response to neural signalling has been questioned. As explored in section 2.2.4.3 of the General Methods, previous studies have implied that unlike other neurotransmitters such as serotonin and noradrenaline, GABA and glutamate are only involved in short distance signalling which may not reach the microdialysis probe (Del Arco et al., 2003). Hence, the extracellular concentrations of glutamate and GABA may therefore not provide a reliable indication of their synaptic exocytotic release (see page 107 for further details).

6.6 Conclusions

The aforementioned limitations may have contributed to the lack of findings in this microdialysis study, however the animal research conducted as a whole has provided valuable insight into the *Neurexin1α* knock out rat model of ASD. This study in particular has highlighted the need for other direct evaluations of synaptic activity in the ASD brain, which could be explored in future animal research using the *Nrxn1α*$^{-/-}$ model.

Chapter 7

General Discussion

7.1 Summary of findings

Evidence to date implicates E-I imbalance in ASD, though thus far E-I has only been investigated at rest in mostly cross-sectional studies. To date, no one has examined the responsivity of the E-I system, which may well be important, especially when looking towards treatment discovery. No single technique can fully capture E-I dynamics in the living brain, therefore I looked at E-I responsivity at different levels, using several modalities, across both humans and an animal model of ASD. For an outline of the levels of investigation conducted, see Figure 7.1.

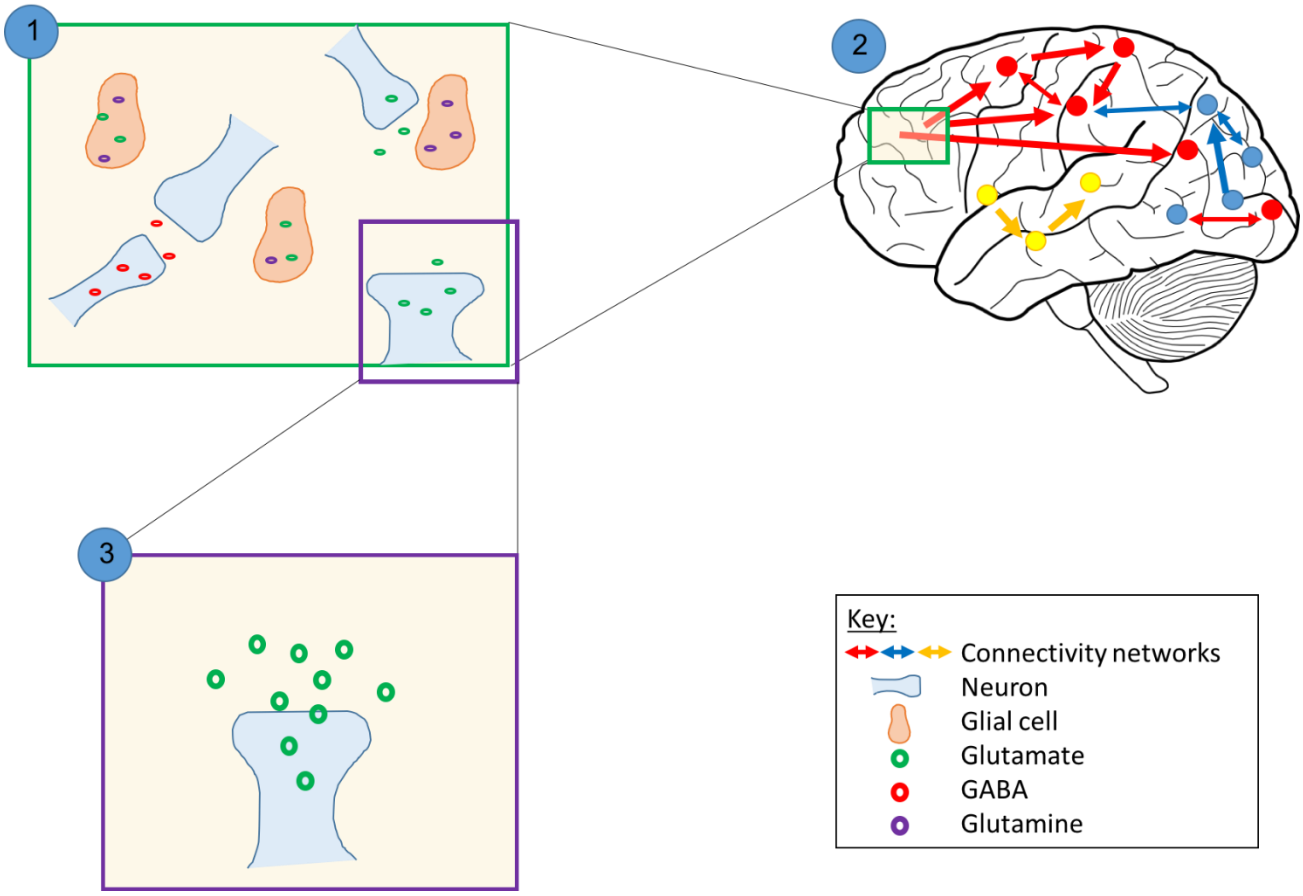

Figure 7.1: Investigating E-I pharmacology at the intracellular, functional and extracellular level

Responsivity to E-I challenge with riluzole was investigated at three levels using different techniques; 1) bulk intracellular measures of E-I metabolites, i.e. the total 'neurotransmitter pool', was measured in humans using [1H]MRS and in animals using *ex vivo* tissue analysis; 2) whole brain functional connectivity was captured in humans using fMRI as a proxy for neuronal activity; and finally, 3) extracellular neurotransmitter efflux was examined in animals via *in vivo* microdialysis.

Boxes indicate E/I 'level' captured by the various techniques. Diagram not to scale.

To first capture E-I dynamics at the intracellular level, I investigated riluzole-evoked changes in bulk tissue levels of GABA, Glx and the inhibitory index (the relative proportion of GABA within the total 'GABA + Glx' pool) using *in vivo* [1H]MRS in the human prefrontal cortex and basal ganglia (Chapters 3 and 4), and *ex vivo* HPLC-MS/MS in a rodent model of ASD (the *Nrxn1α*$^{-/-}$ rat) in equivalent brain regions (Chapter 5). In humans with and without ASD, despite comparable baseline measures of Glx and GABA between groups in the prefrontal cortex, the response to riluzole challenge was diametrically opposite; riluzole increased the inhibitory index in ASD, but decreased it in controls. In the basal ganglia, a group difference in baseline E-I balance was observed, whereby ASD subjects had significantly lower Glx compared to controls. Despite this difference at rest, both groups responded in the same manner to riluzole challenge, with an increase in the inhibitory index. These intracellular findings in the human cohort partially translated to the animal studies. In the *Nrxn1α*$^{-/-}$ rat I recorded lower baseline glutamate in the basal ganglia region (as in humans with ASD), but there was no effect of riluzole on E-I dynamics in either wild type or knock-out animals in any brain region.

Given that tissue E-I balance is thought to determine network activity, I also explored group differences in E-I dynamics at the whole brain connectivity level. Where a group difference in tissue responsivity was observed (prefrontal cortex), the responsivity of functional connectivity of that region with the rest of the brain was examined using resting-state fMRI (Chapter 3). In the ASD group, functional connectivity of the prefrontal cortex was shown to be abnormal at baseline, and was restored to control levels after riluzole administration. Conversely, riluzole had no effect on functional connectivity in the control group; hence again, irrespective of baseline activity, control and ASD subjects significantly differed in their prefrontal response to E-I challenge.

Finally, to examine E-I dynamics at the extracellular level, I explored neurotransmitter efflux into the extracellular space in the living rat brain, using *in vivo* microdialysis (Chapter 6). I hypothesized that differences in E-I dynamics in a rat model of ASD would be present at the extracellular level. I hoped that the findings would inform me what extracellular E-I changes were driving the observed differences in functional connectivity response. However, riluzole had no measurable effect on glutamate or GABA efflux in either brain region in either wild type or *Nrxn1α*$^{-/-}$ rats. For an outline of findings, see Figure 7.2.

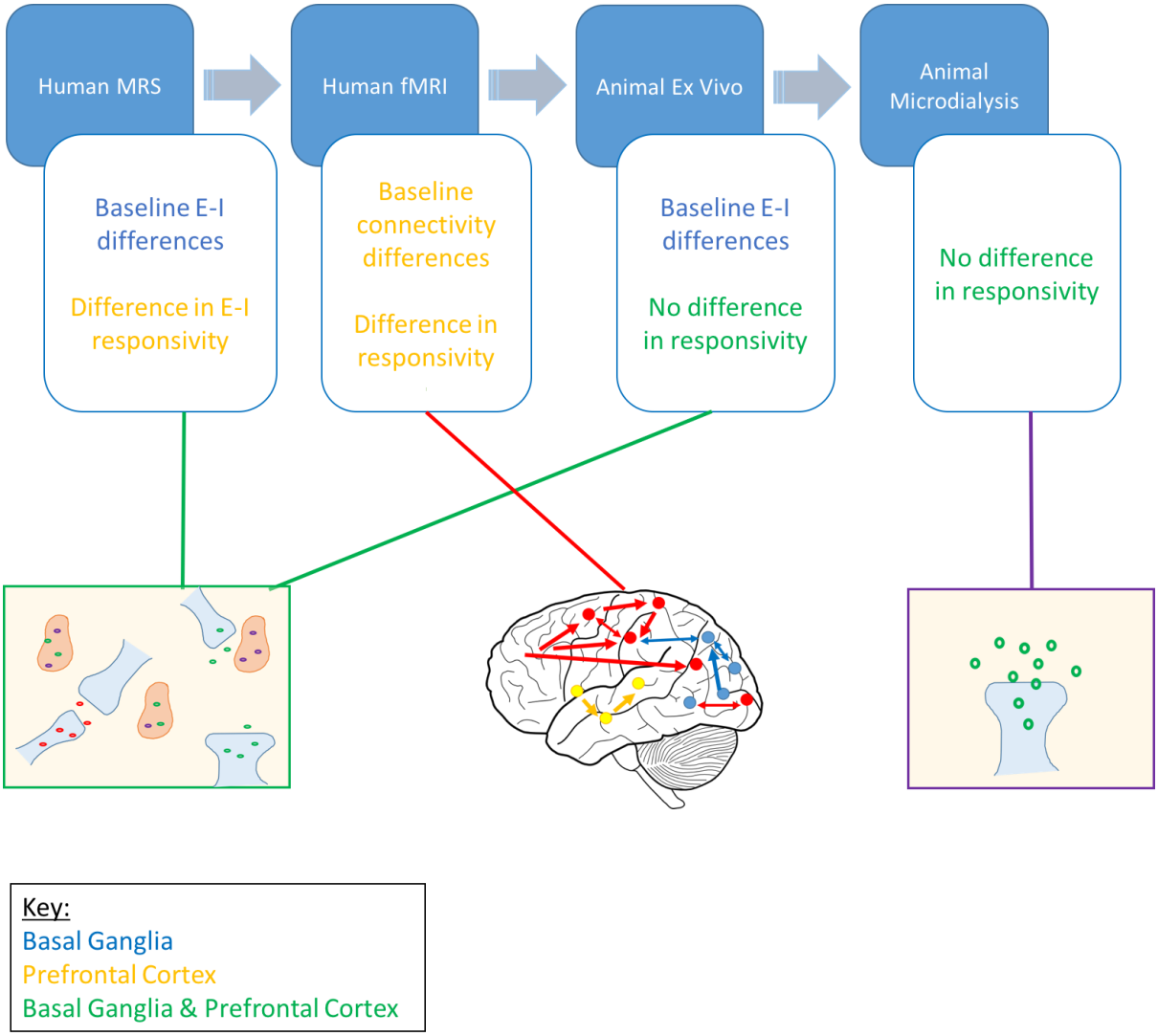

Figure 7.2: Summary of results at each level of investigation

Intracellular measures of E-I (MRS in humans and animal *ex vivo* studies) showed baseline differences in E-I balance in the basal ganglia in men with and without ASD and mice with and without the Nrxn1α gene. In the prefrontal cortex, despite no group difference at baseline, the human study reported a group difference in E-I responsivity. E-I baseline and responsivity differences were also found in functional connectivity measures of the human prefrontal cortex. No effect of riluzole on E-I dynamics was found in microdialysis studies in either brain region.

7.2 E-I dynamics at the intracellular level

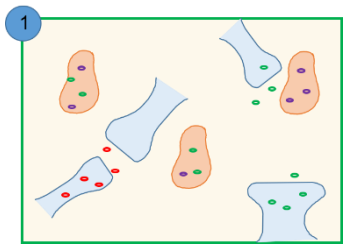

Investigations into bulk tissue E-I dynamics in humans highlighted group differences in regional responsivity to an E-I challenge with riluzole. The findings presented in Chapters 3 and 4 confirm previously reported E-I imbalances at the intracellular level in ASD (Bernardi et al., 2011; Harada et al., 2011; Hassan et al., 2013; Horder et al., 2013; Joshi et al., 2013; Tebartz van Elst et al., 2014) and for the first time, show that E-I balance is open to modulation in adults with ASD. The potential causes for such group differences in regional responsivity profiles are numerous and are discussed in full in Chapter 4.

One potential explanation, is that the cellular composition of the two regions are very different in terms of their relative proportions of neurons to glial cells. Abnormalities in both neuronal, and in particular glial activity have been reported in the prefrontal cortex, but not basal ganglia regions in ASD, which may go some way to explain why the ASD response in the prefrontal cortex is different to that of controls, but the basal ganglia effect is the same. This is speculative however, as MRS does not distinguish between neuronal and glial effects; and though [1H]MRS was able to detect alterations to E-I at rest and when challenged, it is unknown where in the total neurotransmitter 'pool' this signal arises.

In addition to a lack of cellular specificity, the analysis techniques used in humans in this study were also unable to differentiate between some key metabolites, most notably between glutamate (glu) and its metabolite, glutamine (gln). In the present study, excitatory neurotransmitter measures were reported as the combined 'Glx', as is commonly accepted in the literature. Capturing Glx in this way, despite being an indicator of E-I flux, does not account for potential differences in glu-gln ratios, which may be altered in ASD (Cochran et

al., 2015; Shimmura et al., 2013). The importance of eventually investigating glutamine and glutamate levels separately in human studies was suggested by the animal *ex vivo* analyses (Chapter 5). Specifically, there were no group differences in the combined Glx measure in the animal model and WT at baseline in either brain region tested; yet when analysed as individual metabolites, significant differences in baseline glutamine and glutamate were found in the PFC and CPu, respectively. In light of these findings, future MRS studies in people should endeavour to use new techniques which are capable of quantifying both glutamate and glutamine as separate measures (Ramadan et al., 2013), as any group differences in human glutamine levels may have been overlooked here, and thus the combined Glx findings may present a false negative result. A simple way of tackling this problem may be to scan at a higher magnetic field strength, such as 7T, which has proven to be capable of separating the Glx signal, whilst also capturing GABA (Cai et al., 2012; Lally et al., 2016; Wijtenburg, Rowland, Edden, & Barker, 2013).

Likewise, the GABA measure in the present thesis was also potentially contaminated, as it contained macromolecule (MM) signal and was therefore reported as GABA+. New GABA editing techniques allow for the detection of GABA alone (Harris et al., 2015; Henry et al., 2001) and should be considered in addition to separation of the Glx signal to obtain a 'clean' measure of GABA and glutamate in future MRS studies of E-I.

Finally, pre-selecting the MRS voxels restricted data capture to two specific locations, but it is clear from the present thesis (Chapters 3 and 4) and the previous literature (Table 1.3) that E-I imbalances in ASD may be found in multiple regions across the brain. These regions work together in complex networks, therefore, to further investigate E-I dynamics at the

whole brain level, it was necessary to assess the influence of E-I on functional network activity.

7.3 E-I dynamics at the functional level

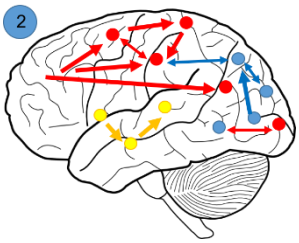

Regional E-I dynamics are thought to regulate the functional connectivity of resting state networks in the brain, yet responsivity of these networks to E-I challenge has not previously been investigated. In Chapter 3, having found group differences in intracellular responsivity of the prefrontal cortex, I next examined responsivity of the anterior cingulate cortex (the core region captured by the MRS voxel) in terms of its connectivity with the rest of the brain.

Riluzole restored absent functional connectivity of prefrontal-posterior networks in the ASD group, and did not alter functional connectivity in the control brain. Thus, for the first time, I showed that functional connectivity of the adult ASD brain is open to pharmacological modulation, and that functional networks in the ASD brain respond differently to controls. Previous studies have indicated that resting tissue measures of glutamate and GABA are predictive of network activity in control subjects (Duncan et al., 2013; Enzi et al., 2012; Horn et al., 2010; Kapogiannis et al., 2013; Kwon et al., 2014), however the present study showed no correlation between MRS and fMRI measures in either controls or those with ASD. This disconnect between bulk measures of neurotransmitter pools and neural activity may be unsurprising. Functional connectivity is a measure of the oxygen demand of brain tissue, which is assumed to be required for neuronal activity. However, this activity could be glutamatergic or GABAergic/excitatory or inhibitory. fMRI is unable to distinguish between the two and is therefore a measure of 'bulk' brain activity, in the same way as MRS is a measure of the bulk (metabolic and active) neurotransmitter pool- hence the two may not necessarily correlate. Particularly in the ASD cohort, the relationship between brain function and tissue metabolite concentration may not be straightforward. Consistent with this, intracellular findings have previously been shown to correlate with functional outputs in

control subjects, but not in those with ASD. For example, in the absence of a group difference in GABA levels in the occipital cortex in adults with and without ASD, Robertson et al. (2016) reported a relationship between GABA levels and performance in binocular rivalry tasks in controls and not ASD. Likewise, Schallmo et al. (2017) recently presented early data indicating modulation of the GABA receptor by lorazepam affected individual perception across control individuals in opposite ways.

Therefore, in an attempt to understand the driving factors behind the fMRI result, I sought to investigate E-I dynamics at the extracellular level using *in vivo* microdialysis in a rodent model of ASD.

7.4 E-I dynamics at the extracellular level

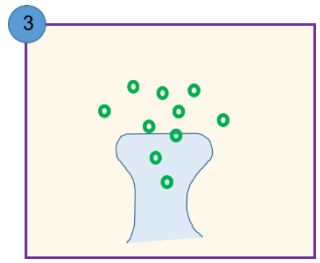

Having established that the *Neurexin1*$\alpha^{-/-}$ rat had comparable baseline E-I balance to ASD (Chapter 5), this model was used to investigate extracellular E-I responsivity. I postulated that there would be group differences in riluzole-evoked E-I efflux between wild type and *Nrxn1*$\alpha^{-/-}$ rats, which would help to further understand what was driving the connectivity findings in the human brain. However, no effect of riluzole was observed on either GABA or glutamate efflux in either the medial prefrontal cortex or caudate putamen.

Whilst extracellular measures provided a step closer to understanding synaptic activity, they are not necessarily indicative of the levels of active neurotransmitters involved in signaling. The efflux of neurotransmitter into the extracellular space may therefore not give sufficient information to understand the complex mechanisms underlying altered E-I neurotransmission, and hence connectivity.

The negative findings from the microdialysis studies could be due to a number of reasons. First, as previously discussed - the concentration of riluzole may have been too low to engage with relevant molecular targets. In previous *in vitro* studies, riluzole altered neurotransmitter efflux when in the micromolar range (Cheramy et al., 1992; Hubert, Delumeau, Glowinski, Prémont, & Doble, 1994; Martin, Thompson, & Nadler, 1993), whereas in my *in vivo* experiment (Chapter 6), riluzole was calculated to be present in nanomolar concentrations. Future studies should therefore aim to investigate the effect of a range of doses. This would be of particular interest as riluzole has been shown to have different effects on E-I balance at different concentrations. For example at low micromolar levels, riluzole reportedly inhibits release of excitatory neurotransmitters and potentiates $GABA_A$ receptor activity, whereas

GABA release is inhibited at 10 fold higher concentrations (Jahn et al., 2008; Martin et al., 1993). In my human experiments, the poly-pharmacology of riluzole at glutamate and GABA systems (in addition to reports of wide-ranging mechanisms of action at ion channels by Bellingham, 2011, and Doble, 1996) was advantageous when attempting to evoke a 'Proof of Concept' response in a heterogeneous cohort of individuals. Yet this same broad range of actions may hinder attempts to understand the effect of the drug on specific targets. For this, further, more directed probes of E-I may be required. I suggest that future experiments could use E-I acting drugs which are more selective for specific targets (for example $mGluR_5$ antagonists such as 2-methyl-6-phenylethyl-pyrididine (MPEP), or $GABA_A$ receptor modulators such as benzodiazepines, both of which have shown promise in preclinical and clinical studies of ASD models and patients (Han et al., 2014; Mehta et al., 2011; Silverman et al., 2010).

7.5 Implications for future research of E-I pharmacology (back-translation)

The present thesis attempted to 'back-translate' from humans to animal models in order to explore the effects of an E-I challenge on neurotransmitter efflux. Going forward, more direct measures of E-I in ASD models are needed.

Possible approaches include electrophysiological techniques such as patch clamp recordings, which have previously identified differences in the neuronal activity of cultured neurons and brain slices from animal models of ASD. For example in cortical neurons, decreased glutamatergic transmission was recorded in ubiquitin protein ligase E3A (UBE3A) mice alongside social and interaction impairments (Smith et al., 2011), and increased GABA

transmission was shown in mice carrying the autism-associated neuroligin 3 point mutation (Tabuchi et al., 2007). *In vitro* electrophysiology may therefore be useful for measuring changes in glutamatergic and GABAergic neuronal activity after riluzole administration. However, these measurements must be carried out *ex vivo*, and are therefore not ideal for capturing the complex environment of the living brain. Equivalent *in vivo* alternatives may be available however, as shown by a recent study in awake macaque monkeys, which demonstrated pharmacological manipulation of E-I balance in the auditory cortex by NMDA channel blockers, ketamine and MK-801, in terms of auditory-evoked-potentials as an electrophysiological biomarker (Holliday et al., 2017).

There is currently no methodology available to directly measure neural activity in the living brain, yet there is hope, as new techniques such as oxygen amperometry can highlight *in vivo* changes in extracellular oxygen, in a similar manner to the BOLD fMRI signal (Bolger et al., 2011; Lowry et al., 2010). Unlike the BOLD signal however, there is a good degree of certainty that recorded changes in oxygen level are functionally related to discrete neural activation events (Li et al., 2011). Future experiments could utilize this technique in awake, freely moving rats, to investigate the effect of riluzole on the activation of specific regions within brain networks.

However, alongside probing E-I regulation of neuronal activity relevant to ASD, it has been noted that glia help maintain E-I balance (Auld & Robitaille, 2003; Domercq et al., 2013; Liang et al., 2006) and may be involved in the pathology of ASD (Bernstein et al., 2009; Durieux et al., 2015; Onore et al., 2012; Shigemori et al., 2015). Furthermore, in addition to an effect on neural activity and neuronal glutamate and GABA release, riluzole has been shown to affect glial mechanisms. For example, riluzole is reported to enhance glutamate

uptake into glia via glutamate transporter GLT-1 (Carbone et al., 2012; Dall'Igna et al., 2013; Yoshizumi et al., 2012), whilst paradoxically also facilitating release of glutamate from glia (Hayashida et al., 2010).

It may be beneficial therefore for future studies to also investigate riluzole's glial-specific mechanisms of action in the atypical brain. The benefits of investigating drug action in different cell types has previously been shown in the field of depression, whereby the discovery of riluzole's effects on glutamate metabolism in astrocytes prompted the exploration of its therapeutic potential as an antidepressant. Indeed, the results supported riluzole-evoked reversal of a depressive like phenotype in rats, via restoration of glutamate homeostasis in glia (Yu et al., 2011). In future, examinations of glial mechanisms may come in the form of investigating drug effects on glial specific targets, such as the GLT-1 and GLAST glutamate transporters (Chaudhry et al., 1995). Together, findings from more in-depth back-translation studies, which dissect the mechanism of action of riluzole will, I hope, inform future clinical studies. It may eventually be possible to identify which groups along the spectrum may respond best to a specific E-I intervention (see Figure 7.3).

Nevertheless, I do not rule out the possibility that the ability of riluzole to affect both neuronal and glial targets may itself be beneficial for a spectrum disorder such as ASD, as it may be able to modulate E-I in a variety of ways in people with varied clinical presentations.

7.6 Implications for future research into E-I acting therapeutics (forward-translation)

In line with this, open label studies in children and adults have provided supportive evidence for the effectiveness of riluzole in patients with psychiatric disorders, including OCD (Coric et al., 2005; Grant et al., 2007), schizophrenia (Farokhnia et al., 2014), depression (Zarate et al., 2004) and generalized anxiety (Mathew et al., 2005). Yet in trials in patients with ASD, the primary outcome of improving core symptoms has not yet been reached. For example, in a study by Ghaleiha et al., riluzole was used as an adjunct to risperidone for the treatment of irritability in 49 children (age 5-12 years) with ASD. Participants in the riluzole treatment group demonstrated improved irritability scores, reduced social withdrawal and lethargy, reduced stereotypical behaviours and reduced hyperactivity. Within the study, more patients within the riluzole group were deemed 'responders' than those in the risperidone-only group, however despite improvements across symptoms, none reached statistical significance, and there were no significant differences in the primary outcome of an improved Clinical Global Impressions (CGI) score (Ghaleiha et al., 2013). Likewise, an open-label study of riluzole in 6 adult men with Fragile X syndrome showed limited improvements in the primary outcome of reduced repetitive behaviours, and again showed no significant change in CGI scores (Erickson et al., 2011). Wink et al., demonstrated moderate improvements in repetitive behaviours and irritability in three adult men with ASD, though the small sample size and lack of a placebo control did not allow for a full review of its efficacy (Wink et al., 2011). Finally, a single case study of one 13 year old girl with ASD reported an observed reduction in screaming and compulsivity after taking riluzole for 6 weeks, but no change in the core symptoms of ASD (Veenstra-Vanderweele, 2010). In this case, and in other studies of children (Mechler et al., 2017), riluzole treatment was terminated due to adverse side effects

(such as mild elevation of liver enzymes), however this is less common in studies of adults, who appear to tolerate riluzole well.

Though the results are positive overall, clinical trials of riluzole are hindered by a lack of significant outcomes, which may potentially be due to the heterogeneity of the participants in the study. Initial stratification of the patient sample, by examining E-I responsivity to a single dose of riluzole, potentially using a protocol as outlined in Chapters 3 and 4 of this thesis, may highlight those patients who are capable of E-I modulation, and therefore more likely to be 'responders'. For example, in Chapter 3, I observed that the extent of riluzole-evoked shift in prefrontal E-I balance was linked to clinical symptom presentation- patients with the most symptoms in the social and communication symptom domains responded the least to riluzole challenge.

Therefore, based on the results outlined in this thesis, an 8 week clinical study, 'Predicting treatment response in ASD', is currently under ethical review for implementation in 2018. This study will aim to invite patients with ASD to undergo an initial MRS scan after a single dose of riluzole, followed by an 8 week period of daily riluzole administration and will examine whether response to a test dose is correlated with outcome. The primary end points for this study will be acute (initial scan) and persistent (8 week scan) riluzole-induced changes in imaging indices (MRS and fMRI) and improvements in clinical scores (from psychometric tests), which I hope will correlate.

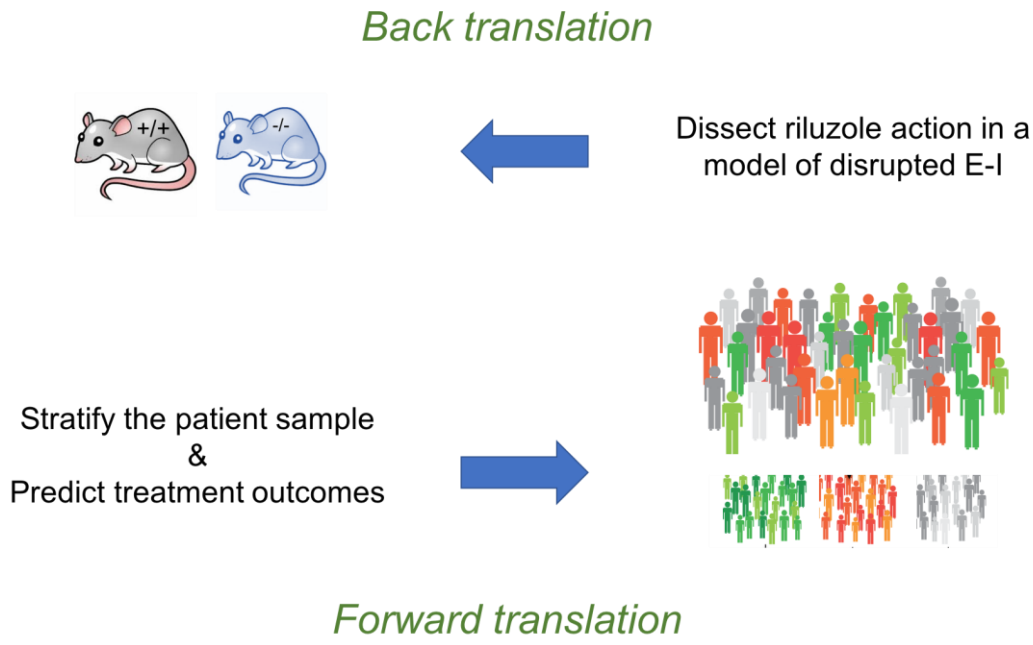

Figure 7.3: Future plans for back and forwards translation of results

7.7 Conclusions

From the outset of this thesis, it was clear that improved treatment targets are required for ASD. In addition, evidence that these targets can be shifted in advance of starting lengthy and expensive clinical trials is much needed. This thesis has begun to address this by identifying the glutamate-GABA system as a dynamic biomarker for ASD, against which drugs can be targeted and individual response to a test dose i.e. 'target-engagement' measured. Over the course of this PhD, I have shown the E-I system in ASD can be modulated, even in the mature adult brain. Additionally, the results presented here indicate the brain in ASD is pharmacologically different to the control brain.

These findings have implications for both back-translation, to better understand the biological mechanisms of E-I in ASD, and forward-translation, towards identifying subgroups of patients likely to respond to a particular drug prior to treatment, thereby working towards a personalized approach to medicine in ASD.

References

Abarca, C., Silva, E., Sepúlveda, M. J., Oliva, P., & Contreras, E. (2000). Neurochemical changes after morphine, dizocilpine or riluzole in the ventral posterolateral thalamic nuclei of rats with hyperalgesia. *European Journal of Pharmacology*, *403*(1–2), 67–74.

Abbara, C., Estournet, B., Lacomblez, L., Lelièvre, B., Ouslimani, A., Lehmann, B., … Diquet, B. (2011). Riluzole pharmacokinetics in young patients with spinal muscular atrophy. *British Journal of Clinical Pharmacology*, *71*(3), 403–410.

Abramowitz, J. S., & Deacon, B. J. (2006). Psychometric properties and construct validity of the Obsessive-Compulsive Inventory-Revised: Replication and extension with a clinical sample. *Journal of Anxiety Disorders*, *20*, 1016–1035.

Accordino, R. E., Kidd, C., Politte, L. C., Henry, C. A., & McDougle, C. J. (2016). Psychopharmacological interventions in autism spectrum disorder. *Expert Opinion on Pharmacotherapy*, *17*(7), 937–952.

Adams, J. B., Johansen, L. J., Powell, L. D., Quig, D., & Rubin, R. A. (2011). Gastrointestinal flora and gastrointestinal status in children with autism--comparisons to typical children and correlation with autism severity. *BMC Gastroenterology*, *11*, 22.

Aggarwal, S., & Angus, B. (2015). Misdiagnosis versus missed diagnosis: diagnosing autism spectrum disorder in adolescents. *Australasian Psychiatry*, *23*(2), 120–123.

AHRQ. (2011). Therapies for children with autism spectrum disorders. *American Family Physician*, *85*(9), 1–4.

Ajram, L. A., Durieux, A. M. S., Carvalho Pereira, A., Velthuis, H. E., Petrinovic, M. M., & McAlonan, G. M. (2018). *The contribution of [1H] Magnetic Resonance Spectroscopy to the study of excitation-inhibition in autism. Prog Neuro-Psychopharm and Biol Psych*. 89, 236-244.

Ajram, L. A., Horder, J., Mendez, M. A., Galanopoulos, A., Brennan, L. P., Wichers, R. H., … McAlonan, G. M. (2017). Shifting brain inhibitory balance and connectivity of the prefrontal cortex of adults with autism spectrum disorder. *Transl Psychiatry*, *7*, e1137.

Al-Hamdan, A. Z., Preetha, P. P., Albashaireh, R. N., Al-Hamdan, M. Z., & Crosson, W. L. (2018). Investigating the effects of environmental factors on autism spectrum disorder in the USA using remotely sensed data. *Environmental Science and Pollution Research*, *25*(8), 7924–7936.

American Psychiatric Association. (2000). *Diagnostic and statistical manual of mental disorders IV*. *American Journal of Psychiatry* (4th ed.). American Psychiatric Publishing: Arlington, VA.

American Psychiatric Association. (2013). *Diagnostic and statistical manual of mental disorders V*. *American Journal of Psychiatry* (5th ed.). American Psychiatric Publishing: Arlington, VA.

Amir, R. E., Van den Veyver, I. B., Wan, M., Tran, C. Q., Francke, U., & Zoghbi, H. Y. (1999). Rett syndrome is caused by mutations in X-linked MECP2, encoding methyl-CpG-binding protein 2. *Nature Genetics*, *23*(2), 185–188.

Analysis group, FMRIB, Oxford, U. (2015). FMRIB Software Library. Retrieved from www.fmrib.ox.ac.uk/fsl

Andersson, M., Horder, J., Mendez, M. A., Tangen, A., Lundberg, J., Gee, A., … Borg, J. (2017). A multicenter positron emission tomography study of GABA receptor availability in adults with autism. In *30th ECNP Congress*. Paris.

Aoki, Y., Kasai, K., & Yamasue, H. (2012). Age-related change in brain metabolite abnormalities in autism: a meta-analysis of proton magnetic resonance spectroscopy studies. *Translational Psychiatry*, *2*, e69.

Ashwood, K. L., Gillan, N., Horder, J., Hayward, H., Woodhouse, E., McEwen, F. S., … Murphy, D. G. (2016). Predicting the diagnosis of autism in adults using the Autism-Spectrum Quotient (AQ) questionnaire. *Psychological Medicine*, 1–10.

Assaf, M., Jagannathan, K., Calhoun, V. D., Miller, L., Stevens, M. C., Sahl, R., … Pearlson, G. D. (2010). Abnormal functional connectivity of default mode sub-networks in autism spectrum disorder patients. *NeuroImage*, *53*(1), 247–256.

Atladóttir, H. Ó., Thorsen, P., Østergaard, L., Schendel, D. E., Lemcke, S., Abdallah, M., & Parner, E. T. (2010). Maternal infection requiring hospitalization during pregnancy and autism spectrum disorders. *Journal of Autism and Developmental Disorders*, *40*(12), 1423–1430.

Auld, D. S., & Robitaille, R. (2003). Glial cells and neurotransmission: an inclusive view of synaptic function. *Neuron*, *40*(2), 389–400.

Avoli, M., & de Curtis, M. (2011). GABAergic synchronization in the limbic system and its role in the generation of epileptiform activity. *Progress in Neurobiology*, *95*(2), 104–132.

Banerjee, A., García-Oscos, F., Roychowdhury, S., Galindo, L. C., Hall, S., Kilgard, M. P., & Atzori, M. (2013). Impairment of cortical GABAergic synaptic transmission in an environmental rat model of autism. *The International Journal of Neuropsychopharmacology*, *16*(06), 1309–1318.

Barkley, & Russell, A. (2011). *Barkley Adult ADHD Rating Scale-IV (BAARS-IV)*. New York: The Guildford Press.

Baron-Cohen, S., Wheelwright, S., Skinner, R., Martin, J., & Clubley, E. (2001). The Autism-Spectrum Quotient (AQ): Evidence from Asperger Syndrome/High-Functioning Autism, Males and Females, Scientists and Mathematicians. *Journal of Autism and Developmental Disorders*, *31*(1), 5–17.

Baudouin, S. J. (2014). Heterogeneity and convergence: the synaptic pathophysiology of autism. *European Journal of Neuroscience*, *39*(7), 1107–1113.

Behar, T. N., Scott, C. A., Greene, C. L., Wen, X., Smith, S. V., Maric, D., … Barker, J. L. (1999). Glutamate Acting at NMDA Receptors Stimulates Embryonic Cortical Neuronal Migration. *J. Neurosci.*, *19*(11), 4449–4461.

Bejjani, A., O'Neill, J., Kim, J. A., Frew, A. J., Yee, V. W., Ly, R., … Levitt, J. G. (2012). Elevated glutamatergic compounds in pregenual anterior cingulate in pediatric autism spectrum disorder demonstrated by1H MRS and 1H MRSI. *PLoS ONE*, *7*(7), e38786.

Bellingham, M. C. (2011). A Review of the Neural Mechanisms of Action and Clinical Efficiency of Riluzole in Treating Amyotrophic Lateral Sclerosis: What have we Learned in the Last Decade? *CNS Neuroscience & Therapeutics*, *17*(1), 4–31.

Belsito, K. M., Law, P. A., Kirk, K. S., Landa, R. J., & Zimmerman, A. W. (2001). Lamotrigine therapy for autistic disorder: a randomized, double-blind, placebo-controlled trial. *Journal of Autism and Developmental Disorders*, *31*(2), 175–181.

Ben-Ari, Y., Khalilov, I., Kahle, K. T., & Cherubini, E. (2012). The GABA excitatory/inhibitory shift in brain maturation and neurological disorders. *The Neuroscientist*, *18*(5), 467–486.

Ben-Yaakov, G., & Golan, H. (2003). Cell proliferation in response to GABA in postnatal hippocampal slice culture. *International Journal of Developmental Neuroscience*, *21*(3), 153–157.

Berg, J. M., & Geschwind, D. H. (2012). Autism genetics: searching for specificity and convergence. *Genome Biology*, *13*(7), 247.

Bernardi, S., Anagnostou, E., Shen, J., Kolevzon, A., Buxbaum, J. D., Hollander, E., … Fan, J. (2011). In vivo 1H-magnetic resonance spectroscopy study of the attentional networks in autism. *Brain Research*, *1380*, 198–205.

Bernstein, H.-G., Steiner, J., & Bogerts, B. (2009). Glial cells in schizophrenia: pathophysiological significance and possible consequences for therapy. *Expert Review of Neurotherapeutics*, *9*(7), 1059–1071.

Berry-Kravis, E., Des Portes, V., Hagerman, R., Jacquemont, S., Charles, P., Visootsak, J., … von Raison, F. (2016). Mavoglurant in fragile X syndrome: Results of two randomized, double-blind, placebo-controlled trials. *Science Translational Medicine*, *8*(321), 321ra5-321ra5.

Besag, F. (2017). Epilepsy in patients with autism: links, risks and treatment challenges. *Neuropsychiatric Disease and Treatment*, *Volume 14*, 1–10.

Bettelheim, B. (1967). The empty fortress: Infantile autism and the birth of the self. *Pediatrics*, *40*(2), 312–313.

Billstedt, E., Gillberg, C., & Gillberg, C. (2005). Autism after adolescence: Population-based 13- to 22-year follow-up study of 120 individuals with autism diagnosed in childhood. *Journal of Autism and Developmental Disorders*, *35*(3), 351–360.

Biswal, B., Yetkin, F. Z., Haughton, V. M., & Hyde, J. S. (1995). Functional connectivity in the motor cortex of resting human brain using echo-planar MRI. *Magnetic Resonance in Medicine : Official Journal of the Society of Magnetic Resonance in Medicine / Society of Magnetic Resonance in Medicine*, *34*(4), 537–541.

Blatt, G. J., Fitzgerald, C. M., Guptill, J. T., Booker, A. B., Kemper, T. L., & Bauman, M. L. (2001). Density and distribution of hippocampal neurotransmitter receptors in autism: an autoradiographic study. *Journal of Autism and Developmental Disorders*, *31*(6), 537–543.

Blüml, S., & Panigrahy, A. (2013). Magnetic Resonance Spectroscopy: Basics. In S. Blüml & A. Panigrahy (Eds.), *MR Spectroscopy of Pediatric Brain Disorders* (X1V ed., pp. 1–401). Springer.

Bolger, F. B., McHugh, S. B., Bennett, R., Li, J., Ishiwari, K., Francois, J., … Lowry, J. P. (2011). Characterisation of carbon paste electrodes for real-time amperometric monitoring of brain tissue oxygen. *Journal of Neuroscience Methods*, *195*(2), 135–142.

Borland, L. M., Shi, G., Yang, H., & Michael, A. C. (2005). Voltammetric study of extracellular dopamine near microdialysis probes acutely implanted in the striatum of the anesthetized rat. *Journal of Neuroscience Methods*, *146*(2), 149–158.

Bourdelais, A. J., & Kalivas, P. W. (1992). Modulation of extracellular gamma-aminobutyric acid in the ventral pallidum using in vivo microdialysis. *Journal of Neurochemistry*, *58*(6), 2311–2320.

Breese, C. R., & Leonard, S. S. (1994). Glutamate Receptor Subtype Expression in Human Postmortem Brain. *Journal of Molecular Neuroscience*, *263*(4), 82–90.

Bristot Silvestrin, R., Bambini-Junior, V., Galland, F., Daniele Bobermim, L., Quincozes-Santos, A., Torres Abib, R., … Gottfried, C. (2013). Animal model of autism induced by prenatal exposure to valproate: Altered glutamate metabolism in the hippocampus. *Brain Research*, *1495*, 52–60.

Brix, M. K., Ersland, L., Hugdahl, K., Grüner, R., Posserud, M.-B., Hammar, Å., … Beyer, M. K. (2015). Brain MR spectroscopy in autism spectrum disorder—the GABA excitatory/inhibitory imbalance theory revisited. *Frontiers in Human Neuroscience*, *9*(June), 1–12.

Brodkin, E. S. (2007). BALB/c mice: Low sociability and other phenotypes that may be relevant to autism. *Behavioural Brain Research*, *176*(1), 53–65.

Brown, M. S., Singel, D., Hepburn, S., & Rojas, D. C. (2013). Increased glutamate concentration in the auditory cortex of persons with autism and first-degree relatives: A 1H-MRS study. *Autism Research*, *6*(1), 1–10.

Brugha, T. S., McManus, S., Bankart, J., Scott, F., Purdon, S., Smith, J., … Meltzer, H. (2011). Epidemiology of autism spectrum disorders in adults in the community in England. *Archives of General Psychiatry*, *68*(5), 459–465.

Bryson, H. M., Fulton, B., & Benfield, P. (1996). Riluzole. A review of its pharmacodynamic and pharmacokinetic properties and therapeutic potential in amyotrophic lateral sclerosis. *Drugs*, *52*(4), 549–563.

Bucan, M., Abrahams, B. S., Wang, K., Glessner, J. T., Herman, E. I., Sonnenblick, L. I., … Hakonarson, H. (2009). Genome-wide analyses of exonic copy number variants in a family-based study point to novel autism susceptibility genes. *PLoS Genetics*, *5*(6), e1000536.

Buescher, A. V, Cidav, Z., Knapp, M., & Mandell, D. S. (2014). Costs of autism spectrum disorders in the United Kingdom and the United States. *JAMA Pediatr*, *168*(8), 721–728.

Burrows, E. L., Laskaris, L., Koyama, L., Churilov, L., Bornstein, J. C., Hill-Yardin, E. L., & Hannan, A. J. (2015). A neuroligin-3 mutation implicated in autism causes abnormal aggression and increases repetitive behavior in mice. *Molecular Autism*, *6*(1), 62.

Buzsáki, G., Kaila, K., & Raichle, M. (2007). Inhibition and Brain Work. *Neuron*, *56*(5), 771–783.

Cai, H.-L., Zhu, R.-H., & Li, H.-D. (2010). Determination of dansylated monoamine and amino acid neurotransmitters and their metabolites in human plasma by liquid chromatography–electrospray ionization tandem mass spectrometry. *Analytical Biochemistry*, *396*(1), 103–111.

Cai, K., Nanga, R. P., Lamprou, L., Schinstine, C., Elliott, M., Hariharan, H., … Epperson, C. N. (2012). The Impact of Gabapentin Administration on Brain GABA and Glutamate Concentrations: A 7T 1H-MRS Study. *Neuropsychopharmacology*, *37*(13), 2764–2771.

Calderoni, S., Bellani, M., Hardan, A. Y., Muratori, F., & Brambilla, P. (2014). Basal ganglia and restricted and repetitive behaviours in Autism Spectrum Disorders: current status and future perspectives. *Epidemiology and Psychiatric Sciences*, *23*(03), 235–238.

Capo, L. C. (2001). Autism, employment, and the role of occupational therapy. *Work*, *16*(3), 201–207.

Carbone, M., Duty, S., & Rattray, M. (2012). Riluzole elevates GLT-1 activity and levels in striatal astrocytes. *Neurochemistry International*, *60*(1), 31–38.

Carlsson, L. H., Norrelgen, F., Kjellmer, L., Westerlund, J., Gillberg, C., & Fernell, E. (2013). Coexisting disorders and problems in preschool children with autism spectrum disorders. *The Scientific World Journal*, *2013*, 213979.

Carvalho Pereira, A., Violante, I. R., Mouga, S., Oliveira, G., & Castelo-Branco, M. (2017). Medial Frontal Lobe Neurochemistry in Autism Spectrum Disorder is Marked by Reduced N-Acetylaspartate and Unchanged Gamma-Aminobutyric Acid and Glutamate + Glutamine Levels. *Journal of Autism and Developmental Disorders*, 1–16.

Castro, J., Mellios, N., & Sur, M. (2013). Mechanisms and therapeutic challenges in autism spectrum disorders: insights from Rett syndrome. *Current Opinion in Neurology*, *26*(2), 154–159.

Centers for Disease Control and Prevention. (2014). Prevalence of autism spectrum disorder among children aged 8 years - autism and developmental disabilities monitoring network, 11 sites, United States, 2010. *Morbidity and Mortality Weekly Report. Surveillance Summaries*, *63*(2), 1–21.

Chana, G., Laskaris, L., Pantelis, C., Gillett, P., Testa, R., Zantomio, D., … Skafidas, E. (2015). Decreased expression of mGluR5 within the dorsolateral prefrontal cortex in autism and increased microglial number in mGluR5 knockout mice: Pathophysiological and neurobehavioral implications. *Brain, Behavior, and Immunity*, *49*, 197–205.

Charles, H. C., Lazeyras, F., Krishnan, K. R., Boyko, O. B., Patterson, L. J., Doraiswamy, P. M., & McDonald, W. M. (1994). Proton spectroscopy of human brain: effects of age and sex. *Prog Neuropsychopharmacol Biol Psychiatry*, *18*(6), 995–1004.

Charman, T., & Baird, G. (2002). Practitioner Review: Diagnosis of autism spectrum disorder in 2-and 3-year-old children. *Journal of Child Psychology and Psychiatry*, *43*(3), 289–305.

Charman, T., Baron-Cohen, S., Swettenham, J., Baird, G., Cox, A., & Drew, A. (2000). Testing joint attention, imitation, and play as infancy precursors to language and theory of mind. *Cognitive Development*, *15*(4), 481–498.

Chaste, P., Sanders, S. J., Mohan, K. N., Klei, L., Song, Y., Murtha, M. T., … Kim, S.-J. (2014). Modest Impact on Risk for Autism Spectrum Disorder of Rare Copy Number Variants at 15q11.2, Specifically Breakpoints 1 to 2. *Autism Research*, *7*(3), 355–362.

Chaudhry, F. A., Lehre, K. P., Lookeren Campagne, M. van, Ottersen, O. P., Danbolt, N. C., & Storm-Mathisen, J. (1995). Glutamate transporters in glial plasma membranes: Highly differentiated localizations revealed by quantitative ultrastructural immunocytochemistry. *Neuron*, *15*(3), 711–720.

Chefer, V. I., Thompson, A. C., Zapata, A., & Shippenberg, T. S. (2009). Overview of brain microdialysis. In *Current Protocols in Neuroscience* (Vol. Chapter 7). NIH Public Access.

Cheramy, A., Barbeito, L., Godeheu, G., & Glowinski, J. (1992). Riluzole inhibits the release of glutamate in the caudate nucleus of the cat in vivo. *Neuroscience Letters*, *147*, 209–212.

Cherkassky, V. L., Kana, R. K., Keller, T. A., & Just, M. A. (2006). Functional connectivity in a baseline resting-state network in autism. *NeuroReport*, *17*(16), 1687–1690.

Chew, D. J., Carlstedt, T., & Shortland, P. J. (2014). The effects of minocycline or riluzole treatment on spinal root avulsion-induced pain in adult rats. *Journal of Pain*, *15*, 664–675.

Ching, M. S. L. L., Shen, Y., Tan, W.-H. H., Jeste, S. S., Morrow, E. M., Chen, X., … Children's Hospital Boston Genotype Phenotype Study Group. (2010). Deletions of NRXN1 (neurexin-1) predispose to a wide spectrum of developmental disorders. *American Journal of Medical Genetics, Part B: Neuropsychiatric Genetics*, *153B*(4), 937–947.

Ciranna, L. (2006). Serotonin as a modulator of glutamate- and GABA-mediated neurotransmission: implications in physiological functions and in pathology. *Current Neuropharmacology*, *4*(2), 101–114.

Clarke, G., Stilling, R. M., Kennedy, P. J., Stanton, C., Cryan, J. F., & Dinan, T. G. (2014). Minireview: Gut microbiota: the neglected endocrine organ. *Mol Endocrinol*, *28*(8), 1221–1238.

Clayton, G. H., Owens, G. C., Wolff, J. S., & Smith, R. L. (1998). Ontogeny of cation-Cl- cotransporter expression in rat neocortex. *Brain Research. Developmental Brain Research*, *109*(2), 281–292.

Clin Calc LLC. (2018). ClinCalc.com.

CMA Microdialysis. (1991). *Microdialysis - principles of recovery*. Stockholm.

Cochran, D. M., Sikoglu, E. M., Hodge, S. M., Edden, R. A. E., Foley, A., Kennedy, D. N., … Frazier, J. A. (2015). Relationship among Glutamine, γ-Aminobutyric Acid, and Social Cognition in Autism Spectrum Disorders. *Journal of Child and Adolescent Psychopharmacology*, *25*(4), 314–322.

Coderre, T. J., Kumar, N., Lefebvre, C. D., & Yu, J. S. C. (2007). A comparison of the glutamate release inhibition and anti-allodynic effects of gabapentin, lamotrigine, and riluzole in a model of neuropathic pain. *Journal of Neurochemistry*, *100*(5), 1289–1299.

Coghlan, S., Horder, J., Inkster, B., Mendez, M. A., Murphy, D. G., & Nutt, D. J. (2012). GABA system dysfunction in autism and related disorders: From synapse to symptoms. *Neuroscience and Biobehavioral Reviews*, *36*(9), 2044–2055.

Collins, G. G. S. (1972). GABA—2-oxoglutarate transaminase, glutamate decarboxylase and the half-life of GABA in different areas of rat brain. *Biochemical Pharmacology*, *21*(21), 2849–2858.

Colovic, M., Zennaro, E., & Caccia, S. (2004). Liquid chromatographic assay for riluzole in mouse plasma and central nervous system tissues. *Journal of Chromatography B: Analytical Technologies in the Biomedical and Life Sciences*, *803*(2), 305–309.

Colvert, E., Tick, B., McEwen, F., Stewart, C., Curran, S. R., Woodhouse, E., … Bolton, P. (2015). Heritability of Autism Spectrum Disorder in a UK Population-Based Twin Sample. *JAMA Psychiatry*, *72*(5), 415–423.

Coric, V., Taskiran, S., Pittenger, C., Wasylink, S., Mathalon, D. H., Valentine, G., … Krystal, J. H. (2005). Riluzole Augmentation in Treatment-Resistant Obsessive–Compulsive Disorder: An Open-Label Trial. *Biological Psychiatry*, *58*(5), 424–428.

Courchesne, E., Pierce, K., Schumann, C. M., Redcay, E., Buckwalter, J. A., Kennedy, D. P., & Morgan, J. (2007). Mapping early brain development in autism. *Neuron*, *56*(2), 399–413.

Croen, L. a., Zerbo, O., Qian, Y., Massolo, M. L., Rich, S., Sidney, S., & Kripke, C. (2015). The health status of adults on the autism spectrum. *Autism*, *19*(7), 814–823.

Dabell, M. P., Rosenfeld, J. A., Bader, P., Escobar, L. F., El-Khechen, D., Vallee, S. E., … Shaffer, L. G. (2013). Investigation of NRXN1 deletions: clinical and molecular characterization. *American Journal of Medical Genetics. Part A*, *161*(4), 717–731.

Dachtler, J., Ivorra, J. L., Rowland, T. E., Lever, C., Rodgers, R. J., & Clapcote, S. J. (2015). Heterozygous deletion of α-neurexin I or α-neurexin II results in behaviors relevant to autism and schizophrenia. *Behavioral Neuroscience*, *129*(6), 765–776.

Dager, S. R., Corrigan, N. M., Richards, T. L., & Posse, S. (2008). Research Applications of Magnetic Resonance Spectroscopy to Investigate Psychiatric Disorders. *Topics in Magnetic Resonance Imaging*, *19*(2), 81–96.

Dall'Igna, O. P., Bobermin, L. D., Souza, D. O., & Quincozes-Santos, A. (2013). Riluzole increases glutamate uptake by cultured C6 astroglial cells. *International Journal of Developmental Neuroscience*, *31*(7), 482–486.

Dawson, G., Webb, S. J., & McPartland, J. (2005). Understanding the Nature of Face Processing Impairment in Autism: Insights From Behavioral and Electrophysiological Studies. *Developmental Neuropsychology*, *27*(3), 403–424.

De Rubeis, S., He, X., Goldberg, A. P., Poultney, C. S., Samocha, K., Cicek, A. E., … Buxbaum, J. D. (2014). Synaptic, transcriptional and chromatin genes disrupted in autism. *Nature*, *515*(7526), 209–215.

de Theije, C. G. M., Wopereis, H., Ramadan, M., van Eijndthoven, T., Lambert, J., Knol, J., … Oozeer, R. (2014). Altered gut microbiota and activity in a murine model of autism spectrum disorders. *Brain, Behavior, and Immunity*, *37*, 197–206.

Debono, M. W., Le Guern, J., Canton, T., Doble, a, & Pradier, L. (1993). Inhibition by riluzole of electrophysiological responses mediated by rat kainate and NMDA receptors expressed in Xenopus oocytes. *European Journal of Pharmacology*, *235*(2–3), 283–289.

Del Arco, A., Martínez, R., & Mora, F. (1998). Amphetamine increases extracellular concentrations of glutamate in the prefrontal cortex of the awake rat: A microdialysis study. *Neurochemical Research*, *23*(9), 1153–1158.

Del Arco, A., Segovia, G., Fuxe, K., & Mora, F. (2003). Changes in dialysate concentrations of glutamate and GABA in the brain: an index of volume transmission mediated actions? *Journal of Neurochemistry*, *85*(1), 23–33.

DeLaPaz, R. L. (1994). Echo-planar imaging. *Radiographics*, *14*, 1045–1058.

Delmonte, S., Gallagher, L., O'Hanlon, E., McGrath, J., & Balsters, J. H. (2013). Functional and structural connectivity of frontostriatal circuitry in Autism Spectrum Disorder. *Front Hum Neurosci*, *7*, 430.

DeLorey, T. M., Handforth, A., Anagnostaras, S. G., Homanics, G. E., Minassian, B. A., Asatourian, A., … Olsen, R. W. (1998). Mice lacking the beta3 subunit of the GABAA receptor have the epilepsy phenotype and many of the behavioral characteristics of Angelman syndrome. *The Journal of Neuroscience : The Official Journal of the Society for Neuroscience*, *18*, 8505–8514.

DeVito, T. J., Drost, D. J., Neufeld, R. W. J., Rajakumar, N., Pavlosky, W., Williamson, P., & Nicolson, R. (2007). Evidence for Cortical Dysfunction in Autism: A Proton Magnetic Resonance Spectroscopic Imaging Study. *Biological Psychiatry*, *61*(4), 465–473.

Dhossche, D., Applegate, H., Abraham, A., Maertens, P., Bland, L., Bencsath, A., & Martinez, J. (2002). Elevated plasma gamma-aminobutyric acid (GABA) levels in autistic youngsters: stimulus for a GABA hypothesis of autism. *Medical Science Monitor : International Medical Journal of Experimental and Clinical Research*, *8*, PR1-R6.

Dichter, G. S., Felder, J. N., Green, S. R., Rittenberg, A. M., Sasson, N. J., & Bodfish, J. W. (2012). Reward circuitry function in autism spectrum disorders. *Soc Cogn Affect Neurosci*, *7*(2), 160–172.

Dickens, A. M., Vainio, S., Marjamaki, P., Johansson, J., Lehtiniemi, P., Rokka, J., … Airas, L. (2014). Detection of Microglial Activation in an Acute Model of Neuroinflammation Using PET and Radiotracers 11C-(R)-PK11195 and 18F-GE-180. *Journal of Nuclear Medicine*, *55*(3), 466–472.

Dickerson, D. D., Overeem, K. a, Wolff, a R., Williams, J. M., Abraham, W. C., & Bilkey, D. K. (2014). Association of aberrant neural synchrony and altered GAD67 expression following exposure to maternal immune activation, a risk factor for schizophrenia. *Translational Psychiatry*, *4*(7), e418.

Dietze, S., & Kuschinsky, K. (1992). Determination of extracellular glutamate after local K+ stimulation in the striatum of non-anaesthetised rats after treatment with dopaminergic drugs - studies using microdialysis. *Journal of Neural Transmission*, *90*(1), 1–11.

Dinnissen, M., Dietrich, A., van den Hoofdakker, B. J., & Hoekstra, P. J. (2014). Clinical and pharmacokinetic evaluation of risperidone for the management of autism spectrum disorder. *Expert Opinion on Drug Metabolism & Toxicology*, *11*(1), 1–14.

Doble, A. (1996). The pharmacology and mechanism of action of riluzole. *Neurology*, *47*, S233–S241.

Dölen, G., Osterweil, E., Rao, B. S. S., Smith, G. B., Auerbach, B. D., Chattarji, S., & Bear, M. F. (2007). Correction of Fragile X Syndrome in Mice. *Neuron*, *56*(6), 955–962.

Domercq, M., Vázquez-Villoldo, N., & Matute, C. (2013). Neurotransmitter signaling in the pathophysiology of microglia. *Frontiers in Cellular Neuroscience*, *7*, 49.

Duncan, N. W., Wiebking, C., Tiret, B., Marja??ska, M., Hayes, D. J., Lyttleton, O., … Northoff, G. (2013). Glutamate Concentration in the Medial Prefrontal Cortex Predicts Resting-State Cortical-Subcortical Functional Connectivity in Humans. *PLoS ONE*, *8*(4), e60312.

Durieux, A. M. S., Fernandes, C., Murphy, D., Labouesse, M. A., Giovanoli, S., Meyer, U., … McAlonan, G. (2015). Targeting Glia with N-Acetylcysteine Modulates Brain Glutamate and Behaviors Relevant to Neurodevelopmental Disorders in C57BL/6J Mice. *Frontiers in Behavioral Neuroscience*, *9*, 343.

Ecker, C., Spooren, W., & Murphy, D. (2013). Developing new pharmacotherapies for autism. *J Intern Med*, *274*(4), 308–320.

Ecker, & Murphy, D. (2014). Neuroimaging in autism--from basic science to translational research. *Nature Reviews. Neurology*, *10*(2), 82–91.

Edden, & Barker, P. B. (2007). Spatial effects in the detection of gamma-aminobutyric acid: improved sensitivity at high fields using inner volume saturation. *Magnetic Resonance in Medicine : Official Journal of the Society of Magnetic Resonance in Medicine / Society of Magnetic Resonance in Medicine*, *58*(6), 1276–1282.

Edden, Puts, N. A. J., Harris, A. D., Barker, P. B., & Evans, C. J. (2014). Gannet: A batch-processing tool for the quantitative analysis of gamma-aminobutyric acid–edited MR spectroscopy spectra. *Journal of Magnetic Resonance Imaging : JMRI*, *40*(6), 1445–1452.

Edden, R., Puts, N., & Barker, P. (2012). Macromolecule-suppressed GABA-edited magnetic resonance spectroscopy at 3T. *Magnetic Resonance in Medicine*, *68*(3), 657–661.

Ehlers, S., & Gillberg, C. (1993). The epidemiology of Asperger syndrome. A total population study. *Journal of Child Psychology and Psychiatry and Allied Disciplines*, *34*(8), 1327–1350.

Elston, G. N. (2003). Cortex, Cognition and the Cell: New Insights into the Pyramidal Neuron and Prefrontal Function. *Cerebral Cortex*, *13*(11), 1124–1138.

Enzi, B., Duncan, N. W., Kaufmann, J., Tempelmann, C., Wiebking, C., & Northoff, G. (2012). Glutamate modulates resting state activity in the perigenual anterior cingulate cortex - A combined fMRI-MRS study. *Neuroscience*, *227*, 102–109.

Erickson, C. A., Weng, N., Weiler, I. J., Greenough, W. T., Stigler, K. A., Wink, L. K., & McDougle, C. J. (2011). Open-label riluzole in fragile X syndrome. *Brain Research*, *1380*, 264–270.

Erlander, M. G., Tillakaratne, N. J., Feldblum, S., Patel, N., & Tobin, a J. (1991). Two genes encode distinct glutamate decarboxylases. *Neuron*, *7*(1), 91–100.

Esclapez, M., Tillakaratne, N. J., Kaufman, D. L., Tobin, A. J., & Houser, C. R. (1994). Comparative localization of two forms of glutamic acid decarboxylase and their mRNAs in rat brain supports the concept of functional differences between the forms. *The Journal of Neuroscience, 14*(3 Pt 2), 1834–1855.

Esclassan, F., Francois, J., Phillips, K. G., Loomis, S., & Gilmour, G. (2015). Phenotypic characterization of nonsocial behavioral impairment in neurexin 1α knockout rats. *Behavioral Neuroscience*, *129*(1), 74–85.

Estes, A., Shaw, D. W. W., Sparks, B. F., Friedman, S., Giedd, J. N., Dawson, G., … Dager, S. R. (2011). Basal ganglia morphometry and repetitive behavior in young children with autism spectrum disorder. *Autism Research*, *4*(3), 212–220.

Etherton, M., Földy, C., Sharma, M., Tabuchi, K., Liu, X., Shamloo, M., … Südhof, T. C. (2011). Autism-linked neuroligin-3 R451C mutation differentially alters hippocampal and cortical synaptic function. *Proceedings of the National Academy of Sciences*, *108*(33), 13764–13769.

Etherton, M. R., Blaiss, C. A., Powell, C. M., & Südhof, T. C. (2009). Mouse neurexin-1alpha deletion causes correlated electrophysiological and behavioral changes consistent with cognitive impairments. *Proceedings of the National Academy of Sciences*, *106*(42), 17998–18003.

Etherton, M. R., Tabuchi, K., Sharma, M., Ko, J., & Südhof, T. C. (2011). An autism-associated point mutation in the neuroligin cytoplasmic tail selectively impairs AMPA receptor-mediated synaptic transmission in hippocampus. *The EMBO Journal*, *30*(14), 2908–2919.

Farokhnia, M., Sabzabadi, M., Pourmahmoud, H., Khodaie-Ardakani, M.-R., Hosseini, S.-M.-R., Yekehtaz, H., … Akhondzadeh, S. (2014). A double-blind, placebo controlled, randomized trial of riluzole as an adjunct to risperidone for treatment of negative symptoms in patients with chronic schizophrenia. *Psychopharmacology*, *231*(3), 533–542.

Fatemi, S. H., & Folsom, T. D. (2015). GABA receptor subunit distribution and FMRP–mGluR5 signaling abnormalities in the cerebellum of subjects with schizophrenia, mood disorders, and autism. *Schizophrenia Research*, *167*(1–3), 42–56.

Fatemi, S. H., Folsom, T. D., Kneeland, R. E., & Liesch, S. B. (2011). Metabotropic glutamate receptor 5 upregulation in children with autism is associated with underexpression of both Fragile X mental retardation protein and GABAA receptor beta 3 in adults with autism. *Anatomical Record (Hoboken, N.J. : 2007)*, *294*(10), 1635–1645.

Fatemi, S. H., Folsom, T. D., Reutiman, T. J., & Lee, S. (2008). Expression of astrocytic markers aquaporin 4 and connexin 43 is altered in brains of subjects with autism. *Synapse*, *62*(7), 501–507.

Fatemi, S. H., Halt, A. R., Stary, J. M., Kanodia, R., Schulz, S. C., & Realmuto, G. R. (2002). Glutamic acid decarboxylase 65 and 67 kDa proteins are reduced in autistic parietal and cerebellar cortices. *Biological Psychiatry*, *52*(8), 805–810.

Fatemi, S. H., Reutiman, T. J., Folsom, T. D., Rooney, R. J., Patel, D. H., & Thuras, P. D. (2010). mRNA and Protein Levels for GABAAα4, α5, β1 and GABABR1 Receptors are Altered in Brains from Subjects with Autism. *Journal of Autism and Developmental Disorders*, *40*(6), 743–750.

Fatemi, S. H., Reutiman, T. J., Folsom, T. D., Rustan, O. G., Rooney, R. J., & Thuras, P. D. (2014). Downregulation of GABAA Receptor Protein Subunits alpha6, beta2, delta, epsilon, gamma2, theta, and rho2 in Superior Frontal Cortex of Subjects with Autism. *Journal of Autism and Developmental Disorders*, *44*(8), 1833–1845.

Fatouros, P. P., Heath, D. L., Beaumont, A., Corwin, F. D., Signoretti, S., AL-Samsam, R. H., … Marmarou, A. (2000). Comparison of NAA Measures by MRS and HPLC. In *Brain Edema XI* (pp. 35–37). Vienna: Springer.

Feng, J., Schroer, R., Yan, J., Song, W., Yang, C., Bockholt, A., … Sommer, S. S. (2006). High frequency of neurexin 1β signal peptide structural variants in patients with autism. *Neuroscience Letters*, *409*(1), 10–13.

Foa, E. B., Huppert, J. D., Leiberg, S., Langner, R., Kichic, R., Hajcak, G., & Salkovskis, P. M. (2002). The obsessive-compulsive inventory: Development and validation of a short version. *Psychological Assessment*, *14*(4), 485–496.

Fox, M. D., Snyder, A. Z., Vincent, J. L., Corbetta, M., Van Essen, D. C., & Raichle, M. E. (2005). From The Cover: The human brain is intrinsically organized into dynamic, anticorrelated functional networks. *Proceedings of the National Academy of Sciences*, *102*(27), 9673–9678.

Friedman, S. D., Shaw, D. W., Artru, A. A., Richards, T. L., Gardner, J., Dawson, G., … Dager, S. R. (2003). Regional brain chemical alterations in young children with autism spectrum disorder. *Neurology*, *60*, 100–107.

Friston, J., Ashburner, J., & Wellcome, K. (1997). Multimodal Image Coregistration and Partitioning - a Unified Framework. *Neuroimage*, *6*(3), 209–217.

Friston, K. J., Worsley, K. J., Frackowiak, R. S. J., Mazziotta, J. C., & Evans, A. C. (1994). Assessing the significance of focal activations using their spatial extent. *Human Brain Mapping*, *1*(3), 210–220.

Frizzo, M. E. dos S., Dall'Onder, L. P., Dalcin, K. B., & Souza, D. O. (2004). Riluzole enhances glutamate uptake in rat astrocyte cultures. *Cellular and Molecular Neurobiology*, *24*(1), 123–128.

Frye, R. E. (2014). Clinical potential, safety, and tolerability of arbaclofen in the treatment of autism spectrum disorder. *Drug, Healthcare and Patient Safety*, *6*, 69–76.

Futai, K., Kim, M. J., Hashikawa, T., Scheiffele, P., Sheng, M., & Hayashi, Y. (2007). Retrograde modulation of presynaptic release probability through signaling mediated by PSD-95–neuroligin. *Nature Neuroscience*, *10*(2), 186–195.

Gaetz, W., Bloy, L., Wang, D. J., Port, R. G., Blaskey, L., Levy, S. E., & Roberts, T. P. L. (2014). GABA estimation in the brains of children on the autism spectrum: measurement precision and regional cortical variation. *NeuroImage*, *86*, 1–9.

Gandal, M. J., Anderson, R. L., Billingslea, E. N., Carlson, G. C., Roberts, T. P. L., & Siegel, S. J. (2012). Mice with reduced NMDA receptor expression: More consistent with autism than schizophrenia? *Genes, Brain and Behavior*, *11*(6), 740–750.

Gao, R., & Penzes, P. (2015). Common mechanisms of excitatory and inhibitory imbalance in schizophrenia and autism spectrum disorders. *Current Molecular Medicine*, *15*(2), 146–167.

Garrity, A. G., Pearlson, G. D., McKiernan, K., Lloyd, D., Kiehl, K. A., & Calhoun, V. D. (2007). Aberrant "Default Mode" Functional Connectivity in Schizophrenia. *American Journal of Psychiatry*, *164*(3), 450–457.

Gauthier, J., Siddiqui, T. J., Huashan, P., Yokomaku, D., Hamdan, F. F., Champagne, N., … Rouleau, G. A. (2011). Truncating mutations in NRXN2 and NRXN1 in autism spectrum disorders and schizophrenia. *Human Genetics*, *130*(4), 563–573.

Geurts, H. M., & Jansen, M. D. (2011). A retrospective chart study: The pathway to a diagnosis for adults referred for ASD assessment. *Autism*, *16*(3), 299–305.

Ghaleiha, A., Mohammadi, E., Mohammadi, M.-R., Farokhnia, M., Modabbernia, A., Yekehtaz, H., … Akhondzadeh, S. (2013). Riluzole as an adjunctive therapy to risperidone for the treatment of irritability in children with autistic disorder: a double-blind, placebo-controlled, randomized trial. *Paediatric Drugs*, *15*(6), 505–514.

Ghanizadeh, A., Tordjman, S., & Jaafari, N. (2015). Aripiprazole for treating irritability in children and adolescents with autism: A systematic review. *Indian Journal of Medical Research*, *142*(3), 269.

Ghaziuddin, M., Ghaziuddin, N., & Greden, J. (2002). Depression in Persons with Autism: Implications for Research and Clinical Care. *Journal of Autism and Developmental Disorders*, *32*(4), 299–306.

Gipson, T. T., Poretti, A., Thomas, E. A., Jenkins, K. T., Desai, S., & Johnston, M. V. (2015). Autism Phenotypes in Tuberous Sclerosis Complex: Diagnostic and Treatment Considerations. *Journal of Child Neurology*, *30*(14), 1871–1876.

Gleason, G., Liu, B., Bruening, S., Zupan, B., Auerbach, A., Mark, W., … Toth, M. (2010). The serotonin1A receptor gene as a genetic and prenatal maternal environmental factor in anxiety. *Proceedings of the National Academy of Sciences*, *107*(16), 7592–7597.

Glessner, J. T., Wang, K., Cai, G., Korvatska, O., Kim, C. E., Wood, S., … Hakonarson, H. (2009). Autism genome-wide copy number variation reveals ubiquitin and neuronal genes. *Nature*, *459*(7246), 569–573.

Glover, G. H. (2011). Overview of functional magnetic resonance imaging. *Neurosurgery Clinics of North America*, *22*(2), 133–139.

Gonçalves, J., Violante, I. R., Sereno, J., Leitão, R. A., Cai, Y., Abrunhosa, A., … Castelo-Branco, M. (2017). Testing the excitation/inhibition imbalance hypothesis in a mouse model of the autism spectrum disorder: in vivo neurospectroscopy and molecular evidence for regional phenotypes. *Molecular Autism*, *8*, 47.

Gotham, K., Risi, S., Pickles, A., & Lord, C. (2007). The autism diagnostic observation schedule: Revised algorithms for improved diagnostic validity. *Journal of Autism and Developmental Disorders*, *37*(4), 613–627.

Graeber, M. B. (2010). Changing Face of Microglia. *Science*, *330*(6005), 783–788.

Grant, P., Lougee, L., Hirschtritt, M., & Swedo, S. E. (2007). An Open-Label Trial of Riluzole, a Glutamate Antagonist, in Children with Treatment-Resistant Obsessive-Compulsive Disorder. *Journal of Child and Adolescent Psychopharmacology*, *17*(6), 761–767.

Grayton, H. M., Missler, M., Collier, D. A., & Fernandes, C. (2013). Altered social behaviours in neurexin 1α knockout mice resemble core symptoms in neurodevelopmental disorders. *PloS One*, *8*(6), e67114.

Greicius, M. (2008). Resting-state functional connectivity in neuropsychiatric disorders. *Current Opinion in Neurology*, *24*(4), 424–430.

Groeneveld, G., van Kan, H., Lie-A-Huen, L., Guchelaar, H.-J., & van den Berg, L. (2008). An Association Study of Riluzole Serum Concentration and Survival and Disease Progression in Patients With ALS. *Clinical Pharmacology & Therapeutics*, *83*(5), 718–722.

Haag, L., Quetscher, C., Dharmadhikari, S., Dydak, U., Schmidt-Wilcke, T., & Beste, C. (2015). Interrelation of resting state functional connectivity, striatal GABA levels, and cognitive control processes. *Human Brain Mapping*, *36*(11), 4383–4393.

Haahr, M. (1998). www.random.org. Retrieved from www.random.org

Hahamy, A., Behrmann, M., & Malach, R. (2015). The idiosyncratic brain: distortion of spontaneous connectivity patterns in autism spectrum disorder. *Nature Neuroscience*, *18*(2), 302–309.

Halonen, L. M., Sinkkonen, S. T., Chandra, D., Homanics, G. E., & Korpi, E. R. (2009). Brain regional distribution of GABAA receptors exhibiting atypical GABA agonism: Roles of receptor subunits. *Neurochemistry International*, *55*(6), 389–396.

Han, S., Tai, C., Jones, C. J., Scheuer, T., & Catterall, W. A. (2014). Enhancement of Inhibitory Neurotransmission by GABA A Receptors Having α 2,3 -Subunits Ameliorates Behavioral Deficits in a Mouse Model of Autism. *Neuron*, *81*(6), 1282–1289.

Harada, M., Taki, M. M., Nose, A., Kubo, H., Mori, K., Nishitani, H., & Matsuda, T. (2011). Non-invasive evaluation of the GABAergic/glutamatergic system in autistic patients observed by MEGA-editing proton MR spectroscopy using a clinical 3 tesla instrument. *Journal of Autism and Developmental Disorders*, *41*(4), 447–454.

Hardan, A. Y., Minshew, N. J., Melhem, N. M., Srihari, S., Jo, B., Bansal, R., … Stanley, J. A. (2008). An MRI and proton spectroscopy study of the thalamus in children with autism. *Psychiatry Research: Neuroimaging*, *163*(2), 97–105.

Harris, A. D., Puts, N. A. J., Barker, P. B., & Edden, R. A. E. (2015). Spectral-editing measurements of GABA in the human brain with and without macromolecule suppression. *Magnetic Resonance in Medicine*, *74*(6), 1523–1529.

Hassan, T. H., Abdelrahman, H. M., Abdel Fattah, N. R., El-Masry, N. M., Hashim, H. M., El-Gerby, K. M., & Abdel Fattah, N. R. (2013). Blood and brain glutamate levels in children with autistic disorder. *Research in Autism Spectrum Disorders*, *7*(4), 541–548.

Hayashida, K., Parker, R. A., & Eisenach, J. C. (2010). Activation of glutamate transporters in the locus coeruleus paradoxically activates descending inhibition in rats. *Brain Research*, *1317*, 80–86.

Haydar, T. F., Wang, F., Schwartz, M. L., & Rakic, P. (2000). Differential Modulation of Proliferation in the Neocortical Ventricular and Subventricular Zones. *The Journal of Neuroscience : The Official Journal of the Society for Neuroscience*, *20*(15), 5764–5774.

Haznedar, M. M., Buchsbaum, M. S., Hazlett, E. a., LiCalzi, E. M., Cartwright, C., & Hollander, E. (2006). Volumetric analysis and three-dimensional glucose metabolic mapping of the striatum and thalamus in patients with autism spectrum disorders. *The American Journal of Psychiatry*, *163*(7), 1252–1263.

He, Y., Benz, A., Fu, T., Wang, M., Covey, D. F., Zorumski, C. F., & Mennerick, S. (2002). Neuroprotective agent riluzole potentiates postsynaptic GABAA receptor function. *Neuropharmacology*, *42*, 199–209.

Hebb, D. O. (1949). *The Organization of Behavior*. *The Organization of Behavior* (Vol. 911).

Hebert, T., Drapeau, P., Pradier, L., & Dunn, R. J. (1994). Block of the rat brain IIA sodium channel alpha subunit by the neuroprotective drug riluzole. *Molecular Pharmacology*, *45*(5), 1055–1060.

Heffner, T. G., Hartman, J. a, & Seiden, L. S. (1980). A rapid method for the regional dissection of the rat brain. *Pharmacology, Biochemistry, and Behavior*, *13*, 453–456.

Helton, S. G., & Lohoff, F. W. (2015). Serotonin pathway polymorphisms and the treatment of major depressive disorder and anxiety disorders. *Pharmacogenomics*, *16*(5), 541–553.

Henry, P. G., Dautry, C., Hantraye, P., & Bloch, G. (2001). Brain gaba editing without macromolecule contamination. *Magnetic Resonance in Medicine*, *45*(3), 517–520.

Hofvander, B., Delorme, R., Chaste, P., Nydén, A., Wentz, E., Ståhlberg, O., … Leboyer, M. (2009). Psychiatric and psychosocial problems in adults with normal-intelligence autism spectrum disorders. *BMC Psychiatry*, *9*, 35.

Holdsworth, S. J., & Bammer, R. (2008). Magnetic resonance imaging techniques: FMRI, DWI, and PWI. *Seminars in Neurology*, *28*(4), 395–406.

Hollander, E., Anagnostou, E., Chaplin, W., Esposito, K., Haznedar, M. M., Licalzi, E., … Buchsbaum, M. (2005). Striatal volume on magnetic resonance imaging and repetitive behaviors in autism. *Biological Psychiatry*, *58*(3), 226–232.

Hollander, E., Phillips, A., Chaplin, W., Zagursky, K., Novotny, S., Wasserman, S., & Iyengar, R. (2005). A Placebo Controlled Crossover Trial of Liquid Fluoxetine on Repetitive Behaviors in Childhood and Adolescent Autism. *Neuropsychopharmacology*, *30*(3), 582–589.

Hollander, E., Soorya, L., Chaplin, W., Anagnostou, E., Taylor, B. P., Ferretti, C. J., … Settipani, C. (2012). A Double-Blind Placebo-Controlled Trial of Fluoxetine for Repetitive Behaviors and Global Severity in Adult Autism Spectrum Disorders. *American Journal of Psychiatry*, *169*(3), 292–299.

Holliday, W. B., Gurnsey, K., Sweet, R. A., & Teichert, T. (2017). A putative electrophysiological biomarker of auditory sensory memory encoding is sensitive to pharmacological alterations of excitatory/inhibitory balance in male macaque monkeys. *Journal of Psychiatry & Neuroscience*, *43*(3), 182–193.

Holmboe, K., Elsabbagh, M., Volein, A., Tucker, L. A., Baron-Cohen, S., Bolton, P., … Johnson, M. H. (2010). Frontal cortex functioning in the infant broader autism phenotype. *Infant Behavior and Development*, *33*(4), 482–491.

Horder, J., Lavender, T., Mendez, M. A., O'Gorman, R., Daly, E., Craig, M. C., … Murphy, D. G. (2013). Reduced subcortical glutamate/glutamine in adults with autism spectrum disorders: a [^{1}H]MRS study. *Translational Psychiatry*, *3*, e279.

Horn, D. I., Yu, C., Steiner, J., Buchmann, J., Kaufmann, J., Osoba, A., … Walter, M. (2010). Glutamatergic and resting-state functional connectivity correlates of severity in major depression - the role of pregenual anterior cingulate cortex and anterior insula. *Frontiers in Systems Neuroscience*, *4*(July), 1–10.

Howlin, P., Goode, S., Hutton, J., & Rutter, M. (2004). Adult outcome for children with autism. *Journal of Child Psychology and Psychiatry and Allied Disciplines*, *45*(2), 212–229.

Howlin, P., Moss, P., Savage, S., & Rutter, M. (2013). Social outcomes in mid- to later adulthood among individuals diagnosed with autism and average nonverbal IQ as children. *Journal of the American Academy of Child and Adolescent Psychiatry*, *52*(6), 572–581.

Hsia, Y., Wong, A. Y. S., Murphy, D. G. M., Simonoff, E., Buitelaar, J. K., & Wong, I. C. K. (2014). Psychopharmacological prescriptions for people with autism spectrum disorder (ASD): a multinational study. *Psychopharmacology*, *231*(6), 999–1009.

Hubert, J. P., Delumeau, J. C., Glowinski, J., Prémont, J., & Doble, A. (1994). Antagonism by riluzole of entry of calcium evoked by NMDA and veratridine in rat cultured granule cells: evidence for a dual mechanism of action. *British Journal of Pharmacology*, *113*(1), 261–267.

Hyder, F., Fulbright, R. K., Shulman, R. G., & Rothman, D. L. (2013). Glutamatergic function in the resting awake human brain is supported by uniformly high oxidative energy. *Journal of Cerebral Blood Flow and Metabolism : Official Journal of the International Society of Cerebral Blood Flow and Metabolism*, *33*(3), 339–347.

Ipser, J. C., Syal, S., Bentley, J., Adnams, C. M., Steyn, B., & Stein, D. J. (2012). 1H-MRS in autism spectrum disorders: a systematic meta-analysis. *Metab Brain Dis*, *27*(3), 275–287.

Isles, A. R., Ingason, A., Lowther, C., Walters, J., Gawlick, M., Stöber, G., … Kirov, G. (2016). Parental Origin of Interstitial Duplications at 15q11.2-q13.3 in Schizophrenia and Neurodevelopmental Disorders. *PLOS Genetics*, *12*(5), e1005993.

Jahn, K., Schlesinger, F., Jin, L. J., Dengler, R., Bufler, J., & Krampfl, K. (2008). Molecular mechanisms of interaction between the neuroprotective substance riluzole and GABAA-receptors. *Naunyn-Schmiedeberg's Archives of Pharmacology*, *378*(1), 53–63.

Jamain, S., Quach, H., Betancur, C., Råstam, M., Colineaux, C., Gillberg, I. C., … Bourgeron, T. (2003). Mutations of the X-linked genes encoding neuroligins NLGN3 and NLGN4 are associated with autism. *Nature Genetics*, *34*, 27–29.

Jann, K., Hernandez, L. M., Beck-Pancer, D., Mccarron, R., Smith, R. X., Dapretto, M., & Wang, D. J. J. (2015). Altered resting perfusion and functional connectivity of default mode network in youth with autism spectrum disorder. *Brain and Behavior*, *5*(9).

Jannsen Pharmaceuticals Ltd, I. (2009). Risperdal [package insert].

Jaramillo, T. C., Liu, S., Pettersen, A., Birnbaum, S. G., & Powell, C. M. (2014). Autism-Related Neuroligin-3 Mutation Alters Social Behavior and Spatial Learning. *Autism Research*, *7*(2), 264–272.

Jehle, T., Bauer, J., Blauth, E., Hummel, A., Darstein, M., Freiman, T. M., & Feuerstein, T. J. (2000). Effects of riluzole on electrically evoked neurotransmitter release. *British Journal of Pharmacology*, *130*, 1227–1234.

Jenkinson, M., Beckmann, C. F., Behrens, T. E. J., Woolrich, M. W., & Smith, S. M. (2012). FSL. *NeuroImage*, *62*(2), 782–790.

Joint Formularly Committee. (2017). *British National Formulary* (74th ed.). London: BMJ Group and Pharmaceutical Press.

Joshi, G., Biederman, J., Wozniak, J., Goldin, R. L., Crowley, D., Furtak, S., … Gönenç, A. (2013). Magnetic resonance spectroscopy study of the glutamatergic system in adolescent males with high-functioning autistic disorder: A pilot study at 4T. *European Archives of Psychiatry and Clinical Neuroscience*, *263*, 379–384.

Just, M. A., Cherkassky, V. L., Keller, T. A., & Minshew, N. J. (2004). Cortical activation and synchronization during sentence comprehension in high-functioning autism: evidence of underconnectivity. *Brain*, *127*(8), 1811–1821.

Just, M. A., Keller, T. A., Malave, V. L., Kana, R. K., & Varma, S. (2012). Autism as a neural systems disorder: a theory of frontal-posterior underconnectivity. *Neuroscience and Biobehavioral Reviews*, *36*(4), 1292–1313.

Kaiser, L. G., Schuff, N., Cashdollar, N., & Weiner, M. W. (2005). Age-related glutamate and glutamine concentration changes in normal human brain: 1H MR spectroscopy study at 4 T. *Neurobiol Aging*, *26*(5), 665–672.

Kalbe, E., Schlegel, M., Sack, A. T., Nowak, D. a., Dafotakis, M., Bangard, C., … Kessler, J. (2010). Dissociating cognitive from affective theory of mind: A TMS study. *Cortex*, *46*(6), 769–780.

Kalkbrenner, A. E., Schmidt, R. J., & Penlesky, A. C. (2014). Environmental Chemical Exposures and Autism Spectrum Disorders: A Review of the Epidemiological Evidence. *Current Problems in Pediatric and Adolescent Health Care*, *44*(10), 277–318.

Kang, D.-W., Ilhan, Z. E., Isern, N. G., Hoyt, D. W., Howsmon, D. P., Shaffer, M., … Krajmalnik-Brown, R. (2018). Differences in fecal microbial metabolites and microbiota of children with autism spectrum disorders. *Anaerobe*, *49*, 121–131.

Kanne, S. M., & Mazurek, M. O. (2011). Aggression in children and adolescents with ASD: Prevalence and risk factors. *Journal of Autism and Developmental Disorders*, *41*(7), 926–937.

Kapogiannis, D., Reiter, D. a., Willette, A. a., & Mattson, M. P. (2013). Posteromedial cortex glutamate and GABA predict intrinsic functional connectivity of the default mode network. *NeuroImage*, *64*(1), 112–119.

Kariuki-Nyuthe, C., Gomez-Mancilla, B., & Stein, D. J. (2014). Obsessive compulsive disorder and the glutamatergic system. *Current Opinion in Psychiatry*, *27*(1), 32–37.

Kattenstroth, G., Tantalaki, E., Südhof, T. C., Gottmann, K., & Missler, M. (2004). Postsynaptic N-methyl-D-aspartate receptor function requires alpha-neurexins. *PNAS*, *101*(8), 2607–2612.

Kim, H.-G., Kishikawa, S., Higgins, A. W., Seong, I.-S., Donovan, D. J., Shen, Y., … Gusella, J. F. (2008). Disruption of Neurexin 1 Associated with Autism Spectrum Disorder. *The American Journal of Human Genetics*, *82*(1), 199–207.

Kohls, G., Chevallier, C., Troiani, V., & Schultz, R. T. (2012). Social "wanting" dysfunction in autism: neurobiological underpinnings and treatment implications. *J Neurodev Disord*, *4*(1), 4–10.

Kratsman, N., Getselter, D., & Elliott, E. (2016). Sodium butyrate attenuates social behavior deficits and modifies the transcription of inhibitory/excitatory genes in the frontal cortex of an autism model. *Neuropharmacology*, *102*, 136–145.

Kubas, B., Kułak, W., Sobaniec, W., Tarasow, E., Łebkowska, U., & Walecki, J. (2012). Metabolite alterations in autistic children: a 1H MR spectroscopy study. *Advances in Medical Sciences*, *57*(1), 152–156.

Kwon, S. H., Scheinost, D., Lacadie, C., Benjamin, J., Myers, E. H., Qiu, M., … Ment, L. R. (2014). GABA, Resting-State Connectivity and the Developing Brain. *Neonatology*, *106*(2), 149–155.

Laarakker, M. C., Reinders, N. R., Bruining, H., Ophoff, R. A., & Kas, M. J. H. (2012). Sex-Dependent Novelty Response in Neurexin-1α Mutant Mice. *PLoS ONE*, *7*(2), e31503.

Lai, M.-C., Lombardo, M. V., Pasco, G., Ruigrok, A. N. V, Wheelwright, S. J., Sadek, S. A., … Baron-Cohen, S. (2011). A Behavioral Comparison of Male and Female Adults with High Functioning Autism Spectrum Conditions. *PLoS ONE*, *6*(6), e20835.

Lai, M.-C., Lombardo, M. V, & Baron-Cohen, S. (2014). Autism. *Lancet*, *383*(9920), 896–910.

Lally, N., An, L., Banerjee, D., Niciu, M. J., Luckenbaugh, D. A., Richards, E. M., … Nugent, A. C. (2016). Reliability of 7T ^{1} H-MRS measured human prefrontal cortex glutamate, glutamine, and glutathione signals using an adapted echo time optimized PRESS sequence: A between- and within-sessions investigation. *Journal of Magnetic Resonance Imaging*, *43*(1), 88–98.

Lampi, K. M., Hinkka-Yli-Salomäki, S., Lehti, V., Helenius, H., Gissler, M., Brown, A. S., & Sourander, A. (2013). Parental age and risk of autism spectrum disorders in a Finnish national birth cohort. *Journal of Autism and Developmental Disorders*, *43*(11), 2526–2535.

Lanciego, J. L., Luquin, N., & Obeso, J. A. (2012). Functional neuroanatomy of the basal ganglia. *Cold Spring Harbor Perspectives in Medicine*, *2*(12), a009621.

Langen, M., Leemans, A., Johnston, P., Ecker, C., Daly, E., Murphy, C. M., … Murphy, D. G. M. M. (2012). Fronto-striatal circuitry and inhibitory control in autism: Findings from diffusion tensor imaging tractography. *Cortex*, *48*(2), 183–193.

Langen, M., Schnack, H. G., Nederveen, H., Bos, D., Lahuis, B. E., de Jonge, M. V., … Durston, S. (2009). Changes in the Developmental Trajectories of Striatum in Autism. *Biological Psychiatry*, *66*(4), 327–333.

Le Liboux, A., Lefebvre, P., Le Roux, Y., Truffinet, P., Aubeneau, M., Kirkesseli, S., & Montay, G. (1997). Single- and multiple-dose pharmacokinetics of riluzole in white subjects. *Journal of Clinical Pharmacology*, *37*(9), 820–827.

Lee, S. H., & Sheng, M. (2000). Development of neuron-neuron synapses. *Current Opinion in Neurobiology*, *10*(1), 125–131.

Lemonnier, E., Degrez, C., Phelep, M., Tyzio, R., Josse, F., Grandgeorge, M., … Ben-Ari, Y. (2012). A randomised controlled trial of bumetanide in the treatment of autism in children. *Translational Psychiatry*, *2*(12), e202.

Levinson, J. N., Chéry, N., Huang, K., Wong, T. P., Gerrow, K., Kang, R., … El-Husseini, A. (2005). Neuroligins Mediate Excitatory and Inhibitory Synapse Formation. *Journal of Biological Chemistry*, *280*(17), 17312–17319.

Levitt, J. G., O'Neill, J., Blanton, R. E., Smalley, S., Fadale, D., McCracken, J. T., … Alger, J. R. (2003). Proton magnetic resonance spectroscopic imaging of the brain in childhood autism. *Biological Psychiatry*, *54*(12), 1355–1366.

Levy, S. E., Giarelli, E., Lee, L.-C., Schieve, L. A., Kirby, R. S., Cunniff, C., … Rice, C. E. (2010). Autism Spectrum Disorder and Co-occurring Developmental, Psychiatric, and Medical Conditions Among Children in Multiple Populations of the United States. *Journal of Developmental and Behavioral Pediatrics*, *31*(4), 267–275.

Leyfer, O. T., Folstein, S. E., Bacalman, S., Davis, N. O., Dinh, E., Morgan, J., … Lainhart, J. E. (2006). Comorbid psychiatric disorders in children with autism: Interview development and rates of disorders. *Journal of Autism and Developmental Disorders*, *36*(7), 849–861.

Li, J., Bravo, D. S., Louise Upton, A., Gilmour, G., Tricklebank, M. D., Fillenz, M., … McHugh, S. B. (2011). Close temporal coupling of neuronal activity and tissue oxygen responses in rodent whisker barrel cortex. *European Journal of Neuroscience*, *34*(12), 1983–1996.

Liang, S.-L., Carlson, G. C., & Coulter, D. A. (2006). Dynamic Regulation of Synaptic GABA Release by the Glutamate-Glutamine Cycle in Hippocampal Area CA1. *Journal of Neuroscience*, *26*(33), 8537–8548.

Libero, L. E., Reid, M. A., White, D. M., Salibi, N., Lahti, A. C., & Kana, R. K. (2015). Biochemistry of the cingulate cortex in autism: An MR spectroscopy study. *Autism Research : Official Journal of the International Society for Autism Research*, *9*(6), 643–657.

Lin, Q. (2013). Submerged fermentation of Lactobacillus rhamnosus YS9 for γ-aminobutyric acid (GABA) production. *Brazilian Journal of Microbiology*, *44*(1), 183–187.

Liu, Z., Li, X., Zhang, J.-T., Cai, Y.-J., Cheng, T.-L., Cheng, C., … Qiu, Z. (2016). Autism-like behaviours and germline transmission in transgenic monkeys overexpressing MeCP2. *Nature*, *530*(7588), 98–102.

Lohith, T. G., Osterweil, E. K., Fujita, M., Jenko, K. J., Bear, M. F., & Innis, R. B. (2013). Is metabotropic glutamate receptor 5 upregulated in prefrontal cortex in fragile X syndrome? *Molecular Autism*, *4*(1), 15.

Lord, C., Risi, S., Lambrecht, L., Cook, E. H., Leventhal, B. L., Dilavore, P. C., … Rutter, M. (2000). The Autism Diagnostic Observation Schedule-Generic: A standard measure of social and communication deficits associated with the spectrum of autism. *Journal of Autism and Developmental Disorders*, *30*, 205–223.

Lord, C., Rutter, M., & Couteur, A. L. (1994). Autism diagnostic interview-revised: A revised version of a diagnostic interview for caregivers of individuals with possible pervasive developmental disorders. *Journal of Autism and Developmental Disorders*, *24*, 659–685.

LoTurco, J. J., Owens, D. F., Heath, M. J. S., Davis, M. B. E., & Kriegstein, A. R. (1995). GABA and glutamate depolarize cortical progenitor cells and inhibit DNA synthesis. *Neuron*, *15*(6), 1287–1298.

Lowry, J. P., Griffin, K., McHugh, S. B., Lowe, A. S., Tricklebank, M., & Sibson, N. R. (2010). Real-time electrochemical monitoring of brain tissue oxygen: A surrogate for functional magnetic resonance imaging in rodents. *NeuroImage*, *52*(2), 549–555.

Lozano, R., Rosero, C. A., & Hagerman, R. J. (2014). Fragile X spectrum disorders. *Intractable & Rare Diseases Research*, *3*(4), 134–146.

Lugnegård, T., Hallerbäck, M. U., & Gillberg, C. (2011). Psychiatric comorbidity in young adults with a clinical diagnosis of Asperger syndrome. *Research in Developmental Disabilities*, *32*(5), 1910–1917.

Luján, R., Shigemoto, R., & López-Bendito, G. (2005). Glutamate and GABA receptor signalling in the developing brain. *Neuroscience*, *130*(3), 567–580.

Lukkes, J. L., Burke, A. R., Zelin, N. S., Hale, M. W., & Lowry, C. A. (2012). Post-weaning social isolation attenuates c-Fos expression in GABAergic interneurons in the basolateral amygdala of adult female rats. *Physiology & Behavior*, *107*(5), 719–725.

Luyster, R., Gotham, K., Guthrie, W., Coffing, M., Petrak, R., Pierce, K., … Lord, C. (2009). The autism diagnostic observation schedule - Toddler module: A new module of a standardized diagnostic measure for autism spectrum disorders. *Journal of Autism and Developmental Disorders*, *39*(9), 1305–1320.

Lydiard, R. B. (2003). The role of GABA in anxiety disorders. *The Journal of Clinical Psychiatry*, *64 Suppl 3*, 21–27.

Mabunga, D. F. N., Gonzales, E. L. T., Kim, J., Kim, K. C., & Shin, C. Y. (2015). Exploring the Validity of Valproic Acid Animal Model of Autism. *Experimental Neurobiology*, *24*(4), 285.

Magistretti, P. J., & Pellerin, L. (1999). Cellular mechanisms of brain energy metabolism and their relevance to functional brain imaging. *Philosophical Transactions of the Royal Society B: Biological Sciences*, *354*(1387), 1155–1163.

Mann, J. J., Oquendo, M. A., Watson, K. T., Boldrini, M., Malone, K. M., Ellis, S. P., … Currier, D. (2014). Anxiety in major depression and cerebrospinal fluid free gamma-aminobutyric acid. *Depression and Anxiety*, *31*(10), 814–821.

Mantz, J., Laudenbach, V., Lecharny, J. B., Henzel, D., & Desmonts, J. M. (1994). Riluzole, a novel antiglutamate, blocks GABA uptake by striatal synaptosomes. *European Journal of Pharmacology*, *257*(1–2), R7-8.

Marrosu, F., Marrosu, G., Rachel, M. G., & Biggio, G. (1987). Paradoxical reactions elicited by diazepam in children with classic autism. *Functional Neurology*, *2*(3), 355–361.

Martin, D. L., & Rimvall, K. (1993). Regulation of gamma-aminobutyric acid synthesis in the brain. *Journal of Neurochemistry*, *60*(2), 395–407.

Martin, D., Thompson, M. A., & Nadler, J. V. (1993). The neuroprotective agent riluzole inhibits release of glutamate and aspartate from slices of hippocampal area CA1. *European Journal of Pharmacology*, *250*(3), 473–476.

Martin, D., Thompson, M. A., & Nadler, J. V. (1993). The neuroprotective agent riluzole inhibits release of glutamate and aspartate from slices of hippocampal area CA1. *European Journal of Pharmacology*, *250*, 473–476.

Martínez-Sanchis, S. (2015). [The role of the prefrontal cortex in the sensory problems of children with autism spectrum disorder and its involvement in social aspects]. *Revista de Neurologia*, *60 Suppl 1*, S19-24.

Mathew, S. J., Amiel, J. M., Coplan, J. D., Fitterling, H. A., Sackeim, H. A., & Gorman, J. M. (2005). Open-label trial of riluzole in generalized anxiety disorder. *The American Journal of Psychiatry*, *162*(12), 2379–2381.

Matson, J. L., & Rivet, T. T. (2008). Characteristics of challenging behaviours in adults with autistic disorder, PDD-NOS, and intellectual disability. *Journal of Intellectual & Developmental Disability*, *33*(4), 323–329.

Matson, J. L., & Shoemaker, M. (2009). Intellectual disability and its relationship to autism spectrum disorders. *Research in Developmental Disabilities*, *30*(6), 1107–1114.

Mattila, M. L., Hurtig, T., Haapsamo, H., Jussila, K., Kuusikko-Gauffin, S., Kielinen, M., … Moilanen, I. (2010). Comorbid psychiatric disorders associated with asperger syndrome/high-functioning autism: A community- and clinic-based study. *Journal of Autism and Developmental Disorders*, *40*(9), 1080–1093.

Mattson, M. P., Lee, R. E., Adams, M. E., Guthrie, P. B., & Kater, S. B. (1988). Interactions between entorhinal axons and target hippocampal neurons: A role for glutamate in the development of hippocampal circuitry. *Neuron*, *1*(9), 865–876.

McDougle, C. J., Kresch, L. E., & Posey, D. J. (2000). Repetitive Thoughts and Behavior in Pervasive Developmental Disorders: Treatment with Serotonin Reuptake Inhibitors. *Journal of Autism and Developmental Disorders*, *30*(5), 427–435.

McDougle, C. J., Naylor, S. T., Cohen, D. J., Volkmar, F. R., Heninger, G. R., & Price, L. H. (1996). A Double-blind, Placebo-Controlled Study of Fluvoxamine in Adults With Autistic Disorder. *Archives of General Psychiatry*, *53*(11), 1001–1008.

Mechler, K., Häge, A., Schweinfurth, N., Glennon, J. C., Dijkhuizen, R. M., Murphy, D., … The TACTICS Consortium. (2017). Glutamatergic Agents in the Treatment of Compulsivity and Impulsivity in Child and Adolescent Psychiatry: a Systematic Review of the Literature. *Zeitschrift Für Kinder- Und Jugendpsychiatrie Und Psychotherapie*, 1–18.

Mehta, M. V., Gandal, M. J., & Siegel, S. J. (2011). mGluR5-Antagonist Mediated Reversal of Elevated Stereotyped, Repetitive Behaviors in the VPA Model of Autism. *PLoS ONE*, *6*(10), e26077.

Mendez, M. A., Horder, J., Myers, J., Coghlan, S., Stokes, P., Erritzoe, D., … Nutt, D. (2013). The brain GABA-benzodiazepine receptor alpha-5 subtype in autism spectrum disorder: A pilot [11C]Ro15-4513 positron emission tomography study. *Neuropharmacology*, *68*, 195–201.

Mescher, M., Merkle, H., Kirsch, J., Garwood, M., & Gruetter, R. (1998). Simultaneous in vivo spectral editing and water suppression. *NMR in Biomedicine*, *11*(6), 266–272.

Mikl, M., Mareček, R., Hluštík, P., Pavlicová, M., Drastich, A., Chlebus, P., … Krupa, P. (2008). Effects of spatial smoothing on fMRI group inferences. *Magnetic Resonance Imaging*, *26*(4), 490–503.

Milane, A., Tortolano, L., Fernandez, C., Bensimon, G., Meininger, V., & Farinotti, R. (2009). Brain and plasma riluzole pharmacokinetics: Effect of minocycline combination. *Journal of Pharmacy and Pharmaceutical Sciences*, *12*(2), 209–217.

Minshawi, N. F., Wink, L. K., Shaffer, R., Plawecki, M. H., Posey, D. J., Liu, H., … Erickson, C. A. (2016). A randomized, placebo-controlled trial of d-cycloserine for the enhancement of social skills training in autism spectrum disorders. *Molecular Autism*, *7*(1), 1–10.

Missler, M., Zhang, W., Rohlmann, A., Kattenstroth, G., Hammer, R. E., Gottmann, K., & Südhof, T. C. (2003). Alpha-neurexins couple Ca2+ channels to synaptic vesicle exocytosis. *Nature*, *423*(6943), 939–948.

Moeschler, J. B., & Shevell, M. (2006). Clinical genetic evaluation of the child with mental retardation or developmental delays. *Pediatrics*, *117*(6), 2304–2316.

Mohammad-Rezazadeh, I., Frohlich, J., Loo, S. K., & Jeste, S. S. (2016). Brain connectivity in autism spectrum disorder. *Current Opinion in Neurology*, *29*(2), 137–147.

Morgan, J. T., Chana, G., Abramson, I., Semendeferi, K., Courchesne, E., & Everall, I. P. (2012). Abnormal microglial–neuronal spatial organization in the dorsolateral prefrontal cortex in autism. *Brain Research*, *1456*, 72–81.

Morgan, J. T., Chana, G., Pardo, C. A., Achim, C., Semendeferi, K., Buckwalter, J., … Everall, I. P. (2010). Microglial Activation and Increased Microglial Density Observed in the Dorsolateral Prefrontal Cortex in Autism. *Biological Psychiatry*, *68*(4), 368–376.

Mori, T., Mori, K., Fujii, E., Toda, Y., Miyazaki, M., Harada, M., … Kagami, S. (2012). Evaluation of the GABAergic nervous system in autistic brain: (123)I-iomazenil SPECT study. *Brain & Development*, *34*(8), 648–654.

Muller, C. L., Anacker, A. M. J., & Veenstra-VanderWeele, J. (2016). The serotonin system in autism spectrum disorder: From biomarker to animal models. *Neuroscience*, *321*, 24–41.

Müller, P. B., & Langemann, H. (1962). Distribution of Glutamic Acid Decarboxylase activity in humna brain. *Journal of Neurochemistry*, *9*(4), 399–401.

Mullins, P. G., McGonigle, D. J., O'Gorman, R. L., Puts, N. A. J., Vidyasagar, R., Evans, C. J., … Wilson, M. (2014). Current practice in the use of MEGA-PRESS spectroscopy for the detection of GABA. *NeuroImage*, *86*, 43–52.

Murphy, D. G. M., Critchley, H. D., Schmitz, N., McAlonan, G., Van Amelsvoort, T., Robertson, D., … Howlin, P. (2002). Asperger syndrome: a proton magnetic resonance spectroscopy study of brain. *Arch Gen Psychiatry*, *59*(10), 885–891.

Myers, S. M., & Johnson, C. P. (2007). Management of children with autism spectrum disorders. *Pediatrics, 120*(5), 1162–1182.

Naaijen, J., Lythgoe, D. J., Amiri, H., Buitelaar, J. K., & Glennon, J. C. (2015). Fronto-striatal glutamatergic compounds in compulsive and impulsive syndromes: A review of magnetic resonance spectroscopy studies. *Neuroscience and Biobehavioral Reviews*, *52*, 74–88.

Naressi, A., Couturier, C., Devos, J. M., Janssen, M., Mangeat, C., De Beer, R., & Graveron-Demilly, D. (2001). Java-based graphical user interface for the MRUI quantitation package. *Magnetic Resonance Materials in Physics, Biology and Medicine*, *12*(2–3), 141–152.

NAS. (2016). Employment in Autism. Retrieved from http://www.autism.org.uk/professionals/employers.aspx

NC3Rs. (2018). 3R's - Strains of Mice and Rats. Retrieved from http://www.3rs-reduction.co.uk/html/8__strains_of_mice.html

Niswender, C. M., & Conn, P. J. (2010). Metabotropic glutamate receptors: physiology, pharmacology, and disease. *Annual Review of Pharmacology and Toxicology*, *50*, 295–322.

Nomi, J. S., & Uddin, L. Q. (2015). Developmental changes in large-scale network connectivity in autism. *NeuroImage: Clinical*, *7*, 732–741.

O'Brien, G., & Pearson, J. (2004). Autism and learning disability. *Autism : The International Journal of Research and Practice*, *8*, 125–140.

Oblak, Gibbs, T. T., & Blatt, G. J. (2009). Decreased GABAA receptors and benzodiazepine binding sites in the anterior cingulate cortex in autism. *Autism Research : Official Journal of the International Society for Autism Research*, *2*(4), 205–219.

Oblak, Gibbs, T. T., & Blatt, G. J. (2010). Decreased GABAB receptors in the cingulate cortex and fusiform gyrus in Autism. *Journal of Neurochemistry*, *114*(5), 1414–1423.

Ogawa, S., Lee, T. M., Nayak, A. S., & Glynn, P. (1990). Oxygenation-sensitive contrast in magnetic resonance image of rodent brain at high magnetic fields. *Magnetic Resonance in Medicine*, *14*(1), 68–78.

Onore, C., Careaga, M., & Ashwood, P. (2012). The role of immune dysfunction in the pathophysiology of autism. *Brain, Behavior, and Immunity*, *26*(3), 383–392.

Otsuka America Pharmaceutical, Inc, J. (2002). ABILFY [package insert].

Packer, A. (2016). Neocortical neurogenesis and the etiology of autism spectrum disorder. *Neuroscience & Biobehavioral Reviews*, *64*, 185–195.

Page, L. A., Daly, E., Schmitz, N., Simmons, A., Toal, F., Deeley, Q., … Murphy, D. G. M. (2006). In vivo 1H-magnetic resonance spectroscopy study of amygdala-hippocampal and parietal regions in autism. *The American Journal of Psychiatry*, *163*, 2189–2192.

Pakkenberg, B., & Gundersen, H. J. G. (1988). Total number of neurons and glial cells in human brain nuclei estimated by the disector and the fractionator. *Journal of Microscopy*, *150*(1), 1–20.

Pavăl, D. (2017). A Dopamine Hypothesis of Autism Spectrum Disorder. *Developmental Neuroscience*, *39*(5), 355–360.

Paxinos, G., & Watson, C. (2009). *The Rat Brain in Stereotaxic Coordinates; Compact, Sixth Edition* (6th ed.). Academic Press.

Pearce, I. A., Cambray-Deakin, M. A., & Burgoyne, R. D. (1987). Glutamate acting on NMDA receptors stimulates neurite outgrowth from cerebellar granule cells. *FEBS Letters*, *223*(1), 143–147.

Pehrson, A. L., & Sanchez, C. (2015). Altered γ-aminobutyric acid neurotransmission in major depressive disorder: A critical review of the supporting evidence and the influence of serotonergic antidepressants. *Drug Design, Development and Therapy*, *9*, 603–624.

Pellicano, E., Dinsmore, A., & Charman, T. (2014). What should autism research focus upon? Community views and priorities from the United Kingdom. *Autism : The International Journal of Research and Practice*, *18*(7), 756–770.

Persico, A. M., & Bourgeron, T. (2006). Searching for ways out of the autism maze: genetic, epigenetic and environmental clues. *Trends in Neurosciences*, *29*(7), 349–358.

Petrinovic, M. M., Hankov, G., Schroeter, A., Bruns, A., Rudin, M., von Kienlin, M., … Mueggler, T. (2016). A novel anesthesia regime enables neurofunctional studies and imaging genetics across mouse strains. *Scientific Reports*, *6*, 24523.

Pilling, S., Baron-Cohen, S., Megnin-Viggars, O., Lee, R., & Taylor, C. (2012). Recognition, referral, diagnosis, and management of adults with autism: summary of NICE guidance. *BMJ*, *344*(1), e4082–e4082.

Pizzarelli, R., & Cherubini, E. (2011). Alterations of GABAergic signaling in autism spectrum disorders. *Neural Plasticity*, *2011*, 297153.

Posey, D. J., Kem, D. L., Swiezy, N. B., Sweeten, T. L., Wiegand, R. E., & McDougle, C. J. (2004). A pilot study of D-cycloserine in subjects with autistic disorder. *American Journal of Psychiatry*, *161*(11), 2115–2117.

Prakriya, M., & Mennerick, S. (2000). Selective depression of low-release probability excitatory synapses by sodium channel blockers. *Neuron*, *26*(3), 671–682.

Prat, C. S., Stocco, A., Neuhaus, E., & Kleinhans, N. M. (2016). Basal ganglia impairments in autism spectrum disorder are related to abnormal signal gating to prefrontal cortex. *Neuropsychologia*, *91*, 268–281.

Purcell, A. E., Jeon, O. H., Zimmerman, A. W., Blue, M. E., & Pevsner, J. (2001). Postmortem brain abnormalities of the glutamate neurotransmitter system in autism. *Neurology*, *57*(9), 1618–1628.

Purkayastha, P., Malapati, A., Yogeeswari, P., & Sriram, D. (2015). A Review on GABA/Glutamate Pathway for Therapeutic Intervention of ASD and ADHD. *Current Medicinal Chemistry*, 1850–1859.

Puts, N. A. J., & Edden, R. A. E. (2012). In vivo magnetic resonance spectroscopy of GABA: A methodological review. *Progress in Nuclear Magnetic Resonance Spectroscopy*, *60*, 29–41.

Qiu, A., Adler, M., Crocetti, D., Miller, M. I., & Mostofsky, S. H. (2010). Basal ganglia shapes predict social, communication, and motor dysfunctions in boys with autism spectrum disorder. *Journal of the American Academy of Child and Adolescent Psychiatry*, *49*(6), 539–551.

Rackayova, V., Pouwels, P. J. W., & Braissant, O. (2017). Creatine in the central nervous system: From magnetic resonance spectroscopy to creatine deficiencies. *Analytical Biochemistry*, *529*, 144–157.

Radyushkin, K., Hammerschmidt, K., Boretius, S., Varoqueaux, F., El-Kordi, A., Ronnenberg, A., … Ehrenreich, H. (2009). Neuroligin-3-deficient mice: Model of a monogenic heritable form of autism with an olfactory deficit. *Genes, Brain and Behavior*, *8*(4), 416–425.

Ramadan, S., Lin, A., & Stanwell, P. (2013). Glutamate and glutamine: A review of in vivo MRS in the human brain. *NMR in Biomedicine*, *26*(12), 1630–1646.

Rane, P., Cochran, D., Hodge, S. M., Haselgrove, C., Kennedy, D. N., & Frazier, J. A. (2015). Connectivity in Autism: A Review of MRI Connectivity Studies. *Harvard Review of Psychiatry*, *23*(4), 223–244.

Ravi, P. R., Vats, R., & Kora, U. R. (2013). Effect of ciprofloxacin and grapefruit juice on oral pharmacokinetics of riluzole in Wistar rats. *Journal of Pharmacy and Pharmacology*, *65*(3), 337–344.

Reagan-Shaw, S., Nihal, M., & Ahmad, N. (2008). Dose translation from animal to human studies revisited. *The FASEB Journal : Official Publication of the Federation of American Societies for Experimental Biology*, *22*(3), 659–661.

Reiersen, A. M., & Todd, R. D. (2008). Co-occurrence of ADHD and autism spectrum disorders: phenomenology and treatment. *Expert Review of Neurotherapeutics*, *8*(4), 657–669.

Research Units on Pediatric Psychopharmacology Autism Network. (2005). Randomized, Controlled, Crossover Trial of Methylphenidate in Pervasive Developmental Disorders With Hyperactivity. *Archives of General Psychiatry*, *62*(11), 1266–1274.

Richetto, J., Calabrese, F., Riva, M. A., & Meyer, U. (2014). Prenatal immune activation induces maturation-dependent alterations in the prefrontal GABAergic transcriptome. *Schizophrenia Bulletin*, *40*(2), 351–361.

Robertson, C. E. E. C. E., Ratai, E.-M. M., Kanwisher, N., Rubenstein, J. L. R., Merzenich, M. M., Canitano, R., … Shah, N. J. (2016). Reduced GABAergic Action in the Autistic Brain. *Current Biology*, *26*(1), 80–85.

Robinson, E. B., Lichtenstein, P., Anckarsater, H., Happe, F., & Ronald, A. (2013). Examining and interpreting the female protective effect against autistic behavior. *Proceedings of the National Academy of Sciences*, *110*(13), 5258–5262.

Rojas, D. C., Peterson, E., Winterrowd, E., Reite, M. L., Rogers, S. J., & Tregellas, J. R. (2006). Regional gray matter volumetric changes in autism associated with social and repetitive behavior symptoms. *BMC Psychiatry*, *6*(1), 56.

Rojas, D. C., Singel, D., Steinmetz, S., Hepburn, S., & Brown, M. S. (2014). Decreased left perisylvian GABA concentration in children with autism and unaffected siblings. *NeuroImage*, *86*, 28–34.

Rothman, D. L., de Feyter, H. M., de Graaf, R. A., Mason, G. F., & Behar, K. L. (2011). 13C MRS studies of neuroenergetics and neurotransmitter cycling in humans. *NMR in Biomedicine*, *24*(8), 943–957.

Rothman, D. L., de Feyter, H. M., Maciejewski, P. K., & Behar, K. L. (2012). Is there in vivo evidence for amino acid shuttles carrying ammonia from neurons to astrocytes. *Neurochemical Research*, *37*(11), 2597–2612.

Rothman, D. L., Petroff, O. A., Behar, K. L., & Mattson, R. H. (1993). Localized 1H NMR measurements of gamma-aminobutyric acid in human brain in vivo. *Proceedings of the National Academy of Sciences*, *90*(12), 5662–5666.

Rowley, N. M., Madsen, K. K., Schousboe, A., & Steve White, H. (2012). Glutamate and GABA synthesis, release, transport and metabolism as targets for seizure control. *Neurochemistry International*, *61*(4), 546–558.

Russell, G., Rodgers, L. R., Ukoumunne, O. C., & Ford, T. (2014). Prevalence of Parent-Reported ASD and ADHD in the UK: Findings from the Millennium Cohort Study. *Journal of Autism and Developmental Disorders*, *44*, 31–40.

Sailasuta, N., Ernst, T., & Chang, L. (2008). Regional variations and the effects of age and gender on glutamate concentrations in the human brain. *Magnetic Resonance Imaging*, *26*(5), 667–675.

Sanofi-Aventis. (2010). Rilutek (riluzole). *Product Monograph*.

SAS Institute. (2018). SAS Missing Data Analysis. Retrieved from https://support.sas.com/rnd/app/stat/procedures/MissingDataAnalysis.html

Sato, W., Kubota, Y., Kochiyama, T., Uono, S., Yoshimura, S., Sawada, R., … Toichi, M. (2014). Increased Putamen Volume in Adults with Autism Spectrum Disorder. *Frontiers in Human Neuroscience*, *8*, 957.

Schallmo, M.-P. (2017). Opposite effects of GABA-A receptor potentiation and GABA concentration on human perceptual performance. In *4th International Symposium on MRS of GABA*. Katholieke Universiteit Leuven.

Scharf, S. H., Jaeschke, G., Wettstein, J. G., & Lindemann, L. (2015). Metabotropic glutamate receptor 5 as drug target for Fragile X syndrome. *Current Opinion in Pharmacology*, *20*, 124–134.

Schipul, S. E., Keller, T. A., & Just, M. A. (2011). Inter-regional brain communication and its disturbance in autism. *Frontiers in Systems Neuroscience*, *5*, 10.

Schmeisser, M. J., Ey, E., Wegener, S., Bockmann, J., Stempel, A. V., Kuebler, A., … Boeckers, T. M. (2012). Autistic-like behaviours and hyperactivity in mice lacking ProSAP1/Shank2. *Nature*, *486*, 256–260.

Schmitz, N., Daly, E., & Murphy, D. (2007). Frontal anatomy and reaction time in Autism. *Neuroscience Letters*, *412*(1), 12–17.

Schmitz, N., Rubia, K., van Amelsvoort, T., Daly, E., Smith, A., & Murphy, D. G. M. (2008). Neural correlates of reward in autism. *British Journal of Psychiatry*, *192*(01), 19–24.

Schuetze, M., Park, M. T. M., Cho, I. Y., MacMaster, F. P., Chakravarty, M. M., & Bray, S. L. (2016). Morphological Alterations in the Thalamus, Striatum, and Pallidum in Autism Spectrum Disorder. *Neuropsychopharmacology*, *41*(11), 2627–2637.

Schutte, J. L., McCue, M. P., Parmanto, B., McGonigle, J., Handen, B., Lewis, A., … Saptono, A. (2015). Usability and Reliability of a Remotely Administered Adult Autism Assessment, the Autism Diagnostic Observation Schedule (ADOS) Module 4. *Telemedicine Journal and E-Health : The Official Journal of the American Telemedicine Association*, *21*(3), 176–184.

Scott, M., Falkmer, M., Girdler, S., & Falkmer, T. (2015). Viewpoints on factors for successful employment for adults with autism spectrum disorder. *PLoS ONE*, *10*(10), e0139281.

Sestito, R. S., Trindade, L. B., de Souza, R. G., Kerbauy, L. N., Iyomasa, M. M., & Rosa, M. L. (2011). Effect of isolation rearing on the expression of AMPA glutamate receptors in the hippocampal formation. *Journal of Psychopharmacology*, *25*(12), 1720–1729.

Shao, Y., Cuccaro, M. L., Hauser, E. R., Raiford, K. L., Menold, M. M., Wolpert, C. M., … Pericak-Vance, M. A. (2003). Fine mapping of autistic disorder to chromosome 15q11-q13 by use of phenotypic subtypes. *American Journal of Human Genetics*, *72*, 539–548.

Sharma, A., & Shaw, S. R. (2012). Efficacy of Risperidone in Managing Maladaptive Behaviors for Children With Autistic Spectrum Disorder: A Meta-Analysis. *Journal of Pediatric Health Care*, *26*(4), 291–299.

Sherwood, C. C., Stimpson, C. D., Raghanti, M. A., Wildman, D. E., Uddin, M., Grossman, L. I., … Hof, P. R. (2006). Evolution of increased glia-neuron ratios in the human frontal cortex. *Proceedings of the National Academy of Sciences*, *103*(37), 13606–13611.

Shigemori, T., Sakai, A., Takumi, T., Itoh, Y., & Suzuki, H. (2015). Altered Microglia in the Amygdala Are Involved in Anxiety-related Behaviors of a Copy Number Variation Mouse Model of Autism. *Journal of Nippon Medical School*, *82*(2), 92–99.

Shimmura, C., Suzuki, K., Iwata, Y., Tsuchiya, K. J., Ohno, K., Matsuzaki, H., … Mori, N. (2013). Enzymes in the glutamate-glutamine cycle in the anterior cingulate cortex in postmortem brain of subjects with autism. *Molecular Autism*, *4*(1), 6.

Shinoda, Y., Sadakata, T., & Furuichi, T. (2013). Animal models of autism spectrum disorder (ASD): a synaptic-level approach to autistic-like behavior in mice. *Experimental Animals*, *62*(2), 71–78.

Shinohe, A., Hashimoto, K., Nakamura, K., Tsujii, M., Iwata, Y., Tsuchiya, K. J., … Mori, N. (2006). Increased serum levels of glutamate in adult patients with autism. *Progress in Neuro-Psychopharmacology and Biological Psychiatry*, *30*, 1472–1477.

Shungu, D. C., Mao, X., Gonzales, R., Soones, T. N., Dyke, J. P., van der Veen, J. W., & Kegeles, L. S. (2016). Brain γ-aminobutyric acid (GABA) detection *in vivo* with the *J* -editing ^{1} H MRS technique: a comprehensive methodological evaluation of sensitivity enhancement, macromolecule contamination and test-retest reliability. *NMR in Biomedicine*, *29*(7), 932–942.

Sibson, N. R., Dhankhar, A., Mason, G. F., Rothman, D. L., Behar, K. L., & Shulman, R. G. (1998). Stoichiometric coupling of brain glucose metabolism and glutamatergic neuronal activity. *Neurobiology*, *95*(January), 316–321.

Silverman, J. L., Tolu, S. S., Barkan, C. L., & Crawley, J. N. (2010). Repetitive self-grooming behavior in the BTBR mouse model of autism is blocked by the mGluR5 antagonist MPEP. *Neuropsychopharmacology*, *35*, 976–989.

Simonoff, E., Pickles, A., Charman, T., Chandler, S., Loucas, T., & Baird, G. (2008). Psychiatric disorders in children with autism spectrum disorders: prevalence, comorbidity, and associated factors in a population-derived sample. *Journal of the American Academy of Child and Adolescent Psychiatry*, *47*(8), 921–929.

Sizoo, B. B., Horwitz, E., Teunisse, J., Kan, C., Vissers, C., Forceville, E., … Geurts, H. (2015). Predictive validity of self-report questionnaires in the assessment of autism spectrum disorders in adults. *Autism*, *19*(7), 842–849.

Smith, S. E. P., Zhou, Y.-D., Zhang, G., Jin, Z., Stoppel, D. C., & Anderson, M. P. (2011). Increased Gene Dosage of Ube3a Results in Autism Traits and Decreased Glutamate Synaptic Transmission in Mice. *Science Translational Medicine*, *3*(103), 103ra97-103ra97.

Song, J. Y., Ichtchenko, K., Südhof, T. C., & Brose, N. (1999). Neuroligin 1 is a postsynaptic cell-adhesion molecule of excitatory synapses. *Proceedings of the National Academy of Sciences*, *96*(3), 1100–1105.

Soomro, G. M. (2012). Obsessive compulsive disorder. *BMJ Clin Evidence*, *2012*, 1004.

Spencer, T. J., Biederman, J., Madras, B. K., Dougherty, D. D., Bonab, A. A., Livni, E., … Fischman, A. J. (2007). Further Evidence of Dopamine Transporter Dysregulation in ADHD: A Controlled PET Imaging Study Using Altropane. *Biological Psychiatry*, *62*(9), 1059–1061.

Spencer, T. J., Biederman, J., Madras, B. K., Faraone, S. V., Dougherty, D. D., Bonab, A. A., & Fischman, A. J. (2005). In vivo neuroreceptor imaging in attention-deficit/hyperactivity disorder: A focus on the dopamine transporter. *Biological Psychiatry*, *57*(11), 1293–1300.

Spielberger, C. D., Gorsuch, R. L., Lushene, R. E., Vagg, P. R., & Jacobs, G. A. (1970). *The State-Trait Anxiety Inventory*. CA: Consulting Psychologists Press.

Spruston, N. (2008). Pyramidal neurons: dendritic structure and synaptic integration. *Nature Reviews. Neuroscience*, *9*(3), 206–221.

Stagg, C. J., Bachtiar, V., Amadi, U., Gudberg, C. A., Ilie, A. S., Sampaio-Baptista, C., … Johansen-Berg, H. (2014). Local GABA concentration is related to network-level resting functional connectivity. *Elife*, *3*, e01465.

Stanfield, A. C., McIntosh, A. M., Spencer, M. D., Philip, R., Gaur, S., & Lawrie, S. M. (2008). Towards a neuroanatomy of autism: a systematic review and meta-analysis of structural magnetic resonance imaging studies. *European Psychiatry*, *23*(4), 289–299.

State, M. W. (2010). Another piece of the autism puzzle. *Nature Genetics*, *42*(6), 478–479.

Stenken, J. A., Church, M. K., Gill, C. A., & Clough, G. F. (2010). How minimally invasive is microdialysis sampling? A cautionary note for cytokine collection in human skin and other clinical studies. *The AAPS Journal*, *12*(1), 73–78.

Sterling, L., Dawson, G., Estes, A., & Greenson, J. (2008). Characteristics associated with presence of depressive symptoms in adults with autism spectrum disorder. *Journal of Autism and Developmental Disorders*, *38*(6), 1011–1018.

Stewart, A. M., Nguyen, M., Wong, K., Poudel, M. K., & Kalueff, A. V. (2014). Developing zebrafish models of autism spectrum disorder (ASD). *Progress in Neuro-Psychopharmacology and Biological Psychiatry*, *50*, 27–36.

Stone, J. M., Dietrich, C., Edden, R., Mehta, M. a, De Simoni, S., Reed, L. J., … Barker, G. J. (2012). Ketamine effects on brain GABA and glutamate levels with 1H-MRS: relationship to ketamine-induced psychopathology. *Molecular Psychiatry*, *17*(7), 664–665.

Südhof, T. C. (2008). Neuroligins and neurexins link synaptic function to cognitive disease. *Nature*, *455*(7215), 903–911.

Sung, B., Lim, G., & Mao, J. (2003). Altered expression and uptake activity of spinal glutamate transporters after nerve injury contribute to the pathogenesis of neuropathic pain in rats. *The Journal of Neuroscience : The Official Journal of the Society for Neuroscience*, *23*, 2899–2910.

Suzuki, K., Sugihara, G., Ouchi, Y., Nakamura, K., Futatsubashi, M., Takebayashi, K., … Mori, N. (2013). Microglial Activation in Young Adults With Autism Spectrum Disorder. *JAMA Psychiatry*, *70*(1), 49.

Tabuchi, K., Blundell, J., Etherton, M. R., Hammer, R. E., Liu, X., Powell, C. M., … Sudhof, T. C. (2007). A neuroligin-3 mutation implicated in autism increases inhibitory synaptic transmission in mice. *Science*, *318*(5847), 71–76.

Tapuhi, Y., Schmidt, D. E., Lindner, W., & Karger, B. L. (1981). Dansylation of amino acids for high-performance liquid chromatography analysis. *Analytical Biochemistry*, *115*(1), 123–129.

Tebartz van Elst, L., Maier, S., Fangmeier, T., Endres, D., Mueller, G. T., Nickel, K., … Perlov, E. (2014). Disturbed cingulate glutamate metabolism in adults with high-functioning autism spectrum disorder: evidence in support of the excitatory/inhibitory imbalance hypothesis. *Molecular Psychiatry*, *19*(12), 1314–1325.

The Autism Genome Project Consortium. (2007). Mapping autism risk loci using genetic linkage and chromosomal rearrangements. *Nature Genetics*, *39*(3), 319–328.

Tseng, K. Y., & O'Donnell, P. (2004). Dopamine – Glutamate Interactions Controlling Prefrontal Cortical Pyramidal Cell Excitability Involve Multiple Signaling Mechanisms. *Neuroscience*, *24*(22), 5131–5139.

Tuchman, R., & Cuccaro, M. (2011). Epilepsy and autism: neurodevelopmental perspective. *Current Neurology and Neuroscience Reports*, *11*, 428–434.

Tuchman, R., Hirtz, D., & Mamounas, L. A. (2013). NINDS epilepsy and autism spectrum disorders workshop report. *Neurology*, *81*(18), 1630–1636.

Tuchman, R., & Rapin, I. (2002). Epilepsy in autism. *Lancet Neurology*, *1*(6), 352–358.

Tyzio, R., Cossart, R., Khalilov, I., Minlebaev, M., Hübner, C. A., Represa, A., … Khazipov, R. (2006). Maternal oxytocin triggers a transient inhibitory switch in GABA signaling in the fetal brain during delivery. *Science*, *314*(5806), 1788–1792.

Uchino, S., & Waga, C. (2015). Novel Therapeutic Approach for Autism Spectrum Disorder: Focus on SHANK3. *Current Neuropharmacology*, *13*(6), 786–792.

UCL. (1991). SPM2. Retrieved from http://www.fil.ion.ucl.ac.uk/spm/software/spm2/

Uddin, L. Q., Supekar, K., & Menon, V. (2013). Reconceptualizing functional brain connectivity in autism from a developmental perspective. *Frontiers in Human Neuroscience*, *7*(August), 458.

UK Government. Autism Act (2009).

UK Government. Think Autism (2014).

USA Food and Drug Administration. (2002). Estimating the safe starting dose in clinical trials for therapeutics in adult healthy volunteers. *US Food and Drug Administration*.

Uzunova, G., Pallanti, S., & Hollander, E. (2016). Excitatory/inhibitory imbalance in autism spectrum disorders: Implications for interventions and therapeutics. *The World Journal of Biological Psychiatry*, *17*(3), 174–186.

van de Lagemaat, L. N., Nijhof, B., Bosch, D. G. M., Kohansal-Nodehi, M., Keerthikumar, S., & Heimel, J. A. (2014). Age-related decreased inhibitory vs. excitatory gene expression in the adult autistic brain. *Frontiers in Neuroscience*, *8*, 394.

van de Ven, V. G., Formisano, E., Prvulovic, D., Roeder, C. H., & Linden, D. E. J. (2004). Functional connectivity as revealed by spatial independent component analysis of fMRI measurements during rest. *Human Brain Mapping*, *22*(3), 165–178.

Van Gelder, N. M., & Elliott, K. A. (1958). Disposition of gamma-aminobutyric acid administered to mammals. *Journal of Neurochemistry*, *3*(2), 139–143.

Vargas, D. L., Nascimbene, C., Krishnan, C., Zimmerman, A. W., & Pardo, C. A. (2005). Neuroglial activation and neuroinflammation in the brain of patients with autism. *Annals of Neurology*, *57*(1), 67–81.

Varoqueaux, F., Jamain, S., & Brose, N. (2004). Neuroligin 2 is exclusively localized to inhibitory synapses. *European Journal of Cell Biology*, *83*(9), 449–456.

Vaswani, M., Linda, F. K., & Ramesh, S. (2003). Role of selective serotonin reuptake inhibitors in psychiatric disorders: a comprehensive review. *Progress in Neuro-Psychopharmacology and Biological Psychiatry*, *27*(1), 85–102.

Veenstra-Vanderweele, J. (2010). Increase in Valproic Acid Levels During Riluzole Treatment in an Adolescent with Autism. *Journal of Child and Adolescent Psychopharmacology*, *20*(2), 163–165.

Veeraiah, P., Noronha, J. M., Maitra, S., Bagga, P., Khandelwal, N., Chakravarty, S., … Patel, A. B. (2014). Dysfunctional Glutamatergic and γ-Aminobutyric Acidergic Activities in Prefrontal Cortex of Mice in Social Defeat Model of Depression. *Biological Psychiatry*, *76*(3), 231–238.

Velez, Lady, Sokoloff, G., Miczek, K. A., Palmer, A. A., & Dulawa, S. C. (2010). Differences in aggressive behavior and DNA copy number variants between BALB/cJ and BALB/cByJ substrains. *Behavior Genetics*, *40*(2), 201–210.

Verkerk, A. J., Pieretti, M., Sutcliffe, J. S., Fu, Y. H., Kuhl, D. P., Pizzuti, A., … Zhang, F. P. (1991). Identification of a gene (FMR-1) containing a CGG repeat coincident with a breakpoint cluster region exhibiting length variation in fragile X syndrome. *Cell*, *65*, 905–914.

Vernon, A. C., So, P.-W., Lythgoe, D. J., Chege, W., Cooper, J. D., Williams, S. C. R., & Kapur, S. (2015). Longitudinal in vivo maturational changes of metabolites in the prefrontal cortex of rats exposed to polyinosinic–polycytidylic acid in utero. *European Neuropsychopharmacology*, *25*(12), 2210–2220.

Viscidi, E. W., Triche, E. W., Pescosolido, M. F., McLean, R. L., Joseph, R. M., Spence, S. J., & Morrow, E. M. (2013). Clinical Characteristics of Children with Autism Spectrum Disorder and Co-Occurring Epilepsy. *PLoS ONE*, *8*(7), e67797.

Vogeley, K., Kirchner, J. C., Gawronski, A., Van Elst, L. T., & Dziobek, I. (2013). Toward the development of a supported employment program for individuals with high-functioning autism in Germany. *European Archives of Psychiatry and Clinical Neuroscience*, *263*(SUPPL.2).

Wake, H., Moorhouse, A. J., Jinno, S., Kohsaka, S., & Nabekura, J. (2009). Resting Microglia Directly Monitor the Functional State of Synapses In Vivo and Determine the Fate of Ischemic Terminals. *Journal of Neuroscience*, *29*(13), 3974–3980.

Walker, J. M. (1994). The Dansyl Method for Identifying N-Terminal Amino Acids. In *Basic Protein and Peptide Protocols* (pp. 321–328). New Jersey: Humana Press.

Wang, Lin, M.-W., Lin, A.-A., & Wu, S.-N. (2008). Riluzole-induced block of voltage-gated Na+ current and activation of BKCa channels in cultured differentiated human skeletal muscle cells. *Life Sciences*, *82*(1–2), 11–20.

Wang, P., Zhao, D., Lachman, H., & Zheng, D. (2018). Enriched expression of genes associated with autism spectrum disorders in human inhibitory neurons. *Translational Psychiatry*, *8*(13), 1–10.

Washington, S. D., Gordon, E. M., Brar, J., Warburton, S., Sawyer, A. T., Wolfe, A., … VanMeter, J. W. (2014). Dysmaturation of the default mode network in autism. *Human Brain Mapping*, *35*(4), 1284–1296.

Wechsler, D. (1999). Wechsler Abbreviated Scale of Intelligence (WASI). *San Antonio, TX: Psychological Corporation.*

Wei, H., Ding, C., Jin, G., Yin, H., Liu, J., & Hu, F. (2015). Abnormal glutamate release in aged BTBR mouse model of autism. *International Journal of Clinical and Experimental Pathology*, *8*(9), 10689–10697.

Wei, Li, Q., Lam, S., Leung, J., Cheung, C., Zhang, X., … McAlonan, G. M. (2016). A single low dose of valproic acid in late prenatal life alters postnatal behavior and glutamic acid decarboxylase levels in the mouse. *Behavioural Brain Research*, *314*, 190–198.

Weng, S.-J., Wiggins, J. L., Peltier, S. J., Carrasco, M., Risi, S., Lord, C., & Monk, C. S. (2010). Alterations of resting state functional connectivity in the default network in adolescents with autism spectrum disorders. *Brain Research, 1313*, 202–214.

Westerink, B. H. C. (2000). Analysis of biogenic amines in microdialysates of the brain. *Journal of Chromatography B: Biomedical Sciences and Applications*, *747*(1–2), 21–32.

Westerink, B. H. C., Hofsteede, H. M., Damsma, G., & de Vries, J. B. (1988). The significance of extracellular calcium for the release of dopamine, acetylcholine and amino acids in conscious rats, evaluated by brain microdialysis. *Naunyn-Schmiedeberg's Archives of Pharmacology*, *337*(4), 373–378.

Whiteside, S. P., Port, J. D., & Abramowitz, J. S. (2004). A meta–analysis of functional neuroimaging in obsessive–compulsive disorder. *Psychiatry Research: Neuroimaging*, *132*(1), 69–79.

Wijtenburg, S. A., Rowland, L. M., Edden, R. A. E., & Barker, P. B. (2013). Reproducibility of brain spectroscopy at 7T using conventional localization and spectral editing techniques. *Journal of Magnetic Resonance Imaging*, *38*(2), 460–467.

Wink, L. K., Erickson, C. A., Stigler, K. A., & McDougle, C. J. (2011). Riluzole in Autistic Disorder. *Journal of Child and Adolescent Psychopharmacology*, *21*(4), 375–379.

Wu, Y., Satkunendrarajah, K., Teng, Y., Chow, D. S.-L., Buttigieg, J., & Fehlings, M. G. (2013). Delayed Post-Injury Administration of Riluzole Is Neuroprotective in a Preclinical Rodent Model of Cervical Spinal Cord Injury. *Journal of Neurotrauma*, *30*(6), 441–452.

Wydra, K., Golembiowska, K., Zaniewska, M., Kamińska, K., Ferraro, L., Fuxe, K., & Filip, M. (2013). Accumbal and pallidal dopamine, glutamate and GABA overflow during cocaine self-administration and its extinction in rats. *Addiction Biology*, *18*(2), 307–324.

Xing, J., Kimura, H., Wang, C., Ishizuka, K., Kushima, I., Arioka, Y., … Ozaki, N. (2016). Resequencing and Association Analysis of Six PSD-95-Related Genes as Possible Susceptibility Genes for Schizophrenia and Autism Spectrum Disorders. *Scientific Reports*, *6*(1), 27491.

Yamamoto, B. K., & Cooperman, M. A. (1994). Differential Effects of Chronic Antipsychotic Drug Treatment on Extracellular Glutamate and Dopamine Concentrations. *The Journal of Neuroscience*, *14*(7), 4159–4166.

Yan, J., Noltner, K., Feng, J., Li, W., Schroer, R., Skinner, C., … Sommer, S. S. (2008). Neurexin 1α structural variants associated with autism. *Neuroscience Letters*, *438*(3), 368–370.

Yanagi, K., Kaname, T., Wakui, K., Hashimoto, O., Fukushima, Y., & Naritomi, K. (2012). Identification of Four Novel Synonymous Substitutions in the X-Linked Genes *Neuroligin 3* and *Neuroligin 4X* in Japanese Patients with Autistic Spectrum Disorder. *Autism Research and Treatment*, *2012*, 1–5.

Yeargin-Allsopp, M., Rice, C., Karapurkar, T., Doernberg, N., Boyle, C., & Murphy, C. (2003). Prevalence of autism in a US metropolitan area. *JAMA*, *289*(1), 49–55.

Yip, J., Soghomonian, J.-J., & Blatt, G. J. (2007). Decreased GAD67 mRNA levels in cerebellar Purkinje cells in autism: pathophysiological implications. *Acta Neuropathologica*, *113*, 559–568.

Yip, J., Soghomonian, J. J., & Blatt, G. J. (2009). Decreased GAD65 mRNA levels in select subpopulations of neurons in the cerebellar dentate nuclei in autism: An in situ hybridization study. *Autism Research*, *2*(1), 50–59.

Yoshizumi, M., Eisenach, J. C., & Hayashida, K. (2012). Riluzole and gabapentinoids activate glutamate transporters to facilitate glutamate-induced glutamate release from cultured astrocytes. *European Journal of Pharmacology*, *677*(1–3), 87–92.

Yu, & Berry-Kravis. (2014). Autism and Fragile X Syndrome. *Seminars in Neurology*, *34*(03), 258–265.

Yu, J., He, X., Yao, D., Li, Z., Li, H., & Zhao, Z. (2011). A sex-specific association of common variants of neuroligin genes (NLGN3 and NLGN4X) with autism spectrum disorders in a Chinese Han cohort. *Behavioral and Brain Functions*, *7*(1), 13.

Yu, Z., Ono, C., Kim, H. B., Komatsu, H., Tanabe, Y., Sakae, N., … Tomita, H. (2011). Four mood stabilizers commonly induce FEZ1 expression in human astrocytes. *Bipolar Disorders*, *13*(5–6), 486–499.

Zapata, A., Chefer, V. I., & Shippenberg, T. S. (2009). Microdialysis in rodents. In *Current protocols in neuroscience* (pp. 1–34). NIH Public Access.

Zarate, C. A., Payne, J. L., Quiroz, J., Sporn, J., Denicoff, K. K., Luckenbaugh, D., … Manji, H. K. (2004). An Open-Label Trial of Riluzole in Patients With Treatment-Resistant Major Depression. *American Journal of Psychiatry*, *161*(1), 171–174.

Zhang, K., Hill, K., Labak, S., Blatt, G. J., & Soghomonian, J.-J. (2014). Loss of glutamic acid decarboxylase (Gad67) in Gpr88-expressing neurons induces learning and social behavior deficits in mice. *Neuroscience*, *275*, 238–247.

Zhang, Rohlmann, A., Sargsyan, V., Aramuni, G., Hammer, R. E., Südhof, T. C., & Missler, M. (2005). Extracellular Domains of -Neurexins Participate in Regulating Synaptic Transmission by Selectively Affecting N- and P/Q-Type Ca2+ Channels. *Journal of Neuroscience*, *25*(17), 4330–4342.

Zhao, H., Tu, Z., Xu, H., Yan, S., Yan, H., Zheng, Y., … Zhang, Y. Q. (2017). Altered neurogenesis and disrupted expression of synaptic proteins in prefrontal cortex of SHANK3-deficient non-human primate. *Cell Research*, *27*, 1293–1297.

Zona, C., Siniscalchi, A., Mercuri, N. B., & Bernardi, G. (1998). Riluzole interacts with voltage-activated sodium and potassium currents in cultured rat cortical neurons. *Neuroscience*, *85*(3), 931–938.

APPENDICES

APPENDIX 1

Review paper: Chapter 1

Progress in Neuropsychopharmacology & Biological Psychiatry 89 (2019) 236–244

Contents lists available at ScienceDirect

Progress in Neuropsychopharmacology & Biological Psychiatry

journal homepage: www.elsevier.com/locate/pnp

The contribution of [1H] magnetic resonance spectroscopy to the study of excitation-inhibition in autism

Laura A. Ajram[a,b,1], Andreia C. Pereira[a,b,c,1], Alice M.S. Durieux[a,b], Hester E. Velthius[a], Marija M. Petrinovic[a,b,*,2], Grainne M. McAlonan[a,b,*,2]

[a] Department of Forensic and Neurodevelopmental Sciences, Institute of Psychiatry, Psychology and Neuroscience, King's College London, 16 De Crespigny Park, London, SE5 8AF, UK

[b] Sackler Institute for Translational Neurodevelopment, Institute of Psychiatry, Psychology and Neuroscience, King's College London, 16 De Crespigny Park, London, SE5 8AF, UK

[c] CIBIT - Coimbra Institute for Biomedical Imaging and Translational Research, Faculty of Medicine, ICNAS - Institute of Nuclear Sciences Applied to Health, University of Coimbra, Polo 3, 3000-548 Coimbra, Portugal

ARTICLE INFO

Keywords:
Autism
Excitation-inhibition
GABA
Glutamate
Magnetic resonance spectroscopy

ABSTRACT

Autism spectrum disorder (ASD) affects over 1:100 of the population and costs the UK more than £32bn and the USA more than $175bn (£104bn) annually. Its core symptoms are social and communication difficulties, repetitive behaviours and sensory hyper- or hypo-sensitivities. A highly diverse phenotypic presentation likely reflects its etiological heterogeneity and makes finding treatment targets for ASD challenging. In addition, there are no means to identify biologically responsive individuals who may benefit from specific interventions. There is hope however, and in this review we consolidate how findings from magnetic resonance spectroscopy (MRS) add to the evidence that differences in the brain's excitatory glutamate and inhibitory γ-aminobutyric acid (GABA) balance may be both a key biomarker and a tractable treatment target in ASD.

1. Introduction

Autism spectrum disorder (ASD) is a highly heterogeneous lifelong neurodevelopmental syndrome characterised by deficits in social reciprocity and communication, and by restricted interests and stereotyped behaviours (DSM-5; American Psychiatric Association, 2013). Its prevalence is growing (Lai et al., 2014) and, in the UK alone, adults with ASD cost the economy over £32 billion/year, i.e. more than heart disease, cancer and stroke combined (Buescher et al., 2014). Therefore, there is a pressing need to identify the underlying biological mechanisms that would provide a basis for the development of ASD stratification markers and treatment options. Progress is happening however, based on accumulating evidence that multiple genetic and environmental risk factors for ASD converge to disrupt the balance between glutamate-mediated excitatory and γ-aminobutyric acid (GABA)-mediated inhibitory neurotransmission; and this may inform treatment targets for the disorder (Nelson and Valakh, 2015; Rubenstein and Merzenich, 2003).

2. Evidence for excitation-inhibition imbalance in autism spectrum disorder

A balanced interaction between glutamate and GABA is essential for synaptic maturation, refinement of neuronal circuitry and subsequently the regulation of cognition, emotion and behaviour (Lujan et al., 2005). An imbalance in excitation-inhibition (E-I) caused by disruption to any component of the glutamate and GABA signalling systems could therefore have potentially far-reaching consequences. Indeed, based on observations such as an increased incidence of epilepsy – a disorder of E-I balance – in individuals with ASD (Bolton et al., 2011; Muhle et al., 2004), and post-mortem evidence of altered expression of proteins involved in glutamate and GABA biosynthesis and neurotransmission in the brains of individuals with ASD (Blatt and Fatemi, 2011; Fatemi et al., 2002, 2009, 2014; Oblak et al., 2009, 2010, 2011; Purcell et al., 2001; Shimmura et al., 2013; Yip et al., 2007), E-I imbalance has been suggested to be a 'common final pathway' in ASD (Nelson and Valakh, 2015; Rubenstein and Merzenich, 2003).

* Corresponding authors at: Department of Forensic and Neurodevelopmental Sciences, The Sackler Institute for Translational Neurodevelopment, Institute of Psychiatry, Psychology and Neuroscience, King's College London, 16 De Crespigny Park, London, SE8 5AF, UK.
E-mail addresses: marija-magdalena.petrinovic@kcl.ac.uk (M.M. Petrinovic), grainne.mcalonan@kcl.ac.uk (G.M. McAlonan).
[1] Shared first authorship. These authors contributed equally to this work.
[2] Shared last authorship. These authors contributed equally to this work.

https://doi.org/10.1016/j.pnpbp.2018.09.010
Received 16 May 2018; Received in revised form 14 September 2018; Accepted 20 September 2018
Available online 21 September 2018

Genetic studies are in line with this proposal. For example, studies of ASD susceptibility genes have repeatedly identified chromosome 15q11-13 as a particular region of interest as 1–3% of all ASD cases were reported to be associated with duplications in this region (Moreno-De-Luca et al., 2013; Urraca et al., 2013). This chromosomal region contains genes for three $GABA_A$ receptor subtype genes (i.e. β3, γ3 and α5). Mutations in this region, especially in the β3 subunit, convey a high risk for ASD and have been linked to repetitive symptoms and insistence on sameness (Chaste et al., 2014; Isles et al., 2016; Shao et al., 2003). Direct evidence for the link between $GABA_A$-β3 and ASD has also been generated from a β3 knock-out mouse. These mice have behaviours analogous to the condition; they also have seizures, which are a frequent comorbid complication of ASD caused by E-I imbalance (DeLorey et al., 1998). In addition, we and others have reported that environmental risk factors for ASD, such as prenatal exposure to maternal inflammation or the anti-epilepsy medication valproate, disrupt gene and protein expression across GABA pathways and trigger behavioural features which mimic the human condition (Fatemi et al., 2008; Fukuchi et al., 2009; Giovanoli et al., 2014; Meyer et al., 2011; Wei et al., 2016).

There is also good evidence for genetic abnormalities in glutamatergic signalling pathways in ASD and related conditions. This has, in part, been built on the advances made in fragile X syndrome, the most common genetic form of ASD, which is caused by a single gene mutation affecting fragile X mental retardation protein (FMRP) (Verkerk et al., 1991). FMRP negatively regulates postsynaptic glutamate receptor synthesis (including metabotropic glutamate receptor 5; mGluR5) by binding to ribosomes and stalling translation of target mRNAs (Darnell et al., 2011). mRNA translation at the synapse is then increased (Bear et al., 2004), leading to excess excitatory activity, enhanced long term depression, and ASD-like pathology in animal models (Lozano et al., 2014; Yu and Berry-Kravis, 2014). Lower levels of FMRP are found in individuals with idiopathic ASD (i.e. ASD without a known cause) who have a concomitant increase in mGluR5 (Fatemi et al., 2011; Fatemi and Folsom, 2011). In addition to alterations to metabotropic receptors in ASD, genetic aberrations have also been linked to ionotropic glutamate receptors, namely N-methyl-D-aspartate (NMDA) receptors. However, the picture is complex, and both increases and decreases in NMDA receptor function have been associated with the ASD phenotype (Gandal et al., 2012).

GABA and glutamate signalling in ASD may also be indirectly derailed by mutations in genes coding for proteins that stabilise GABAergic and glutamatergic synapses. For example, alterations of neurexin and neuroligin cell adhesion molecules (Ching et al., 2010; Jamain et al., 2003), postsynaptic density protein 95 (PSD-95) and/or Shank scaffold proteins (Uchino and Waga, 2015; Xing et al., 2016) confer a high risk for ASD. These molecules anchor pre- and post-synaptic neuron terminals and disruptions of the molecular assembly of the synapse can potentially cause E-I imbalance (Futai et al., 2007; Südhof, 2008). Consistent with this, neurexin 1-α (*Nrxn1-α*) knock-out mice show a reduction in spontaneous and evoked neurotransmitter release (Kattenstroth et al., 2004; Missler et al., 2003; Zhang, 2005) accompanied by behavioural abnormalities that resemble some of the core ASD symptoms of social impairment and inflexibility/stereotypy (Grayton et al., 2013). Similarly, mice with mutations in the neuroligin 3 gene (*Nlgn3*) exhibit brain-region specific synaptic dysfunction (e.g. a shift of synaptic transmission towards inhibition in the somatosensory cortex and towards excitation in the hippocampus) and impairments in social behaviour that mimic ASD (Burrows et al., 2015; Etherton et al., 2011a, 2011b; Jaramillo et al., 2014; Radyushkin et al., 2009; Tabuchi et al., 2007). Such "multiple" E-I anomalies, that can be not only brain region- but even neural circuit-specific, as shown in multiple animal models of ASD (Horder et al., 2018; Lee et al., 2017; Nelson and Valakh, 2015) further exemplify the complexities of defining and measuring the E-I (im)balance in ASD.

Finally, the metabolism of glutamate and GABA is tightly interlinked so an alteration in either metabolite may potentially affect the other. The enzyme glutaminase catalyses the glutamate to glutamine cycle, allowing glutamine to be stored in astrocytes or converted to glutamate in both glutamatergic and GABAergic neurons (Rowley et al., 2012). In excitatory neurons, glutamate is transported into vesicles via vesicular glutamate transporters, whereas in inhibitory neurons, glutamate is first converted to GABA by the glutamic acid decarboxylase and then transported to vesicles via vesicular GABA transporters. Upon release, the neurotransmitters are taken up by high affinity membrane transporters and returned into neurons and surrounding glia, where they are recycled. Thus, GABA, glutamate and glutamine are in constant flux. In ASD however, the levels of the multiple enzymes controlling glutamine-glutamate-GABA cycles are altered (Fatemi et al., 2002; Shimmura et al., 2013; Yip et al., 2007), and so glutamine-glutamate-GABA metabolism is likely to be atypical in the ASD brain.

How these diverse E-I anomalies might act mechanistically has been the subject of a number of recent comprehensive reviews (Foss-Feig et al., 2017; Gao and Penzes, 2015; Gatto and Broadie, 2010; Lee et al., 2017; Mullins et al., 2016; Nelson and Valakh, 2015; Uzunova et al., 2016). For example, Yizhar et al. (2011) have shown that increase of a cellular E-I balance in the mouse medial prefrontal cortex (mPFC) elicits elevated rhythmic high-frequency (gamma) activity (a disease correlate in clinical conditions; Orekhova et al., 2007) and social dysfunction. Furthermore, it was recently shown that reducing the E-I ratio by either reducing the excitability of pyramidal neurons or by increasing the excitability of inhibitory parvalbumin-positive neurons in the mPFC rescued social deficits in mice lacking the *CNTNAP2* gene, which has been implicated in ASD (Selimbeyoglu et al., 2017). Maintenance of E-I balance is thus essential to network function as not only functional, but also structural properties of neural circuits are defined by inter-neuronal communication.

3. [1H] Magnetic resonance spectroscopy evidence for E-I imbalance in ASD

The hypothesis that the glutamine-glutamate-GABA system is altered in ASD has also been addressed by using [1H] magnetic resonance spectroscopy (MRS) as a non-invasive method to measure tissue levels of E-I metabolites in the living human brain (Ford and Crewther, 2016; Schur et al., 2016). In brief, [1H]MRS uses the nuclear magnetic resonance properties of hydrogen atoms to generate a frequency spectrum (as opposed to the image in MR imaging) (Govindaraju et al., 2000; Juchem and Rothman, 2014; Stagg et al., 2011) in which different metabolites are identified by the position of their signal peak, i.e. chemical shift, along the frequency axis (in units of 'parts per million'; ppm). [1H]MRS metabolite levels can then be quantified by calculating the area under the corresponding peaks or by fitting the in vivo spectra to a basis set, i.e. linear combinations of measured or simulated model spectra of metabolites (Edden et al., 2014; Naressi et al., 2001; Provencher, 1993). [1H]MRS is not without limitations however. For an adequate signal-to-noise ratio, standard single voxel [1H]MRS data is acquired from a predefined and relatively large brain volume-unit (usually around 4–8 cm^3) (Stagg et al., 2011; Zhu and Barker, 2011) compared with conventional MR image resolution (typically around 1–10 mm^3) (Blüml, 2013). Therefore, both grey and white matter is usually sampled within the same voxel. To avoid errors when quantifying metabolites, these so-called 'partial volume' effects need to be corrected by segmenting spectroscopic voxel according to different tissue contents (Dager et al., 2008; Quadrelli et al., 2016). As shown in Table 1, most of the studies reported using tissue segmentation, however, exact approaches varied considerably between studies which might contribute to inconsistencies in the literature. Such partial volume effects are minimised in [1H]MRS imaging (MRSI), a less frequently used extension of [1H]MRS that allows data from multiple adjacent small (1 cm^3 and below) voxels to be acquired simultaneously (Blüml, 2013; Oz et al., 2014; Schneider, 2016; Zhu and Barker, 2011).

Table 1
Summary of [1H]MRS studies reporting Glx, Glu and/or GABA+ levels in ASD.

Citation	ASD group N	Age (years)	[1H] MRS sequence (TR/TE/Av)	Quantification method (tissue segmentation)	Brain areas investigated (cm^3)	Metabolite concentrations in ASD participants compared with controls		
						Glx	Glu	GABA+
Paediatric studies		Range						
Friedman et al. (2006)	45	3–4	1.5 T MRSI PEPSI (2000/20,272/na)	Estimated concentration (Y)	Grey matter (na) White matter (na)	NSD NSD	na	na
DeVito et al. (2007)	26	6–17	3 T MRSI (1800/135/na)	Estimated concentration (Y)	Grey matter (na) White matter (na) Cerebellum (na)	Lower in ASD NSD Lower in ASD	na	na
Hardan et al. (2008)	18	8–15	1.5 T MRSI STEAM (1600/20/4)	Estimated concentration (Y)	(L/R) Thalamus (5.8)	NSD	na	na
Harada et al. (2011)	12	2–11	3 T STEAM (5000/15/48) 3 T MEGA-PRESS (2500/68/256)	Estimated concentration (Y)	(L) Frontal lobe (27) Lenticular nuclei (27)	na	NSD NSD	Lower in ASD NSD
Bejjani et al. (2012)	8 26	7–15 6–17	1.5 T PRESS (1500/25/256) 1.5 T MRSI PRESS (1500/30/8)	Estimated concentration (Y)	(L/R) Anterior cingulate cortex (2.4–3.6) (L/R) Anterior cingulate cortex (1.1)	Higher in ASD Higher in ASD (R)	na	na
Kubas et al. (2012)	12	8–15	1.5 T PRESS (1500/35/192)	Creatine ratios (na)	(L/R) Frontal lobe (na)	Lower in ASD	na	Lower in ASD
Corrigan et al. (2013)	45	3–4	1.5 MRSI	Estimated concentration (Y)	Grey matter (na) White matter (na)	NSD Lower in ASD	na	na
	31	6–7	PEPSI (2000/20/na)		Grey matter (na) White matter (na)	NSD NSD		
	29	9–10			Grey matter (na) White matter (na)	NSD NSD		
Hassan et al. (2013)	10	6–14	1.5 T PRESS (1500/30/3)	Estimated concentration (na)	Anterior cingulate cortex (8) (L) Striatum (8) (L) Cerebellum (8) (L) Frontal lobe (8)	na	Higher in ASD Higher in ASD Higher in ASD Higher in ASD	na
Joshi et al. (2013)	7	12–17	4 T 2D-JPRESS (2000/30–250/16,32)	Estimated concentration (Y)	Anterior cingulate cortex (8) (L/R) Medial temporal lobe (3.38)	na	Higher in ASD NSD	na
Doyle-Thomas et al. (2014)	20	7–18	3 T MRSI (2000/30/na)	Creatine ratios (na)	(L/R) Caudate (na) (L/R) Putamen (na) (L/R) Thalamus (na)	NSD Higher in ASD NSD	na	na
Gaetz et al. (2014)	17	11	3 T MEGA-PRESS (1500/68/256)	Creatine ratios (Y)	(L) Motor cortex (27) (L) Auditory cortex (24) Visual cortex (27)	na	na	Lower in ASD Lower in ASD NSD
Rojas et al. (2014)	17	14	3 T MEGA-PRESS (2500/70/512)	Creatine ratios (Y)	(L) Auditory cortex (36)	na	na	Lower in ASD
Brix et al. (2015)	14	10	3 T PRESS (1500/35/128) 3 T MEGA-PRESS (1500/68/256)	Estimated concentration Creatine ratios (Y)	(L) Anterior cingulate cortex (27)	NSD	na	NSD
Cochran et al. (2015)	13	13–17	3 T PRESS (2000/28/128) 3 T MEGA-PRESS (2000/68/320)	Estimated concentration Total creatine ratios (Y)	Anterior cingulate cortex (8 for PRESS, 18 for MEGA-PRESS)	na	NSD	NSD
Drenthen et al. (2016)	15	14–18	3 T PRESS (2000/35/128) 3 T MEGA-PRESS (2000/68/320)	Creatine ratios (Y)	Occipital cortex (27)	na	NSD	NSD
Naaijen et al. (2016)	51	8–13	3 T PRESS (3000/30/96)	Estimated concentration (Y)	Anterior cingulate cortex (8) (L) Dorsal striatum (8)	na	Higher in ASD NSD	na
Goji et al. (2017)	34	2–12	3 T STEAM (5000/15/48)	Estimated concentration (na)	Anterior cingulate cortex (6 for STEAM, 27 for PRESS)	NSD	na	NSD
	23	4–9	3 T PRESS (2500/68/256)		(L) Cerebellum (6 for STEAM, 27 for PRESS)	NSD		NSD
Hegarty et al. (2017)	47 twin pairs	10	3 T MRSI PRESS (2300/35/na)	Total creatine ratios (Y)	(L/R) Thalamus (4.5)	Lower in ASD (L)	na	na

(*continued on next page*)

Table 1 (*continued*)

Citation	ASD group N	Age (years)	[1H] MRS sequence (TR/TE/Av)	Quantification method (tissue segmentation)	Brain areas investigated (cm^3)	Metabolite concentrations in ASD participants compared with controls		
						Glx	Glu	GABA+
Ito et al. (2017)	112	4–14	3 T STEAM (5000/15/48)	Creatine ratios (na)	Anterior cingulate cortex (6 for STEAM, 27 for MEGA-PRESS)	NSD	NSD	Lower in ASD
	114	3–14	3 T MEGA-PRESS (2500/68/256)		(L) Cerebellum (6 for STEAM, 27 for MEGA-PRESS)	NSD	Higher in ASD	Lower in ASD
Port et al. (2017)	16	6–14	3 T MEGA-PRESS (1500/68/256)	Creatine ratios (Y)	(L) Auditory cortex (24)	na	na	Lower in ASD
Puts et al. (2017)	35	8–12	3 T MEGA-PRESS (2000/68/320)	Estimated concentration (Y)	(R) Sensorimotor cortex (27) Occipital cortex (27)	na	na	Lower in ASD NSD
Cavalho Pereira et al. (2018)	27	9–18	3 T MEGA-PRESS (1500/68/392)	Estimated concentration Total creatine ratios (Y)	Medial prefrontal cortex (27)	NSD	na	NSD
Adult studies		Mean (SD)						
Page et al. (2006)	25	35 (11)	1.5 T PRESS (3000/35/160)	Estimated concentration Total creatine ratios (Y)	(R) Amygdala – hippocampal complex (6) (R) Parietal lobe (8)	Higher in ASD NSD	na	na
Bernardi et al. (2011)	14	29 (6)	3 T MRSI PRESS (2000/30/na)	Estimated concentration (na)	(L/R) Anterior cingulate cortex (0.56) (L/R) Thalamus (0.56) (L/R) Temporo-parietal junction (0.56) (L/R) Intraparietal sulcus (0.56)	Lower in ASD (R) NSD NSD NSD	na	na
Aoki et al. (2012)	24	29 (6)	3 T STEAM (3000/15/128)	Estimated concentration (Y)	Medial prefrontal cortex (8)	NSD	na	na
Brown et al. (2013)	13	36 (6)	3 T PRESS (2000/30/192)	Estimated concentration (na)	(L/R) Auditory cortex (7.5)	Higher in ASD	Higher in ASD	na
Horder et al. (2013)	28	28 (6)	1.5 T PRESS (3000/30/na)	Estimated concentration (Y)	(L) Basal ganglia (6) (L) Dorsolateral prefrontal cortex (7.68) (L) Medial parietal lobe (8)	Lower in ASD NSD NSD	na	na
Tebartz van Elst et al. (2014)	29	35 (9)	3 T PRESS (3000/30/na)	Estimated concentration (Y)	Anterior cingulate cortex (8) (L) Cerebellum (8)	Lower in ASD NSD	Lower in ASD NSD	na
Libero et al. (2015)	19	27 (1)	3 T PRESS (2000/80/128)	Creatine ratios (Y)	Anterior cingulate cortex (5.4) Posterior cingulate cortex (10.8)	NSD NSD	na	na
Robertson et al. (2015)	20	29 (9)	3 T MEGA-PRESS (1500/68/320)	Estimated concentration (Y)	Visual cortex (18.75) (L) Motor cortex (18.75)	NSD NSD	na	NSD NSD
Libero et al. (2016)	20	26 (1)	3 T PRESS (2000/80/128)	Estimated concentration Total creatine ratios (Y)	Anterior cingulate cortex (5.4) Posterior cingulate cortex (10.8)	NSD NSD	na	na
Ajram et al. (2017)	17	33 (2)	3 T MEGA-PRESS (2000/68/na)	Estimated concentration (Y)	Dorsomedial prefrontal cortex (30)	NSD	na	NSD
Endres et al. (2017)	24	40 (10)	3 T PRESS (1500/30/256)	Estimated concentration (Y)	Anterior cingulate cortex (15) (L) Dorsal prefrontal cortex (15.63)	NSD NSD	na	na
Port et al. (2017)	15	21 (1)	3 T MEGA-PRESS (1500/68/256)	Creatine ratios (Y)	(L) Auditory cortex (24)	na	na	NSD
Horder et al. (2018)	25	30(1)	3 T MEGA-PRESS (2000/68/368)	Estimated concentration (Y)	(L) Striatum (26.25) Medial prefrontal cortex (30)	Lower in ASD NSD	Lower in ASD NSD	NSD NSD
Kirovski et al. (2018)	12	28(6)	3 T MEGAPRESS (1500/68/240)	Estimated concentration (Y)	(R) Dorsolateral prefrontal cortex (8) (R) Superior temporal sulcus (8)	na	na	NSD

Estimated concentration refers to water- or external reference-scaled metabolites.

ASD, autism spectrum disorder; Av, number of averages; GABA+, γ-aminobutyric acid + macromolecules; Glx, glutamate + glutamine; Glu, glutamate; L, left; MRS, magnetic resonance spectroscopy; MRSI, magnetic resonance spectroscopy imaging; MEGA-PRESS, Meshcher-Garwood point-resolved spectroscopy; na, not applicable; NSD, not statistically different; PEPSI, proton echo planar spectroscopy imaging; PRESS, point-resolved spectroscopy; R, right; ROI, region of interest; STEAM, stimulated echo acquisition mode; TR, repetition time (ms); TE, echo time (ms); Y, reported.

However, MRSI is often associated with reduced spectral resolution, non-uniform water suppression and voxel bleeding artefact (i.e. signal contamination from neighbouring voxels into the voxel-of-interest), therefore single voxel [1H]MRS remains the technique of choice (Astrakas and Argyropoulou, 2016; Blüml, 2013; Duarte et al., 2012; Jansen et al., 2006).

This large volume also means that [1H]MRS samples tissue metabolites within both neurons and glia and in both intra-and extra-cellular space (Dager et al., 2008). Therefore, to account for possible variation in voxel tissue composition, some studies report metabolite concentrations as ratios to total creatine (creatine + phosphocreatine; tCr), which is assumed to be present at constant concentration in brain tissue and cerebrospinal fluid (Gussew et al., 2012). However, as an alternative to tCr ratios, water has been used as a reference because tCr itself can be altered in neurodevelopmental conditions (Alger, 2010). Finally, depending on technical factors, such as the magnetic field strength, it is not always possible to differentiate between glutamate and glutamine due to the overlap of their resonant peaks, and the combined signal termed Glx is commonly reported (Table 1), and thus is only a proxy measure of glutamate. Similarly, the GABA signal usually also has a contribution from 'macromolecules', and is denoted as GABA + (Edden et al., 2012; Henry et al., 2001; Mikkelsen et al., 2017; Near et al., 2011).

Despite these limitations, [1H]MRS is safe and therefore, in contrast to other in vivo imaging modalities such as positron emission tomography, it can be used repeatedly, and also in children. Indeed, many [1H]MRS studies of E-I metabolites in ASD have been conducted in paediatric populations. The initial studies focused on the glutamatergic system, reporting Glx and glutamate (Glu), with reduced levels found in the cortical grey matter, frontal lobes, thalamus and cerebellum in children with ASD (DeVito et al., 2007; Hegarty et al., 2017; Kubas et al., 2012) (Table 1). However, this was not replicated by others, with either no difference in Glx/Glu observed between ASD and control participants in cortical and subcortical areas (Brix et al., 2015; Cavalho Pereira et al., 2018; Cochran et al., 2015; Doyle-Thomas et al., 2014; Drenthen et al., 2016; Friedman et al., 2006; Goji et al., 2017; Harada et al., 2011; Hardan et al., 2008; Ito et al., 2017; Joshi et al., 2013; Naaijen et al., 2016) or higher levels reported in ASD – in the anterior cingulate cortex, frontal lobes, striatum (Bejjani et al., 2012; Doyle-Thomas et al., 2014; Joshi et al., 2013; Hassan et al., 2013; Naaijen et al., 2016) and cerebellum (Hassan et al., 2013; Ito et al., 2017) (Table 1).

By definition, ASD is a neurodevelopmental condition and how the brain matures is acknowledged to be quite different to even age matched controls (Amaral et al., 2008; Aoki et al., 2012; Redcay and Courchesne, 2005). Thus, results of [1H]MRS studies in ASD – as other MR modalities – may vary depending on the age group sampled. For example, Corrigan et al. (2013) have reported lower Glx in the cerebral white matter of 3–4-year-old children; however, there was no change in Glx when the same children were scanned again at age 6–7 and 9–10 years; and no difference in grey matter Glx at any age in childhood (Table 1). However, even in adulthood, when the brain may be expected to have fully matured, [1H]MRS studies of glutamate have generated conflicting findings. Lower Glx/Glu has been reported in the anterior cingulate cortex in ASD adults (Bernardi et al., 2011; Tebartz van Elst et al., 2014) (Table 1), but others have observed no significant difference in Glx between ASD adults and controls in this cortical region (Endres et al., 2017; Libero et al., 2015, 2016) (Table 1). Horder et al. (2013, 2018) reported lower Glx/Glu in the basal ganglia of adults with ASD, but unchanged cortical levels (Table 1).

In addition to differences in study samples and brain regions examined, different [1H]MRS sequences for quantification of Glx and/or Glu have been employed in the studies reviewed here (Table 1). While conventional [1H]MRS sequences (e.g. STEAM, PRESS) were used by most, unedited (equivalent to a PRESS) (Horder et al., 2018; Robertson et al., 2015) as well as the difference MEGA-PRESS spectra (edit ON-edit OFF subtraction; please see below) (Ajram et al., 2017; Cavalho Pereira et al., 2018) were also used to quantify Glx and/or Glu (Table 1).

In order to sample GABA, customised spectral editing sequences, such as Meshcher-Garwood Point-resolved spectroscopy (MEGA-PRESS) carried out at 3 T or higher field strengths are required (Mescher et al., 1998; Mullins et al., 2014). In MEGA-PRESS, a GABA signal can be resolved from the more prominent Cr + PCr signal at 3 ppm by applying an editing pulse (edit ON) to the GABA signal at 1.9 ppm interleaved with edit OFF pulse (no frequency-selective editing pulses applied, or if applied, at a different frequency) (Cleve et al., 2015; Long et al., 2015; Maddock et al., 2016; Mescher et al., 1998; Mullins et al., 2014; Shungu et al., 2016). The application of this editing pulse results in the co-editing of other molecules present in the final spectrum, namely the Glx at 3.75 ppm and 'macromolecules' at 3 ppm (Cleve et al., 2015; O'Gorman et al., 2011). Thus, the GABA signal at 3 ppm is commonly reported as GABA + (Table 1). Furthermore, due to low tissue concentration of GABA, MEGA-PRESS requires larger ROI volumes (typically around 27 cm^3) and longer acquisition times ideally between 7 and 10 min (Mikkelsen et al., 2018). This was generally applied in all but two reviewed study (Kirovski et al., 2018; Kubas et al., 2012) (Table 1). In ASD, most studies of [1H]MRS GABA + have been conducted only in the last four years (Table 1). The majority have recruited children (Brix et al., 2015; Cavalho Pereira et al., 2018; Cochran et al., 2015; Drenthen et al., 2016; Gaetz et al., 2014; Goji et al., 2017; Harada et al., 2011; Ito et al., 2017; Kubas et al., 2012; Puts et al., 2017; Rojas et al., 2014), with three studies involving only adults (Ajram et al., 2017; Horder et al., 2018; Kirovski et al., 2018; Robertson et al., 2015), and one combining children and adults (Port et al., 2017). The pattern of GABA + differences in ASD compared to typically developing controls is a little more consistent than for Glx and Glu, with either lower measures or no difference in regional GABA + reported. Thus, lower GABA + has been found in the motor, auditory and frontal cortices and in the sensorimotor regions, anterior cingulate cortex and cerebellum (Gaetz et al., 2014; Harada et al., 2011; Ito et al., 2017; Kubas et al., 2012; Port et al., 2017; Puts et al., 2017; Rojas et al., 2014), whereas others have observed no differences in GABA + in the prefrontal and occipital cortices (Ajram et al., 2017; Brix et al., 2015; Cavalho Pereira et al., 2018; Cochran et al., 2015; Drenthen et al., 2016; Gaetz et al., 2014; Goji et al., 2017; Horder et al., 2018; Puts et al., 2017; Robertson et al., 2015), lenticular nuclei (Harada et al., 2011), motor cortex (Robertson et al., 2015), superior temporal sulcus (Kirovski et al., 2018), basal ganglia (Horder et al., 2018) and cerebellum (Goji et al., 2017) (Table 1).

Reduction in GABA in the somatosensory cortex has been associated with altered tactile function in children with ASD (Puts et al., 2017). Interestingly, developmental tactile perception abnormalities due to a loss of presynaptic inhibition of somatosensory neuron transmission have been shown to result in ASD-related social interaction deficits in mice (Orefice et al., 2016). However, even in the absence of group differences in GABA +, a role for GABA in ASD has still been argued based on findings that [1H]MRS GABA + levels in ASD are inversely correlated with scores on the Autism Spectrum Screening Questionnaire (Brix et al., 2015) and with the communication and delayed development scores of the Autism Diagnostic Interview – Revised (Cavalho Pereira et al., 2018). More difficult to disentangle are the results from Robertson et al. (2015). In their study, occipital GABA + measures were equivalent in ASD and control groups, but the ASD group had a deficit in the performance of a binocular rivalry test of visual function thought to rely upon visual cortical E-I balance. The authors went on to show that a positive correlation between GABA + and performance on a binocular rivalry task in control group was not evident in the ASD group, and suggested that the results supported an impairment in 'inhibitory signalling' in ASD (Robertson et al., 2015). This may well be the case, but because [1H]MRS captures the metabolites within a composite of cell types and does not capture active neurotransmission, it is

impossible to say with certainty.

4. E-I flux in ASD

One perspective on this constellation of [1H]MRS findings in ASD, is that their range may mirror the etiological and phenotypical heterogeneity of the spectrum as well as the variety in the typically developing control groups used for comparison. For example, [1H]MRS measures of glutamate and GABA+ differ even within the typically developing population (Bogner et al., 2010; Brix et al., 2017; Kaiser et al., 2005; O'Gorman et al., 2011; Sailasuta et al., 2008).

Another consideration for the field is that, in the main, indices of glutamate and GABA have been assessed separately in ASD; yet the results have been interpreted in terms of E-I balance (Dickinson et al., 2016). It could be argued that a true imbalance can only be uncovered if the level of each metabolite is reported. Thus, if a GABA decrease is accompanied by a glutamate decrease, then the system may remain balanced. Moreover, until recently, the logic of trying to capture metabolites within a glutamine-glutamate-GABA cycle that is constantly changing or in 'flux' in cohorts with and without ASD, has not been questioned. We now suggest that replication difficulties in cross-sectional studies of glutamate and GABA pathways in ASD arise, at least in part, because they sample only one part of an E-I system, which is a 'moving target'. As described earlier, the regulatory enzymes controlling this dynamic system are altered in ASD, and so E-I flux in ASD is therefore very likely to be atypical.

Supporting this hypothesis, there is now evidence that [1H]MRS is sensitive to changes in E-I flux elicited by pharmacological probes that challenge the system. This comes initially from studies in rats, which have established that [1H]MRS can reliably capture changes in glutamate and GABA levels following pharmacological interventions (Waschkies et al., 2014). Specifically, [1H]MRS was used to track the E-I response to pharmacologically relevant doses of compounds with a known mechanism of action on GABAergic and glutamatergic neurotransmission, namely vigabatrin, 3-mercaptopropionate, tiagabine, methionine sulfoximine, and riluzole. Clear drug dose-[1H]MRS effect relationships were demonstrated, with changes as low as 6% in glutamate and 12% in GABA reliably measured using [1H]MRS. The authors concluded that quantitative [1H]MRS of glutamate and GABA may usefully reveal E-I 'target engagement' – in other words, the interaction of a drug with its biological goal (Waschkies et al., 2014). We have recently extended this approach to humans. Using [1H]MRS, we found that the anti-glutamate and pro-GABA drug riluzole increased the proportion of GABA+ relative to the total level of GABA+ and Glx metabolites in the prefrontal cortex in ASD, but decreased it in controls, despite a comparable baseline between groups (Ajram et al., 2017).

This difference in E-I 'responsivity' in ASD has important implications for the development of pharmacological treatments for ASD, as it suggests that drugs may not act in the ASD brain the same way as in the typically developing brain. That is, selecting a compound for a trial/treatment in ASD based on its mechanism of action in the typical brain may not always be appropriate. Moreover, the response to pharmacological treatments in ASD may itself be heterogeneous. This may, for instance, explain why some – but not all – individuals with ASD can have paradoxical responses to $GABA_A$/benzodiazepine receptor agonists; usually these medications have a sedative effect, but 'excitation' has at times been reported in individuals with ASD (Lemonnier et al., 2012; Marrosu et al., 1987). It may also explain some of the trial disappointments in ASD. For example, lamotrigine, an anticonvulsant, was proposed to be a potential treatment for ASD because it inhibits synaptic glutamate release in excitatory neurons. Unfortunately, it did not improve clinical outcomes in children with ASD (Belsito et al., 2001). A similar failure followed the use of D-cycloserine, a partial agonist at the NMDA glutamate receptor (Belsito et al., 2001; Minshawi et al., 2016; Posey et al., 2004).

5. Conclusions

We conclude that disruption within E-I systems could serve as a biomarker for ASD. However, we extend this observation to suggest that E-I systems in the ASD brain are pharmacologically atypical. However, the picture is far from straight-forward. This means that we need better strategies, potentially including [1H]MRS, to examine the biological response or target engagement to proposed treatments in sub-groups of individuals with ASD. The identification of more pharmacologically homogeneous sub-groups within the spectrum may inform a new generation of biologically-driven clinical trials and avoid the time and expense (and failure) of un-stratified large-scale studies.

Author contributions

L.A.A., M.M.P., and G.M.M. designed the study. L.A.A., A.M.S.D., A.C.P., H.E.V., M.M.P., and G.M.M. wrote the manuscript. All authors contributed to and approved the final manuscript.

Role of the funding source

L.A.A was supported by the Autism Speaks (grant no. 8132) and by an MRC CASE Postgraduate Studentship Award (MR/K01725X/1). Assistance was also provided by The Sackler Centre for Translational Neurodevelopment at King's College London; and EU-AIMS (European Autism Interventions), which receives support from the Innovative Medicines Initiative Joint Undertaking under grant agreement no. 115300, the resources of which are composed of financial contributions from the European Union's Seventh Framework Programme (grant FP7/2007-2013). Additional funding was provided by Autistica UK (A.C.P.), MRC Centre for Neurodevelopmental Disorders (MRC-CNDD; MR/N026063/1) and The National Institute for Health Research (NIHR) Biomedical Research Centre for Mental Health at South London and Maudsley NHS Foundation Trust and Institute of Psychiatry, Psychology and Neuroscience at King's College London. The views expressed are those of the authors and not necessarily those of the NHS, the NIHR or the Department of Health, UK. The funding sources had no involvement in the decision to submit this article for publication, nor in its design.

Declarations of interest

None.

References

Ajram, L.A., Horder, J., Mendez, M.A., Galanopoulos, A., Brennan, L.P., Wichers, R.H., et al., 2017. Shifting brain inhibitory balance and connectivity of the prefrontal cortex of adults with autism spectrum disorder. Transl. Psychiatry 7, e1137.

Alger, J.R., 2010. Quantitative proton magnetic resonance spectroscopy and spectroscopic imaging of the brain: a didactic review. Top. Magn. Reson. Imaging 21, 115–128.

Amaral, D.G., Schumann, C.M., Nordahl, C.W., 2008. Neuroanatomy of autism. Trends Neurosci. 31, 137–145.

American Psychiatric Association, 2013. Diagnostic and Statistical Manual of Mental Disorders, 5th ed. American Psychiatric Press, Arlington.

Aoki, Y., Abe, O., Yahata, N., Kuwabara, H., Natsubori, T., Iwashiro, N., et al., 2012. Absence of age-related prefrontal NAA change in adults with autism spectrum disorders. Transl. Psychiatry 2, e178.

Astrakas, L.G., Argyropoulou, M.I., 2016. Key concepts in MR spectroscopy and practical approaches to gaining biochemical information in children. Pediatr. Radiol. 46, 941–951.

Bear, M.F., Huber, K.M., Warren, S.T., 2004. The mGluR theory of fragile X mental retardation. Trends Neurosci. 27, 370–377.

Bejjani, A., O'Neill, J., Kim, J.A., Frew, J.F., Jee, V.W., Ly, R., et al., 2012. Elevated glutamatergic compounds in pregenual anterior cingulate in pediatric autism spectrum disorder demonstrated by1H MRS and 1H MRSI. PLoS One 7, e38786.

Belsito, K.M., Law, P.A., Kirk, K.S., Landa, R.J., Zimmerman, A.W., 2001. Lamotrigine therapy for autistic disorder: a randomized, double-blind, placebo-controlled trial. J. Autism Dev. Disord. 31, 175–181.

Bernardi, S., Anagnostou, E., Shen, J., Kolevzon, A., Buxbaum, J.D., Hollander, E., et al.,

2011. In vivo 1H-magnetic resonance spectroscopy study of the attentional networks in autism. Brain Res. 1380, 198–205.
Blatt, G.J., Fatemi, S.H., 2011. Alterations in GABAergic biomarkers in the autism brain: research findings and clinical implications. Anat. Rec. (Hoboken) 294, 1646–1652.
Blüml, S., 2013. Magnetic resonance spectroscopy: basics. In: Blüml, S., Panigrahy, A. (Eds.), MR Spectroscopy of Pediatric Brain Disorders. Springer, New York, pp. 11–23.
Bogner, W., Gruber, S., Doelken, M., Stadlbauer, A., Ganslandt, O., Boettcher, U., et al., 2010. In vivo quantification of intracerebral GABA by single-voxel 1H-MRS—how reproducible are the results? Eur. J. Radiol. 73, 526–531.
Bolton, P.F., Carcani-Rathwell, I., Hutton, J., Goode, S., Howlin, P., Rutter, M., 2011. Epilepsy in autism: features and correlates. Br. J. Psychiatry 198, 289–294.
Brix, M.K., Ersland, L., Hugdahl, K., Grüner, R., Posserud, M.B., Hammar, A., et al., 2015. Brain MR spectroscopy in autism spectrum disorder—the GABA excitatory/inhibitory imbalance theory revisited. Front. Hum. Neurosci. 9, 1–12.
Brix, M.K., Ersland, L., Hugdahl, K., Dwyer, G.E., Grüner, R., Noeske, R., et al., 2017. Within- and between-session reproducibility of GABA measurements with MR spectroscopy. J. Magn. Reson. Imaging 46, 421–430.
Brown, M.S., Singel, D., Hepburn, S., Rojas, D.C., 2013. Increased glutamate concentration in the auditory cortex of persons with autism and first-degree relatives: A (1)H-MRS study. Autism Res. 6, 1–10.
Buescher, A.V., Cidav, Z., Knapp, M., Mandell, D.S., 2014. Costs of autism spectrum disorders in the United Kingdom and the United States. JAMA Pediatr. 168, 721–728.
Burrows, E.L., Laskaris, L., Koyama, L., Churilov, L., Bornstein, J.C., Hill-Yardin, E.L., et al., 2015. A neuroligin-3 mutation implicated in autism causes abnormal aggression and increases repetitive behavior in mice. Mol. Autism 6, 62.
Cavalho Pereira, A., Violante, I.R., Mouga, S., Oliveria, G., Castelo-Branco, M., 2018. Medial frontal lobe neurochemistry in autism spectrum disorder is marked by reduced N-acetylaspartate and unchanged gamma-aminobutyric acid and glutamate + glutamine levels. J. Autism Dev. Discord. 48, 1467–1482.
Chaste, P., Sanders, S.J., Mohan, K.N., Klein, L., Song, Y., Murtha, M.T., et al., 2014. Modest impact on risk for autism spectrum disorder of rare copy number variants at 15q11.2, specifically breakpoints 1 to 2. Autism Res. 7, 355–362.
Ching, M.S.L., Shen, Y., Tan, W., Jeste, S.S., Shafali, S.J., Morrow, E.M., Chen, X., et al., 2010. Deletions of NRXN1 (Neurexin-1) predispose to a wide spectrum of developmental disorders. Am. J. Med. Genet. B. Neuropsychiatr. Genet. 153B, 937–947.
Cleve, M., Gussew, A., Reichenbach, J.R., 2015. In vivo detection of acute pain-induced changes of GABA+ and Glx in the human brain by using functional 1H MEGA-PRESS MR spectroscopy. NeuroImage 105, 67–75.
Cochran, D.M., Sikoglu, E.M., Hodge, S.M., Edden, R.A.E., Foley, A., Kennedy, D.N., et al., 2015. Relationship among glutamine, γ-aminobutyric acid, and social cognition in autism spectrum disorders. J. Child Adolesc. Psychopharmacol. 25, 314–322.
Corrigan, N.M., Shaw, D.W., Estes, A.M., Richards, T.L., Munson, J., Friedman, S.D., et al., 2013. Atypical developmental patterns of brain chemistry in children with autism spectrum disorder. JAMA Psychiat. 70, 964–974.
Dager, S.R., Corrigan, N.M., Richards, T.L., Posse, S., 2008. Research applications of magnetic resonance spectroscopy to investigate psychiatric disorders. Top. Magn. Reson. Imaging 19, 81–96.
Darnell, J.C., Van Driesche, S.J., Zhang, C., Hung, K.Y., Mele, A., Fraser, C.E., 2011. FMRP stalls ribosomal translocation on mRNAs linked to synaptic function and autism. Cell 146, 247–261.
Delorey, T.M., Handforth, A., Anagnostaras, S.G., Homanics, G.E., Minassian, B.A., Asatourian, A., Fanselow, M.S., et al., 1998. Mice lacking the beta3 subunit of the GABAA receptor have the epilepsy phenotype and many of the behavioral characteristics of angelman syndrome. J. Neurosci. 18, 8505–8514.
Devito, T.J., Drost, D.J., Neufeld, R.W., Rajakumar, N., Pavlosky, W., Williamson, P., et al., 2007. Evidence for cortical dysfunction in autism: a proton magnetic resonance spectroscopic imaging study. Biol. Psychiatry 61, 465–473.
Dickinson, A., Jones, M., Milne, E., 2016. Measuring neural excitation and inhibition in autism: different approaches, different findings and different interpretations. Brain Res. 1648, 277–289.
Doyle-Thomas, K.A.R., Card, D., Soorya, L.V., Wang, A.T., Fan, J., Anagnostou, E., 2014. Metabolic mapping of deep brain structures and associations with symptomatology in autism spectrum disorders. Res. Autism Spectr. Disord. 8, 44–51.
Drenthen, G.S., Barendse, E.M., Aldenkamp, A.P., van Veenendaal, T.M., Puts, N.A., Edden, R.A., et al., 2016. Altered neurotransmitter metabolism in adolescents with high-functioning autism. Psychiatry Res. 256, 44–49.
Duarte, J.M., Lei, H., Mlynarik, V., Gruetter, R., 2012. The neurochemical profile quantified by in vivo 1H NMR spectroscopy. NeuroImage 61, 342–362.
Edden, R.A., Puts, N.A., Barker, P.B., 2012. Macromolecule-suppressed GABA-edited magnetic resonance spectroscopy at 3T. Magn. Reson. Med. 68, 657–661.
Edden, R.A., Puts, N.A., Harris, A.D., Barker, P.B., Evans, C.J., 2014. Gannet: a batch-processing tool for the quantitative analysis of gamma-aminobutyric acid-edited MR spectroscopy spectra. J. Magn. Reson. Imaging 40, 1445–1452.
Endres, D., Tebartz Van Elst, L., Meyer, S.A., Feige, B., Nickel, K., Bubl, A., et al., 2017. Glutathione metabolism in the prefrontal brain of adults with high-functioning autism spectrum disorder: an MRS study. Mol. Autism 8, 10.
Etherton, M., Földy, C., Sharma, S., Tabuchi, K., Liu, X., Shamloo, M., et al., 2011a. Autism-linked neuroligin-3 R451C mutation differentially alters hippocampal and cortical synaptic function. PNAS 108, 13764–13769.
Etherton, M.R., Tabuchi, K., Sharma, M., Ko, J., Südhof, T.C., 2011b. An autism-associated point mutation in the neuroligin cytoplasmic tail selectively impairs AMPA receptor-mediated synaptic transmission in hippocampus. EMBO J. 30, 2908–2919.
Fatemi, S.H., Folsom, T.D., 2011. Dysregulation of fragile × mental retardation protein and metabotropic glutamate receptor 5 in superior frontal cortex of individuals with autism: a postmortem brain study. Mol. Autism 2, 6.
Fatemi, S.H., Halt, A.R., Stary, J.M., Kanodia, R., Schulz, S.C., Realmuto, G.R., 2002. Glutamic acid decarboxylase 65 and 67 kDa proteins are reduced in autistic parietal and cerebellar cortices. Biol. Psychiatry 52, 805–810.
Fatemi, S.H., Reutiman, T.J., Folsom, T.D., Huang, H., Oishi, K., Mori, S., et al., 2008. Maternal infection leads to abnormal gene regulation and brain atrophy in mouse offspring: implications for genesis of neurodevelopmental disorderss. Schizophr. Res. 99, 56–70.
Fatemi, S.H., Reutiman, T.J., Folsom, T.D., Thuras, P.D., 2009. GABA(A) receptor downregulation in brains of subjects with autism. J. Autism Dev. Disord. 39, 223–230.
Fatemi, S.H., Folsom, T.D., Kneeland, R.E., Liesch, S.B., 2011. Metabotropic glutamate receptor 5 upregulation in children with autism is associated with underexpression of both Fragile X Mental retardation protein and GABAA receptor beta 3 in adults with autism. Anat. Rec. (Hoboken) 294, 1635–1645.
Fatemi, S.H., Reutiman, T.J., Folsom, T.D., Rustan, O.G., Rooney, R.J., Thuras, P.D., 2014. Downregulation of GABAA receptor protein subunits alpha6, beta2, delta, epsilon, gamma2, theta, and rho2 in superior frontal cortex of subjects with autism. J. Autism Dev. Disord. 44, 1833–1845.
Ford, T.C., Crewther, D.P., 2016. A comprehensive review of the (1)H-MRS metabolite spectrum in autism spectrum disorder. Front. Mol. Neurosci. 9, 14.
Foss-Feig, J.H., Adkinson, B.D., Ji, J.L., Yang, G., Srihari, V.H., McPartland, J.C., et al., 2017. Searching for cross-diagnostic convergence: neural mechanisms governing excitation and inhibition balance in schizophrenia and autism spectrum disorders. Biol. Psychiatry 81, 848–861.
Friedman, S.D., Shaw, D.W., Artru, A.A., Dawson, G., Petropoulous, H., Dager, S.R., 2006. Gray and white matter brain chemistry in young children with autism. Arch. Gen. Psychiatry 63, 786.
Fukuchi, M., Nii, T., Ishimaru, N., Minamino, A., Hara, D., Takasaki, I., et al., 2009. Valproic acid induces up- or down-regulation of gene expression responsible for the neuronal excitation and inhibition in rat cortical neurons through its epigenetic actions. Neurosci. Res. 65, 35–43.
Futai, K., Kim, M.J., Hashikawa, T., Scheiffele, P., Sheng, M., Hayashi, Y., 2007. Retrograde modulation of presynaptic release probability through signaling mediated by PSD-95–neuroligin. Nat. Neurosci. 10, 186–195.
Gaetz, W., Bloy, L., Wang, D.J., Port, R.G., Blaskey, L., Levy, S.E., Roberts, T.P., 2014. GABA estimation in the brains of children on the autism spectrum: measurement precision and regional cortical variation. NeuroImage 86, 1–9.
Gandal, M.J., Anderson, R.L., Billingslea, E.N., Carlson, G.C., Roberts, T.P., Siegel, S.J., 2012. Mice with reduced NMDA receptor expression: more consistent with autism than schizophrenia? Genes Brain Behav. 11, 740–750.
Gao, R., Penzes, P., 2015. Common mechanisms of excitatory and inhibitory imbalance in schizophrenia and autism spectrum disorders. Curr. Mol. Med. 15, 146–167.
Gatto, C.L., Broadie, K., 2010. Genetic controls balancing excitatory and inhibitory synaptogenesis in neurodevelopmental disorder models. Front. Synaptic. Neurosci. 2, 4.
Giovanoli, S., Weber, L., Meyer, U., 2014. Single and combined effects of prenatal immune activation and peripubertal stress on parvalbumin and reelin expression in the hippocampal formation. Brain Behav. Immun. 40, 48–54.
Goji, A., Ito, H., Mori, K., Harada, M., Hisaoka, S., Toda, Y., et al., 2017. Assessment of anterior cingulate cortex (ACC) and left cerebellar metabolism in asperger's syndrome with proton magnetic resonance spectroscopy (MRS). PLoS One 12, e0169288.
Govindaraju, V., Young, K., Maudsley, A.A., 2000. Proton NMR chemical shifts and coupling constants for brain metabolites. NMR Biomed. 13 (3), 129–153.
Grayton, H.M., Missler, M., Collier, D.A., Fernandes, C., 2013. Altered social behaviours in neurexin 1 knockout mice resemble core symptoms in neurodevelopmental disorders. PLoS One 8, e67114.
Gussew, A., Erdtel, M., Hiepe, P., Rzanny, R., Reichenbach, J.R., 2012. Absolute quantitation of brain metabolites with respect to heterogeneous tissue compositions in (1) H-MR spectroscopic volumes. MAGMA 25, 321–333.
Harada, M., Taki, M.M., Nose, A., Kubo, H., Mori, K., Nishitani, H., et al., 2011. Non-invasive evaluation of the GABAergic/glutamatergic system in autistic patients observed by MEGA-editing proton MR spectroscopy using a clinical 3 tesla instrument. J. Autism Dev. Disord. 41, 447–454.
Hardan, A.Y., Minshew, N.J., Melhem, N.M., Srihari, S., Jo, B., Bansal, R., et al., 2008. An MRI and proton spectroscopy study of the thalamus in children with autism. Psychiatry Res. 163, 97–105.
Hassan, T.H., Abdelrahman, H.M., Abdel Fattah, N.R., El-Masry, N.M., Hashim, H.M., El-Gerby, K.M., et al., 2013. Blood and brain glutamate levels in children with autistic disorder. Res. Autism Spectr. Disord. 7, 541–548.
Hegarty, J.P., Gu, M., Spielman, D.M., Cleveland, S.C., Hallmayer, J.F., Lazzeroni, L.C., et al., 2017. A proton MR spectroscopy study of the thalamus in twins with autism spectrum disorder. Prog. Neuro-Psychopharmacol. Biol. Psychiatry 81, 153–160.
Henry, P.G., Dautry, C., Hantraye, P., Bloch, G., 2001. Brain GABA editing without macromolecule contamination. Magn. Reson. Med. 45, 517–520.
Horder, J., Lavender, T., Mendez, M.A., O'Gorman, R., Daly, E., Craig, M.C., et al., 2013. Reduced subcortical glutamate/glutamine in adults with autism spectrum disorders: A [1H]MRS study. Transl. Psychiatry 3, e279.
Horder, J., Petrinovic, M.M., Mendez, M.A., Bruns, A., Takumi, T., Spooren, W., et al., 2018. Glutamate and GABA in autism spectrum disorder-a translational magnetic resonance spectroscopy study in man and rodent models. Transl. Psychiatry 8, 106.
Isles, A.R., Ingason, A., Lowther, C., Walters, J., Gawlick, M., Stöber, G., et al., 2016. Parental origin of interstitial duplications at 15q11.2-q13.3 in schizophrenia and neurodevelopmental disorders. PLoS Genet. 12, e1005993.
Ito, H., Mori, K., Harada, M., Hisaoka, S., Toda, Y., Mori, et al., 2017. A proton magnetic resonance spectroscopic study in autism spectrum disorder using a 3-tesla clinical magnetic resonance imaging (MRI) system: the anterior cingulate cortex and the left cerebellum. J. Child Neurol. 32, 731–739.
Jamain, S., Quach, H., Betancur, C., Rastam, M., Colineaux, C., Gillberg, C., et al., 2003.

Mutations of the X-linked genes encoding neuroligins NLGN3 and NLGN4 are associated with autism. Nat. Genet. 34, 27–29.
Jansen, J.F., Backes, W.H., Nicolay, K., Kooi, M.E., 2006. 1H MR spectroscopy of the brain: absolute quantification of metabolites. Radiology 240, 318–332.
Jaramillo, T.C., Liu, S., Pettersen, A., Birnbaum, S.G., Powell, C.M., 2014. Autism-related neuroligin-3 mutation alters social behavior and spatial learning. Autism Res. 7, 264–272.
Joshi, G., Biederman, J., Wosniak, J., Goldin, R.L., Crowley, D., Furtak, S., et al., 2013. Magnetic resonance spectroscopy study of the glutamatergic system in adolescent males with high-functioning autistic disorder: a pilot study at 4T. Eur. Arch. Psychiatry Clin. Neurosci. 263, 379–384.
Juchem, C., Rothman, D.L., 2014. Basis of magnetic resonance. In: Stagg, C., Rothman, D.L. (Eds.), Magnetic Resonance Spectroscopy. Academic Press, San Diego, pp. 3–14.
Kaiser, L.G., Schuff, N., Cashdollar, N., Weiner, M.W., 2005. Age-related glutamate and glutamine concentration changes in normal human brain: 1H MR spectroscopy study at 4 T. Neurobiol. Aging 26, 665–672.
Kattenstroth, G., Tantalaki, E., Südhof, T.C., Gottmann, K., Missler, M., 2004. Postsynaptic N-methyl-D-aspartate receptor function requires alpha-neurexins. PNAS 101, 2607–2612.
Kirovski, M., Suo, C., Enticott, P.G., Yücel, M., Fitzgerald, P.B., 2018. Sex-linked differences in gamma-aminobutyric acid (GABA) are related to social functioning in autism spectrum disorder. Psychiatry Res. 274, 19–22.
Kubas, B., Kulak, W., Sobaniec, W., Tarasow, E., Lebkowska, U., Walecki, J., 2012. Metabolite alterations in autistic children: a 1H MR spectroscopy study. Adv. Med. Sci. 57, 152–156.
Lai, M.C., Lombardo, M.V., Baron-Cohen, S., 2014. Autism. Lancet 383, 896–910.
Lee, E., Lee, J., Kim, E., 2017. Excitation/inhibition imbalance in animal models of autism spectrum disorders. Biol. Psychiatry 81, 838–847.
Lemonnier, E., Degrez, C., Phelep, M., Tyzio, R., Josse, F., Grandgeorge, M., et al., 2012. A randomised controlled trial of bumetanide in the treatment of autism in children. Transl. Psychiatry 2, e202.
Libero, L.E., Deramus, T.P., Lahti, A.C., Deshpande, G., Kana, R.K., 2015. Multimodal neuroimaging based classification of autism spectrum disorder using anatomical, neurochemical, and white matter correlates. Cortex 66, 46–59.
Libero, L.E., Reid, M.A., White, D.M., Salibi, N., Lahti, A.C., Kana, R.K., 2016. Biochemistry of the cingulate cortex in autism: an MR spectroscopy study. Autism Res. 9, 643–657.
Long, Z., Dyke, J.P., Ma, R., Huang, C.C., Louis, E.D., Dydak, U., 2015. Reproducibility and effect of tissue composition on cerebellar γ-aminobutyric acid (GABA) MRS in an elderly population. NMR Biomed. 28, 1315–1323.
Lozano, R., Rosero, C.A., Hagerman, R.J., 2014. Fragile X spectrum disorders. Intractable Rare Dis. Res. 3, 134–146.
Lujan, R., Shigemoto, R., Lopez-Bendito, G., 2005. Glutamate and GABA receptor signalling in the developing brain. Neuroscience 130, 567–580.
Maddock, R.J., Casazza, G.A., Fernandez, D.H., Maddock, M.I., 2016. Acute modulation of cortical glutamate and GABA content by physical activity. J. Neurosci. 36, 2449–2457.
Marrosu, F., Marrosu, G., Rachel, M.G., Biggio, G., 1987. Paradoxical reactions elicited by diazepam in children with classic autism. Funct. Neurol. 2, 355–361.
Mescher, M., Merkle, H., Kirsch, J., Garwood, M., Gruetter, R., 1998. Simultaneous in vivo spectral editing and water suppression. NMR Biomed. 11, 266–272.
Meyer, U., Feldon, J., Dammann, O., 2011. Schizophrenia and autism: both shared and disorder-specific pathogenesis via perinatal inflammation? Pediatr. Res. 69, 26R–33R.
Mikkelsen, M., Barker, P.B., Bhattacharyya, P.K., Brix, M.K., Buur, P.F., Cecil, K.M., 2017. Big GABA: edited MR spectroscopy at 24 research sites. NeuroImage 159, 32–45.
Mikkelsen, M., Loo, R.S., Puts, N.A.J., Edden, R.A.E., Harris, A.D., 2018. Designing GABA-edited magnetic resonance spectroscopy studies: Considerations of scan duration, signal-to-noise ratio and sample size. J. Neurosci. Methods 303, 86–94.
Minshawi, N.F., Wink, L.K., Shaffer, R., Plawecki, M.H., Posey, D.J., Liu, H., et al., 2016. A randomized, placebo-controlled trial of D-cycloserine for the enhancement of social skills training in autism spectrum disorders. Mol. Autism 7, 2.
Missler, M., Zhang, W., Rohlmann, A., Kattenstroth, G., Hammer, R.E., Gottmann, K., et al., 2003. Alpha-neurexins couple Ca2+ channels to synaptic vesicle exocytosis. Nature 423, 939–948.
Moreno-De-Luca, D., Sanders, S.J., Willsey, A.J., Mulle, J.G., Lowe, J.K., Geschwind, D.H., et al., 2013. Using large clinical data sets to infer pathogenicity for rare copy number variants in autism cohorts. Mol. Psychiatry 18, 1090–1095.
Muhle, R., Trentacoste, S.V., Rapin, I., 2004. The genetics of autism. Pediatrics 113, e472–e486.
Mullins, P.G., Mcgonigle, D.J., O'Gorman, R.L., Puts, N.A., Vidyasagar, R., Evans, C.J., Cardiff Symposium On, M.R.S.O.G., Edden, R.A., 2014. Current practice in the use of MEGA-PRESS spectroscopy for the detection of GABA. NeuroImage 86, 43–52.
Mullins, C., Fishell, G., Tsien, R.W., 2016. Unifying views of autism spectrum disorders: a consideration of autoregulatory feedback loops. Neuron 89, 1131–1156.
Naaijen, J., Zwiers, M.P., Amiri, H., Williams, S.C., Durston, S., Oranje, B., et al., 2016. Fronto-striatal glutamate in autism spectrum disorder and obsessive compulsive disorder. Neuropsychopharmacology 42, 2466–2467.
Naressi, A., Couturier, C., Castang, I., De Beer, R., Graveron-Demilly, D., 2001. Java-based graphical user interface for MRUI, a software package for quantitation of in vivo/medical magnetic resonance spectroscopy signals. Comput. Biol. Med. 31, 269–286.
Near, J., Simpson, R., Cowen, P., Jezzard, P., 2011. Efficient gamma-aminobutyric acid editing at 3T without macromolecule contamination: MEGA-SPECIAL. NMR Biomed. 24, 1277–1285.
Nelson, S.B., Valakh, V., 2015. Excitatory/inhibitory balance and circuit homeostasis in autism spectrum disorders. Neuron 87, 684–698.
Oblak, A., Gibbs, T.T., Blatt, G.J., 2009. Decreased GABAA receptors and benzodiazepine binding sites in the anterior cingulate cortex in autism. Autism Res. 2, 205–219.
Oblak, A.L., Gibbs, T.T., Blatt, G.J., 2010. Decreased GABA(B) receptors in the cingulate cortex and fusiform gyrus in autism. J. Neurochem. 114, 1414–1423.
Oblak, A.L., Gibbs, T.T., Blatt, G.J., 2011. Reduced GABAA receptors and benzodiazepine binding sites in the posterior cingulate cortex and fusiform gyrus in autism. Brain Res. 1380, 218–228.
O'Gorman, R.L., Michels, L., Edden, R.A., Murdoch, J.B., Martin, E., 2011. In vivo detection of GABA and glutamate with MEGA-PRESS: reproducibility and gender effects. J. Magn. Reson. Imaging 33, 1262–1267.
Orefice, L.L., Zimmerman, A.L., Chirila, A.M., Sleboda, S.J., Head, J.P., Ginty, D.D., 2016. Peripheral mechanosensory neuron dysfunction underlies tactile and behavioral deficits in mouse models of ASDs. Cell 166, 299–313.
Orekhova, E.V., Stroganova, T.A., Nygren, G., Tsetlin, M.M., Posikera, I.N., Gillberg, C., et al., 2007. Excess of high frequency electroencephalogram oscillations in boys with autism. Biol. Psychiatry 62, 1022–1029.
Oz, G., Alger, J.R., Barker, P.B., Bartha, R., Bizzi, A., Boesch, C., 2014. Clinical proton MR spectroscopy in central nervous system disorders. Radiology 270, 658–679.
Page, L.A., Daly, E., Schmitz, N., Simmons, A., Toal, F., Deeley, Q., et al., 2006. In vivo 1H-magnetic resonance spectroscopy study of amygdala-hippocampal and parietal regions in autism. Am. J. Psychiatry 163, 2189–2192.
Port, R.G., Gaetz, W., Bloy, L., Wang, D., Blaskey, L., Kuschner, E.S., et al., 2017. Exploring the relationship between cortical GABA concentrations, auditory gamma-band responses and development in ASD: evidence for an altered maturational trajectory in ASD. Autism Res. 10, 593–607.
Posey, D.J., Kem, D.L., Swiezy, N.B., Sweeten, T.L., Wiegand, R.E., McDougle, C.J., 2004. A pilot study of D-cycloserine in subjects with autistic disorder. Am. J. Psychiatry 161, 2115–2117.
Provencher, S.W., 1993. Estimation of metabolite concentrations from localized in vivo proton NMR spectra. Magn. Reson. Med. 30, 672–679.
Purcell, A.E., Jeon, O.H., Zimmerman, A.W., Blue, M.E., Pevsner, J., 2001. Postmortem brain abnormalities of the glutamate neurotransmitter system in autism. Neurology 57, 1618–1628.
Puts, N.A.J., Wodka, E.L., Harris, A.D., Crocetti, D., Tommerdahl, M., Mostofsky, S.H., et al., 2017. Reduced GABA and Altered Somatosensory Function in Children with Autism Spectrum Disorder. Autism Res. 10, 608–619.
Quadrelli, S., Mountford, C., Ramadan, S., 2016. Hitchhiker's guide to voxel segmentation for partial volume correction of in vivo magnetic resonance spectroscopy. Magn. Reson. Insights 9, 1–8.
Radyushkin, K., Hammerschmidt, K., Boretius, S., Varoqueaux, F., El-Kordi, A., Ronnenberg, A., et al., 2009. Neuroligin-3-deficient mice: model of a monogenic heritable form of autism with an olfactory deficit. Genes Brain Behav. 8, 416–425.
Redcay, E., Courchesne, E., 2005. When is the brain enlarged in autism? a meta-analysis of all brain size reports. Biol. Psychiatry 58, 1–9.
Robertson, C.E., Ratai, E., Kanwisher, N., 2015. Reduced GABAergic action in autistic brain. Curr. Biol. 26, 80–85.
Rojas, D.C., Singel, D., Steinmetz, S., Hepburn, S., Brown, M.S., 2014. Decreased left perisylvian GABA concentration in children with autism and unaffected siblings. NeuroImage 86, 28–34.
Rowley, N.M., Madsen, K.K., Schousboe, A., Steve White, H., 2012. Glutamate and GABA synthesis, release, transport and metabolism as targets for seizure control. Neurochem. Int. 61, 546–558.
Rubenstein, J.L.R., Merzenich, M.M., 2003. Model of autism: increased ratio of excitation/inhibition in key neural systems. Genes Brain Behav. 2, 255–267.
Sailasuta, N., Ernst, T., Chang, L., 2008. Regional variations and the effects of age and gender on glutamate concentrations in the human brain. Magn. Reson. Imaging 2, 667–675.
Schneider, J.F., 2016. MR spectroscopy in children: protocols and pitfalls in non-tumorous brain pathology. Pediatr. Radiol. 46, 963–982.
Schur, R.R., Draisma, L.W., Wijnen, J.P., Boks, M.P., Koevoets, M.G., Joels, M., 2016. Brain GABA levels across psychiatric disorders: a systematic literature review and meta-analysis of (1) H-MRS studies. Hum. Brain Mapp. 37, 3337–3352.
Selimbeyoglu, A., Kim, C.K., Inoue, M., Lee, S.Y., Hong, A.S.O., Kauvar, I., et al., 2017. Modulation of prefrontal cortex excitation/inhibition balance rescues social behavior in CNTNAP2-deficient mice. Sci. Transl. Med. 9.
Shao, Y., Cuccaro, M.L., Hauser, E.L., Raiford, K.L., Menold, M.M., Wolpert, C.M., et al., 2003. Fine mapping of autistic disorder to chromosome 15q11-q13 by use of phenotypic subtypes. Am. J. Hum. Genet. 72, 539–548.
Shimmura, C., Suzuki, K., Iwata, Y., Tsuchiya, K.L., Ohno, K., Matsuzaki, H., et al., 2013. Enzymes in the glutamate-glutamine cycle in the anterior cingulate cortex in postmortem brain of subjects with autism. Mol. Autism 4, 6.
Shungu, D.C., Mao, X., Donzales, R., Soones, T.R., Dyke, J.P., van der Veen, J.W., et al., 2016. Brain γ-aminobutyric acid (GABA) detection in vivo with the J -Editing 1 H MRS technique: a comprehensive methodological evaluation of sensitivity enhancement, macromolecule contamination and test-retest reliability. NMR Biomed. 29, 932–942.
Stagg, C.J., Bachtiar, V., Johansen-Berg, H., 2011. What are we measuring with GABA magnetic resonance spectroscopy? Commun. Integr. Biol. 4, 573–575.
Südhof, T.C., 2008. Neuroligins and neurexins link synaptic function to cognitive disease. Nature 455, 903–911.
Tabuchi, K., Blundell, J., Etherton, M.R., Hammer, R.E., Liu, X., Powell, C.M., et al., 2007. A neuroligin-3 mutation implicated in autism increases inhibitory synaptic transmission in mice. Science 318, 71–76.
Tebartz Van Elst, L., Maier, S., Fangmeier, T., Endres, D., Mueller, G.T., Nickel, K., et al., 2014. Disturbed cingulate glutamate metabolism in adults with high-functioning autism spectrum disorder: evidence in support of the excitatory/inhibitory imbalance

hypothesis. Mol. Psychiatry 19, 1314–1325.
Uchino, S., Waga, C., 2015. Novel therapeutic approach for autism spectrum disorder: focus on SHANK3. Curr. Neuropharmacol. 13, 786–792.
Urraca, N., Cleary, J., Brewer, V., Pivnick, E.K., McVicar, K., Thibert, R.L., et al., 2013. The interstitial duplication 15q11.2-q13 syndrome includes autism, mild facial anomalies and a characteristic EEG signature. Autism Res. 6, 268–279.
Uzunova, G., Pallanti, S., Hollander, E., 2016. Excitatory/inhibitory imbalance in autism spectrum disorders: implications for interventions and therapeutics. World J. Biol. Psychiatry 17, 174–186.
Verkerk, A.J., Pieretti, M., Sutcliffe, J.S., Fu, Y.H., Kuhl, D.P., Pizutti, A., et al., 1991. Identification of a gene (FMR-1) containing a CGG repeat coincident with a breakpoint cluster region exhibiting length variation in Fragile X syndrome. Cell 65, 905–914.
Waschkies, C.F., Bruns, A., Müller, S., Kapps, M., Borroni, E., von Kinelin, M., et al., 2014. Neuropharmacological and neurobiological relevance of in vivo (1)H-MRS of GABA and glutamate for preclinical drug discovery in mental disorders. Neuropsychopharmacology 39, 2331–2339.
Wei, R., Li, Q., Lam, S., Lueng, J., Cheung, C., Zhang, X., et al., 2016. A single low dose of valproic acid in late prenatal life alters postnatal behavior and glutamic acid decarboxylase levels in the mouse. Behav. Brain Res. 314, 190–198.
Xing, J., Kimura, H., Wang, C., Ishizuka, K., Kushima, I., Arioka, Y., et al., 2016. Resequencing and association analysis of six PSD-95-related genes as possible susceptibility genes for schizophrenia and autism spectrum disorders. Sci. Rep. 6, 27491.
Yip, J., Soghomonian, J., Blatt, G.J., 2007. Decreased GAD67 mRNA levels in cerebellar Purkinje cells in autism: pathophysiological implications. Acta Neuropathol. 113, 559–568.
Yizhar, O., Fenno, L.E., Prigge, M., Schneider, F., Davidson, T.J., O'Shea, D.J., et al., 2011. Neocortical excitation/inhibition balance in information processing and social dysfunction. Nature 477, 171–178.
Yu, T., Berry-Kravis, E., 2014. Autism and Fragile X syndrome. Semin. Neurol. 34, 258–265.
Zhang, W., 2005. Extracellular domains of-neurexins participate in regulating synaptic transmission by selectively affecting N- and P/Q-Type Ca2+ channels. J. Neurosci. 25, 4330–4342.
Zhu, H., Barker, P.B., 2011. MR spectroscopy and spectroscopic imaging of the brain. Methods Mol. Biol. 711, 203–226.

APPENDIX 2

Patient Information Sheet

Institute of Psychiatry
at The Maudsley

Prof. Declan Murphy
Head of Department
Forensic and
Neurodevelopmental Sciences
PO Box 50

KING'S College LONDON

Information Sheet: Version 4, 29 August 2013

Brain chemistry in Autism Spectrum

Principal Investigator: Dr Grainne McAlonan

Invitation:
You are being invited to take part in a research study. Before you decide if you want to take part, it is important for you to understand why the research is being done and what it will involve. Please take time to read the following information carefully and discuss it with others if you wish. Ask us if there is anything that is not clear. Take your time to decide whether or not you wish to take part in the study. You will be given a copy of this form. Thank you for reading this.

What is the purpose of the study?
Autism spectrum disorder (ASD) is a group of related conditions including autism and Asperger's syndrome. There is evidence that ASD may be caused by differences in the levels of two signalling chemicals in the brain, GABA and glutamate. However, direct evidence is missing.

This study aims to measure GABA and glutamate in the brain of people with and without ASD using an MRI brain scanning technique called magnetic resonance spectroscopy (MRS). We hope that longer-term the results of our study will improve diagnosis of ASD and confirm a potential novel treatment target (the glutamate-GABA system).

We wish to measure glutamate and GABA at 'rest' (when taking an inactive "dummy" pill or placebo) and when 'activated' by a single dose of the drug probe ***Riluzole.*** Riluzole temporarily alters GABA and glutamate activity in the brain.

What if I don't want to take part?
Whether you agree to participate or not in this study does not in any way affect your clinical care (if any). If you do decide to take part, you can still decide to leave the study, at any time in the future, for any or no reason.

What will happen to me if I take part?
If you decide to take part in the study, you will attend our research centre at the Institute of Psychiatry, London, on two separate visits. The two visits will be about one week apart (e.g. Friday

one week, and then the next Friday) and last about 3 hours. We will ask you to fill out some short questionnaires and also carry out some assessments with one of the research team. If you have an ASD, we will confirm diagnosis, either (with your permission) by checking a recent clinic record if available, or by an assessment with you and/or an informant, depending on what is practical.

On each visit, you will have an MRS scan which lasts about 60 minutes. Before the scan, you will be given a tablet to take. The tablet will contain either a 50 milligram dose of riluzole, or a placebo ('dummy pill'). You will not know which tablet you are getting on each occasion. After the scan, we will ask you to complete a short interview and checklist with the doctor and we will ask you to wait for one hour to make sure you are ok before going home.

Will I be compensated for my time and travel expenses?
We will reimburse your travel expenses, and also pay you in compensation for your time, £60 per session, (i.e. £120 if you complete the study.) For more details please contact one of the researchers.

What is riluzole?
Riluzole is licenced for the treatment of Amyotrophic Lateral Sclerosis (ALS, "Lou Gehrig's Disease"). More recently it has been shown to improve mood symptoms in adults and symptoms of OCD in children with and without ASD. It works by altering glutamate and GABA transmission in the nervous system and is thought to protect against neuronal damage. People with ALS take at least 50 mg riluzole every day. In this study Riluzole is used as a drug probe not a treatment, therefore you will only take a one-off standard single dose of 50 mg.

Riluzole has a good safety profile even when used in children. Examples of adverse effects following regular treatment are headache, nausea, chest symptoms and liver problems, but these are very rare and disappear when the drug is stopped. You will only have a single dose of Riluzole, therefore it is extremely unlikely that you will experience any problems as a result of taking the drug. However, a doctor will be present throughout the study.

What is MRS scanning?
The type of scan we use is called a Magnetic Resonance Spectroscopy (MRS) scan. The scanner is a magnet and does not involve the use of harmful radiation such as X-rays.

You cannot have a scan if there is any chance that you have magnetic metal inside your body. For example, you must not be scanned if you have a pacemaker, if you have ever had surgery on your eyes, heart, or head; of if you have suffered an injury that might have left metal fragments in your body. Dental fillings and braces, however, are generally *safe* for MRS scanning, because they are not made of magnetic metal. A radiographer will go over a list of possible risks with you before scanning begins.

There is a microphone inside the MRI scanner so that you can talk to us at any time during the procedure. Some people can feel claustrophobic inside the scanner. If you feel uncomfortable we can stop the scanning immediately. The scanner is noisy, so you will be provided with ear plugs for your comfort. However, if you feel any distress we will stop the scan and assess any discomfort you may experience. You may choose whether you wish to continue and stop the study at any point.
This is a research scan and is not designed to provide clinical information. Therefore, we will not routinely feedback any of the results to you. If, however anything obviously abnormal shows up on the scan, we will inform you and (with your permission) your G.P.

Will my data be kept confidential?
The information obtained from your study is covered by the Data Protection Act. The computerised information is protected by a software and hardware barrier and the records are handled in the same way as hospital records. Only members of the research team or responsible persons from the NHS Trust, where it is relevant to your taking part in this research, will have access to your data and only with permission from the Principal Investigator. We will ensure this data is kept strictly confidential and use a subject number to code your data separately from your personal information.

Are there any reasons why I can't take part in the study?
This is a small study therefore you **can't** take part in the study if you are:

. Female
. Aged under 18 years, **or over 60 years**
. Taking certain regular medications (discuss with researcher)
. Diagnosed with a major psychiatric illness
. Diagnosed with a medical or genetic illness which is linked to autistic spectrum disorders e.g. epilepsy or Fragile X.
. Suffering from any kind of liver disease; or have ever suffered a serious head injury.
. Drinking more than 28 units of alcohol per week, **or a very heavy smoker** or using illegal drugs, or have been a heavy user of these substances in the past **(discuss with researcher)**.
. Not safe to have an MRI e.g. you have a cardiac pacemaker or any other metal implants in your body.
. Learning disabled
. Claustrophobic, or feel that you would be unable to lie still on your back for a period of 1 hour.

Who has reviewed the study?
This study has been review by the NHS Research Ethics Committee London – Camden & Islington.

If you have further queries, or would like more information, please feel free to contact us: Dr. Andreina Mendez on **0207 848 0934** or email **maria.mendez@kcl.ac.uk**
Dr. Jamie Horder on **0207 848 0476** or email **jamie.horder@kcl.ac.uk**

Addendum

Complaints procedure:
In case of any complaint please contact a member of the team in the first instance. The NHS complaints procedure for our Trust is provided at http://www.slam.nhs.uk/patients/frequently-asked-questions/complaints

If the team have been unable to resolve your concerns and you want to make a formal complaint you can contact the Trust's Chief Executive or Complaints Department:
Complaints Department, Maudsley Hospital, 111 Denmark Hill, London. SE5 8AZ
Telephone: 020 3228 2444/2499
Email: Complaints@slam.nhs.uk

If you have something you want to say about our services, you can also visit the Patient Opinion website. This is an independent site which has been set up to give people the opportunity to tell their story about their experience of using NHS services. See www.patientopinion.org.uk

APPENDIX 3
Patient Consent Form

Institute of Psychiatry
at The Maudsley

Prof. Declan Murphy
Head of Department
Forensic and Neurodevelopmental Sciences
PO Box 50
De Crespigny Park
Denmark Hill
London
SE5 8AF

KING'S College LONDON

CONSENT FORM FOR STUDY OF BRAIN CHEMISTRY IN AUTISM SPECTRUM
Version 2, submission date 08 March 2013

IN CONFIDENCE

Have you read the information sheet about this study? **Yes / No**

Do you understand that you are free to withdraw from the study at any time, without having to give a reason for withdrawing, and without influencing current or future treatment? **Yes / No**

Do you understand that relevant sections of your medical notes and data collected during the study, may be looked at by responsible individuals from the study team, or from the NHS Trust, where it is relevant to your taking part in this research. Do you give permission for these individuals to have access to your records? **Yes / No**

Do you understand that all the information will be kept strictly confidential within the research team? **Yes / No**

Do you understand that your GP will be aware that you are participating in the study, but will only be informed if there are any clinically significant results? **Yes/No**

DO YOU CONSENT TO TAKE PART IN THIS STUDY? **Yes/No**

Your Name (capitals) ……

Your Signature ……

Researcher Name ……

Researcher Signature ……

Date of Consent ……

APPENDIX 4

Inclusion and Exclusion criteria for human MRI study

Criteria	Reasoning	Exceptions
Males	Unknown effect of MRI on pregnancy	-
Right handed	Data was collected from the left Basal Ganglia; therefore, only right-handed participants were recruited to avoid possible lateralisation effects	
Aged 18-60	Adults only	-
IQ > 70 As assessed by Wechsler Abbreviated Scale of Intelligence (WASI) (Wechsler, 1999)	Symptom scores of those with IQ < 70 may be confounded by potential learning difficulties	-
No major comorbid medical illness e.g. epilepsy	Modulating the GABA system may trigger seizures in those with pre-existing disposition	-
No major comorbid psychiatric diagnosis	To ensure any observed pathophysiology and	ADHD, Anxiety and Depression (if not medicated) may be

	symptoms are due to autism alone	considered on an individual basis due to the high association of these conditions with ASD
No regular medication use	Potential drug-drug interaction with riluzole	Non-psychotropic medication may be considered if taken consistently over the study duration
No recent (at least 1yr) use of illicit substances	Potential drug-drug interaction with riluzole	-
No drug allergy	In particular those acting on the GABA/Glutamate system	Common allergies e.g. penicillin
No contraindication for MRI	MRI safety	-
Alcohol intake < 28 units/week	Excessive alcohol consumption may modulate GABA receptor pharmacology	-
Tobacco intake < 4/day	Nicotine increases brain GABA levels	Due to paired design, heavy smokers may be considered if necessary

APPENDIX 5

An *in vitro* experiment to assess recovery of the microdialysis probes

A5.1 Background

Microdialysis probes sample from their immediate vicinity, and are therefore not representative of the wider brain region we intend to capture (see Figure A1). To an extent, this is due to several factors which impact upon the dialysing property of the probe, also known as the probes 'recovery'. For example, recovery may depend upon the flow rate, temperature, length of the microdialysis probe and molecular weight of the substance. Therefore, the sample concentration in the microdialysis effluent may be an underestimation of the true extracellular or regional brain concentration. To calculate the sample concentration in the entire region, it is necessary to 'scale up' the concentrations we obtain from LC/MS-MS analyses.

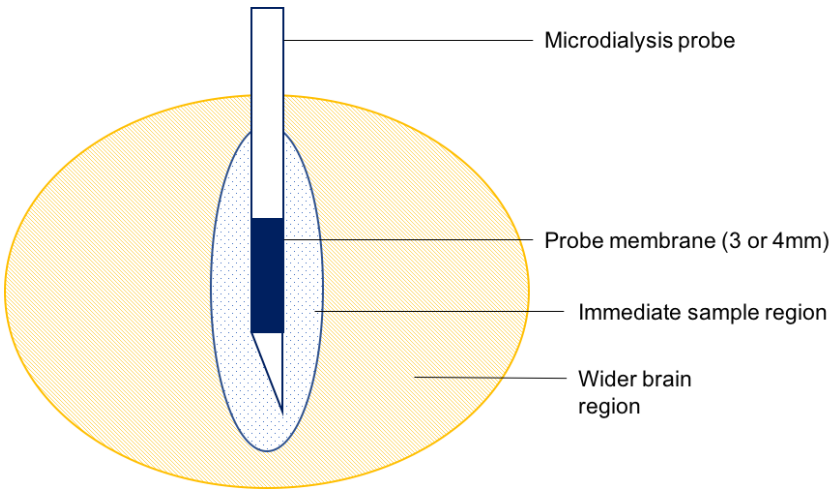

Figure A1: Schematic representation of microdialysis probe recovery efficacy

The microdialysis probe samples from the immediate vicinity (navy dots), and is therefore

not representative of the concentration of sample in the wider brain region (yellow). *Diagram not to scale.*

Previous studies have estimated the percentage recovery of glutamate and GABA in different probe lengths (CMA Microdialysis, 1991), however the recovery of riluzole is as yet unknown. It is particularly important to assess the level of riluzole in the brain regions sampled, in order to know whether any changes in brain neurochemistry are a result of an efficacious riluzole concentration.

By measuring the concentration of riluzole in the microdialysis probe effluent after dialysing artificial cerebrospinal fluid (aCSF) containing a known concentration of riluzole, it is possible to calculate the percentage recovery of riluzole by the probe, and ultimately gain a more accurate estimate the amount of riluzole in the brain region sampled.

A5.2 Methods

An initial concentration curve of riluzole from 0.1-10ng/ml (Sigma, UK) in aCSF (NaCl (141mM), KCl (5mM), MgCl2 (0.8mM) and CaCl2 (1.5mM)) was analysed to calibrate the LC-MS/MS apparatus.

Six stock samples of riluzole were diluted in aCSF in Eppendorf tubes at a concentration of 1ng/ml (37^{o}C). Three 3mm and three 4mm probes were perfused with aCSF at 1.5µl/min and placed into each stock Eppendorf tube. Three consecutive 20 min samples were collected from each probe. Samples were then immediately frozen on dry ice and stored -80°C pending analysis by LC-MS/MS (see General Methods section 2.2.6 for full details). The calculated amounts of riluzole from each of the three 20 min samples were averaged, then divided by

the concentration of the stock sample, and multiplied by 100 to give an estimation of percentage recovery for each probe.

A5.3 Results and discussion

The average accuracy for LC-MS/MS detection of riluzole from the known standards was 96.2 ± 1.4%. The average percentage recovery for riluzole using the 3mm probe was 4.7 ± 0.3 %, compared to 7.5 ± 0.4 % with the 4mm probe (see Table A1). The higher recovery of the 4mm probe is to be expected, as the larger surface area would allow for more riluzole to pass into the probe.

Probe Length	**Percentage Recovery Mean (±SEM)**	**Scale factor**
3mm	4.7 (0.3)	21
4mm	7.5 (0.4)	13

Table A1. *In vitro* recovery of 3mm and 4mm microdialysis probes for riluzole

The percentage recovery was converted to a scale factor (100 / average recovery), this factor can be multiplied by the reported concentration of riluzole in *in vivo* microdialysis samples, to determine an estimate of riluzole levels- see Chapter 6 for further details.

Whilst attempts were made to replicate the *in vivo* scenario, for example by conducting the experiment at physiological temperatures, it is impossible to fully translate the results from *in vitro* to the living brain, where more complex interactions may also play a role in altering probe recovery. However, the scale factors determined in this short study allow for a more accurate assessment of the *in vivo* microdialysis data presented in Chapter 6.

APPENDIX 6

Index and metabolite changes in response to riluzole in the basal ganglia and prefrontal cortex of adults with ASD

		Mean (SEM)						RM ANOVA Between groups		RM ANOVA Within groups		RM ANOVA Drug*Group Intercept	
Region	**Measure**	**Control**			**ASD**			***F***	***p***	***F***	***p***	***F***	***p***
		n	**Placebo**	**Riluzole**	**n**	**Placebo**	**Riluzole**						
Basal Ganglia	**Index**	*13*	.765 (.01)	.783 (.01)	*13*	.795 (.01)	.810 (.01)	2.8	.108	4.4	**.048**	.31	.505
	GABA	*13*	4.06 (.2)	4.40 (.2)	*15*	3.84 (.3)	4.16 (.2)	1.2	.291	3.6	.069	.37	.550
	GLX	*16*	1.19 (.08)	1.22 (.02)	*15*	1.06 (.06)	1.02 (.06)	4.9	**.034**	.07	.936	.35	.562
Prefrontal Cortex	**Index**	*14*	.725 (.2)	.714 (.2)	*13*	.709 (.2)	.731 (.2)	.4	.847	2.3	.146	4.3	**.049**
	GABA	*15*	3.29 (.1)	3.25 (.2)	*14*	3.01 (.2)	3.50 (.2)	.25	.875	1.2	.275	3.1	.091
	GLX	*16*	1.23 (.04)	1.25 (.05)	*13*	1.21 (.05)	1.26 (.04)	.06	.808	1.1	.31	.15	.698

Metabolite and E-I changes in the basal ganglia and prefrontal cortex of controls and ASD subjects in the presence and absence of riluzole.

Index and GABA RM-ANOVA analyses are corrected for state anxiety measures. GABA and GLX mean and SEM are expressed as ($x10^{-4}$). Significant p values are highlighted in bold. Degrees of freedom=1 for each analysis. Repeated measures ANOVA displays between group (effect of diagnosis), within group (effect of drug treatment) and drug by group interactions.